# Synthesis of Strained Ring Systems for Bioorthogonal Labeling Applications

a dissertation by


**Balázs R. Varga**

**Supervisor: Dr. Péter Kele**

principal investigator

**Graduate School of Chemistry**

Chair: Prof. György Inzelt PhD, DSc

**Program of Synthetic Chemistry, Materials Science and Biomolecular Chemistry**

Head: Prof. András Perczel, PhD, DSc


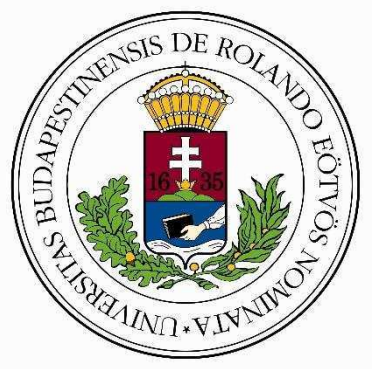



Eötvös Loránd University

Faculty of Natural Sciences


Budapest, 2014.

# Abstract

The synthesis of a novel cyclooctyne and the preparation of reactive and relatively less lipophilic trans cyclooctenes was accomplished.

First a synthetically challenging benzocyclooctyne derivative as a new and simple, directly conjugatable copper-free click reagent, **C**arb**o**xymethyl **m**ono**b**enzo-cycl**o**octyne, COMBO was prepared in 4 synthetic steps in 2 business days. This simple, non-fluorinated copper-free click reagent shows excellent reaction kinetics, which was further supported by theoretical calculations. The appending carboxylic function offers direct use for further conjugation to biomolecules or fluorescent labels. Its use in bioorthogonal labeling schemes was demonstrated on a COMBO-modified fluorescent label employed in glycan imaging of HeLa cells modified metabolically with azidosialic acid residues on its glycan structures.

Next, a series of novel hydrophilic trans cyclooctenes were prepared by chemical and photochemical routes. Some of these compounds display comparable or better kinetics than the commonly used TCO-OH. On these compounds stability and kinetic studies were performed and their applicability was demonstrated by bioorthogonal imaging experiments of PARP protein in HT1080 cells.

# Acknowledgments

I would like to thank Dr. Péter Kele and Dr. Scott A. Hilderbrand for their infinite patience and great number of corrections. I would also like to thank all the members of the “Lendület” Chemical Biology Research Group for their continuous help in practical matters. Furthermore I would like to thank my parents for their support. Special thanks is due to Kim Eunha and Krisztina Hegyi for the live cell imaging experiments, to Mihály Kállay for the computational data, to Szabolcs Béni for his assistance with the NMR experiments, Soma Vesztergom for the valuable discussions concerning kinetic measurements, and to the Szostak lab for the use of the stop flow system.

# Table of Contents

# List of Figures

# List of Schemes

# List of Tables

# List of Abbreviations

| | |
|---|---|
| $Ac_4ManAz$ | peracetylated mannose azide |
| CuAAC | copper catalysed azide-alkyne 1,3-dipolar cycloaddition |
| DCM | dichloromethane |
| Δ | heating |
| DMF | N,N-dimethylformamide |
| DMSO | dimetthyl sulfoxide |
| GC-MS | gas chomatograpy with mass spectrometry detection |
| HOMO | highest occupied molecular orbital |
| HRMS | high resolution mass spectrometry |
| HT1080 | a fibrosarcoma cell line |
| IR | infra red (light) |
| LUMO | lowest unoccupied molecular orbital |
| MS | mass spectrometry |
| NMR | Nuclear Magnetic Resonance |
| PBS | phosphate buffered saline |
| $R_f$ | retention factor |
| rt | room temperature |
| SPAAC | strain-promoted 1,3-dipolar azide-alkyne cycloaddition |
| $^t$Bu | tert buthyl |
| TCO | trans cyclooctene |
| TEA | triethyl amine |
| THF | tetrahydrofurane |
| TLC | thin layer chromatography |
| Ts | p-toluol-sulfonyl |
| UV | ultraviolet |

# 1.§. Introduction

Imaging techniques used to visualize subcellular structures and dynamic interactions of biomolecules play an increasing role in modern molecular biology. Until recently, the most prominent techniques were those based on green fluorescent protein (GFP) and its derivatives, the discovery for which the Nobel Prize was awarded in 2008. Although the merits of the GFP related discoveries and techniques are indisputable it cannot be used for imaging biomolecules that are not directly encoded in the genome (e.g. lipids, nucleotides, saccharides). Post-translational modifications of proteins are also impossible using GFPs. In such cases the use of exogenously delivered probes are the method of choice. It is crucial that these synthetic imaging agents do not alter the function, structure and fate of the labeled biomolecule and the chemical transformation used to covalently implement these probes to the target biomatter is chemoselective, high yielding and proceed within a reasonable time domain. At the same time neither the reagents nor the products are toxic. Chemical transformations meeting all these criteria were collected under the term bioorthogonal.

In other words, bioorthogonal functional groups are non-toxic, biologically inert (bio), and they react selectively and quasi quantitatively with their complementary function (orthogonal) at speeds comparable with that of biochemical reactions. Quite understandably, there are only a few reactions that can fulfill these very strict conditions.

Among bioorthogonal transformations probably the 1,3-dipolar cycloaddition of azides with cyclooctynes and the inverse electron demand Diels-Alder reaction of tetrazines and trans cyclooctenes are the most valuable ones.

The goal of our work was to make improvements to these two methods by developing new reagents. First this was accomplished by the introduction of a novel cyclooctyne termed COMBO, which displays good kinetics and has a relatively low lipophilicity compared to reactants within the same kinetic range. Then we aimed at synthetizing new trans cyclooctenes with low lipophilicity to minimize undesired non-specific secondary interactions with the cell membranes and other subcellular structures.

## 1.1.§. Bioorthogonal chemistry

The discovery of GFPs and their introduction to molecular biology research was a major breakthrough in modern biochemical research. On the one hand GFPs made it possible to localize proteins and to understand e.g. transport mechanisms or protein-protein interactions. On the other hand GFPs also contributed to the easier purification and molecular analysis of tagged proteins. GFP based methodologies have their limitations though. They cannot be used for tagging biomolecules that are not directly encoded in the genome. Such are lipids, nucleotides and saccharides, for example. These molecules are very important because of the role they play in signal transduction. Post-translational modifications of proteins is another limitation for the use of fluorescent proteins[1]. These limitations can be overcome by using bioconjugates of small synthetic probes. Bioconjugation is the process of linking two or more molecules of which at least one is a biomolecule. Reagents for bioconjugation should be stable in aqueous systems, and reactions need to be able to proceed in water. Furthermore, as biomolecules are present only in low concentrations, the reaction rates need to be exceptionally high in order to obtain the desired modifications within a reasonable time frame.

It is also crucial how these synthetic probes are introduced to the system of interest. In addition to the requirements for bioconjugation, such covalent modification of biomatter should involve non-toxic reactants and products, and just like reactions for bioconjugation in general, they should proceed at reasonable rates and high yields under physiological conditions (bio). Additionally, they should be free of any cross-reactivity with other functionalities (orthogonality), especially reactivity with naturally occurring functional groups. The structural perturbation caused by the artificial functional group must be minimal so that the target molecule's natural bioactivity is not altered to a significant degree.

Reactions meeting all these criteria are collected under the term bioorthogonal. It is a term used to broadly define any chemical reaction that can occur in a living system without interfering with any of the system's native biochemical processes[2]. Such transformations use chemically inert non-natural functional groups that are non-reactive, stable. They react, however, when interacting with their complementary bioorthogonal pair and so bioorthogonal ligations allows for the selective and controlled introduction of labels, in proteins as well as on cell-surfaces of living cells and even in live animals[3]. The

concept of bioorthogonality was introduced by Bertozzi in 2000[4]. It should be noted that it is an extension of the 'click chemistry' concept developed by Sharpless, The significance of bioorthogonal reactions lies in the possibility of covalently manipulating biomolecules under physiological conditions and in the ability to study biomolecules in their natural environment.

## 1.2.§. Bioorthogonal reactions

Bioorthogonal tagging schemes usually follow a two-step procedure. At first, the biomolecule in question is tagged with a so-called chemical reporter. Chemical reporters are defined as "non-native, non-perturbing chemical handles that can be modified in living systems through highly selective reactions with exogenously delivered probes". Chemical reporters can be introduced i) metabolically by using modified biomolecular bulding blocks, ii) chemically by taking advantage of unique and rare moieties with distinct chemical affinity, or iii) in case of proteins, by genetic encoding of bioorthogonalized amino acids. Following the introduction of the chemical reporters it is modified selectively with an exogenous probe harboring a complementary bioorthogonal function[1].

In the last decade the set of reactions that can be used as bioorthogonal was delineated and literally limited to a few transformations. Such reactions are: i) the so-called Staudinger ligation between azides and phosphanes, ii) the phototriggered cycloaddition of tetrazoles and alkenes, iii) the dipolar cycloaddition of alkynes and azides that can be either catalyzed by Cu(I)-salts or promoted by ring strain, and iv) the inverse electron demand Diels-Alder reactions of tetrazines and strained alkenes (**Scheme 1.**). Of these bioorthogonal reactions probably the strain-promoted azide-alkyne cycloaddition (SPAAC) of azides and cyclooctynes and the inverse electron demand Diels-Alder (iEDDA) reactions of tetrazines and cyclooctenes are the most valuable ones.

### 1.2.1.§. Reaction between tetrazoles and alkenes

From these four reaction schemes it is maybe the phototriggered cycloaddition of tetrazoles and alkenes (**Scheme 1.**, ii)) that is the least frequently used. The advantage of this reaction is that it makes it possible to control the spatial and time distribution of the reactive species. Especially noteworthy is the work of the Lin group, which examined the

1,3 dipolar cycloaddition reaction of O-allyl tyrosine and nitrile imines which are formed by in situ photodegradation of tetrazoles by 302 nm UV light. The reactivity with different double bonds depends on the nature of substituents on the tetrazole: selectivity to O-allyl tyrosine was achieved by a fine tuning of substituent effects[5].

Another remarkable feature of this reaction is that the products are fluorescent whilst the reactants not, enabling low-background fluorescent labeling schemes. As a further development of this method the Lin group designed such tetrazoles that undergo decomposition at higher wavelengths e.g. at 365 nm, so the damage caused by short wavelength irradiation could be minimized[6].

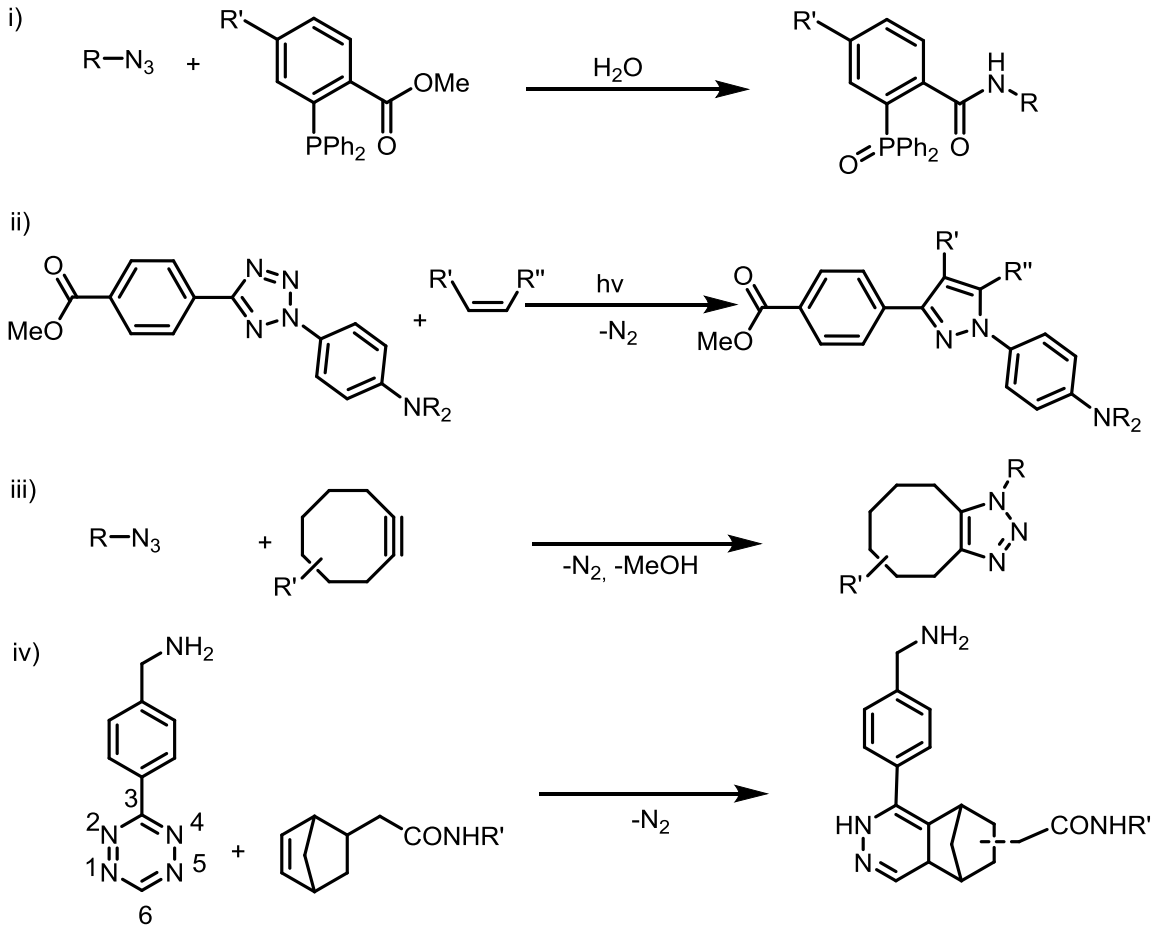


**Scheme 1. i) Staudinger ligation reaction between azides and phosphanes; ii) phototriggered cycloaddition of tetrazoles and alkenes; iii) dipolar cycloaddition of cyclooctynes and azides; iv) inverse electron demand Diels-Alder reactions of tetrazines and norbornenes.**

The phototriggered cycloaddition of tetrazoles and alkenes have found some limited application, but due to the fact that it necessitates the use of UV light it is far not as widespread as the use of azides in bioorthogonal reactions.

### 1.2.2.§. Azides in bioorthogonal reactions

The use of organic azides as most common reagents in bioorthogonal tagging schemes is due to the favorable characteristics of this functional group. Azides are small, highly energetic yet quite stable species. They react readily and selectively, however, with terminal alkynes or cyclooctynes (SPAAC) and phosphanes (Staudinger-ligation) even in the presence of several other functional groups in biological media. Also the azide moiety generally has only minimal effect on the structure of the substrate into which it is introduced[7].

The first azide employing bioorthogonal reaction is the Staudinger ligation (**Scheme 1, i)**) developed by the Bertozzi group. While it has proven to be a selective and efficient reaction, it is relatively slow and its reagents have limited shelf-stability due to the spontaneous oxidation of phosphanes[8].

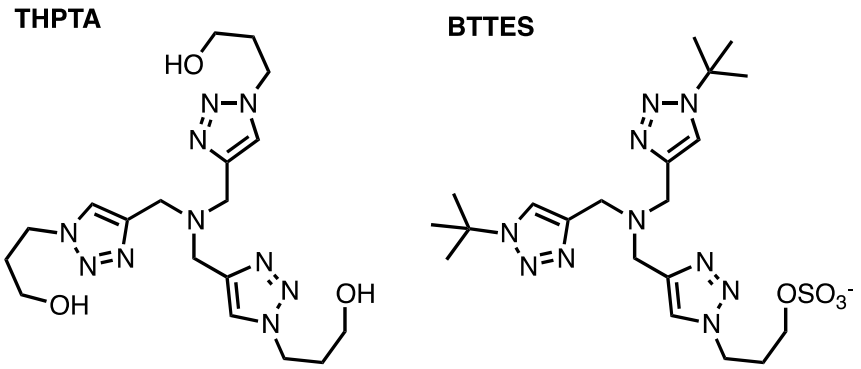


**Figure 1. TFPTA and BTTES: two ligands that diminish copper toxicity in in vivo experiments.**

Next the Cu(I)-catalyzed azide-alkyne cycloaddition was developed. While it has found wide application in chemical biology research, the required Cu(I)-catalyst is toxic to living systems[9]. A recent study by the Finn group shows that the addition of certain ligands significantly reduces the toxic effects and increases the reaction rates[10]. They also showed that the use of THPTA (**Figure 1.**) as a ligand in a 5:1 ratio compared to Cu(I) decreases copper toxicity to such a degree that all cell types tested survive and show consistent labeling using CuAAC[11]. A further improved ligand (BTTES, **Figure 1.**) introduced by the Wu group made CuAAC applicable for live zebrafish labeling[12]. While toxicity issues of Cu(I) can be overcome by the addition of ligands, bioorthogonal labeling without the need of a metal catalyst and additional ligands is preferred.

In bioorthogonal tagging schemes either the azide or the complementary terminal alkyne or cyclooctyne is introduced as part of the chemical reporter. The exogenous probe is then carrying the congeneric function. Typically the degree of metabolic incorporation of the azide labeled metabolites (e.g. sugars) into natural structures does not correspond to the degree of incorporation of the natural derivative. One example is the incorporation of peracetylated N-azidoacetylmannosamine ($Ac_4$ManNAz) into glycan structures of surface glycoproteins in forms of N-azidoacetyl sialic acid (SiaNAz). In other examples the alkyne is incorporated into the sialoglycan structure. In this latter case metabolic incorporation was found to be 25% more efficient compared to the azido-derivative[13]. Other examples use cyclooctynilated amino acids that are genetically encoded into target protein structures. These cyclooctyne motifs then can be targeted e.g. with azide bearing fluorogenic probes[14].

The SPAAC of simple cyclooctynes and azides is relatively slow (the second order rate constant is around $2 \times 10^{-3}$ $dm^3$ $mol^{-1}$ $s^{-1}$), so there was an increasing need to find ways to accelerate the reaction. This was first achieved by incorporating electron-withdrawing groups next to the triple bond such as the gem-difluoromethylene unit in DIFO (**Figure 2**.)[15]. This increases the second order rate constant some 20 fold (to around $4 \times 10^{-2}$ $dm^3$ $mol^{-1}$ $s^{-1}$) relative to cyclooctyne. This is due to polarizing the alkyne which in turn lowers the energy of its LUMO resulting in a lowered activation energy of the SPAAC.

Another way to increase reactivity is to increase ring strain in the core cyclooctyne. The C–C–C angle in cyclooctyne itself is ~155°. By introducing more strain this angle can be reduced further, causing the ground state to be more resembling the transition state geometry which leads to further increase in reactivity[16].

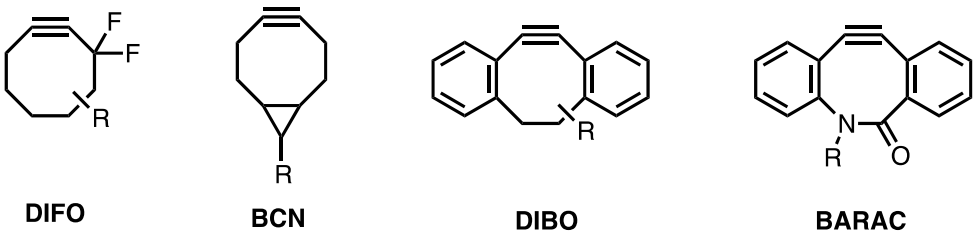


**Figure 2. Strategies to improve cyclooctyne reactivity: gem-difluoro group in DIFO, increased ring strain in BCN, DIBO and BARAC.**

A class of highly strained alkynes are the dibenzocyclooctynes. The Boons group

designed DIBO (**Figure 2.**) which contains two fused aryl rings in the cyclooctyne system. Aryl fusion enhances reactivity both by increased ring strain and conjugation. Cycloaddition of DIBO with benzyl azide gives a rate constant of $k_2 = 5.67 \times 10^{-2}$ $dm^3$ $mol^{-1}$ $s^{-1}$, a value very similar to that for DIFO, although this value was found in more polar methanol as opposed to acetonitrile[17].

Another way to increase ring strain in cyclooctynes was demonstrated by the work of van Delft et al[18]. They installed a cyclopropane ring in the cyclooctyne opposite to the triple bond (BCN, **Figure 2.**). The cyclopropane ring indeed increased ring strain which led to remarkable rate acceleration. The two isomers of BCN display rate constants of 0.11 $dm^3$ $mol^{-1}$ $s^{-1}$ for exo-BCN and 0.14 $dm^3$ $mol^{-1}$ $s^{-1}$ for endo-BCN.

Finally, the reaction rate could be further improved by incorporating an amide bond into the aryl fused system like in BARAC (**Figure 2.**). The extra strain increased the second order rate constant to 0.96 $dm^3$ $mol^{-1}$ $s^{-1}$ [19].

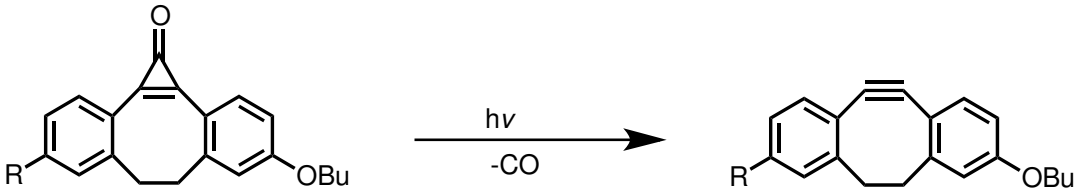


**Scheme 2. Formation of dibenzocyclooctyne from cyclopropenone.**

Cyclooctynes could also be prepared in photoinduced reaction from cyclopropanones (**Scheme 2.**). These cyclopropanones can undergo in situ decomposition by irradiating with 350 nm UV light in vivo[20].

While SPAAC found widespread applications, typical problems encountered include background labeling due to hydrophobic interactions with cell membranes and non-specific binding to serum proteins. Also the faster cyclooctynes like BCN are not shelf-stable or show cross-reactivity with thiols (BARAC and DIFO). Most cyclooctynes need to be prepared via lengthy and low yielding synthetic routes, thus making the routine use of cyclooctynes difficult[3].

### 1.2.3.§. Reaction of tetrazines with alkenes

In 2008 the inverse electron demand Diels-Alder reaction of tetrazines with ring strained cyclic alkenes was reported as a possible bioothogonal reaction using both disubstituted[21] and monosubstituted[22] tetrazines. One of the first reported reactions of this

kind that were used in molecular imaging employed a norbornene and a non-symmetrical benzylamino tetrazine derivative (**Scheme 1. , iv**)), but reaction kinetics was still relatively slow, although much faster than the SPAAC of azides with cyclooctynes. Later, the reaction of trans-cyclooctenol (TCO-OH) with benzylamino tetrazine was reported (**Scheme 3.**)[23]. This led to an increase in reactivity by one order of magnitude.

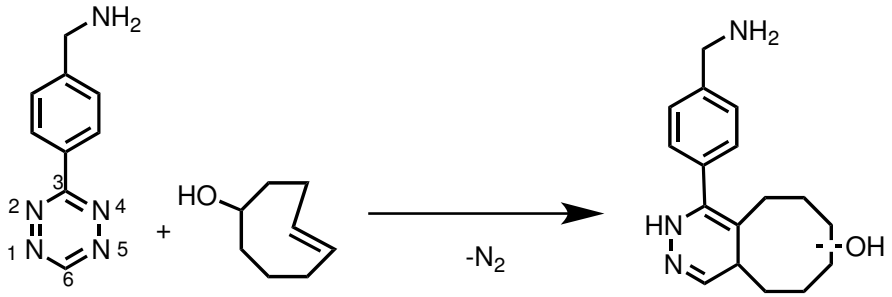


**Scheme 3. Reaction of benzylamino tetrazine with TCO-OH.**

The biggest benefit of the cyclooctene - benzylamino tetrazine based ligation is that it is 4 orders of magnitude faster than most of the other bioorthogonal reactions used. Also by the use of tetrazines it is possible to devise so-called turn on probes[24].

### 1.2.4.§. Mutually orthogonal reaction pairs

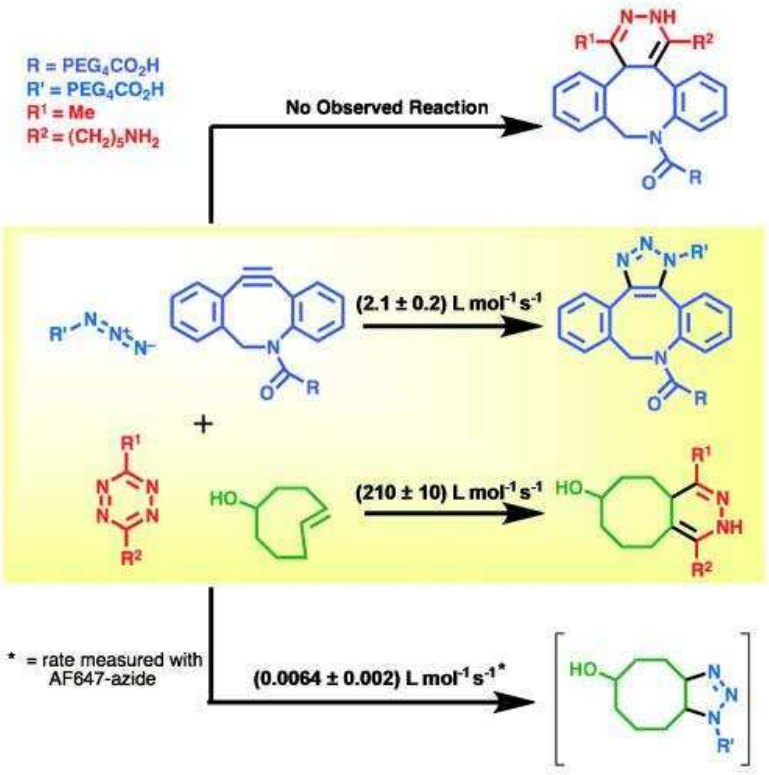


**Figure 3. Mutually orthogonal reaction pairs[25].**

One of the most appealing features of tetrazine - cyclooctene iEDDA and SPAAC click chemistry is that it is possible to design such reaction pairs that the two types of reactions be mutually orthogonal. Typically cyclooctynes can undergo both iEDDA and SPAAC and these two reactions cannot be performed simultaneously unless the steric properties of the cyclooctyne make it virtually unreactive towards tetrazines. Such systems include DIBO like compounds having fused benzene rings as cyclooctynes and unsymmetrical methyl tetrazines (**Figure 3.**)[25]. According to DFT (density functional theory) calculations the reduced reaction rate of tetrazines and dibenzocyclooctyne is due to the significantly raised distortion energy necessary to attain the first transition state in iEDDA reactions[26].

## 1.3.§. Reaction mechanisms

### 1.3.1.§. The mechanism of 1,3-dipolar cycloadditions

In the 1,3-dipolar cycloaddition a 4 electron system reacts with a 2 electron system. However, in this case the 4 electrons are part of a three atomic framework. Nitrones, nitrile-oxides and azides are all examples for such 1,3-dipolar systems (**Figure 4.**).

**Figure 4. Some selected 1,3-dipoles.**

These can react with dipolarophiles, for example with alkenes or alkynes. Azides react with terminal alkynes, but since they are not very reactive this reaction needs a copper (I) catalyst.

There is literature evidence that it is not the frontier molecular orbital (FMO) interactions or reaction thermodynamics, but rather the differences in the energy ($\Delta E_d^{\ddagger}$) required to distort the 1,3-dipole and the dipolarophile during the transition state (TS) that controls the barrier heights for different 1,3-dipoles [27]. Activation, distortion and interaction energies for cycloaddition of an azide with an alkyne are shown in **Figure 5.**

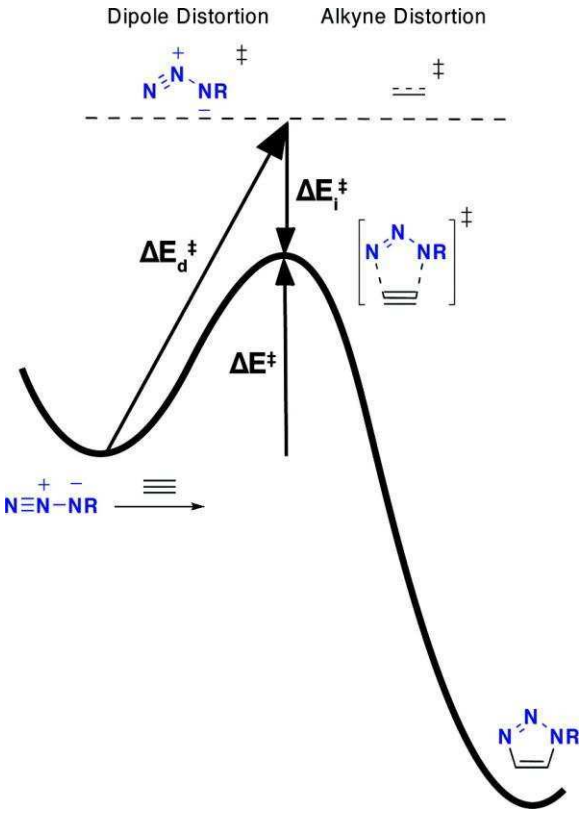


**Figure 5. Activation, distortion and interaction energies for cycloaddition of an azide with an alkyne[27].**

The B3LYP transition structures (**Figure 6.**) are concerted and nearly synchronous, with only minor preference for C-N bond formation with the unsubstituted nitrogen dipole. The cyclooctyne transition structures are slightly earlier with longer forming C-N bond lengths and larger N-N-N dipole when compared to the acetylene transition structure.

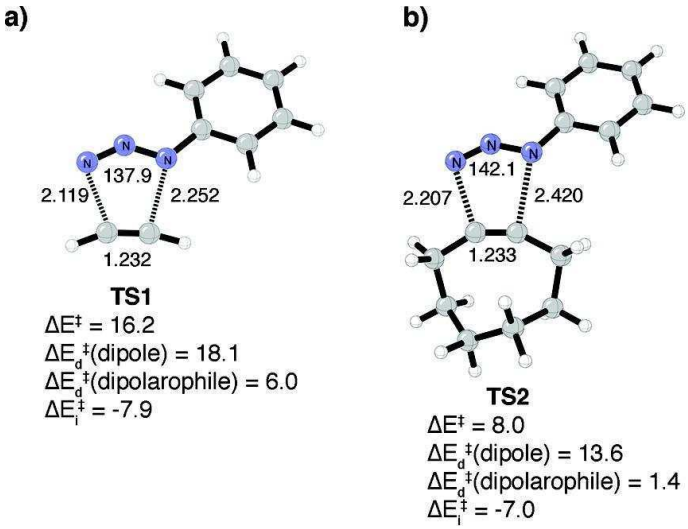


**Figure 6. Transition stuctures for the reactions of a) acetylene and b) cyclooctene with azide[27].**

Also the transition structure of phenyl azide + acetylene (**TS1)** has the azide N-N-N angle distorted to 138° from its ground state angle of 173°, while for the transition state involving cyclooctyne (**TS2)** the N-N-N angle only distorts to 142°. As for the triple bond, the linear H-C-C angles of acetylene bends to 158° and 166° in the transition state (**TS1**). Cyclooctyne is already more bent in the ground state with C-C-C angles of 153° and 155°.

In **TS1** there is a large barrier because there is a 24.1 kcal/mol distortion energy penalty to deform phenyl azide and acetylene into their transition state geometries. The interaction energy of -7.9 kcal/mol (a sum of all electrostatic, charge-transfer, and repulsion interactions) lowers the barrier height to 16.2 kcal/mol.

In the transition state for cycloocytne (**TS2**) only 1.4 kcal/ mol of alkyne distortion energy is required; this is 4.6 kcal/mol less than observed for acetylene. The distortion energy of phenyl azide in the TS involving cyclooctyne decreases by 4.5 kcal/mol compared to acetylene due to the earlier transition state of this reaction. It is primarily these two contributions that further decrease the barrier to 8.0 kcal/mol for the reaction of cyclooctyne and azide[27].

### 1.3.2.§. The mechanism of Diels-Alder reactions

The Diels-Alder (DA) reaction represents a special case of [4+2] cycloadditions. Two main types of DA reaction are distinguished: normal and inverse electron demand Diels-Alder reactions. The reaction partners in both cases involve a conjugated diene and an alkene or alkyne. The diene can be open chained (**Scheme 4.**) or cyclic (**Scheme 5.**) with

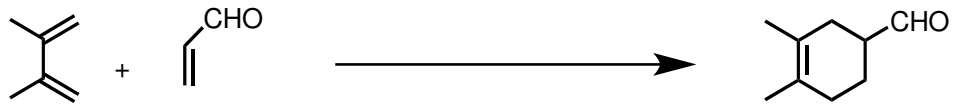


**Scheme 4. Reaction of open chained diene in Diels-Alder reaction.**

the only criterion that it must be able to take the necessary s-cis conformation. In the case of open chained dienes this is always possible, though the s-trans conformation is more stable. Those dienes that can assume only the s-trans conformation cannot undergo Diels-Alder reactions.

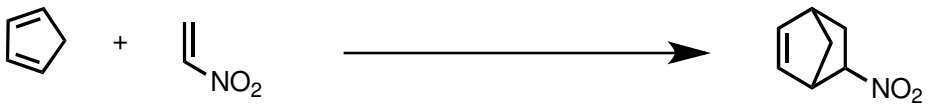


**Scheme 5. Reaction of cyclic diene in Diels-Alder reaction.**

In the case of normal electron demand Diels-Alder reaction the reactivity is improved if the dienophile is electron deficient so bears electron withdrawing substituents conjugated to the double or triple bond. Simple alkenes react with dienes only to a negligible degree. Conjugated carbonyl, nitrile, nitro or sulfon groups containing alkenes and aril-alkenes, vinyl ethers, vinyl esters, haloalkenes, on the other hand, are good dienophiles.

The reaction proceeds in a stereospecific manner. The stereochemistry of the starting alkene is reflected in the product: cis and trans dienophiles give the two diastereomers of the same product. A classic example for this is the reaction between maleic and fumarates with cis butadiene (**Scheme 6.**).

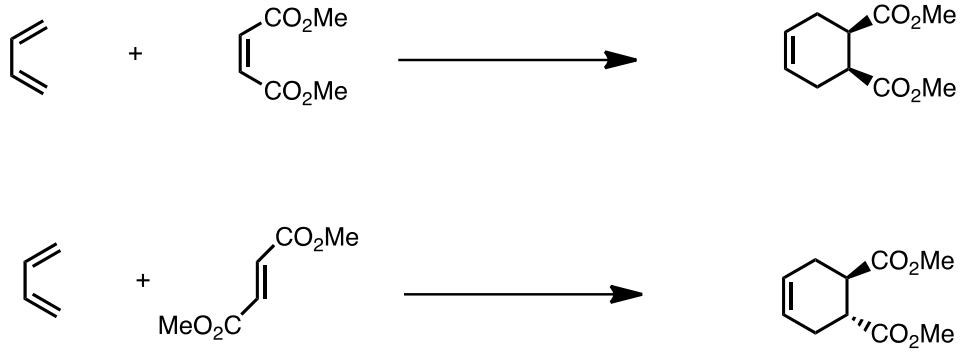


**Scheme 6. Reaction of butadiene with maleic and fumaric esters.**

It can be seen immediately that the relative stereochemistry of the ester groups in the starting material keep their relative position in the product. The reason for this becomes clear when examining the molecular orbitals of the starting materials (**Figure 7**.).

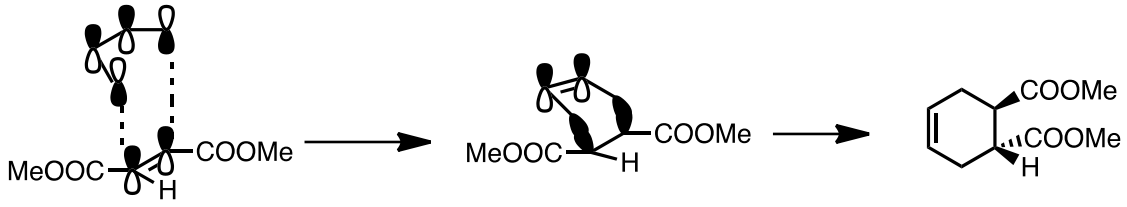


**Figure 7. Interaction of molecular orbitals in DA.**

According to frontier orbital theory[28], because of symmetry reasons, an overlap is

necessary between the frontier molecular orbitals of the diene and the dienophile (**Figure 8.**) in a way that minimizes the energy difference between the interacting molecular


**Figure 8. Overlap between the frontier molecular orbitals of the diene and the dienophile in a Diels-Alder reaction.**

orbitals (**Figure 9.**). This makes the difference between the neutral, the normal electron demand and the inverse electron demand Diels-Alder reactions. In the neutral Diels–Alder reactions the difference between the HOMO and LUMO of both reactants is similar. In the normal electron demand Diels-Alder reaction the relatively high energy HOMO of the electron rich diene interacts with the relatively low energy LUMO of the electron deficient dienophile, because there is a reduced $HOMO_{diene}$–$LUMO_{dienophile}$ separation (compared to the $HOMO_{dienophile}$–$LUMO_{diene}$ separation) which dominates the reactivity.

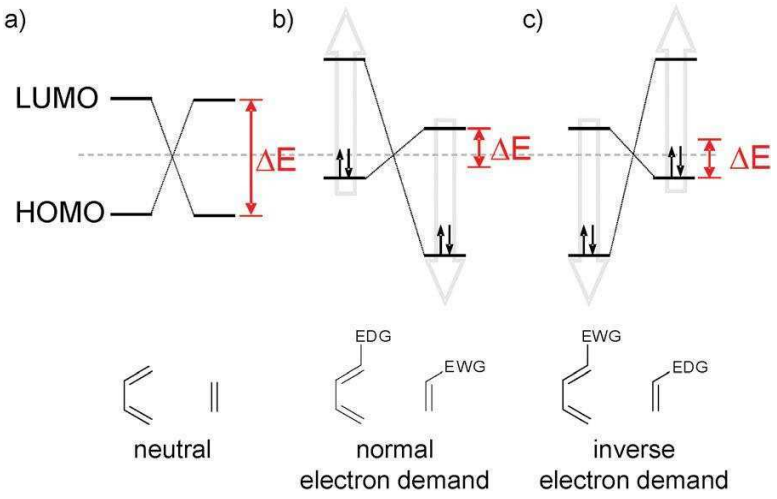


**Figure 9. The neutral, the normal electron demand and the inverse electron demand reactions[29].**

On the contrary in the inverse electron demand Diels-Alder reaction the relatively low energy LUMO of the electron deficient diene interacts with the relatively high energy HOMO of the electron rich dienophile, so that these reactions are governed by the $HOMO_{dienophile}$–$LUMO_{diene}$ gap[30].

### 1.3.3.§. The inverse electron demand reactions of tetrazines

The highly electron deficient tetrazines are excellent reaction partners in inverse electron demand Diels-Alder reactions especially if they contain electron withdrawing substituents. Like many other Diels–Alder reactions, the reaction of tetrazines with dienophiles is a concerted reaction and is characterized by second-order kinetics. The reaction seems to proceed in two steps. An initial [4+2] cycloaddition between tetrazine as diene and the olefin as dienophile is the rate determining step. The reaction presumably goes through a dinitrogen-bridged adduct which is transformed immediately to a 4,5-dihydro-pyridazine when the reaction partner was an alkene or to a pyridazine when the reaction partner was an alkyne by loss of nitrogen (**Scheme 7.**)[31]. The 4,5-dihydro-pyridazine can undergo a subsequent 1,3-prototropic isomerization leading to the corresponding 1,4-dihydro-isomer.

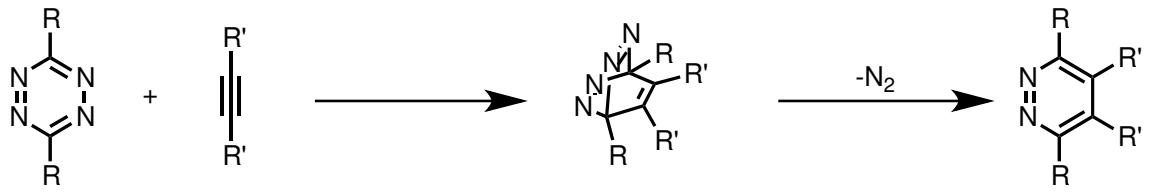


**Scheme 7. Reaction of tetrazines with dienophiles**

As Sauer showed[32, 33, 34], the reactivity depends to a great degree on the substituents of the dienophile, namely the reaction is much faster if the double or triple bond bears an electron donating substituent which raises the HOMO of the dienophile. On the tetrazine side, in general, electron-withdrawing substituents at 3- and 6-positions of the tetrazine lower the LUMO of the diene and thus accelerate iEDDA while electron- donating substituents cause the reaction rates to be slower[28]. Reactivity greatly depends also on the distortion energy needed to reach the transition state geometry and so steric effects play a central role. Sterically demanding substituents on both reaction partners raise the distortion energy[26] needed to attain the transition state. On the other hand, ring strain of the dienophile accelerates iEDDA reactions by reducing the activation energy both by a raising the $HOMO_{dienophile}$ and reducing the distortion energy. For this reason norbornenes or cyclooctynes and cyclooctenes show a great acceleration when compared to open chain alkenes or alkynes.

Sauer has also shown that as a result of these steric effects only one substituent

containing unsymmetric tetrazines react up to three orders of magnitude faster than their symmetric analogs[35]. This means that by the choice of the right reagents the second order rate constant can change up 9 orders of magnitude[36]. Also it is of practical importance that the iEDDA reaction of tetrazines show a significant acceleration in aqueous media[37].

## 1.4.§. Goals

The goal of our research was to develop new cyclooctynes with improved reactivity in SPAAC by introducing additional ring strain in a fused ring system without the need for two benzene rings on the one hand and to develop less lipophilic trans cyclooctenes that also display better kinetics than the parent TCO-OH on the other hand. To reach this latter aim we planned to introduce additional strain by incorporating polar atoms into the cyclooctene ring or polar substituents onto the cyclooctene scaffold. These aimed structures are summarized in **Figure 10.**

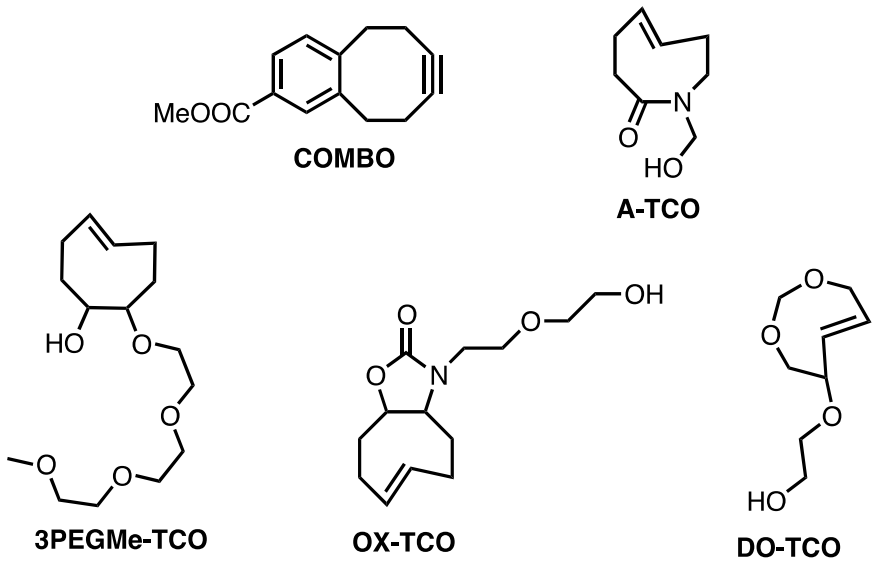


**Figure 10. The new monobenzo-cyclooctyne (COMBO) and new hydrophilic trans-cyclooctenes**

# 2.§. Results and discussion

## 2.1.§. Synthesis and properties of COMBO

Since the introductory use of cyclooctynes as bioorthogonally usable reagents, a series of cyclooctyne derivatives were developed as reagents that enable implementation of chemical reporters or labels by means of SPAAC (**Figure 11.**). The rationale for the development of strained alkynes is to develop reagents with faster reaction kinetics to bring the SPAAC reaction speed comparable to its copper mediated version. There are two major approaches that increase the reactivity of cyclooctynes towards azides. Either the energy of the LUMO of the alkyne is lowered by strongly electron withdrawing groups, typically by gem-difluoro substituents α to the alkyne (e.g. DIFO, DIFBO, **Figure 7.**) or the ring-strain is increased further (DIBO, BARAC, BCN, **Figure 11.)**[15, 18, 19, 38, 39]

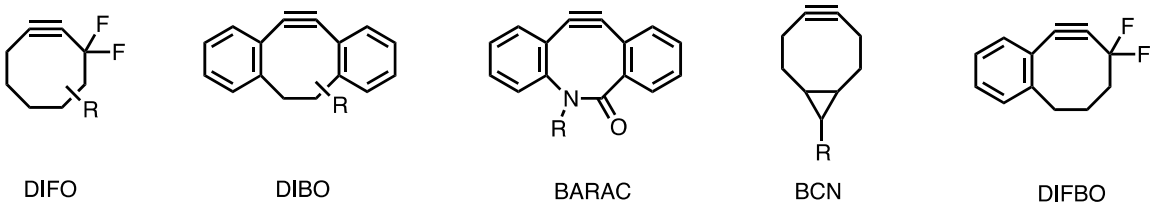


**Figure 11. Cyclooctyne based reagents.**

Very recently, Bertozzi and co-workers have published their results with gem-difluoro benzocyclooctyne with aryl fusion at the 3-4 position of the cycloalkyne ring (DIFBO, **Figure 11.**)[4]. Although fast reaction rates were observed with this reagent, it was also prone to undergo a fast and spontaneous homo-trimerization process due to the presence of the gem-difluoro substituents.

### 2.1.1.§. Synthesis of COMBO

Trying to keep the balance between activity and stability, our interest turned to monobenzocyclooctynes with aryl fusion at the 5-6 positions of the cyclooctyne as a recent theoretical investigation by Goddard et al. suggested that such regioisomers of monobenzocyclooctynes could be excellent reagents[40]. It is noteworthy that the ring strain in these monobenzocyclooctynes is predicted to be comparable to that of dibenzocyclooctynes while the $A^{1,3}$ strain - a problem that compromises the reactivity of

dibenzocyclooctynes[40] - is lowered during the cycloaddition process, thus possibly leading to cyclooctynes with lowered energies of activation in SPAAC with respect to dibenzocyclooctynes (**Figure 12.** and **Figure 13.**).

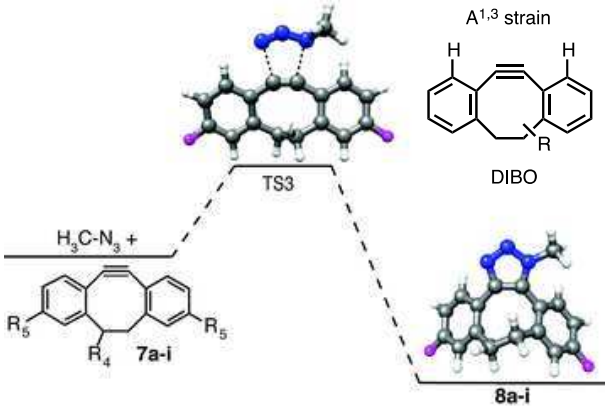


| Reactant | $R_5$ | $\Delta E^{\ddagger}$ | $\Delta G^{\ddagger}$ |
|---|---|---|---|
| **7a** | $NH_2$ | 12.2 | 25.5 |
| **7b** | OMe | 11.6 | 24.9 |
| **7c** | OEt | 11.7 | 25.1 |
| **7d** | $N(CH_3)_2$ | 12.2 | 25.7 |
| **7e** | H | 12.3 | 25.5 |
| **7f** | F | 11.8 | 25.2 |
| **7g** | Cl | 11.7 | 25.0 |
| **7h** | $NO_2$ | 11.2 | 25.1 |
| **7i** | CN | 11.3 | 24.7 |

**Figure 12. Transition state structures and activation barriers for different DIBO derivatives[6].**

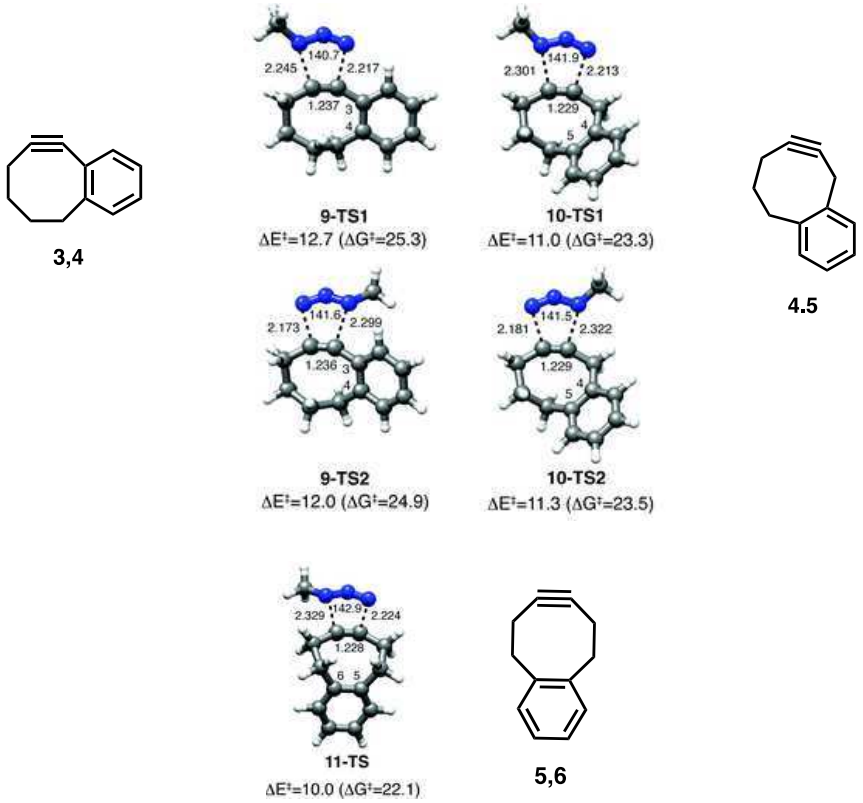


**Figure 13. Transition state structures and calculated activation energies for azide-benzocyclooctyne cycloaddition[6].**

The study of Goddard et al. suggested that the regioisomer having the 5,6 ring fusion holds promise to be a powerful copper free click reagent.

Based on these studies, we decided to synthetize 5,6,9,10-tetrahydro-7,8-dehydro-benzocyclooctene, a novel cyclooctyne having considerable ring strain and lacking $A^{1,3}$ strain during reaction with azides. First, we looked for easily accessible precursors of this highly reactive cyclooctyne (**Figure 14.**) based on our knowledge of previously applied reaction routes towards cyclooctynes.

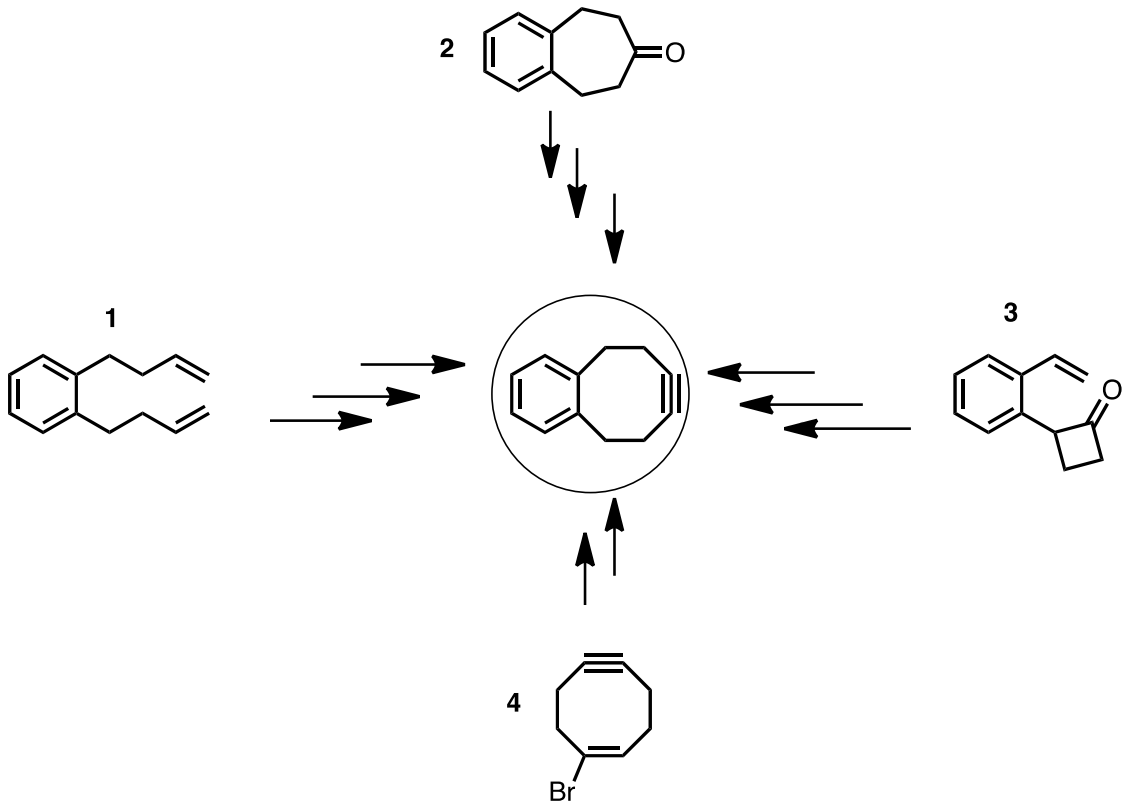


**Figure 14. Possible precursors for 5,6,9,10-tetrahydro-7,8-dehydro-benzocyclo-octene.**

Common problems encountered in former synthetic routes of cyclooctynes were the large number of reaction steps. Moreover, these schemes are often based on the use of unique techniques or harsh reaction conditions during the synthesis, thus leading to less reliable procedures with relatively low yields. Our goal was to devise synthetic routes that employ widely used techniques and mild reaction conditions, especially in the last step of synthesis.

In reference to 5-6 aryl fused cyclooctynes Krebs and Meier et al. noted this regioisomer thermally unstable and in their works only the more stable 3-4 benzannulated regioisomer was achieved in poor yields[41]. We believe that the reason for their results is lying behind harsh conditions (e.g. 190 °C) applied when forming the alkyne moiety.

Therefore we sought for classical chemical transformations that allow mild conditions without the need for expensive and sensitive reagents.

We have identified 1,2-di(but-3-en-1-yl)benzene (**1**), 8,9-dihydro-5H-benzo[7] annulen-7(6H)-one (**2**) and 2-(2-vinylphenyl)cyclobutanone (**3**) as possible precursors (**Figure 14.**). The basic assumption in our retrosynthetic analysis was that first we prepare 5,6,9,10-tetrahydro-benzocyclooctene (**6, Scheme 8., route a**), or 5,6,9,10-tetrahydro-benzo-[8]annulen-7(8*H*)-one (**8, Scheme 8., route** *c*) or its C-TMS analog 8-(trimethyl silyl)-5,6,9,10-tetrahydrobenzo [8]annulen-7(8H)-one, which we hoped to prepare from a known benzosuberone (**7, Scheme 8., route b),** as the key precursors of the cyclooctyne. The preparation of these intermediates would have followed established literature procedures for 5,6,9,10-tetrahydrobenzo[8]annulen-7(8*H*)-one (**8**)[42] or literature analogies for 5,6,9,10-tetrahydro-benzocyclooctene (**6**)[43] and 8-(trimethylsilyl)-5,6,9,10-tetrahydro-benzo[8] annulen-7(8H)-one[4].

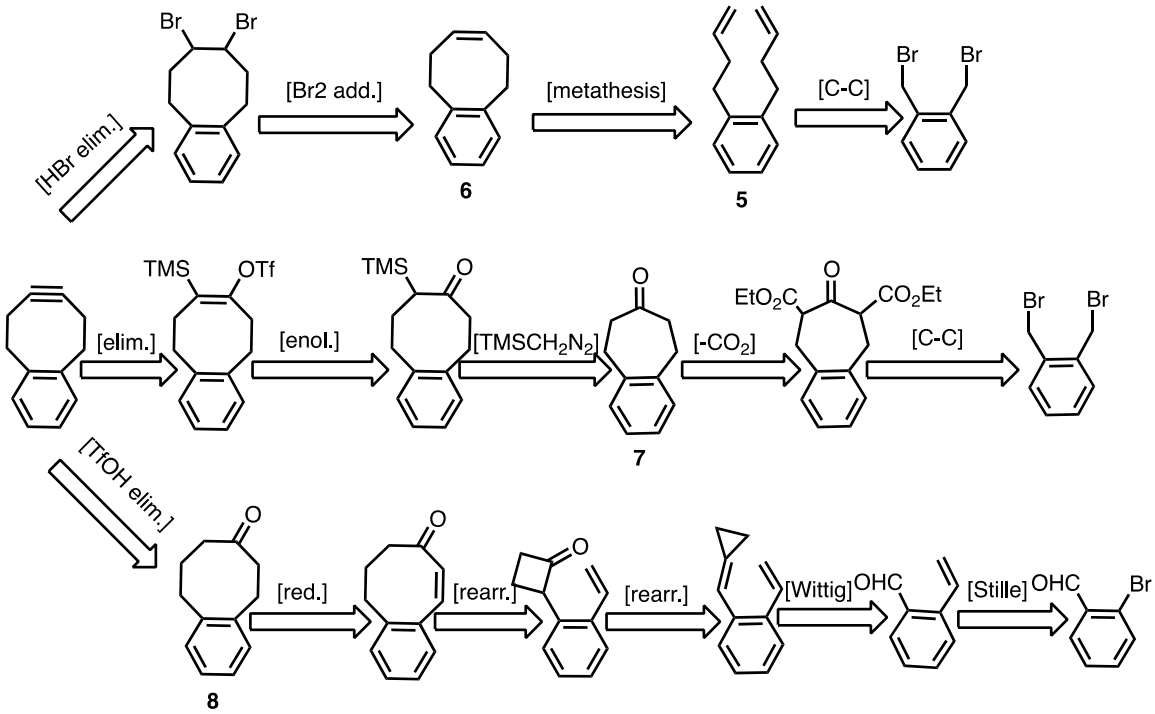


**Scheme 8. Retrosynthetic analysis for the synthesis of 5,6,9,10-tetrahydro-7,8-dehydro-benzocyclooctene routes a, b and c.**

For the ring closing metathesis (RCM) of 1,2-di(but-3-en-1-yl)benzene (**5**) we used 1 mM substrate in the presence of 10 mol% Grubbs II catalyst in refluxing dichloro

methane. However, the reaction did not lead to the desired 5,6,9,10-tetrahydro-benzocyclooctene **(6),** but rather oligomers of the starting material were obtained.

We prepared 8,9-dihydro-5H-benzo[7]annulen-7(6H)-one (**7**) following a literature procedure and attempted ring expansion using $TMSCH_2N_2$. The reaction furnished some 5,6,9,10-tetrahydrobenzo[8]annulen-7(8*H*)-one **(8)** alongside with unidentified byproducts instead of the desired 8-(trimethylsilyl)-5,6,9,10-tetrahydrobenzo[8]annulen-7(8H)-one. The preparation of larger quantities of 5,6,9,10-tetrahydrobenzo[8]annulen-7(8*H*)-one **(8)** proceeded smoothly as described in the literature[8], but attempts to prepare the enol-triflate and to eliminate TfOH have failed.

We recognized that these attempts were unsuccessful presumably because of high activation barriers when we tried to introduce a double bond into the fused cyclooctane-benzene ring system. So we looked for alternative reaction routes in which strain is introduced at an earlier stage. We have devised a route where the synthesis of carboxymethyl-monobenzocyclooctyne, COMBO (2-methoxycarbonyl-5,6,9,10-tetra-hydro-7,8-dehydro-benzocyclooctene) was aimed. It is noteworthy that COMBO lacks fluorine substituents and carry a carboxylic function that allows for further modification (**Scheme 9.**). The reaction scheme includes key intermediate (E)-1-bromocyclooct-1-en-5-yne (**12**)[10],which was hoped to react smoothly with electron deficient dienes in an inverse electron demand Dield-Alder (IEDDA) reaction.

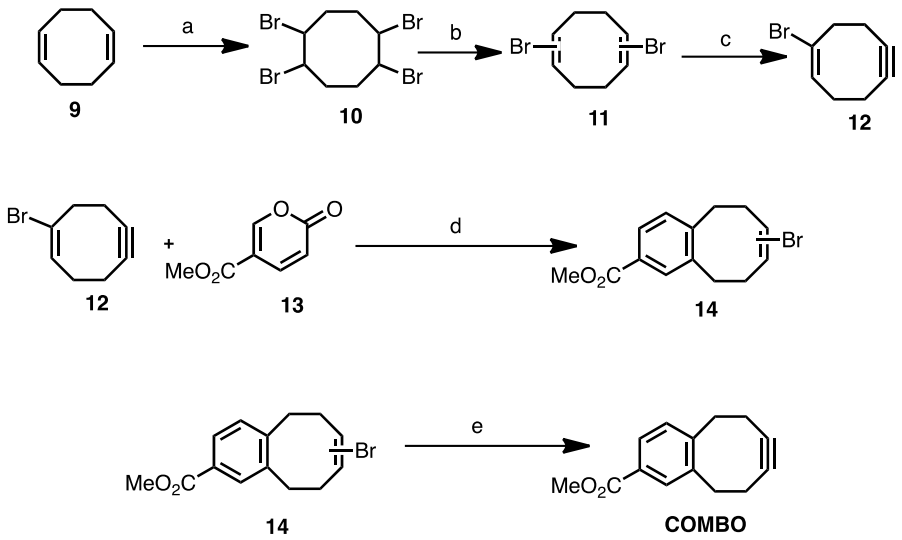


**Scheme 9. Synthesis of carboxy-monobenzocyclooctyne. a) $Br_2$, $CH_2Cl_2$, 0 °C, 85%; b) tBuOK, $Et_2O$, r.t., 83%; c) tBuOK, 18-crown-6 ether, hexane, r.t. d) r.t. 36% for two steps; e) tBuOK, 18-crown-6 ether, hexane, 58 °C, 47%.**

The synthesis started from commercially available 1,5-cyclooctadiene (**9**) that was tetrabrominated in the first step to give **10**. Partial elimination using tBuOK at room

temperature resulted in bis-vinyl-bromide, **11** that was subjected to further elimination using the same base in the presence of 18-crown-6 ether in hexane resulting in eneyne **12**[44]. The key step in the synthetic routine was the formation of the fused ring system with the possibility of incorporating a function that allows further conjugation. Therefore we have chosen commercially available methyl-coumalate, **13** an electron deficient diene that can be a possible reaction partner for eneyne **12**[45]. To our delight, the inverse electron demand Diels-Alder reaction took place chemoselectively affording bromo-benzocyclooctene, **14**. Modularity of the synthetic routine at this point allows for the introduction of other aryl rings by applying different dienes, e.g. further 2H-pyran-2-ones, tetrazines etc. to access a variety of monoarylcyclooctynes. The resulting bromo-benzocyclooctene was directly used in the next step. Formation of the cyclooctyne by means of HBr elimination was brought about by treatment with tBuOK in the presence of 18-crown-6 ether, which afforded carboxymethyl-monobenzocyclooctyne, COMBO in reasonable yields. Hydrolysis under strongly basic conditions at 30 °C for 2 h, followed by acidic work up gave COMBO-acid in 92 % yield indicating that the benzocyclooctyne moiety is stable under these conditions.

### 2.1.2.§. Investigation of the stability of COMBO

We have further investigated the stability of COMBO by monitoring its $^1$H NMR spectra under various conditions: (25±0.1) °C in $CD_3CN$:$D_2O$ 3:1 v/v for 44 h (**Figure 15.**), then at (37±0.1) °C in $CD_3CN$ for 9 h (**Figure 16.**). A potential background reaction with a biologically relevant reagent was studied at (25±0.1) °C in $CD_3CN$:$D_2O$ 1:1 v/v with three-fold molar excess of glutathione (15 mM COMBO and 45 mM glutathione) for 14 h (**Figure 17.**).

While there was no significant change in $CD_3CN$:$D_2O$ 3:1 v/v after 44 h (ca. 5% decomposition), approximately 9% of COMBO reacted in the presence of glutathione after 14 h. We observed considerable decomposition (ca. 30% after 9 h) of COMBO in acetonitrile at 37 °C, but interestingly no decomposition in the first two hours of the experiment.

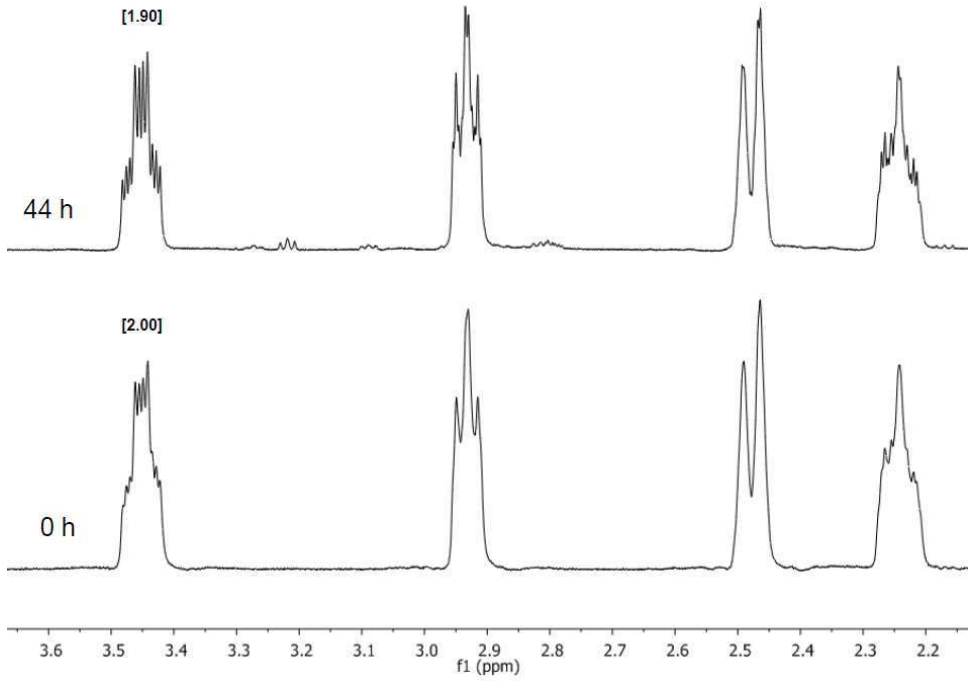


**Figure 15. Aliphatic region of the $^{1}$H-NMR spectra of COMBO in $CD_3CN$: $D_2O$ 3:1 v/v at 25 °C at preset time intervals (numbers in brackets correspond to integral values).**

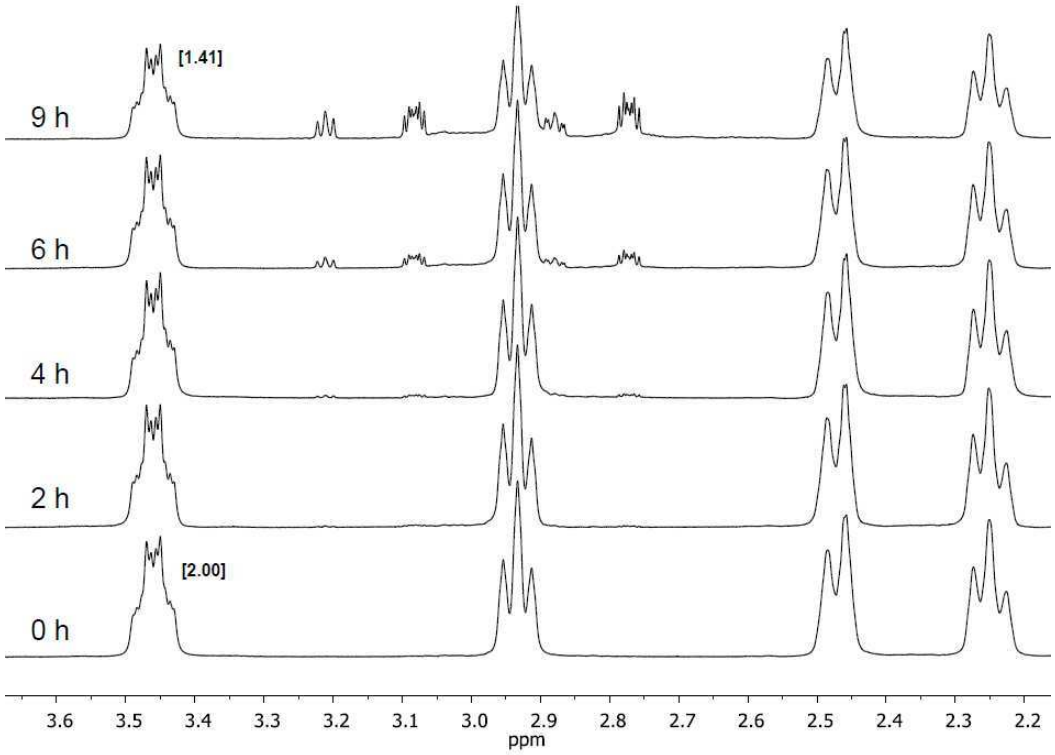


**Figure 16. Aliphatic region of the $^{1}$H-NMR spectra of COMBO in $CD_3CN$ at 37 °C at preset time intervals (numbers in brackets correspond to integral values).**

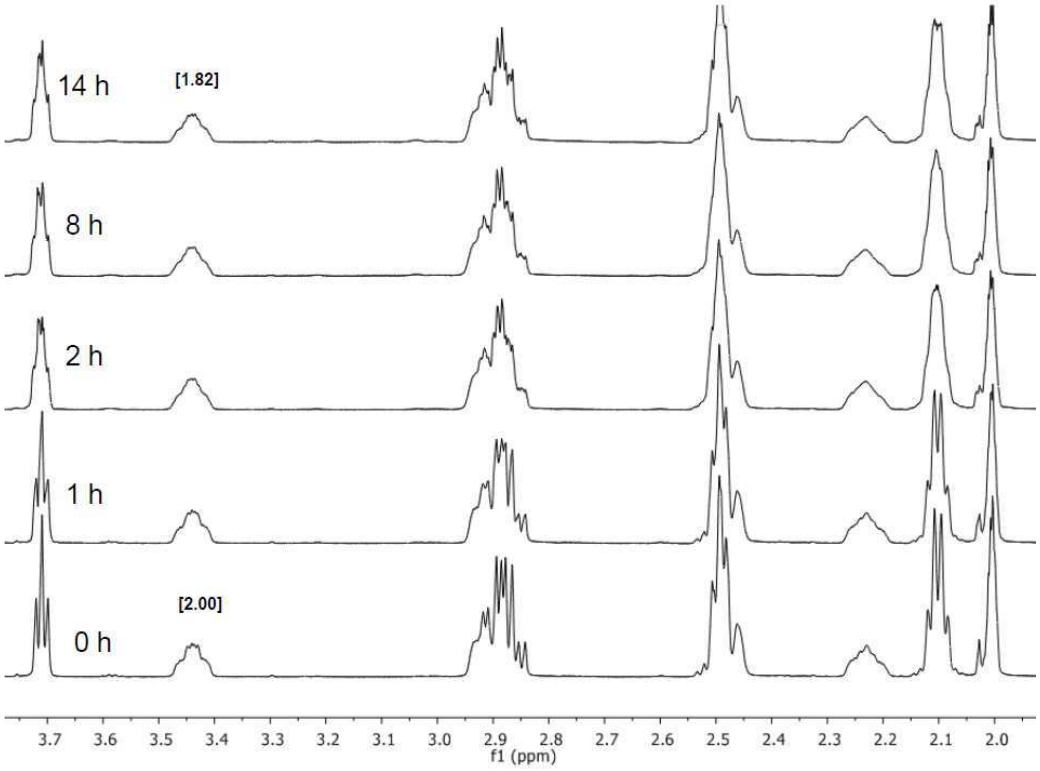


**Figure 17. Aliphatic region of the $^1$H-NMR spectra of COMBO / glutathione in $CD_3CN$: $D_2O$ 1:1 v/v at 25 °C at preset time intervals (numbers in brackets correspond to integral values).**

### 2.1.3.§. Kinetic measurements

Next, we elaborated the reactivity of COMBO towards azides. For this, benzyl azide (**15**) was used as a model reaction partner in strain-promoted azide-alkyne cycloaddition reactions. As expected, the only products formed were the ca. 1:1 mixture of triazol regioisomers (compounds **16** on **Scheme 10.**). We measured kinetics both in $CD_3CN$ and in $CD_3CN$:$D_2O$ 4:3 v/v at 25 °C.

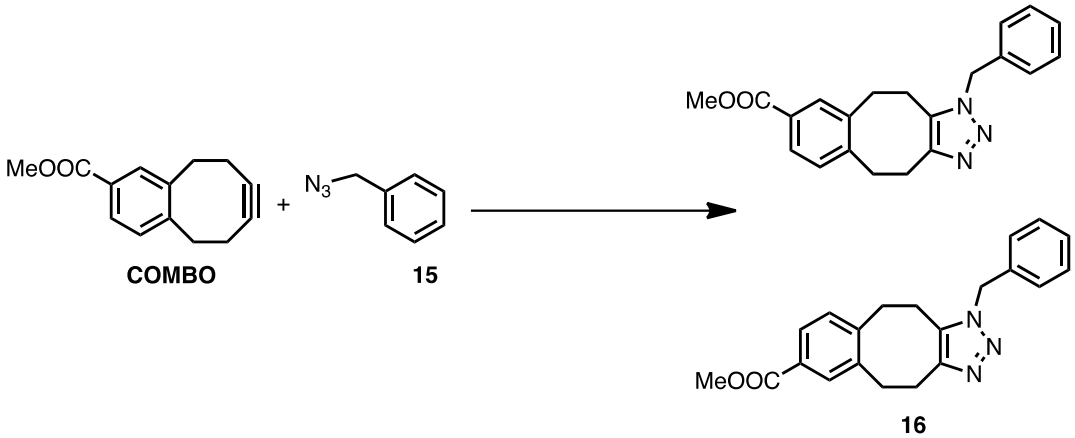


**Scheme 10. The cycloaddition of COMBO and benzyl azide.**

### 2.1.3.1.§. Cycloaddition of COMBO with benzyl azide in $CD_3CN$ at 25 °C

For the $^1$H-NMR monitoring of cycloaddition of COMBO with benzyl azide, stock solutions of COMBO and benzyl-azide were prepared (64 mM each). Aliquots of these solutions were loaded to an NMR tube, mixed thoroughly using vortex and then inserted into a 600 MHz Varian NMR spectrometer immediately. The accuracy of the loadings was checked by integration (see **Figure 18.**). Spectra were measured at 25±0,1 °C over 15 minutes at preset time-intervals (Δt=18,9 s). Experiments were performed in triplicate

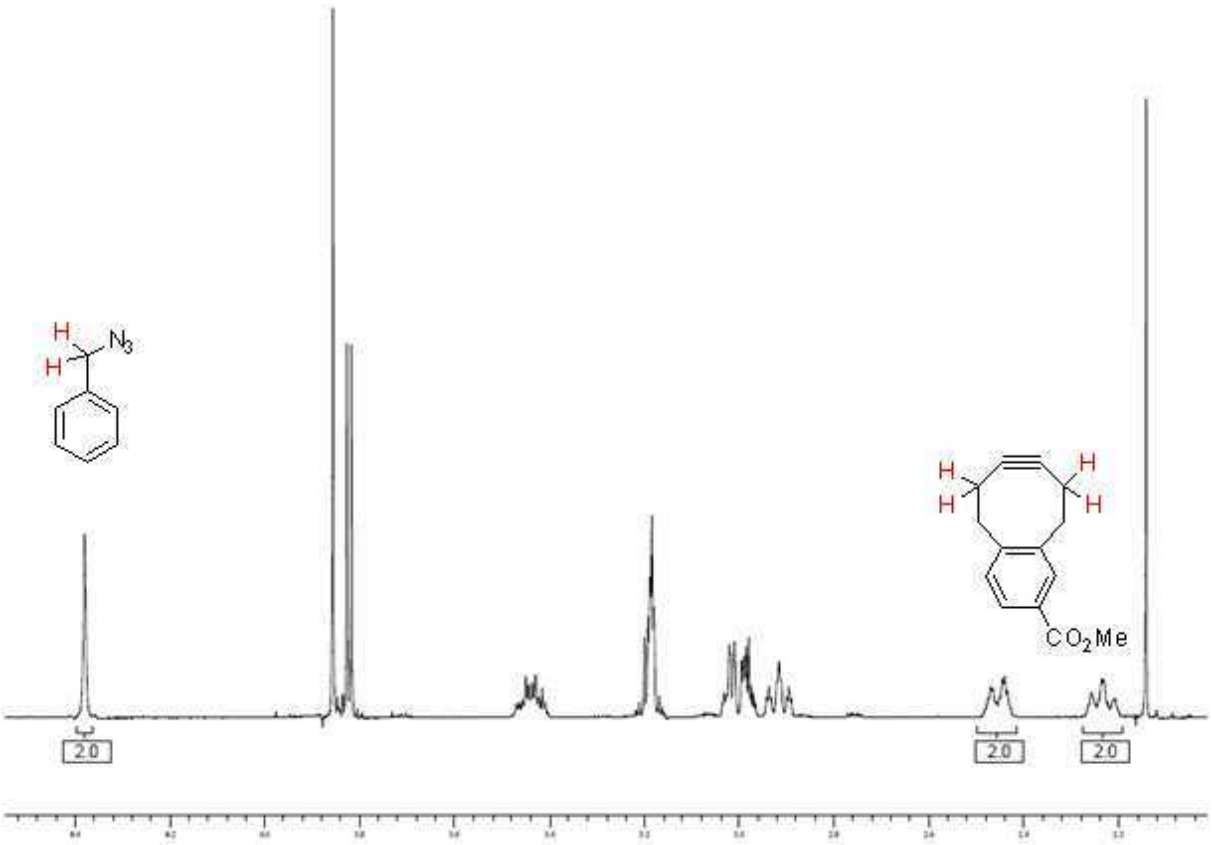


**Figure 18. Integrals for designated protons of benzyl azide and COMBO at 0 min of the measurements in $CD_3CN$.**

For the determination of the second order rate constants the change in the peak-integral of the benzyl azide methylene protons was followed. We plotted both $\frac{1}{c}$ and $c$ versus time (see **Figure 19.**) and the second order rate constants $k_2$ were determined using equations $\frac{1}{c} - \frac{1}{c_0} = k_2 \times t$ and, $c = \frac{1}{c_0^{-1} + k_2 \times t}$ respectively, where $c_0$ is the concentration of benzyl-azide at the beginning of the measurements and t denotes time. The rate constants were determined using the first 21 measurement points by non-weighted fit in all cases.

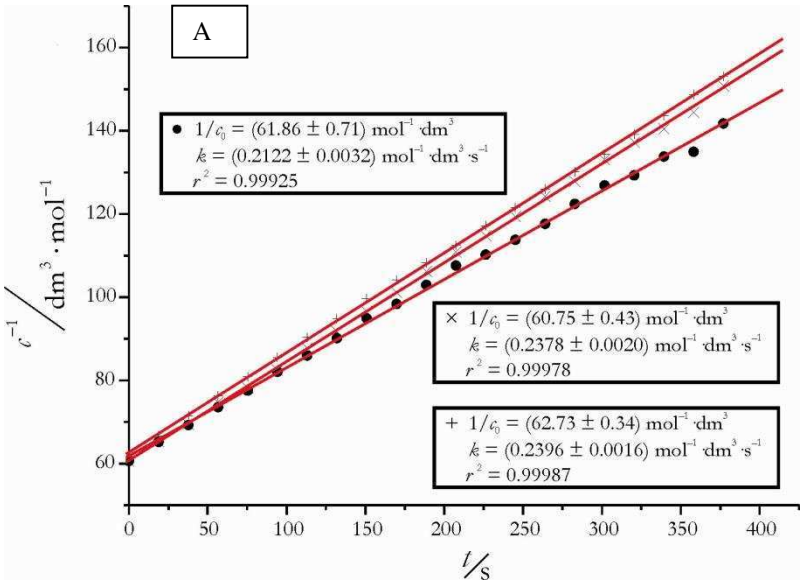


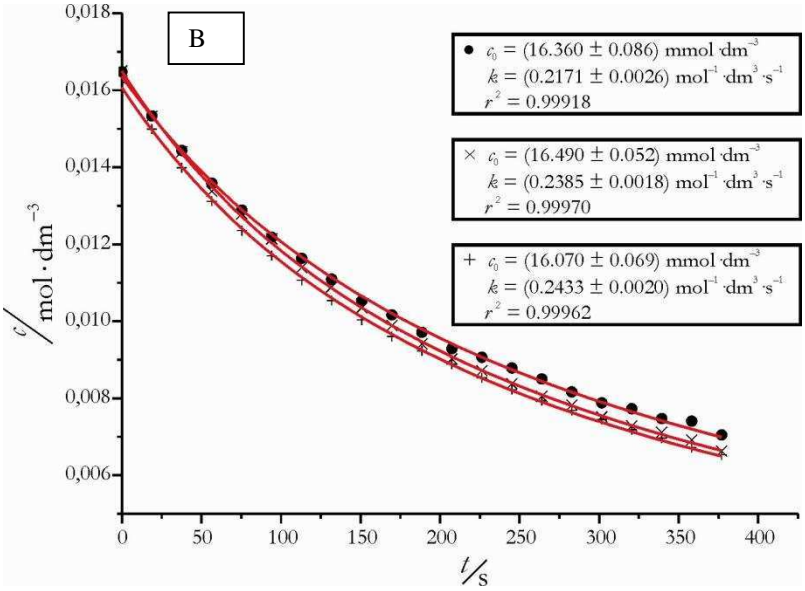


**Figure 19. Linear (A) and non-linear (B) rate plots for the cycloaddition of COMBO with benzyl azide in $CD_3CN$.**

When determining the average value of the rate constant we used the reciprocal of the error of individual values as weighting factor, thus taking the values with smaller errors with bigger factors. Denoting the individual values of $k_2$ as $k_{2_i}$ and the individual errors as $\delta_i$ the weighted average is:

$$k_2 = \frac{\sum_3^{i=1} \frac{1}{\delta_i} * k_i}{\sum_3^{i=1} \frac{1}{\delta_i}} \quad \text{and the error is:} \quad error = \sqrt{\sum_{i=1}^{3} \left(\frac{\partial k_2}{\partial \delta_i} \delta_i\right)^2}$$

$k_{2(linear)} = (0.233 \pm 0.006)\ \mathrm{dm^3 \cdot mol^{-1} \cdot s^{-1}}$

$k_{2(nonlinear)} = (0.235 \pm 0.006)\ \mathrm{dm^3 \cdot mol^{-1} \cdot s^{-1}}$

**2.1.3.2.§.Cycloaddition of COMBO with benzyl azide in $CD_3CN$:$D_2O$ 4:3 v/v at 25 °C**

For the $^1$H-NMR monitoring of cycloaddition of COMBO with benzyl azide in acetonitrile:water mixture, stock solutions of COMBO (47 mM in $CD_3CN$:$D_2O$ 4:3 v/v) and benzyl-azide (63 mM in $CD_3CN$:$D_2O$ 4:3 v/v) were prepared. 400 µl of COMBO solution and 300 µl of the benzyl-azide solution were loaded into an NMR tube, mixed thoroughly using vortex and then inserted into a 600 MHz Varian NMR spectrometer immediately. The accuracy of the loadings was checked by integration (see **Figure 20.**). Spectra were measured at 25±0,1 °C over 10 minutes at preset time-intervals (Δt=13,3 s). Experiments were performed in triplicate.

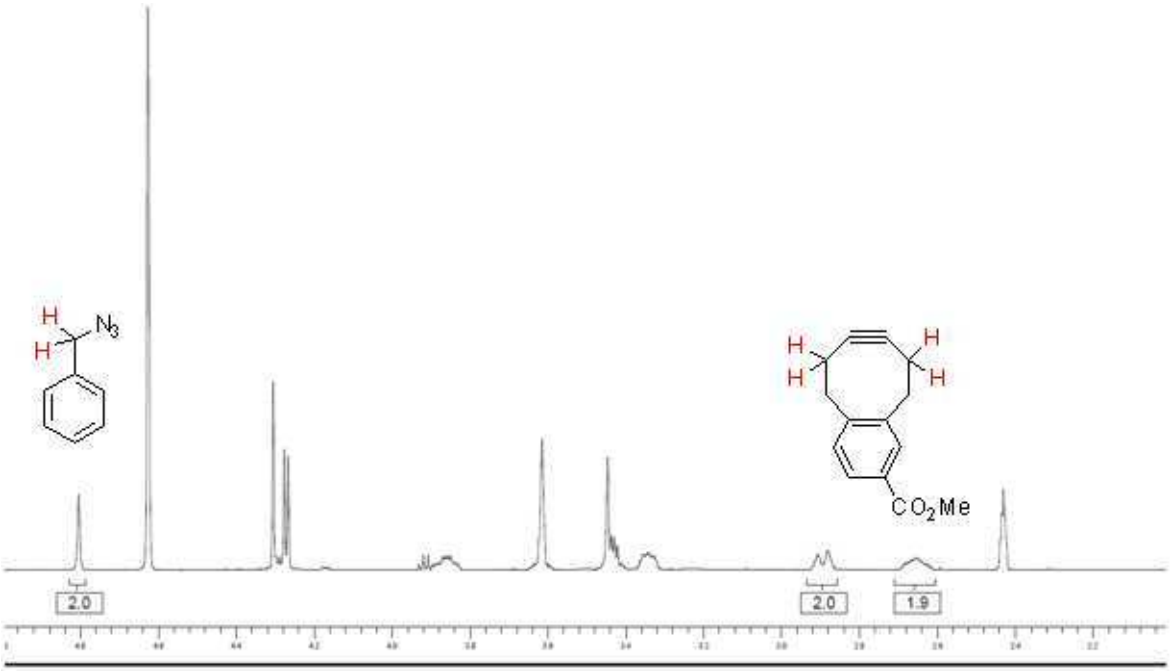


**Figure 20. Integrals for designated protons of benzyl azide and COMBO at 0 min in $CD_3CN$:$D_2O$ 4:3 v/v**

The determination of the second order rate constants proceeded the same as described above, using the first 13 measurement points (**Figure 21.**).

$k_{2(linear)} = (0.768 \pm 0.008)\ \mathrm{dm^3 \cdot mol^{-1} \cdot s^{-1}}$

$k_{2(nonlinear)} = (0.795 \pm 0.007)\ \mathrm{dm^3 \cdot mol^{-1} \cdot s^{-1}}$

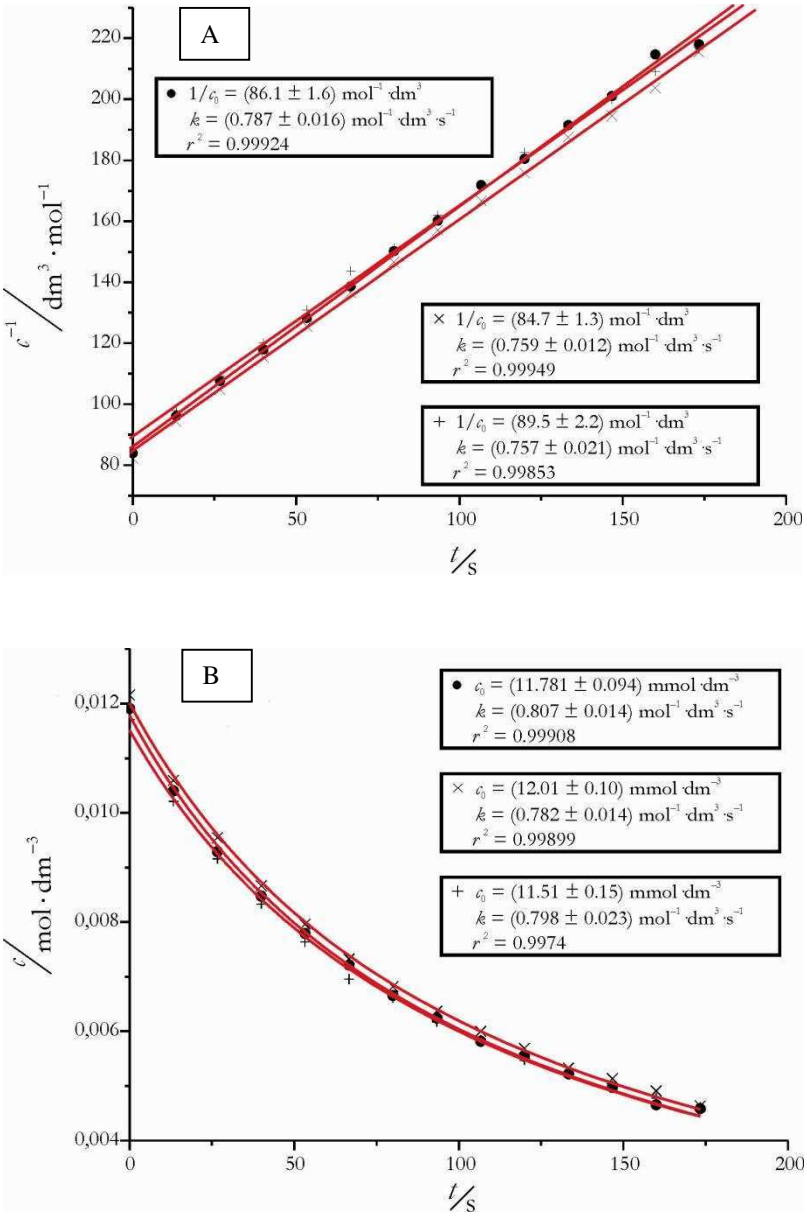


**Figure 21. Linear (A) and non-linear (B) rate plots for the cycloaddition of COMBO with benzyl azide in $CD_3CN$:$D_2O$ 4:3 v/v.**

The results have indicated a second order rate constant of $k_2$ = (0.235 ± 0.006) $M^{-1}s^{-1}$ in acetonitrile, which is quite similar to that of the fluorinated regioisomer, DIFBO[39]. As expected, the rate constant was even larger in a more polar medium ($k_2$ = 0.795 ± 0.007 $M^{-1}s^{-1}$ in water-acetonitrile 3:4 v/v). In comparison with DIFO[1] and DIBO[38], COMBO showed ca. 3 and 5 times faster reaction rates. Direct comparison with BCN[3] is not possible, as kinetic data in acetonitrile were not reported for this reagent, however, the fact that BCN shows comparable kinetics only in a much more polar medium implies the superior reactivity of COMBO (**Table 1.**). The only reported reagent showing better reactivity than COMBO is the biarylazacyclooctynone, BARAC[5]. However, the smaller

size and direct conjugability of COMBO together with its much lower lipophilicity due to the presence of only one aromatic ring ($^c$logP values are 1.9 and 4.5 for COMBO and BARAC, respectively) justify the use of COMBO as an alternative to BARAC.

**Table 1. Second order rate constants ($k_2$/ $M^{-1}s^{-1}$) of cyclooctynes**

| DIFBO | DIFO | BARAC | DIBO | BCN(endo/exo) | COMBO |
|---|---|---|---|---|---|
| 0.22[a] | 0.08[a] | 0.96[a] | 0.05[a] | 0.14 / 0.11[b] | 0.24[a] |
| | | | | 0.29 / 0.19[c] | 0.80[d] |

[a] acetonitrile [b] water:acetonitrile (1:3 v/v)
[c] water:acetonitrile (2:1 v/v) [d] water:acetonitrile (3:4 v/v)

### 2.1.4.§. Computational studies

As gem-diluorinated compounds usually show increased reactivity relative to their non-fluorinated derivatives, we were surprised to see that the reaction rates for DIFBO and COMBO were yet comparable. To explain the experimentally observed reaction rates we carried out density functional theory (DFT) calculations for the cycloadditions of methyl azide with DIFBO and COMBO using the B3LYP functional as well as the 6-311++G** basis set implemented in the Gaussian 03 suite[46]. The geometries for the reactants and transition states were optimized, and the activation barriers ($\Delta E^{\ddagger}$) and Gibbs energies of activation ($\Delta G^{\ddagger}$) were computed. The basis set superposition error was corrected by the counterpoise method. We note that similar procedures have been successfully employed for the cycloaddition of azides with alkynes and expected to have an error of less than 2 kcal/mol for the corresponding barrier heights[27, 47,] The lowest-energy transition-state structures for DIFBO and COMBO are displayed in **Figure 22.**, where the calculated $\Delta E^{\ddagger}$ and $\Delta G^{\ddagger}$ values are also presented (for more details see the Appendix). The barrier heights support the slightly increased reactivity of COMBO with respect to DIFBO. It is instructive to inspect the reason for this somewhat unexpected finding. It was demonstrated in previous studies that the reactivity of cyclooctynes is mainly controlled by two factors: the gap of the frontier molecular orbitals (FMOs) and the strain of the cyclooctyne ring[1,13]. The energies of the FMOs are influenced by several factors: the presence of the fluorine substituents and the phenyl ring as well as the hyperconjugation between the π-orbitals of the triple-bond and the σ-orbitals of the cyclooctyne ring (see Appendix). The HOMO and LUMO are lower in energy for DIFBO than those for COMBO, while the resulting FMO gap is somewhat narrower for COMBO.

As of the ring strain, we can conclude that, in contrast to DIFBO, the equilibrium structure of COMBO is slightly more bent and closer to the transition-state of the reaction. The narrower FMO gap and the less distortion energy required to achieve the transition state are presumably the main reasons for the lower barrier height of COMBO.

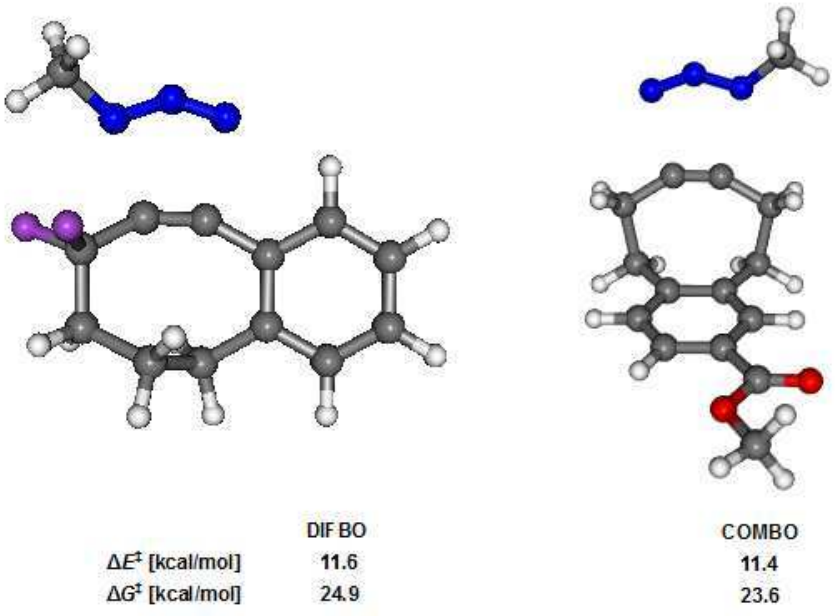


**Figure 22. Lowest-energy transition-state structures and barrier heights for DIFBO and COMBO.**

### 2.1.5.§. Lipophilicity – reactivity relationship of cyclooctyne derivatives

Basic features determine whether a reactant is suitable for bioconjugation are reactivity, selectivity and tendency for non-specific binding. First, high reactivity is necessary for applications under the highly dilute conditions tipically used in vivo. Second, any bioorthogonal ligation becomes unsuitable for in vivo use if cross-reactivity with naturally occurring functionality is present or if there is lipophilic, non-specific binding to proteins or membranes. For example, lipophilic binding to blood albumins followed by irreversible covalent attachment seems to be responsible for the considerable difference between in vitro and in vivo characteristics of some cyclooctynes[48]. During in vitro control experiments, covalent reaction with thiol-containing proteins may also occur[17]. The most reactive cyclooctynes reported in the literutere are DIBO, DIBAC and BARAC, all three containing two aromatic rings (**Figure 23.**)

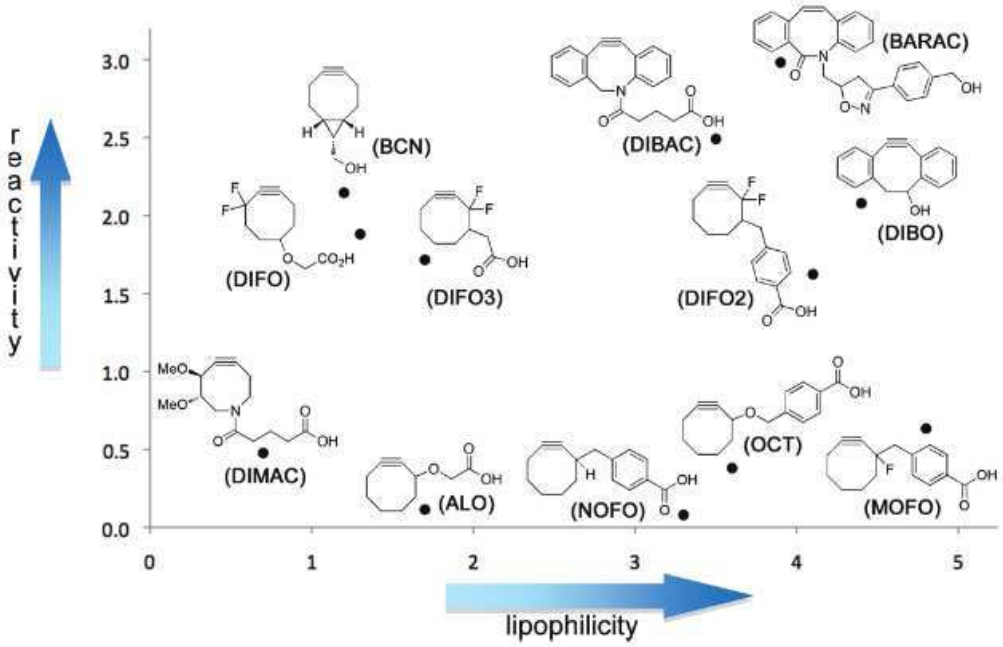


**Figure 23. Reaction rate (-log($k_2$∗$10^3$)) vs. lipophilicity ($^c$LogP) for cyclooctynes reported in the literature[49].**

Aromatic rings increase the lipophilicity (see **Figure 23.**) and the chance to engage in hydrophobic interactions with membranes and proteins. This makes COMBO with its sole aromatic ring even more appealing. We have seen that its reactivity is reasonably close to BARAC, while it is expected to be much less lipophilic.

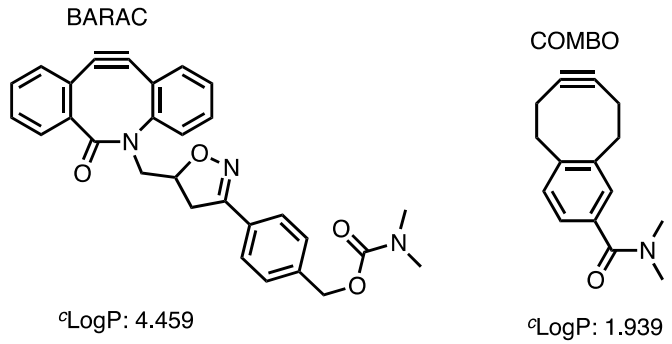


**Figure 24. $^c$LogP values of the N-methylamide derivatives of COMBO and BARAC**

$^c$LogP values were calculated using BioByte (embedded in ChemDraw Ultra 12) for the N-methylamide derivative of both COMBO and BARAC and indeed COMBO proved to be much less lipophilic (**Figure 24.**)

### 2.1.6.§. Labeling of azido-glycoproteins on Cells and Imaging by Fluorescence Microscopy

Next, we wanted to see the applicability of fluorescently tagged COMBO reagents in live cell staining experiments. For this, COMBO-acid was conjugated to a fluorescein-piperazine derivative[50] by means of amide bond formation to furnish COMBO-Flu.

First we have examined the dose dependency of COMBO-Flu reagent on U937 cells that were modified metabolically with azidosialic acid on their surface glycans. The dose-dependence of COMBO-Flu was assessed using flow cytometry (FACS) on U937 cells. Results have shown that COMBO-Flu staining of cells was efficient in the micromolar range too (**Figure 25**). These results suggest that COMBO-based fluorescent stains are useful reagents for live cell and real-time imaging purposes.

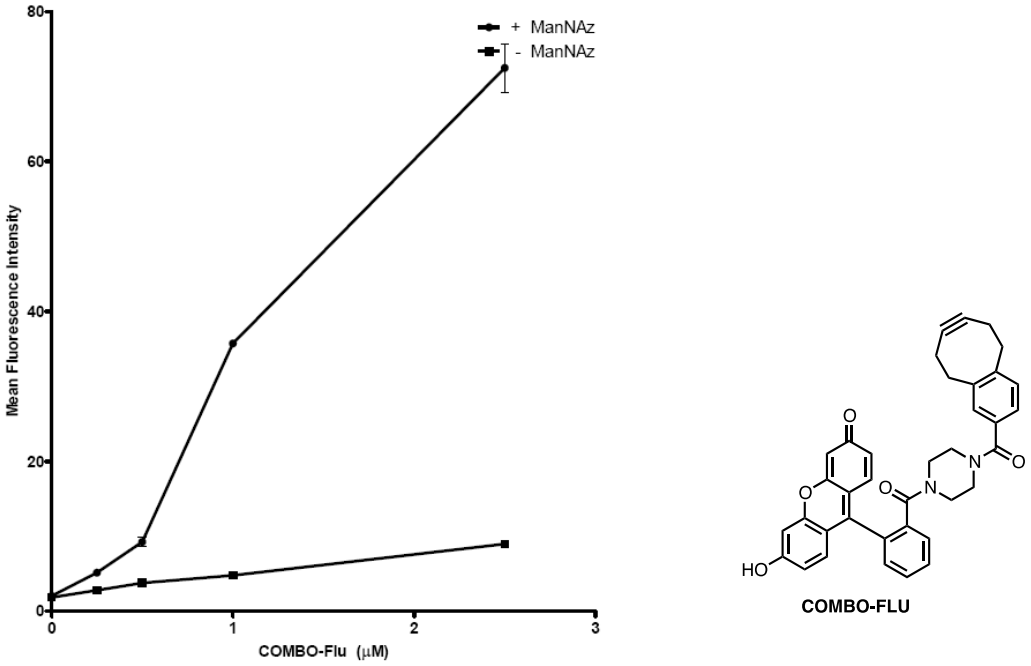


**Figure 25. The structure of COMBO-FLU and dose-dependence of COMBO-Flu staining. U937 cells with or without azido glycans were stained with different concentrations of COMBO-Flu and measured by FACS..**

Live cell imaging was performed on HeLa cells also metabolically modified with $Ac_4$ManNAz on their glycan structures (see the experimental part)[11]. The cells incorporate $Ac_4$ManNAz and express it as azidosialic acid in their glycoproteins at the trans-Golgi network, which are then targeted mainly to the plasmamembrane. The as-modified cells were stained with 12.5 µM COMBO-Flu.

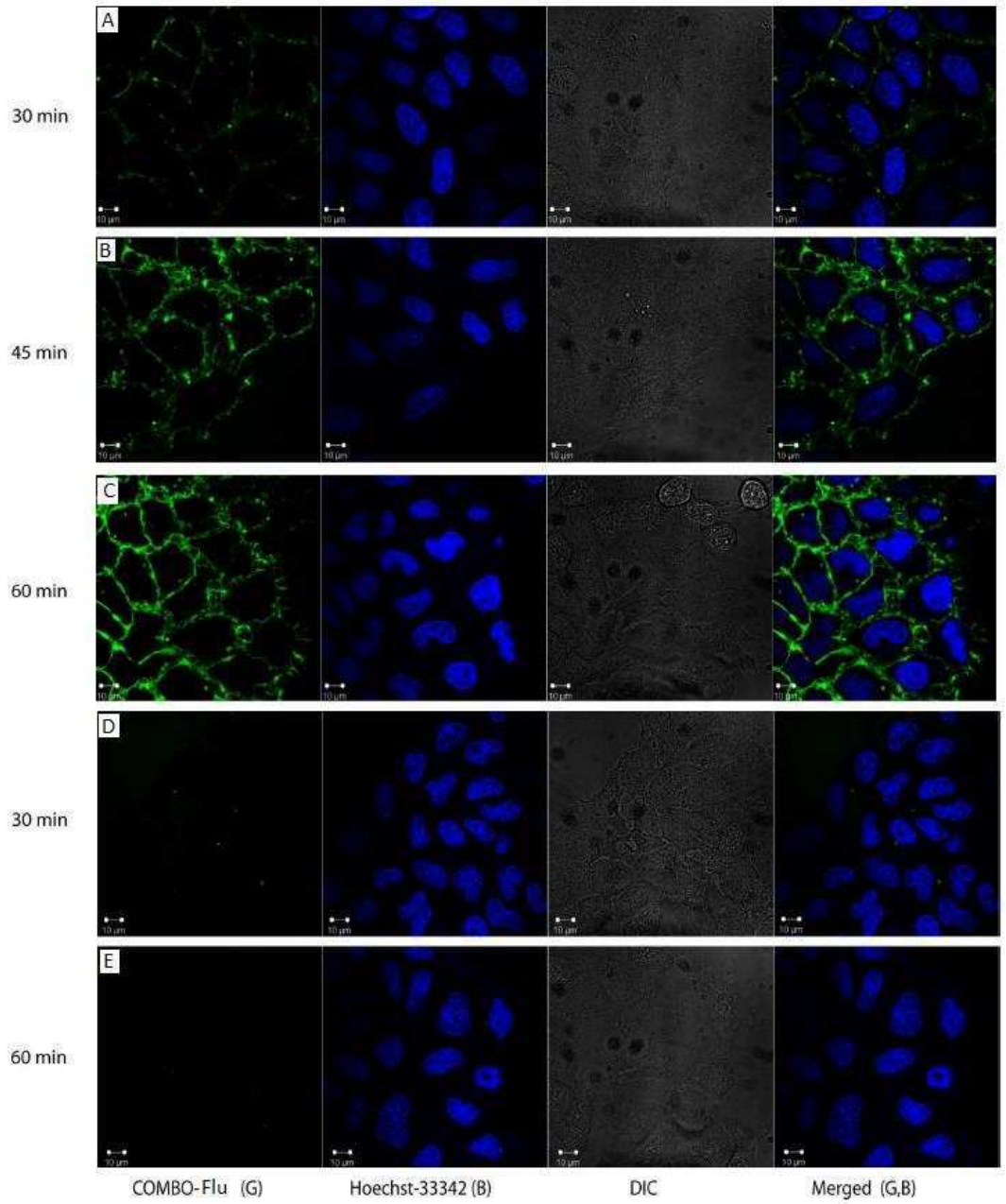


**Figure 26. Top: images of COMBO-Flu stained live HeLa cells treated (A-C) and not treated with $Ac_4$ManNAz (D-E). COMBO-Flu was applied at 12.5 µM concentration along with 40 µM Hoechst 33342 for nuclear staining. G: green channel, B: blue channel.**

Cells were also stained with 5 µM COMBO-Flu for 1 h at the above conditions. The cells showed efficient azide specific labeling with no significant background fluorescence

(**Figure 26.** A-E). The live staining appeared efficient at 5 μM concentration for 1 h, too (**Figure 27.**).

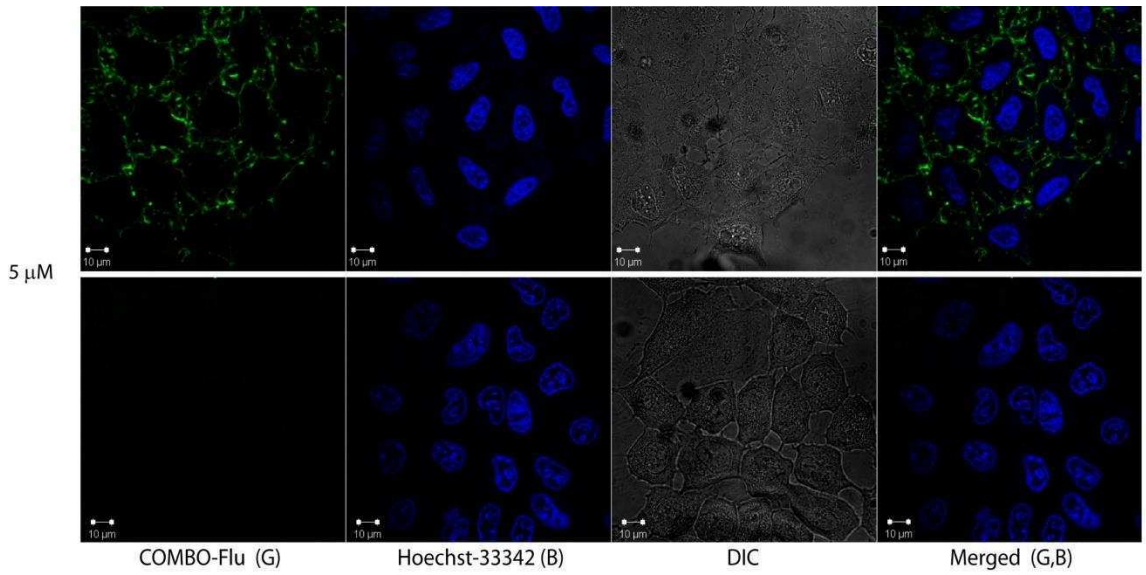


**Figure 27. Live staining of azide-modified (top row) and non-modified (bottom row) HeLa cells with 5 μM COMBO-Flu. Cells were left to incorporate $Ac_4$ManAz for 2 days, then washed and stained with COMBO-Flu in culture conditions for 1 h.**

### 2.1.7.§. Conclusion

In conclusion, we have synthesized a non-fluorinated monobenzocyclooctyne that showed excellent stability and reactivity in aqueous media. We found that this monoarylcyclooctyne has similar reactivity to a related difluorinated benzocyclooctyne, which was also supported by theoretical calculations. Not only does the absence of fluorine incorporation reduce the number of synthetic steps and increase stability, but also offers a more economical access to a rapid bioorthogonal reagent. The applicability of this reagent was tested in cell membrane labeling experiments using a fluorescent COMBO derivative. The fact that COMBO is easily prepared in a couple of classical synthetic transformation steps and shows excellent reaction kinetics would allow this compound to be used in several applications (e.g. bioorthogonal labeling schemes, materials science etc.).

The small size, low lipophilicity and the fast reaction rate suggest that COMBO- based reagents are promising tools in real-time and whole cell imaging experiments. Another fluorescent derivative of COMBO (COMBO-Rhodamine conjugate, COMBO-Rhod) was also synthesized and is currently being used in the labeling of artificial organelles (in collaboration with Dr. Stefan Schiller, Universität Freiburg)

## 2.2.§. Synthesis and properties of trans cyclooctenes

The introduction of the TCO-tetrazine based cycloadditions by the Fox group in 2008[21] was a major breakthrough in bioorthogonal chemistry. The good stability of the reaction partners and the excellent kinetics made these reagents an ideal tool for bioorthogonal labeling experiments. The initial method used a dipyridil-tetrazine derivative which reacted with (E)-cyclooctene-4-enol (trans cyclooctenol, **TCO-OH**) with a second order rate constant of $k_2 = (2000 \pm 400)$ $dm^3mol^{-1}s^{-1}$ at 25 °C in 9:1 methanol/water. The Hilderbrand group introduced a novel asymmetrical benzyl amino tetrazine derivative, which showed even better kinetics with **TCO-OH** ( $k_2 = (33585 \pm 326)$ $dm^3mol^{-1}s^{-1}$ in PBS at 37 °C) [51] and an excellent stability (15% decomposition observed after 15 h in fetal bovine serum (FBS) at 20.0 °C) [22, 23]. The past few years saw numerous applications of this chemistry[52,53,54,55,56] and attempts to optimize the tetrazine reactivity/stability relationship[57,58].

The major problem encountered in these applications came from the high lipophilicity of trans cyclooctenol (**TCO-OH**), an 8 membered carbon ring, lacking any other polar substituents than the OH used for conjugation. Lipohilicity increases undesired nonspecific binding and so it became important to develop TCO derivatives with decreased lipophilicity. Also as investigations in tetrazine chemistry did not lead to new reagents that would have more favorable reactivity/stability relationship, it became more important to look into the cyclooctene chemistry to improve reaction kinetics.

As we mentioned in the introduction, from a practical standpoint there are three routes that allow the routine synthesis of substituted trans cyclooctenes. In the first route bicyclic bromo cyclopropanes are treated with silver perchlorate in the presence of a nucleophile.

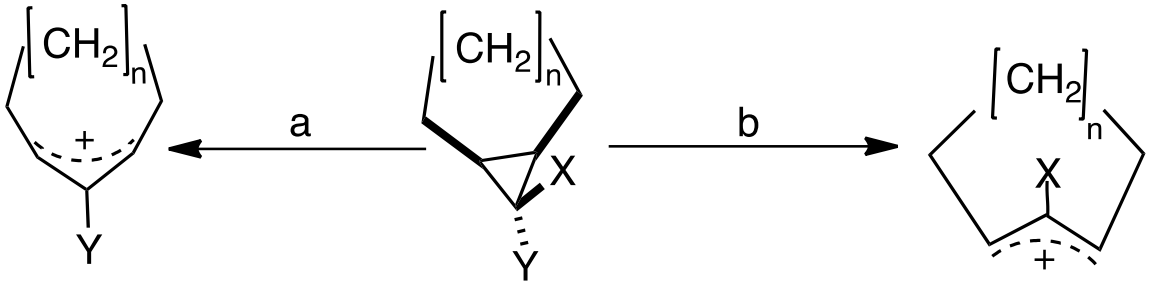


**Scheme 11. Formation of cis and trans cycloalkenes from bicyclic bromocyclopropanes[59].**

If the bromo substituent is in the endo position then this leads to the cis cycloalkane. When the bromo substituent is in the exo position, however, the ring opening leads to the trans cycloalkane (**Scheme 11.**). The second route employs the ring opening of nitrosoureas. The reaction proceeds through the formation of a diaza intermediate and just like with bromo cyclopropanes, formation of the trans congener is preferred from the exo isomer (**Scheme 12.**).

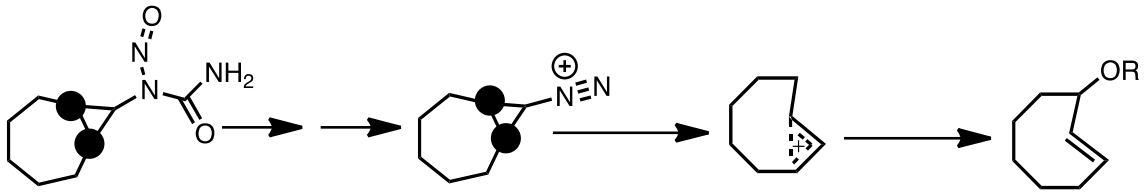


**Scheme 12. Formation of trans cyclooctenes from nitrosourea.**

The third route employs a continuous-flow photochemical transformation of cis cyclooctene. The trans cyclooctene product is bound selectively to $AgNO_3$ impregnated silica support while the unreacted cis form is returned to the reaction vessel (**Figure 28.**). Continuous removal of the product shifts the otherwise unfavorable equilibrium. After completion of the reaction the trans cyclooctene is decomplexed from the $AgNO_3$ impregnated silica either by aqueous $NH_3$ or saturated NaCl.

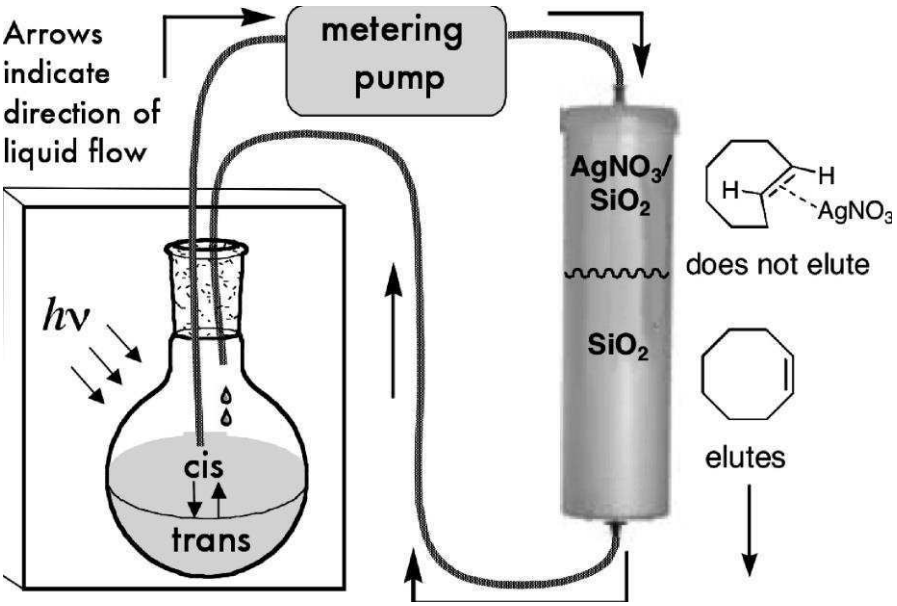


**Figure 28. Experimental setup for continuous-flow synthesis of TCO[60].**

In our investigation we first looked for possible ways to increase both the polarity and reactivity of cyclooctenes. For this purpose we envisioned incorporating endocyclic oxygens into the 8 membered ring. The average length of a $Csp^3$-$Csp^3$ bond is 1.53 Å, while an average $Csp^3$-O bond in a $Csp^3$-O-$Csp^3$ system is 1.43 Å[61]. Exchanging one carbon for oxygen in the eight membered ring causes a 0.2 Å shortening in the overall bond lengths, while exchanging two carbons for oxygens causes a 0.4 Å shortening, thus leading to increased ring strain in these systems. Our basic assumption was that the increased strain would ultimately translate to improved reactivity in the inverse electron demand Diels-Alder reaction.

### 2.2.1.§. Synthesis of TCOs

Jendrall[62] already reported a synthesis for trans cyclooctenes incorporating an endocyclic acetal moiety. He prepared (5 RS, 7 RS)-7-Methoxy-1,3-dioxacyclooct-5(E)-ene, a stable bishetero trans cyclooctene, which showed an increased reactivity in [2+2] cycloadditions in nonpolar media relative to trans cyclooctene. Our synthesis (**Scheme 13.**), which is a modification of Jendralla's method, started from commercially available dioxepin **17** which was reacted with methyl diaza acetate in the presence of catalytic $Rh_2(OAc)_4$ to furnish cyclopropyl carboxylate **18,** which was subsequently subjected to hydrolysis using aqueous LiOH.

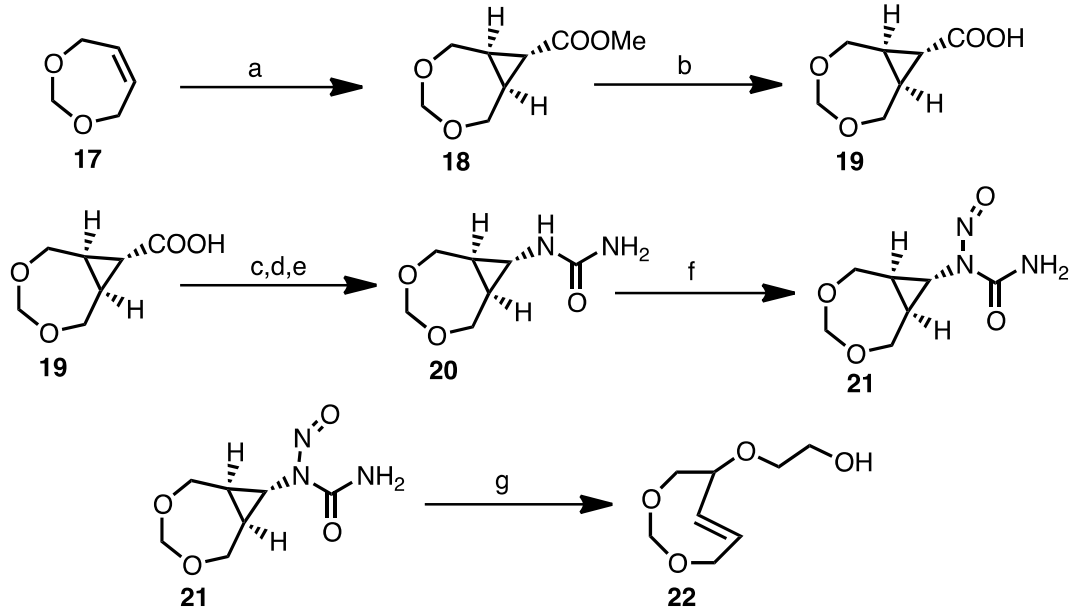


**Scheme 13. Synthesis of DO-TCO. a) $N_2CHCOOMe$, 0.24 mol% $Rh_2(OAc)_4$, r.t., 44%; b) LiOH, water, THF, r.t., 93%; c) $Et_3N$, ethyl chloroformate, acetone, 0 °C; d) $NaN_3$, water; e) toluene, 105 °C, $NH_3$ in THF, 0 °C, 88% for three steps; f) NaOAc, $N_2O_4$, $Et_2O$, 0 °C, 72%; g) $NaHCO_3$, ethylene glycol, r.t., 32%.**

The resulting acid **19** was transformed to the urea **20** in excellent yields using the Curtius rearrangement. Nitrosation using $N_2O_4$ in diethyl ether afforded nitrosourea **21** in good yields. In the last step we used ethylene glycol as solvent and nucleophile in the ring opening in order to convert **21** to a new cyclooctene (**22, DO-TCO**) having an OH handle for further conjugation. This synthesis involves eight steps and four intermediates are isolated. In our first attempts we achieved only poor yields, so we decided to look for an alternate route that would decrease the number of steps and time needed for the synthesis.

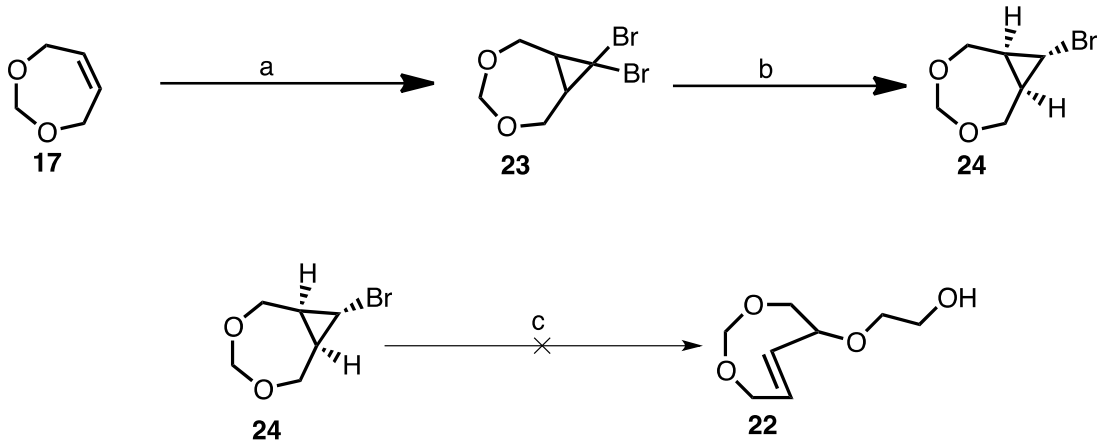


**Scheme 14. Attempt for the synthesis of DO-TCO. a) $CHBr_3$, $Et_3N$, cetrimonium bromide, $CH_2Cl_2$, 50% NaOH in water, r.t., 62%; b) BuLi, $Et_2O$, -78 °C then water, -78 → 0 °C, 70%; c) $AgClO_4$, ethylene glycol, r.t.**

This synthetic route again starts from dioxepin **17** but in the first step we formed the dibromo cyclopropane **23** by dibromo carbene addition under phase transfer conditions. **23** was subsequently subjected to Br-Li exchange resulting in a Li carbenoid, the quenching of which resulted in the exo bromo derivative **24**. We tried to convert **24** to the trans cyclooctene **22** using the general method, however, this step failed to furnish the desired product even using higher concentrations of $AgClO_4$ and extended reaction times (**Scheme 14.**).

Kinetic studies of DO-TCO (**22**) in PBS at 37 °C gave a second order rate constant of $k_2 = (332 \pm 3)$ dm$^3$ mol$^{-1}$ s$^{-1}$ for the reaction with benzylamino tetrazine (see details for kinetic measurements later), which is two orders of magnitude lower than the values measured for TCO-OH. This result is surprising, given that DO-TCO (**22**) is expected to have much larger internal strain than TCO-OH. In order to examine if this lower reactivity is caused by the incorporation of endocyclic oxygens or by the ether group

adjacent to the trans double bond, we decided to synthetize EG-TCO (**28**, **Scheme 15.**), which is a direct analog of DO-TCO **(22).**

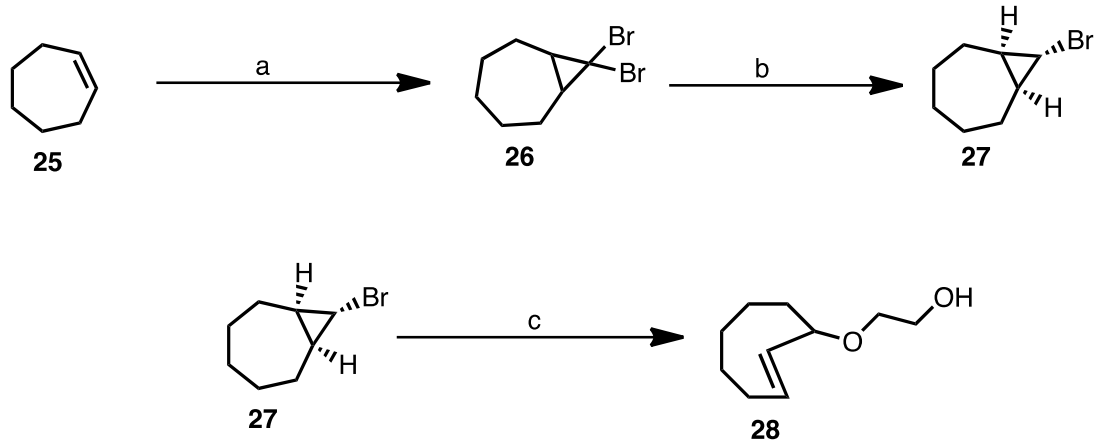


**Scheme 15. Synthesis of EG-TCO. a) $CHBr_3$, tBuOK, pentane, 0 °C, 80%; b) BuLi, THF, $Et_2O$, -100 °C then MeOH, -78→0 °C, 70%; c) $AgClO_4$, ethylene glycol, r.t., 62%.**

Our synthesis started from **25**, which was reacted with dibromo carbene to form **26**, which was converted to **27** through Li-carbenoid intermediate**. 27** reacted promptly with ethylene glycol to furnish **28** in the presence of $AgClO_4$. Surprisingly, the second order rate constant for **28** proved to be only $k_2 = (600 \pm 6)$ dm$^3$ mol$^{-1}$ s$^{-1}$ in PBS at 37 °C. While it is still fifty times lower than the second order rate constant for TCO-OH, it is twice of the value measured for DO-TCO **(22).** Clearly, these values indicate that the relatively low reactivity of EG-TCO and DO-TCO in the inverse electron demand Diels-Alder reaction with benzyl amino tetrazine is to a great degree, a result of steric hindrance exerted by the nearby ether group. This fact alone though does not explain the even lower kinetics of the more strained DO-TCO compared to EG-TCO. Literature studies show that in general there is considerable rate acceleration when aqueous solutions are used as media in Diels-Alder reactions[63]. It seems that this acceleration is due to two factors. First, there is a stabilizing interaction coming from the hydrogen bonds between water and the activated complex. Second, the reaction rate is enhanced by so-called hydrophobic effect. During the activation process the hydrophobic surface area of the reactants is reduced and this provides an additional driving force for the reaction. These effects could be accounted for the slower reaction rates of DO-TCO with benzyl amino tetrazine relative to EG-TCO: in the reaction of the DO-TCO the hydrophobic interactions cannot play such a prominent role as in the reaction of the EG-TCO, because of the highly increased

polarity of the cyclooctene. This proposal, however, needs to be further studied in solvent dependent kinetic experiments.

Next, we decided to turn our attention to possible TCO analogs lacking the steric hindrance of the appending ether group yet having increased polarity and ring strain. For this purpose we devised compound **34** (**Scheme 16.**), a trans cyclooctene that incorporates an endocyclic amide. The endocyclic amide bond introduces polarity, but to a much lesser degree than endocyclic oxygens. At the same time it introduces extra strain and this likely would lead to increased reactivity towards tetrazines. Our hope was, that since increase in polarity is slighter in **A-TCO** than in DO-TCO, the relatively apolar nature of A-TCO would still allow for considerable aqueous acceleration, while the increased strain would lead to a superior reagent in terms of kinetics when compared to TCO-OH, with lower tendency for non-specific binding in labeling experiments due to decreased lipophilicity.

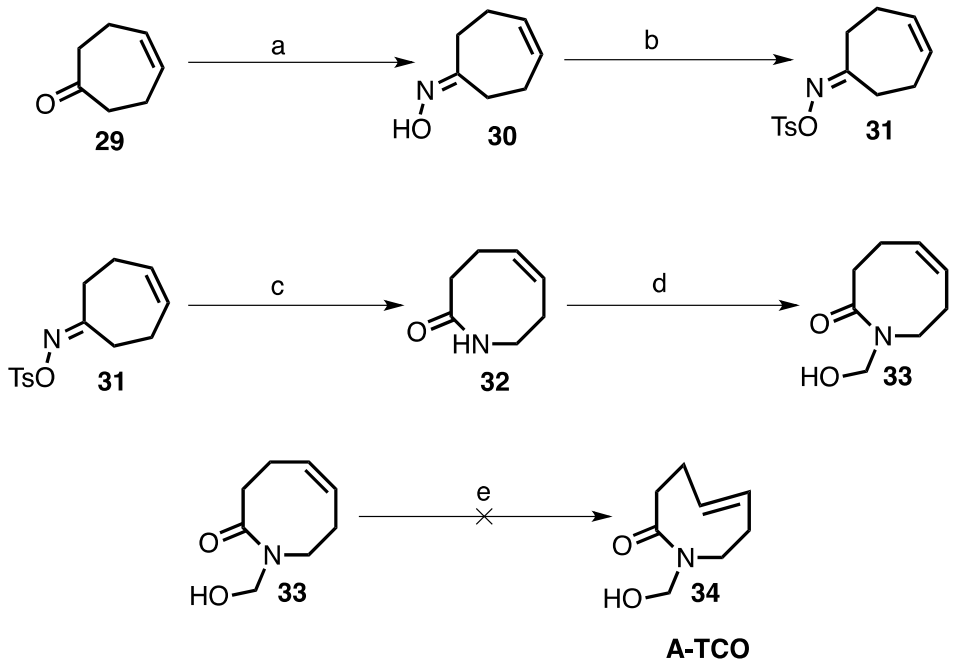


**Scheme 16. Attempt for the synthesis of Amido-TCO. a) $NH_2OH \cdot HCl$, $NaHCO_3$, MeOH, r.t., 99%; b) p-TsCl, pyridine, $CH_2Cl_2$, r.t.; c) $K_2CO_3$, THF, water, r.t., 78% for two steps; d) KOH, 37% formaldehyde, ethanol, reflux, 83%; e) hv, methyl benzoate, 1 vol% MeOH in $Et_2O$, r.t.**

Our synthesis of **34** started from cycloheptenone **29**, which was prepared following literature procedures[64]. This was converted to the endocyclic amide l-aza-2-ketocyclooct-5-ene **(32)** in 3 steps through the oxime **30** and tosyl oxime **31** using slight modifications of literature procedures[65]. **32** was treated with aqueous formaldehyde in refluxing ethanol

in the presence of catalytic KOH to furnish **33**, a novel aza-ketocyclooctene derivative. We tried to convert **33** to the trans cyclooctene **34** using the general method, but our attempts failed and $^1$H NMR of both the reaction mixture and the column content showed the presence of unidentified degradation products, but no trans compounds.

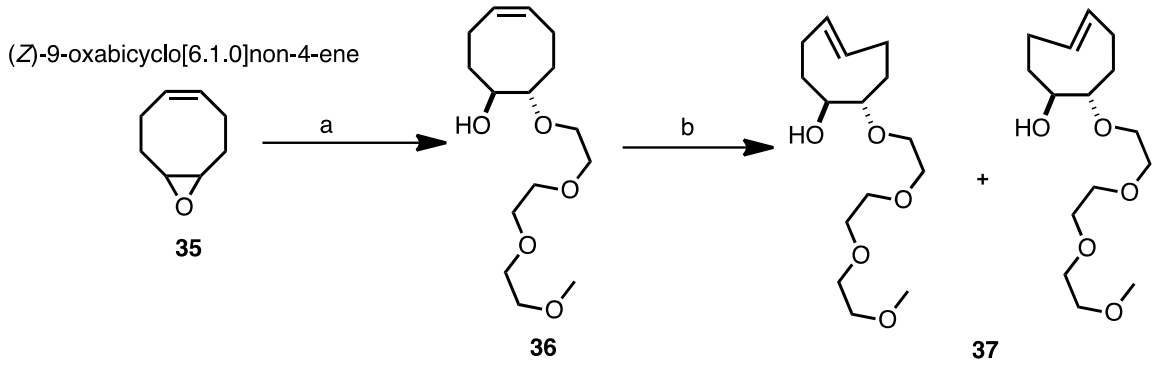


**Scheme 17. Synthesis of 3PEGMe-TCO. a) 3PEGMe, Er(OTf)$_3$, r.t., 41%; b) hv, methyl benzoate, 4:1 Et$_2$O/hexanes, 64%.**

Since our attempts to increase reactivity through the introduction of extra ring strain and to decrease lipophilicity through the incorporation of polar moieties into the ring had failed, we designed trans cyclooctenes **37** (**3PEGMe-TCO**) and **40** (**OX-TCO**) (**Schemes 17.** and **18.**). These have no additional ring strain yet bear highly polar substituents but not too close to the reaction center. What is common in both types of compounds is that their structure is composed of a highly polar exocyclic moiety and a non-polar ring module. We had a reason to think that this would diminish the "hydrophobic effect" in aqueous media less than endocyclic polar moieties.

Our synthesis of **37** (**Scheme 18.**) started from **(Z)-9-oxabicyclo[6.1.0]non-4-ene (35)** by converting it to **36** in reaction with triethylene glycol monomethyl ether (**3PEGMe**) in the presence of erbium triflate[66]. To our delight**, 36** could be distilled from the product mixture following an aqueous work-up and while it still contained some 10% of 3PEGMe, luckily was free of double bond containing impurities. As such, we could subject **36** to photochemical reaction after the distillation without further purification. While the photochemical reaction for TCO proceeds in hexane or pentane, with 3PEGMe-TCO we had to use a 4:1 Et$_2$O/hexane mixture, so that the unreacted cis compound could elute from the column. We also tried pure Et$_2$O as solvent for this reaction but we got too much silver plating, which indicates that some of the silver complex co-eluted with the cis compound. The photochemical reaction gave **37** as a 1:1 mixture. Typically, the product-$AgNO_3$ complex was eluted from the silica column using 500 mL Et$_2$O containing 20%

DCM and 20% MeOH. The resulting organics were extracted using an aqueous 10% $AgNO_3$ solution (3 X 30 mL). The combined aqueous phases were washed with DCM (5 X 20 mL), which was discarded. This removed the remaining cis compound and other impurities. The $AgNO_3$ trans cyclooctene complex could be decomplexed either by the addition of saturated NaCl or saturated $NH_3$ solution.

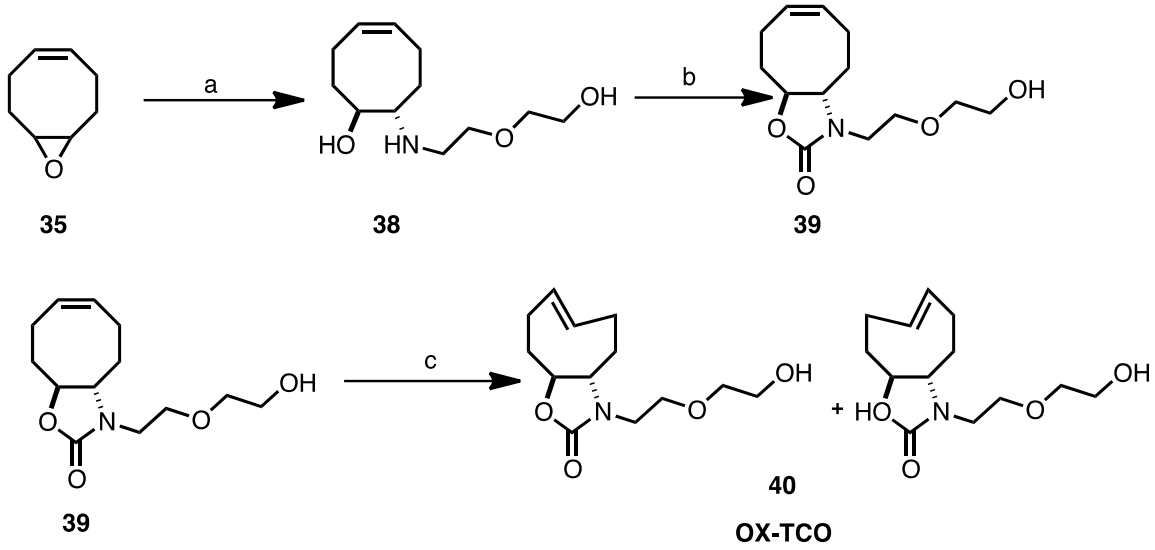


**Scheme 18. Synthesis of OX-TCO. a) 2-(2-aminoethoxy) ethanol, MW, 130 °C, 85%; b) N,N′-disuccinimidyl carbonate, $Et_3N$, acetonitrile, r.t., 92%; c) hν, methyl benzoate, 1 vol% MeOH in $Et_2O$, 82%.**

For the synthesis of compounds **40** (**Scheme 18.**) we proceeded again from (Z)-9-oxabicyclo[6.1.0]non-4-ene **(35),** reacting it first with 2-(2-aminoethoxy) ethanol, in a microwave reactor, at 130 °C constant temperature mode. This gave **38** which was then reacted with N,N-disuccinimidyl carbonate overnight yielding compound **39** in excellent yields. **39** was subjected to the photochemical reaction following the standard procedure. In this case even pure $Et_2O$ was not polar enough to ensure continuous elution of the unreacted starting material from the $AgNO_3$ impregnated silica and there was still a lot of starting material even after prolonged reaction times, so we had to add 1% MeOH to the reaction mixture. When more MeOH was added, silver leaching became too extensive and the reaction flask needed to be cleaned every few hours. While a typical continuous-flow photochemical reaction in the original report lasts less than 24 hours[21], with **39** we needed to run it for around 72 hours to minimize the amount of unreacted cis compound (being around 9% at the end) and the reaction flask needed to be cleaned several times because of the silver plating observed on the inner surface of the glass. The remaining cis isomer could be removed by dissolving the mixture in as much 10% aqueous $AgNO_3$

solution so that it contained 0.9 – 1.0 equiv silver relative to the trans isomers and then washing this solution with DCM several times. The aqueous phase could then be treated with brine or ammonia solution and the trans isomers extracted with DCM. When we tried the same process using multiple equivalents of $AgNO_3$, then there was still a significant amount of cis isomer present in the purified sample.

### 2.2.2.§. Synthesis of NHS carbamates

Next we prepared NHS carbamates from **DO-TCO**, **3PEGMe-TCO** and **OX-TCO** (**Scheme 19.**), using N,N´ -disuccinimidyl carbonate as reagent in the presence of $Et_3N$ in acetonitrile at room temperature. In the case of **37** and **40**, we used an isomeric mixture of the trans compounds for the conversion to the NHS carbamates (for simplicity only

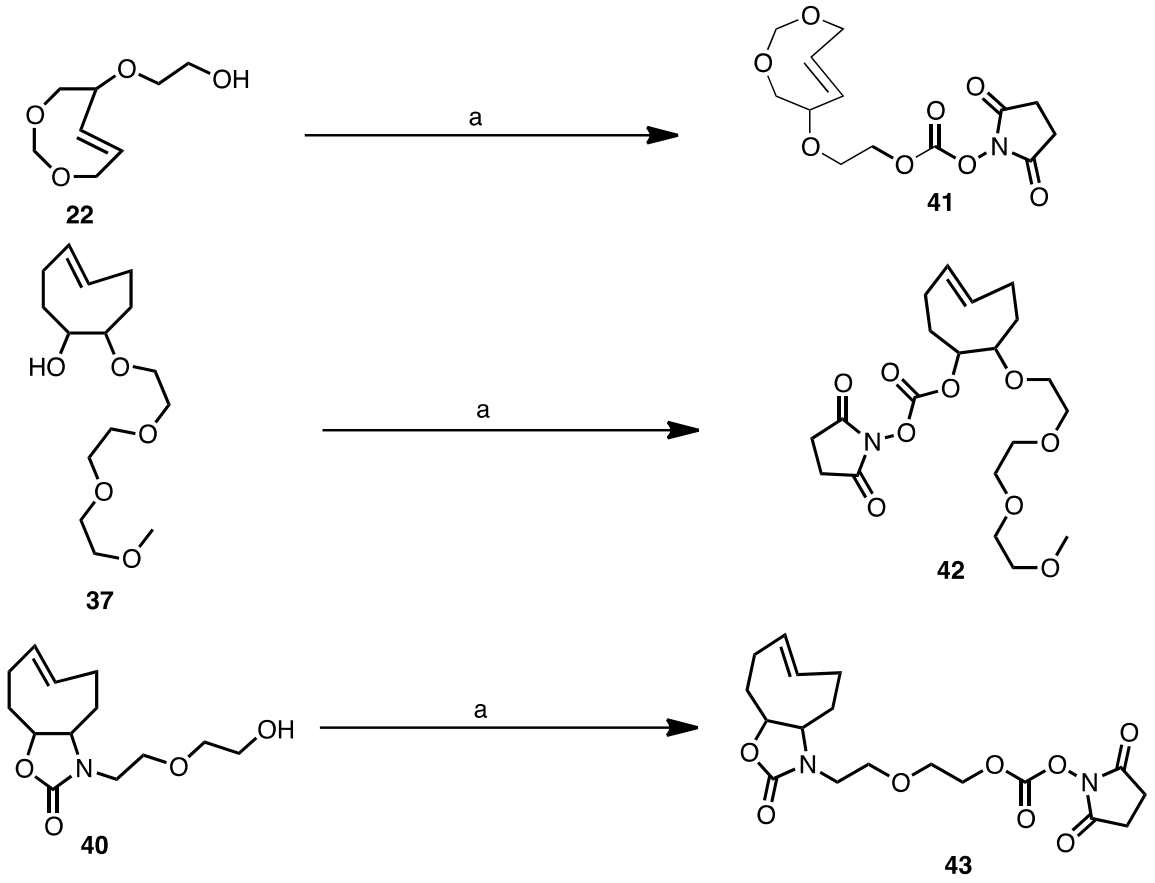


**Scheme 19. Preparation of NHS carbamates from TCOs. a) MeCN, $Et_3N$, *N,N'*-disuccinimidyl carbonate, r.t., 83% for 41, 37% for 42, 71%for 43.**

of the isomers is shown for both compounds in **Scheme 19.**). Luckily, the two isomers of **42** could be isolated on silica, so we were able to perform kinetic measurements for both isomers of **37**, while in the case of **40** we had to measure kinetics on the 4:1 mixture of isomers. We did not identify which of the two possible structures of **37** correspond to the

first and to the second isomer isolated. Nevertheless, the two second order rate constants are $k_2 = (20643 \pm 387)$ $dm^3mol^{-1}s^{-1}$ and $k_2 = (108041 \pm 2418)$ $dm^3mol^{-1}s^{-1}$ in PBS at 37 °C for the reaction with benzylamino tetrazine. This difference in rate constants for the two isomers may seem unexpected, however, literature examples show that there can be even up to one order of magnitude difference in the reactivities of different isomers of TCOs in reactions with tetrazines depending on the position (axial or equatorial) of the substituent opposite to the trans double bond[67]. The isomer mixture of **40** gave a second order rate constant of $k_2 = (29242 \pm 636)$ $dm^3$ $mol^{-1}$ $s^{-1}$ under the same conditions. This aligns well with the reactivity of **TCO-OH**.

### 2.2.3.§. Synthesis of PARP1 inhibitor conjugates

In order to assess the potential use of the new TCOs (**DO-TCO**, **3PEGMe-TCO** and **OX-TCO**), we decided to perform imaging experiments using a previously studied model system.

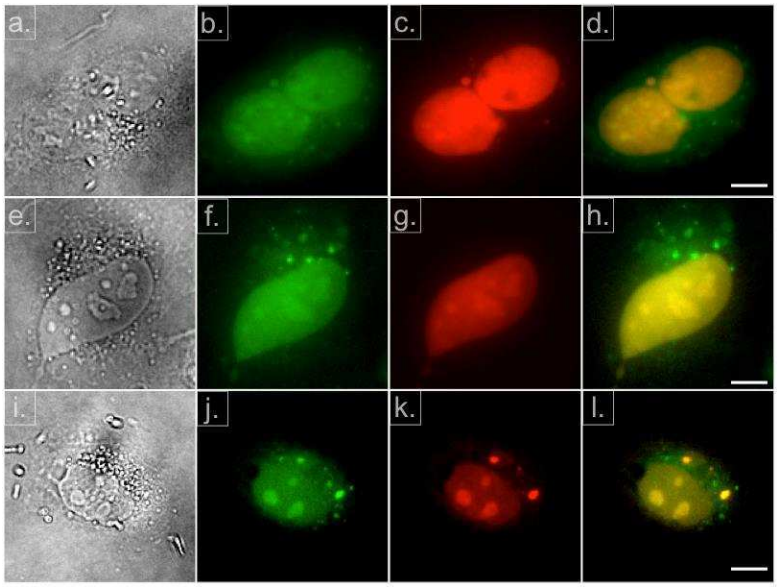


**Figure 29. Bioorthogonal imaging of PARP protein in HT1080 cells. HT1080 cells (expressing PARP1 fused to mCherry) were treated with 5 µM compound 45 (a-d), 47 (e-h) and 46 (i-l) for 30 minutes. After washing with growth media three times for 5 minutes each, cells were incubated for 30 minutes with 1 µM of CFDA-Tz for bio-orthogonal reaction inside the live cells. Following fixation, 40x images were collected by deconvolution microscopy a,e,i) bright field images; b,f,j) Olaparib-TCO/Tz-CFDA staining; c,g,k) PARP1-mCherry, d,h,l) merged images. Scale bar: 10 µm.**

We choose **PARP1** imaging using a PARP inhibitor, **AZD2281**. It has been shown that the 4-NH-piperazine of **AZD2281** tolerates a diverse range of capping groups without

significantly decreasing PARP1 binding affinity[68]. A previous study reported

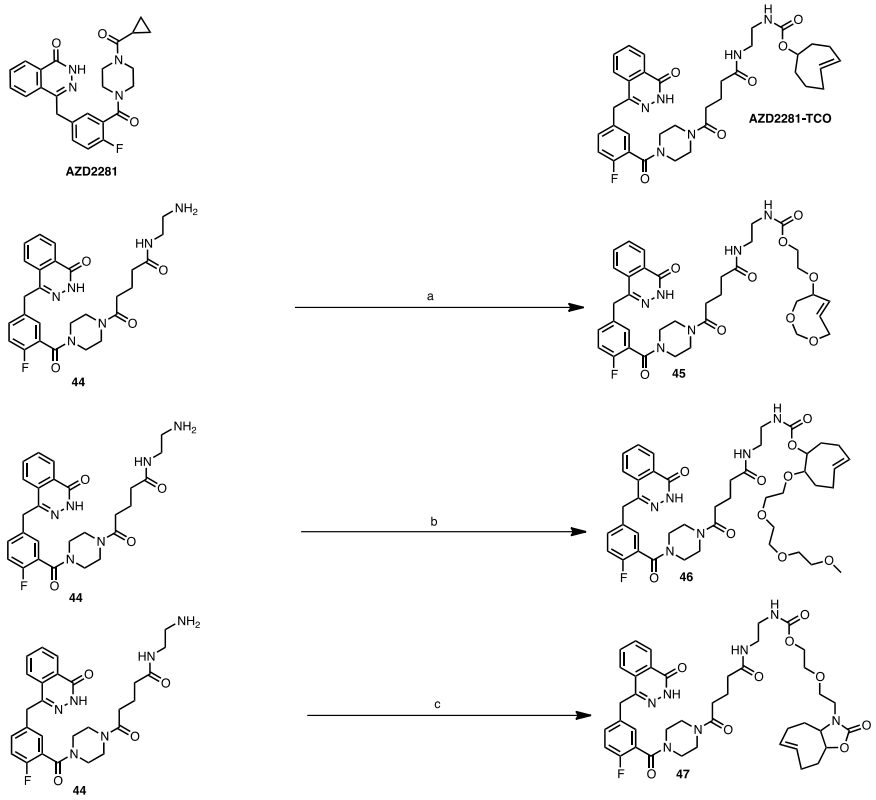


**Scheme 20. Preparation of AZD2281 conjugates. a) DMF, $Et_3N$, then 41 in DCM, r.t., 54%; b) DMF, $Et_3N$, then 42 in DCM, r.t., 70%; c) DMF, $Et_3N$, then 43 in DCM, r.t., 74%.**

**AZD2281-TCO**, which modification of **AZD2281** using the NH-piperazine anchor point. **AZD2281-TCO** was then used in live-cell imaging with fluorophore-tetrazine derivatives[69]. Similarly we prepared **AZD2281-DO-TCO**, **AZD2281-3PEGMe-TCO** and **AZD2281-OX-TCO** and the originally reported **AZD2281-TCO** (**Scheme 20.**) in order to compare their performance in in vivo imaging experiments. The conjugates were tested in imaging experiments (see the experimental part). A significant advantage of the new trans cyclooctene derivatives lies in their better solubility in DMSO/water mixtures. Sample preparation using our compounds was significantly easier than with **AZD2281-TCO**. Bio-orthogonal imaging experiments of PARP protein in HT1080 cells (expressing PARP1 fused to mCherry) were successful with all three new compounds, but we could not yet observe a significant difference between **AZD2281-TCO** and our products (**Figure 29.**). Further experiments would be needed to assess the potential of **DO-TCO**, **3PEGMe-TCO** and **OX-TCO**.

### 2.2.4.§. Comparison of $^{c}$LogP values of our and previous TCOs

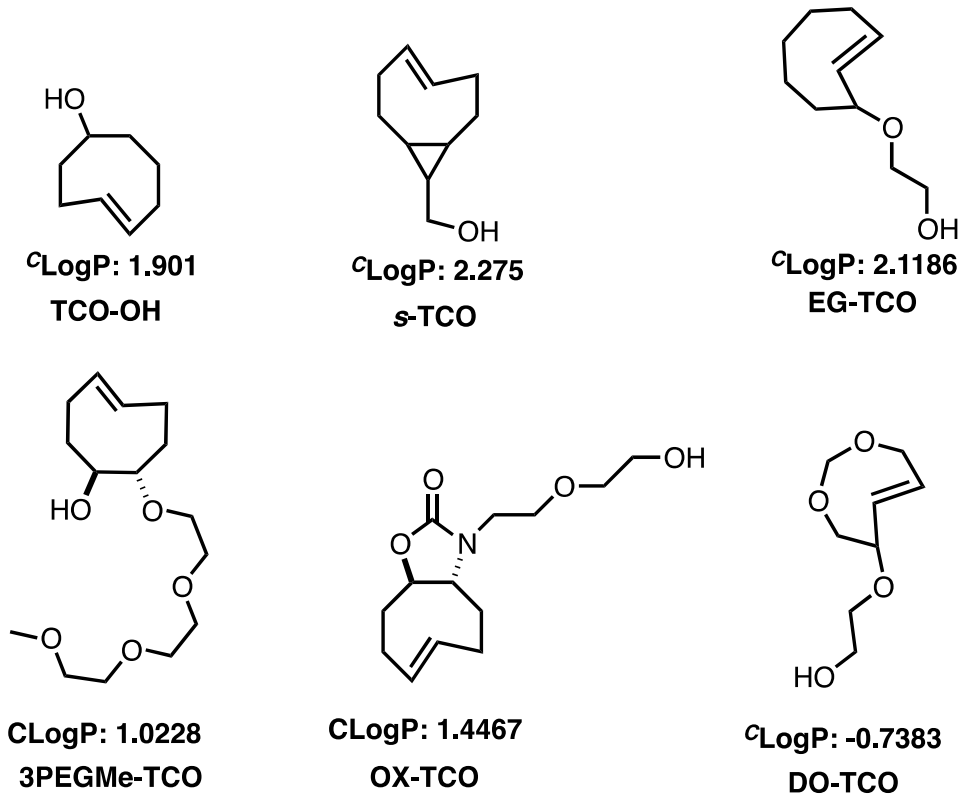


**Figure 30. $^{c}$LogP values of previously reported and our trans cyclooctenes as calculated by BioByte embedded in CS ChemDraw Ultra 12.**

**Figure 30.** shows calculated $^{c}$LogP values for **TCO-OH**, **s-TCO** and our trans cyclooctene derivatives. It can be seen that adding a glycol moiety (**EG-TCO**) almost does not affect the $^{c}$LogP value at all, while a longer polar chain can make a significant difference. Incorporation of oxygen into the cyclooctene ring itself shifts the $^{c}$LogP drastically.

### 2.2.5.§. Stability of TCOs

We stored bulk samples of all three new cyclooctenes at –20 °C for six months. None of them showed any kind of degradation or isomerization by $^{1}$H NMR and signals from the double bond region disappeared in all cases when reacting with 1,2,4,5-tetrazine.

During our experiments we observed that **3PEGMe-TCO** and **OX-TCO** display a very similar stability to **TCO-OH**, but we had concerns about **DO-TCO**, because of the increased strain. When (E)-2-((5,8-dihydro-4H-1,3-dioxocin-5-yl)oxy)ethanol (**22, DO-TCO**) was stored in $D_2O$ only isomerization to the cis isomer was observed as confirmed

by $^{1}$H NMR. We obtained authentic spectrum of the cis isomer separately with deliberate isomerization using traces of iodine. The spontaneous isomerization took almost 5 days at 37 °C and more than 12 days at room temperature. Presence of white light did not accelerate the reaction. The isomerization did not prove to be of any integer order but after an initial period it best approached zero order and the half-life decreased with lower concentrations (**Figures 31.** and **32.**) .

As we will see later, **s-TCO** also showed some 5% isomerization after 14 hours in $D_2O$:DMSO-$d^6$ 10:1 at room temperature. With **DO-TCO** we observed similar degree of isomerization only after 63 hours at room temperature in $D_2O$.

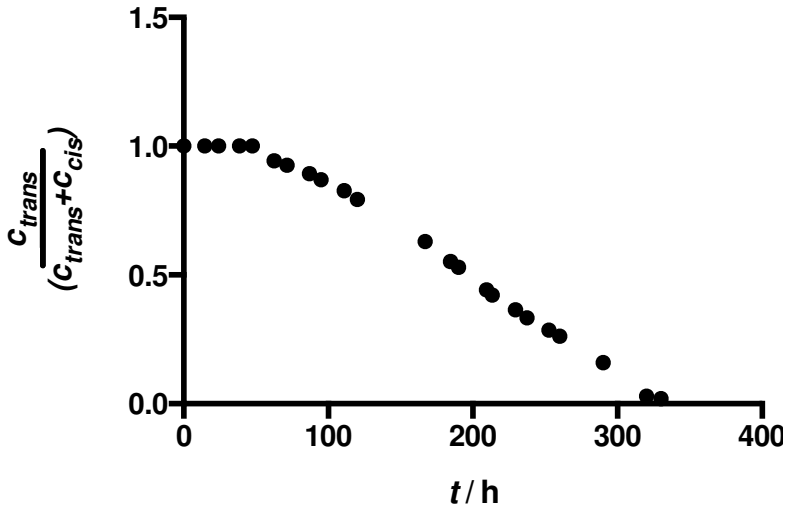


**Figure 31. Isomerization of DO-TCO at room temperature.**

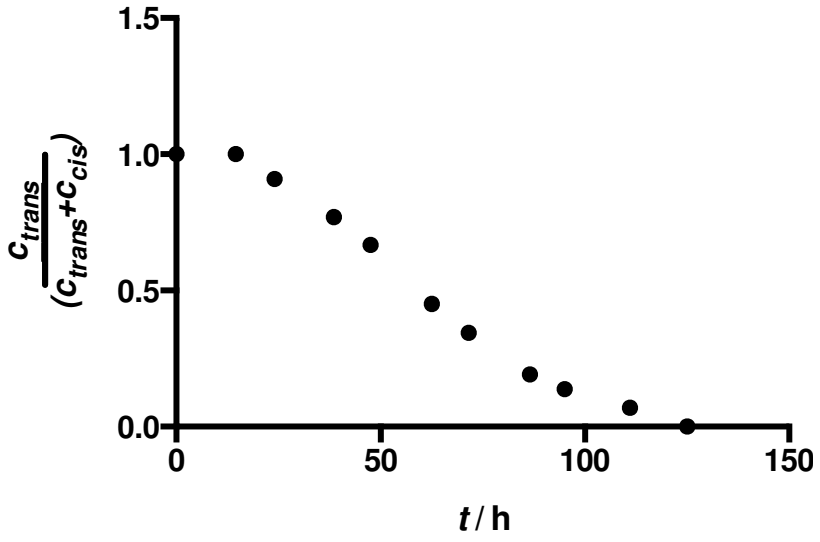


**Figure 32. Isomerization of DO-TCO at 37 °C.**

We performed stability studies in the presence of various nucleophiles at 37 °C. The solvent was $D_2O$:DMSO-$d^6$ 10:1 v/v. The solutions were made by the dilution of a stock solution prepared in DMSO-$d^6$. We used 20 mM end concentration of the cyclooctenes, except for the s-TCO, which was used in 10 mM end concentration because of poorer solubility: a 20 mM solution could not be prepared by dilution with $D_2O$ from DMSO-$d^6$ stock solution without the precipitation of **s-TCO**. Nucleophiles mercaptoethanol and cysteine were used in 48 mM end concentration. It should be noted that cysteine precipitated very soon from the solution. In all cases reactions were followed by $^1$H NMR. **s-TCO** isomerized very fast in the presence of mercaptoethanol, so we performed a control experiment in which **s-TCO** was kept in $D_2O$:DMSO-$d^6$ 10:1 v/v at room temperature. Measurements were taken in the following intervals: mercaptoethanol: 0 h, 2 h, 11 h, 17 h and 25 h; cysteine: 0 h, 6 h and 14 h; **s-TCO** without nucleophile at room temperature: 1 h, 7 h and 14 h.

**TCO-OH**, **EG-TCO**, **OX-TCO** did not show any change under the aforementioned conditions. **3PEGMe-TCO** did not show any degradation in the presence of cysteine, however, it isomerized to the cis isomer in the presence of mercaptoethanol (**Table 2.**). **s-TCO** and **DO-TCO** both showed isomerization of the trans isomer to the cis isomer in the presence of cysteine as the main reaction (**Table 5.** and **Table 7.**). In the presence of mercaptoethanol isomerization of **DO-TCO** and **s-TCO** occurred together with unidentified side reactions as the emergence of complex patterns in the aliphatic region suggests. These observations are summarized in **Table 3.** and **Table 4.** In each case we calculated the ratio of the integrals of the cis double bond to the sum of the integrals of the cis and trans double bonds.

**Table 2. Isomerization of 3PEGMe-TCO in the presence of mercaptoethanol at 37 °C.**

| t (h) | $I_{cis}$ | $I_{trans}$ | $I_{trans} / (I_{cis}+I_{trans})$ |
|---|---|---|---|
| 0 | 0.17 | 2 | **0.922** |
| 2 | 0.48 | 2 | **0.807** |
| 11 | 0.66 | 2 | **0.752** |
| 17 | 0.69 | 2 | **0.744** |
| 25 | 0.74 | 2 | **0.730** |

**Table 3. Isomerization of DO-TCO in the presence of mercaptoethanol at 37 °C.**

| t (h) | $I_{cis}$ | $I_{trans}$ | $I_{trans} / (I_{cis}+I_{trans})$ |
|---|---|---|---|
| 0 | 0 | 2 | **1** |
| 2 | 0.18 | 2 | **0.917** |
| 11 | 0.38 | 2 | **0.840** |
| 17 | 0.42 | 2 | **0.826** |
| 25 | 0.79 | 2 | **0.717** |

**Table 4. Isomerization of s-TCO in the presence of mercaptoethanol at 37 °C.**

| t (h) | $I_{cis}$ | $I_{trans}$ | $I_{trans} / (I_{cis}+I_{trans})$ |
|---|---|---|---|
| 0 | 1.19 | 2 | **0.627** |
| 2 | 87 | 2 | **0.023** |
| 11 | 2 | 0 | **0** |
| 17 | 2 | 0 | **0** |
| 25 | 2 | 0 | **0** |

**Table 5. Isomerization of DO-TCO in the presence of cysteine at 37 °C.**

| t (h) | $I_{cis}$ | $I_{trans}$ | $I_{trans} / (I_{cis}+I_{trans})$ |
|---|---|---|---|
| 0 | 0 | 2 | **1** |
| 6 | 2 | 0 | **0** |
| 14 | 2 | 0 | **0** |

**Table 6. Isomerization of s-TCO in the presence of cysteine at 37 °C.**

| t (h) | $I_{cis}$ | $I_{trans}$ | $I_{trans} / (I_{cis}+I_{trans})$ |
|---|---|---|---|
| 0 | 0.19 | 2 | **0.913** |
| 6 | 1.07 | 2 | **0.652** |
| 14 | 8.42 | 2 | **0.192** |

**Table 7. Isomerization of s-TCO in $D_2O$:DMSO-$d^6$ 10:1 v/v at room temperature.**

| t (h) | $I_{cis}$ | $I_{trans}$ | $I_{trans} / (I_{cis}+I_{trans})$ |
|---|---|---|---|
| 0 | 0 | 2 | **1** |
| 1 | 0.03 | 2 | **0.985** |
| 7 | 0.06 | 2 | **0.971** |
| 14 | 0.1 | 2 | **0.952** |

From these data we can conclude that while **TCO-OH**, **EG-TCO**, **OX-TCO** and **3PEGMe-TCO** are relatively stable in the presence of thiol nucleophiles, **DO-TCO** and **s-TCO** undergo significant isomerization/decomposition. In the presence of mercaptoethanol most of the **s-TCO** disappeared within the first two hours of the experiment, while **DO-TCO** was almost unaffected within the same period. On the contrary, in the presence of cysteine the isomerization of **DO-TCO** proved to be much faster than that of **s-TCO**: while for the former no trans compound was present after 6 hours, the latter still contained 65% trans isomer.

### 2.2.6.§. Tetrazine Kinetics with Cyclooctenes

Kinetic measurements were performed with benzylamino tetrazine and excessive amounts of cyclooctenes, using an Applied Photophysics Stopped-Flow spectrophotometer. Stock solutions of reactants in DMSO were diluted in PBS pH 7.4 to a final concentration of 1 vol% DMSO. Solutions of these reactants were loaded into the individual chambers of the instrument and equilibrated to 37°C for 10 min. The concentration of benzylamino tetrazine after the samples were mixed by the spectrometer in a 1:1 v/v ratio was 50, 75 or 150 μM depending on the cyclooctene used. The decrease of the benzylamino tetrazine absorbance measured at 515 nm was monitored at regular intervals between 0.075 s and 10 s depending on the cyclooctene used. For trials shorter than 1 s (**TCO-OH**, **OX-TCO** and **3PEGMe-TCO**) 1000 and for trials longer than 1 s (**EG-TCO** and **DO-TCO**) 10000 data points were collected. We performed measurements at five different concentrations for each cyclooctene (see **Table 8.**). The $k_{obs}$ ($s^{-1}$) values were calculated using the Prism 6 software package and the results of 6 runs were averaged for each cyclooctene concentration. The average $k_{obs}$ values were then plotted against the concentration of cyclooctenes to yield the second order rate constant

$k_2$=($dm^3$ $mol^{-1}$ $s^{-1}$) from the slope of the line with the error from the standard deviation in the slope calculated in Prism 6.

**Table 8. Experimental setup and the second rate constants for the reaction of cyclooctenes with benzylamino tetrazyne in PBS at 37 °C. n denotes the number of data points collected.**

| Cyclooctene | $c_{cyclooctene}$ (mM) | $c_{tetra}$ (μM) | Run time (s) | n | $k_2$ ($dm^3.mol^{-1}.s^{-1}$) |
|---|---|---|---|---|---|
| TCO | 1.42, 1.65 1.89, 2.13 2.36 | 75 | 0.15 | 1000 | $33585 \pm 326$ |
| EG-TCO | 2.57, 3.00 3.43, 3.86 4.23 | 150 | 6 | 10000 | $600 \pm 6$ |
| DO-TCO | 2.57, 3.00 3.43, 3.86 4.23 | 150 | 10 | 10000 | $332 \pm 3$ |
| OX-TCO | 1.2, 1.4, 1.6, 1.8, 2.6 | 50 | 0.175 | 1000 | $29242 \pm 636$ |
| 3PEGMe-$TCO_A$ | 0.90, 1.16, 1.55, 1.93, 2.71 | 75 | 0.2 | 1000 | $20643 \pm 387$ |
| 3PEGMe-$TCO_B$ | 0.81, 1.04, 1.39, 1.74, 2.43 | 75 | 0.075 | 1000 | $108041 \pm 2418$ |

Representative data for the slowest (**DO-TCO**) and the fastest (**3PEGMe-$TCO_B$**) kinetics are given in **Figures 33** to **36**. Details for **TCO-OH**, **EG-TCO**, **3PEGMe-$TCO_A$** and **OX-TCO** are given in the appendix.

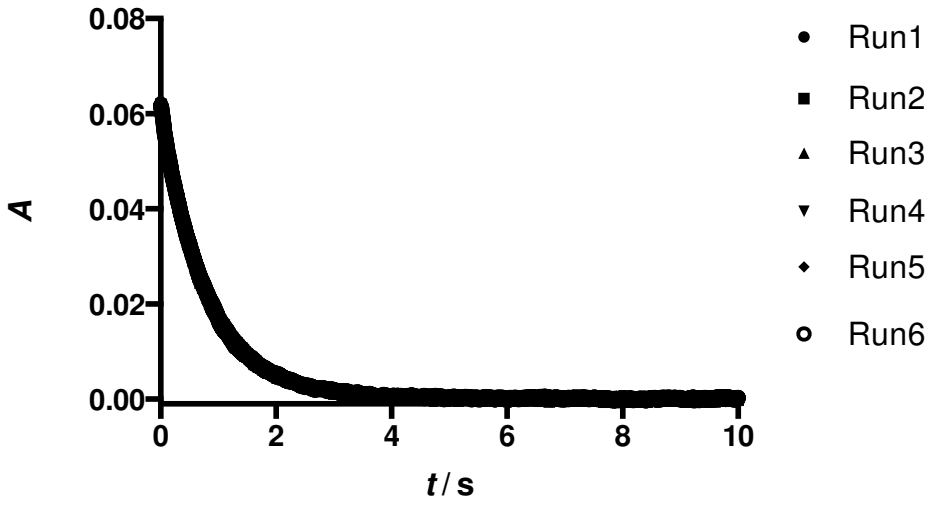


**Figure 33. Absorbance vs time, 150 μM tetrazine, 4.5 mM DO-TCO.**

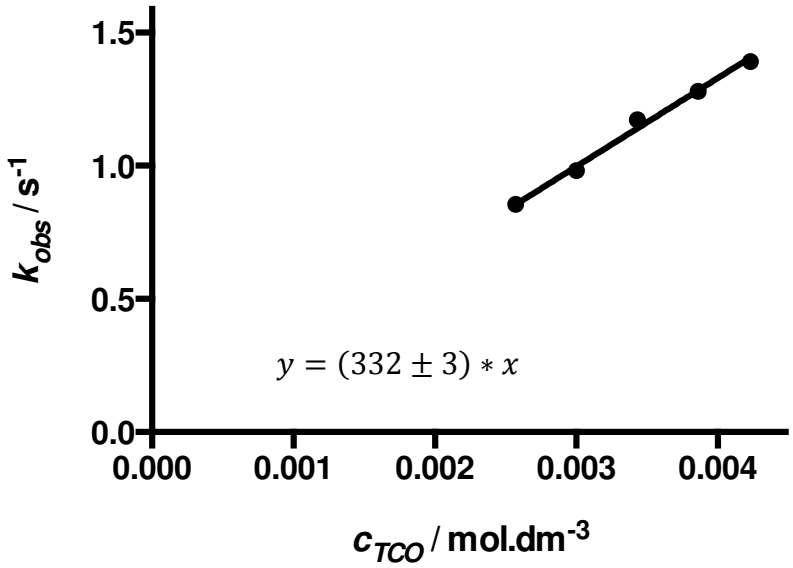


**Figure 34. Linear fit to the pseudo first order rate constants for DO-TCO.**

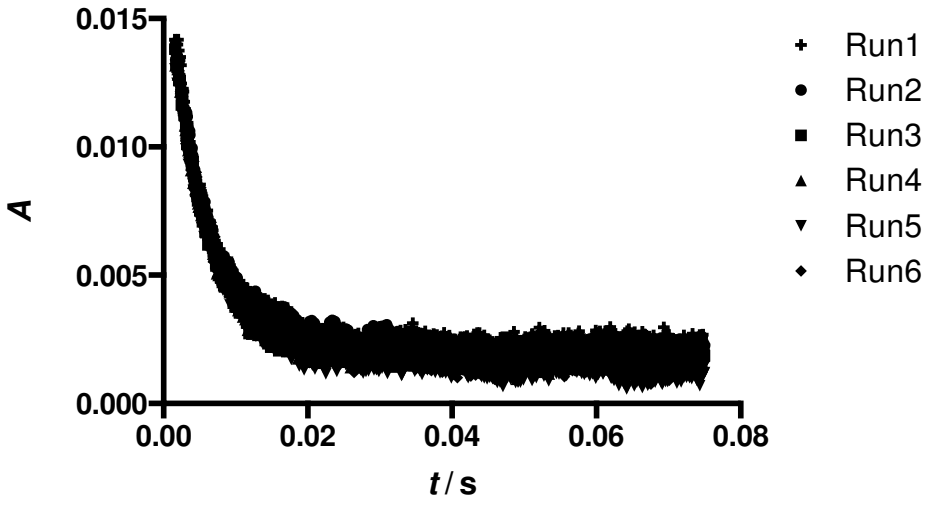


**Figure 35. Absorbance vs time, 75 μM tetrazine, 3.5 mM 3PEGMe-TCO$_B$.**

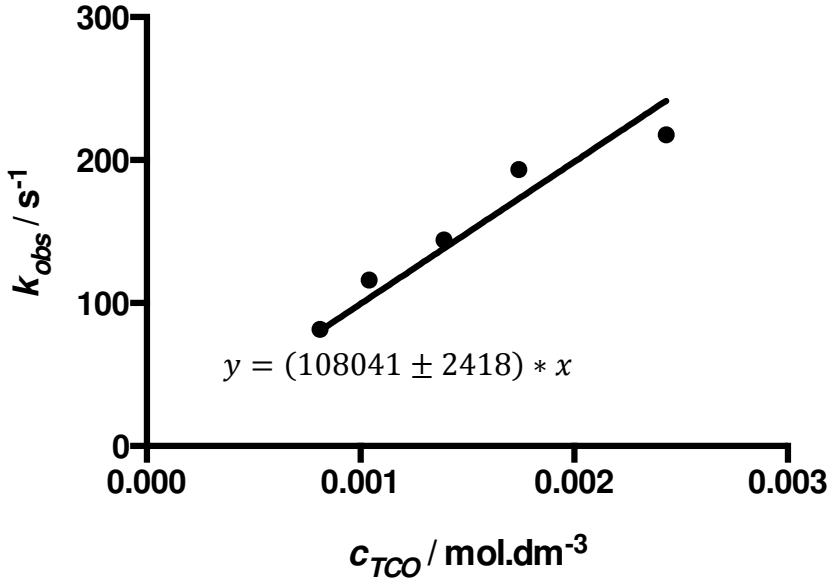


**Figure 36. Linear fit to the pseudo first order rate constants for 3PEGMe-TCO$_B$.**

### 2.2.7.§. Conclusion

In summary we synthetized novel trans cyclooctenes **DO-TCO**, **3PEGMe-TCO** and **OX-TCO**. All of these compound display significantly lower lipophilicity than **TCO-OH**. While the second order rate constant for the reaction of **DO-TCO** and benzyl amino tetrazine is significantly lower than for **TCO-OH**, **3PEGMe-TCO** and **OX-TCO** display similar or better kinetics. The stability of the new trans cyclooctenes proved to be satisfactory (**DO-TCO**) or excellent (**3PEGMe-TCO** and **OX-TCO**) in the presence of thiols. Bioorthogonal imaging experiments of PARP protein in HT1080 cells (expressing PARP1 fused to mCherry) were successful with all three new compounds.

As part of our further research we wish to prepare **3PEGMe-EG-TCO** (**Figure 37.**) in order to make possible the tosylation and substitution to fluorine through the EG linker. Direct tosylation of **3PEGMe-TCO** is not possible due to an attack of the trans double bond on the tosylation site. Furthermore, we envision the preparation of a new **DO-TCO** derivative (**NDO-TCO**, **Figure 37.**) in which the linker is removed from the position next to the double bond and thus does not impede the cycloaddition reaction. As a further improvement we wish to prepare **syn-OX-TCO**, which based on patent literature precedence should display significantly better kinetics than **OX-TCO**.

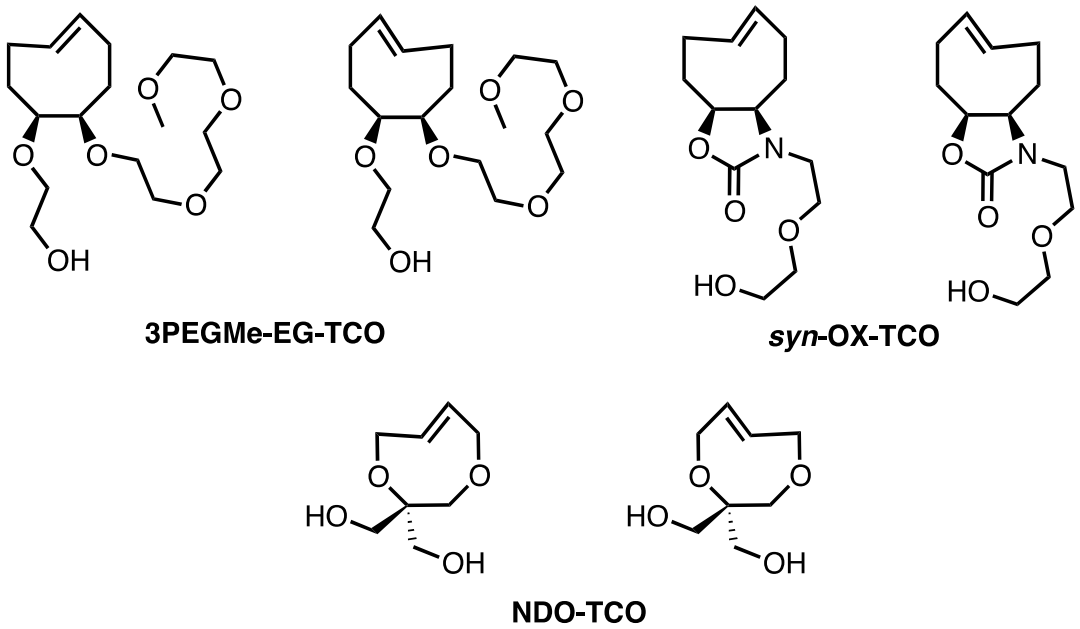


**Figure 37. New TCOs planned to be synthesised.**

# 3.§. Experimental

## 3.1.§. General Considerations

Unless otherwise noted, all reactions and manipulations were performed in dry glassware under air at ambient temperature. NMR spectra were recorded using a 600 MHz Varian VNMRS spectrometer, a Varian 500 MHz, a Bruker 400 MHz or a Bruker 250 MHz spectrometer. $^{1}H$ or $^{13}C$ NMR chemical shifts are reported vs. $Me_4Si$ and were determined by reference to the residual $^{1}H$ or $^{13}C$ solvent peaks. Splitting patterns are designated as s (singlet), d (doublet), t (triplet), q (quadruplet), m (multiplet), dd (doublet of a doublets), dt (doublet of triplets), td (triplet of doublets) and dq (doublet of quadruplets). Solvent signals were supressed using DSG (embedded in MestreNova) where necessary.

A combination gas chromatography and low-resolution mass spectrometry were carried out on an Agilent 6890N gas chromatograph (30 m x 0.25 mm column with 0.25 μm HP-5MS coating, He carrier gas) and an Agilent 5973 mass spectrometer (Ion source: EI +, 70 eV, 230 °C; interface: 300 °C). IR spectra were obtained on a Bruker IFS55 spectrometer on a single-reflection diamond attenuated total reflectance (ATR) unit. All melting points were measured on a Büchi 501 apparatus. For COMBO, its precursors and derivatives the exact masses were determined with an Agilent 6230 time-of-flight mass spectrometer. Samples were introduced by the Agilent 1260 Infinity LC system and the mass spectrometer was operated in conjunction with a JetStream source in positive/negative ion mode. Reference masses of m/z 121.050873 and 922.009798 or 119.03632 and 966.000725 were used to calibrate the mass axis during analysis. For the trans cyclooctenes, their precursors and derivatives the high-resolution electrospray ionization (ESI) mass spectra were obtained on a Bruker Daltonics APEXIV 4.7 Tesla Fourier Transform mass spectrometer (FT-ICR-MS) in the Department of Chemistry Instrumentation Facility at the Massachusetts Institute of Technology.

Unless otherwise noted, reagents were from commercial suppliers, notably Sigma-Aldrich, Fisher Scientific, Acros Organics, TCI America, Chem-Impex, Oakwood Chemical and Crescent Chemicals. Ethylene glycol was dried over 4 Å molecular sieves as an approximately 20 vol% solution in DCM/MeOH 4:1. It was considered sufficiently dry when the water content was less than 5 mol% as determined by $^{1}H$ NMR. If necessary,

multiple batches of dry molecular sieves were used to achieve the desired level of dryness. The photochemical reactions were performed in a Rayonet PRP-100 system. Microwave experiments were performed in a CEM Discover system. Analytical thin-layer chromatography (TLC) was performed on Polygram SIL G/UV 254 pre-coated plastic TLC plates with 0.25 mm silica gel from Macherey-Nagel + Co. Visualisation was performed with a 254 nm UV lamp or by using an aqueous solution of $KMnO_4$ (a solution of $KMnO_4$ (1.5 g), $K_2CO_3$ (10 g) and 10 % aqueous NaOH (1.25 $cm^3$ in water (200 $cm^3$)).

Silica gel column chromatography was carried out with Flash silica gel (0.040–0.063 mm) from Merck. For the flash chromatography a CombiFlash $R_f$ 200 system was used.

8,8-dibromobicyclo[5.1.0]octane (26) and (1R,7S,8r)-8-bromobicyclo[5.1.0] octane (27)[70], 4,7-dihydro-1,3-dioxepin (17)[71], methyl diazoacetate[72], Rhodamine piperazine chloride [73] and 4-[[4-Fluoro-3-(4-(N-(2-aminoethyl)-5-oxo-pentanamide) piperazine-1-carbonyl) phenyl] methyl]-2H-phthalazin-1-one (PARP1 inhibitor)[68] were prepared using standard literature procedures.

## 3.2.§. Procedures

### 3.2.1.§. Preparation of COMBO and its derivatives

**1,2,5,6-tetrabromocyclooctane (10)[74]**

To a solution of 1,5-cis-cyclooctadiene (240 mg, 2.20 mmol, 1.0 equiv) in $CH_2Cl_2$ (8 $cm^3$) was slowly added bromine (800 mg, 5.00 mmol, 2.3 equiv) dissolved in $CH_2Cl_2$ (8 $cm^3$) at -78 °C under argon atmosphere. The resulting mixture was allowed to warm to room temperature and then stirred for another 3 hours at which point saturated $Na_2S_2O_3$ solution (10 $cm^3$) was added and stirring was continued for 10 min. The two layers were separated and the aqueous phase was extracted twice with $CH_2Cl_2$ (2 X 8 $cm^3$). The combined organic layers were dried over $MgSO_4$, filtered and the solvent was evaporated. To the resulting thick oil 2 $cm^3$ of cold hexane was added, which effected crystallization. The crystals were filtered off and washed with cold hexane (1.5 $cm^3$) to afford the desired product as a white crystalline solid (695 mg, 73%). The filtrate was concentrated on silica and purified on a short silica pad using hexane as eluent to provide further 120 mg (13%) of the desired product, which consisted of two isomers in a ratio of 58:42. Yield: 86%, $R_f$ =0.21 and 0.34 (in hexane), respectively.

Major isomer:

$^{1}$H NMR (600 MHz, $CDCl_3$) δ 4.76 (d, J = 2.5 Hz, 4H) 2.82 (d, J = 13.1 Hz, 4H) 2.12 (d, J = 12.8 Hz, 4H); $^{13}$C NMR (150 MHz, $CDCl_3$) δ 57.3, 26.5.

Minor isomer :

$^{1}$H NMR (600 MHz, $CDCl_3$) δ 4.57 (d, J = 7.1 Hz, 4H), 2.59-2.51 (m, 4H), 2.46-2.37 (m, 4H); $^{13}$C NMR (150 MHz, $CDCl_3$) δ 58.3, 31.5.

**(1E,5E)-1,5-dibromocycloocta-1,5-diene and (1E,5E)-1,6-dibromocycloocta-1,5-diene (11)[44]**

Powdered 1,2,5,6-tetrabromocyclooctane (428 mg, 1.00 mmol, 1.0 equiv) and KO$^{t}$Bu (450 mg, 4.00 mmol, 4.0 equiv) were mixed in a round- bottom flask and cooled to -78 °C under argon atmosphere. To this mixture diethyl ether (20 $cm^3$) was added while stirred. The resulting suspension was allowed to warm to room temperature and stirred till the completion of the reaction (6h) at which point saturated $NH_4Cl$ solution (5 $cm^3$) and water (5 $cm^3$) were added and the stirring was continued for another 10 minutes. The resulting two layers were separated and the aqueous phase was extracted three times with ethyl acetate (3 X 8 $cm^3$). The combined organic layers were dried over $MgSO_4$, filtered and the crude product was concentrated onto silica and purified on a short column using hexane as eluent. This procedure resulted in 200 mg (83%) of colourless oil, which solidified upon standing. $R_f$ = 0.46 (hexane). Product consists of two isomers in a ratio of 63:37.

Major isomer:

$^{1}$H NMR (600 MHz, $CDCl_3$) δ 6.09 (t, J = 7.1 Hz, 2H), 2.83 (m, 4H), 2.41 (q, J = 6.9 Hz, 4H); $^{13}$C NMR (150 MHz, $CDCl_3$) δ 129.5, 124.4, 38.3, 27.4.

Minor isomer:

$^{1}$H NMR (600 MHz, $CDCl_3$) δ 6.04 (m, 2H) 2.91 (s, 4H) 2.35 (m, 4H); $^{13}$C NMR (150 MHz, $CDCl_3$) δ 129.8, 123.8, 38.0, 27.6.

**(E)-methyl 8-bromo-5,6,9,10-tetrahydrobenzo[8]annulene-2-carboxylate and (E)-methyl 7-bromo-5,6,9,10-tetrahydrobenzo[8]annulene-2-carboxylate (14)**

$KO^tBu$ (168 mg, 1.50 mmol, 4.0 equiv) and 18 – crown – 6 ether (25 mg, 0.095 mmol, 0.25 equiv) were suspended in hexane (20 $cm^3$) and a solution of a mixture of (1E, 5E)-1,5-dibromocycloocta-1,5-diene and (1E, 5E)-1,6-dibromocycloocta-1,5-diene (100 mg, 0.38 mmol, 1.0 equiv) in hexane (5 $cm^3$) was added to it dropwise under argon atmosphere with continuous stirring. The stirring has been continued for 110 minutes (or until the consumption of the starting material) and then quenched by adding saturated $NH_4Cl$ (5 $cm^3$) and water (5 $cm^3$). The two phases were separated and the water phase was extracted three times with ethyl acetate (3 X 5 $cm^3$). Methyl coumalate (48 mg, 0.31 mmol, 0.82 equiv) was added to the combined organic phases and the resulting solution was stirred overnight. The solvent was then removed on a rotary evaporator and the crude product was purified by column chromatography (hexane:ethyl acetate, 20:1 v/v). White crystalline solid, 40 mg (36%), $R_f$= 0.50 (hexane:ethyl acetate, 10:1 v/v).

$^1H$ NMR (600 MHz, $CDCl_3$) δ 7.84-7.78 (m, 3H) 7.74 (d, J = 1.5 Hz, 1H), 7.18 (d, J = 7.9 Hz, 1H), 7.11 (d, J = 7.7 Hz, 1H), 5.82 (m, 2H), 3.90 (s, 3H), 3.89 (s, 3H), 3.13-3.00 (m 8H), 2.48 (m, 4H); $^{13}C$ NMR (150 MHz, $CDCl_3$) δ 167.11, 167.10, 144.9, 144.1, 139.6, 138.8, 131.6, 131.2, 130.6, 130.1, 130.0, 129.8, 128.5, 128.29, 127.9, 127.7, 123.8, 123.5, 51.9, 51.9, 39.4, 39.0, 33.2, 33.1, 33.0, 32.8, 29.6, 29.4; IR (ν / $cm^{-1}$): 2948.7, 1713.3, 1607.8, 1430.3, 1269.3; GC-MS (M/z): 215(83%), 216(15%), 263(7%), 265(9%), 294(3%), 296(8%); mp: 55.4-55.8 °C.

**COMBO**

$KO^tBu$ (210 mg, 1.87 mmol, 2.5 equiv) and 18-crown-6 ether (50 mg, 0.19 mmol, 0.25 equiv) were suspended in hexane (80 $cm^3$) under argon atmosphere. This suspension was heated to 58 °C[75], then a solution of **14** (220 mg, 0.75 mmol, 1.0 equiv) in hexane (30 $cm^3$) was added under continuous stirring. During the addition the colour of the suspension turned orange. Stirring was continued for 30 minutes, at which time the suspension was cooled. The precipitate was filtrated off and washed with ethyl acetate (2 x 10 $cm^3$), then ice (20 g) was added to the solution. After shaking, the resulting two layers were separated and the organic phase was washed with water (1 X 20 $cm^3$). To the

organic phase then 0.5 M $AgNO_3$ solution was added (2 X 20 $cm^3$) and shaken vigorously (2 X 5 min). The collected aqueous phases were washed wit hexane (3 X 10 $cm^3$). Then hexane (10 $cm^3$) and cooled $NH_4OH$ solution (25%, 15 $cm^3$) were added and the resulting mixture was shaken. The two phases were separated and the aqueous phase was extracted with hexane (3 X 10 $cm^3$). The combined organic layers were dried over $MgSO_4$, filtered and the hexane removed on a rotary evaporator. Colourless oily material which solidified upon standing at -20 °C, 75 mg (47 %).

$^1$H NMR (600 MHz, $CD_3CN$) δ 7.85 (d, J = 1.9 Hz, 1H), 7.81 (dd, J = 7.9, 1.9 Hz, 1H), 7.32 (d, J = 7.9 Hz, 1H), 3.85 (s, 3H), 3.49-3.39 (m, 2H), 2.92 (tt, J = 12.8, 2.9 Hz, 2H), 2.50-2.41 (m, 2H), 2.28-2.19 (m, 2H); $^{13}$C NMR (150 MHz, $CD_3CN$) δ 167.6, 148.2, 143.1, 132.5, 132.2, 129.5, 128.4, 100.1, 99.9, 52.6, 38.1, 38.0, 23.1, 22.9; IR (ν / $cm^{-1}$): 2929.6, 1712.2, 1433.7, 1288.0, 1265.2; GC-MS (M/z): 155(45%), 167(17%), 171(15%), 199(19%).

**COMBO-acid**

**COMBO** (40 mg, 0.19 mmol, 1.0 equiv) was added to a round-bottom flask which was then flushed with argon and then charged with dioxane (3 $cm^3$). LiOH (90 mg, 3.76 mmol, 20 equiv) was taken up in water (1 $cm^3$) and added to the solution dropwise during continuous stirring. The stirring was continued for 2 hours at 30 °C under argon atmosphere, then the reaction was quenched with 1 N HCl (5 $cm^3$). To the resulting suspension $CH_2Cl_2$ was added (10 $cm^3$). The two phases were separated and the aqueous phase was extracted with $CH_2Cl_2$ (3 X 5 $cm^3$). The combined organic phases were dried over $MgSO_4$ and the solvent was removed on a rotary evaporator. The resulting pale yellow solid was washed once with hexane (1 $cm^3$). White powder, 35 mg (92%).

$^1$H NMR (600 MHz, $CDCl_3$) δ 7.95-7.91 (m, 2H), 7.28 (d, J = 8.5 Hz, 1H), 3.47 (apparent q, J = 12.1 Hz, 2H), 2.92 (apparent t, J = 14.0 Hz, 2H), 2.54-2.45 (m, 2H), 2.37-2.28 (m, 2H); $^{13}$C NMR (150 MHz, $CDCl_3$) δ 170.7, 147.8, 141.6, 132.5, 131.2, 128.5, 127.4, 99.3, 98.8, 37.7, 37.5, 22.7, 22.5; IR (ν / $cm^{-1}$): 2924.4, 2557.3, 1674.1, 1609.9, 1566.7, 1440.6, 1307.6, 1294.1, 1274.3; HRMS (ESI) calcd. for $C_{13}H_{11}O_2$ $[M-H]^-$: 199.0759, found: 199.0761; mp: 158.1-158.6 °C (decomp.).

**COMBO-Rhod**

In a round-bottom flask **COMBO-acid** (20 mg, 0.10 mmol, 1.0 equiv) HBtU (35 mg, 0.094 mmol, 0.94 equiv) and HOBt x $H_2O$ (16 mg, 0.10 mmol, 1.0 equiv) were mixed and dissolved in anhydrous acetonitrile (6 $cm^3$). To the resulting solution EDIPA (36 µl, 26 mg, 0.2 mmol, 2.0 equiv) and Rhodamine piperazine chloride (56 mg, 0.12 mmol, 1.2 equiv) were added. The solution was stirred for 4 hours at room temperature. The solvent was removed on a rotary evaporator and the crude product was purified by column chromatography ($CH_2Cl_2$:MeOH, 20:1 v/v). Scarlet crystalline solid, 60 mg (89%). $R_f$ = 0.33 ($CH_2Cl_2$:MeOH, 20:1 v/v)

$^1$H NMR (600 MHz, $CDCl_3$) δ 7.67 (br s, 2H), 7.54 (br s, 1H), 7.34 (br s, 1H), 7.25-7.17 (m, 5H), 7.01-6.72 (m, 4H), 3.61 (m, 8H), 3.55-3.34 (m, 8H), 3.39 (t, J = 12.3 Hz, 2H), 2.85 (t, J = 11.9 Hz, 2H), 2.43 (d, J = 15.0 Hz, 2H), 2.26 (t, J = 13.7 Hz, 2H), 1.32 (t, J = 6.8 Hz, 12H); $^{13}$C NMR (150 MHz, $CDCl_3$): 167.7, 157.8, 155.7, 155.6, 143.7, 141.8, 132.0, 131.1, 130.4, 130.2, 130.1, 129.8, 127.6, 125.5, 114.2, 114.1, 114.0, 113.8, 99.3, 99.1, 46.1, 41.9, 37.5, 37.4, 22.6, 22.5, 12.6; IR (ν / $cm^{-1}$): 2922.5, 2242.3, 1630.0, 1585.3, 1528.5, 1411.3, 1335.3, 1246.5; HRMS (ESI) calcd. for $C_{45}H_{49}N_4O_3$ $[M+H]^+$: 693.3799, found: 693.3767; mp: 111.4-112.0 °C (decomp.).

**COMBO-Flu**

**COMBO acid** (10 mg, 0.05 mmol, 1.0 equiv), HBtU (18 mg, 0.047 mmol, 0.95 equiv) and HOBt·$H_2O$ (8 mg, 0.05 mmol, 1.0 equiv) were mixed in a round- bottomed flask and dissolved in anhydrous DMF (2 $cm^3$). Subsequently, ethyldiisopropylamine (18 mL) and fluorescein–piperazine (20 mg, 0.05 mmol, 1.0 equiv) were added to the resulting solution, which was stirred for 3 h at room temperature under an argon atmosphere. The reaction mixture was then directly loaded onto a silica column and the product was purified using $CH_2Cl_2$:MeOH (20:1 to 10:1 v/v) as the eluent to give an orange crystalline solid (25 mg, 86 %). $R_f$ = 0.67 ($CH_2Cl_2$:MeOH, 9 :1 v/v)

$^1$H NMR (600 MHz, $CDCl_3$) δ 7.68 (br s, 2 H), 7.54 (br s, 1 H), 7.41 (t, J = 3.9 Hz, 1 H), 7.21 (d, J = 7.6 Hz, 1 H), 7.17-7.06 (m, 4 H), 6.74-6.70 (m, 4H), 3.53-3.33 (broad s 8H), 3.47 (td, J = 12.7, 2.7Hz, 2H), 2.85 (t, J = 11.3 Hz, 2H), 2.46 (d, J = 14.6 Hz, 2H), 2.20–

2.30 ppm (m, 2H); $^{13}$C NMR (150 MHz, $CDCl_3$) δ 171.2, 168.3, 157.5, 150.87, 144.2, 142.2, 135.2, 132.8, 131.6, 131.3, 131.1, 130.8, 130.3, 130.0, 129.7, 127.6, 125.4, 115.6, 104.1, 99.3, 99.2, 47.5, 42.2, 37.6, 37.6, 22.7, 22.6; IR (neat, ν / $cm^{-1}$) = 2923.9, 2853.8, 1728.1, 1590.4, 1458.0, 1258.0; HRMS (ESI): m/z calcd for $C_{37}H_{31}N_2O_5$ $[M+H]^+$: 583.2227; found: 583.2222.

**COMBO-Benzylazide adduct (16)**

**COMBO** (21 mg, 0.100 mmol, 1.0 equiv) was dissolved in acetonitrile (3 $cm^3$) and benzyl-azide was added (14 mg, 0.105 mmol, 1.05 equiv). The mixture was stirred for 2 h, then the solvent was removed and the resulting solid was washed with hexane (1 X 300 μl). White solid, 32 mg (91%).

$^1$H NMR (600 MHz, $CD_3CN$): 7.70 (d, J = 1.7 Hz, 1H), 7.67 (dd, J = 7.9, 1.8 Hz, 1H), 7.60 (dd, J = 7.9, 1.8 Hz, 1H), 7.38 (d, J = 1.7 Hz, 1H), 7.34-7.21 (m, 6H), 7.17 (d, J = 7.9 Hz, 1H), 6.92 (m, 2H), 6.85 (m, 3H), 5.36 (s, 4H), 3.83 (s, 3H), 3.82 (s, 3H), 3.24-3.15 (m, 8H), 3.04-2.96 (m, 8H); $^{13}$C NMR (150 MHz, $CD_3CN$): 167.5, 167.4, 146.7, 145.8, 144.5, 144.4, 141.5, 140.6, 137.0, 137.0, 133.4, 133.3, 131.8, 131.7, 131.2, 131.2, 129.8, 129.7, 129.6, 129.4, 128.9, 128.8, 128.5, 128.3, 127.9, 127.8, 52.5, 52.5, 52.0, 51.9, 32.3, 32.0, 31.2, 31.0, 27.3, 27.0, 24.7, 24.6; IR (ν / $cm^{-1}$): 2952.3, 2175.5, 1711.6, 1608.0, 1575.3, 1496.5, 1436.3, 1374.9, 1267.4, 1225.1; HRMS (ESI) calcd. for $C_{21}H_{21}N_3O_2$ $[M+H]^+$: 347.1707, found: 347.1708; mp: 113.3-114.0 °C.

### 3.2.2.§. Preparation of trans cyclooctenes and their derivatives

**(1R,7S,8r)-methyl 3,5-dioxabicyclo[5.1.0]octane-8-carboxylate (18)[62]**

Rhodium acetate (250 mg, 0.57 mmol, 2.4 X $10^{-3}$ equiv) was dissolved in 4,7-dihydro-1,3-dioxepine (240 g). To this was added a solution of methyl diazoacetate (240 g, 2.4 mol, 1.0 equiv) in 4,7-dihydro-1,3-dioxepine (350 g) at the rate of 1 drop per second (4 h total approximately). The total amount of 4,7-dihydro-1,3-dioxepine used equals to 2.5 equiv with respect to methyl diazoacetate. After stirring the reaction overnight, excess 4,7-dihydro-1,3-dioxepine was removed by vacuum distillation. To the remaining residue $Et_2O$ and petroleum ether were added (1:1 mixture, 150 mL). After storing overnight at -20 °C the resulting crystals were filtered giving pure (1R,7S,8r)-methyl 3,5-dioxabicyclo[5.1.0]octane-8-carboxylate (47 g, 11.4%). A second batch of product was

obtained from the filtrate by removal of the solvent and subsequent distillation. Additional (1R,7S,8r)-methyl 3,5-dioxabicyclo[5.1.0]octane-8-carboxy late was obtained by collecting fractions distilling between 90 °C and 120 °C at 3 to 6 mBar. This gave semi pure (1R,7S,8r)-methyl 3,5-dioxabicyclo[5.1.0]octane-8-carboxylate (150 g, 36%) containing less than 10% impurities. Both the pure and semi-pure product were suitable for subsequent reactions.

$^{1}$H NMR (500 MHz, $CDCl_3$) δ 4.92 (d, J = 7.2 Hz, 1H), 4.20 (d, J = 7.2 Hz, 1H), 4.14 (dt, J = 13.1, 2.0 Hz, 2H), 3.99 – 3.94 (m, 2H), 3.68 (s, 3H), 2.13 (t, J = 4.9 Hz, 1H), 1.80-1.77 (m, 2H); $^{13}$C NMR (101 MHz, $CDCl_3$) δ 174.11, 99.76, 68.52, 51.76, 27.46, 18.87; HRMS (ESI) calcd. for $C_8H_{13}O_4$ $[M+H]^+$: 173.0808, found: 173.0809.

**(1R,7S,8r)-3,5-dioxabicyclo[5.1.0]octane-8-carboxylic acid (19)[62]**

(1R,7S,8r)-methyl 3,5-dioxabicyclo[5.1.0]octane-8-carboxylate (43 g, 0.25 mol, 1.00 equiv) was dissolved in THF (30 mL). To this solution water (30 mL) was added and the mixture was cooled in an ice bath. To this was added slowly LiOH (12 g, 0.50 mol, 2.00 equiv) in water (120 mL), the resulting mixture was stirred for 2.5 h at room temperature. After stirring for 2.5 h at room temperature, the reaction was quenched by addition of 5 N HCl (80 mL, prepared from a 10 N HCl stock solution and ice). The mixture was extracted with DCM (5 X 50 mL) and the solvents were removed by rotary evaporation. Trituration of the resulting residue with petroleum ether afforded pure (1R,7S,8r)-3,5-dioxabicyclo[5.1.0]octane-8-carboxylic acid (36.9 g, 93%) as a white crystalline solid.

1H NMR (500 MHz, CDCl3) δ 4.93 (dd, J = 7.1, 1.8 Hz, 1H), 4.25-4.09 (m, 3H), 3.97 (d, J = 13.0 Hz, 2H), 2.12 (t, J = 4.8 Hz, 1H), 1.84 (dd, J = 5.1, 2.7 Hz, 2H); 13C NMR (126 MHz, CDCl3) δ 179.87, 99.72, 68.35, 28.20, 18.82.

**1-((1R,7S,8r)-3,5-dioxabicyclo[5.1.0]octan-8-yl)urea (20)[62, 76]**

To a solution of (1R,7S,8r)-3,5-dioxabicyclo[5.1.0]octane-8-carboxylic acid (2.70 g, 17.1 mmol, 1.0 equiv) in acetone (12 mL), $Et_3N$ (1.99 g, 19.6 mmol, 1.15 equiv) in acetone (24 mL) was added dropwise at 0 °C. To the resulting solution ethyl chloroformate (2.32 g, 21.3 mmol, 1.25 equiv) in acetone (6 mL) was added at 0 °C. The ethyl chloroformate addition resulted in the formation of a white precipitate. This

suspension was stirred at 0 °C for 30 min and then sodium azide (1.71 g, 26.3 mmol, 1.54 equiv) in water (3 mL) was added. On the addition of the sodium azide a light pink color developed. The resulting suspension was maintained at 0 °C for 1 h with stirring and then was poured on ice. The resulting homogeneus mixture was extracted with toluene. (10 X 20 mL) The organic phase was dried over $MgSO_4$ for 16 h, concentrated to 50 mL on a rotary evaporator and heated to 100 – 105 °C until the gas evolution ceased. The yellow solution was cooled to 0 °C and ammonia (68.2 mL of 0.5 M solution in THF, 34.1 mmol, 2.00 equiv) was added slowly. The resulting white suspension was stirred for 1 h at room temperature. After stirring, the THF was removed by rotary evaporation, the suspension was cooled to 0 °C, the white precipitate was filtered, and then washed with a few mL of $Et_2O$ and petroleum ether and dried yielding 1-((1R,7S,8r)-3,5-dioxabicyclo[5.1.0]octan-8-yl)urea (2.58 g, 88%) as a white solid.

$^1$H NMR (500 MHz, DMSO-$d_6$) δ 6.11 (d, J = 3.9 Hz, 1H), 5.42 (s, 2H), 4.70 – 4.39 (m, 2H), 4.22 – 3.96 (m, 2H), 3.72 (d, J = 12.1, 2H), 2.75 (dd, J = 3.7, 3.7 Hz, 1H), 1.45 – 1.08 (m, 2H). $^{13}$C NMR (126 MHz, DMSO-$d_6$) δ 158.97, 99.76, 70.32, 33.11, 26.17.

**1-((1R,7S,8r)-3,5-dioxabicyclo[5.1.0]octan-8-yl)-1-nitrosourea (21)[62]**

To a suspension of 1-((1R,7S,8r)-3,5-dioxabicyclo[5.1.0]octan-8-yl)urea (55.0 g, 319.4 mmol, 1.00 equiv) and sodium acetate (52.0 g, 638.9 mmol, 2.00 equiv) in $Et_2O$ (600 mL) was added liquid $N_2O_4$ (39 g, 425 mmol, 1.33 equiv) dissolved in $Et_2O$ (500 mL) at -45 °C. The mixture was subsequently stirred at 0-10 °C for 1.5 h. After stirring, the solids were filtered off, washed with cold $Et_2O$ (3 X 30 mL) which was kept in order to be worked up later. The solid residue was extracted with DCM until only white precipitate remained on the filter. This necessitated some 20 X 50 mL DCM. The combined DCM extracts were concentrated by rotary evaporation, 50 mL hexane was added, and the resulting yellow precipitate was filtered giving 1-((1R,7S,8r)-3,5-dioxabicyclo [5.1.0]octan-8-yl)-1-nitrosourea (38 g, 59%). A second batch of product was obtained from the remaining $Et_2O$ reaction solution. The $Et_2O$ reaction solution was washed several times with cold saturated $NaHCO_3$ and concentrated to 40 mL by rotary evaporation. To this concentrate was added hexanes (20 mL). Filtration of the precipitate gave an additional 8 g (13%) of 1-((1R,7S,8r)-3,5-dioxabicyclo[5.1.0]octan-8-yl)-1-nitrosourea with a combined yield of 46 g (72%).

$^{1}$H NMR (250 MHz, DMSO-$d_6$) δ 7.98 (s, 1H), 7.84-7.56 (m, 1H), 4.80 (d, J = 7.4 Hz, 1H), 4.27-4.06 (m, 3H), 3.93 (d, J = 12.8 Hz, 2H), 2.57 (t, J = 4.5 Hz, 1H), 1.37 (t, J = 3.3 Hz, 2H); $^{13}$C NMR (63 MHz, DMSO-$d_6$) δ 154.00, 99.05, 68.23, 27.64, 26.18.

**(E)-2-((5,8-dihydro-4H-1,3-dioxocin-5-yl)oxy)ethanol (22)**

1-((1R,7S,8r)-3,5-dioxabicyclo[5.1.0]octan-8-yl)-1-nitrosourea (2.0 g, 10 mmol, 1.0 equiv) and sodium bicarbonate (1.68 g, 20 mmol, 2.0 equiv) were mixed and to the mixture ethylene glycol (8 mL, 128 mmol, 12.8 equiv) was added. The resulting suspension was stirred until the yellow color disappeared (4 h), then the crude reaction mixture was added to saturated aqueous $NaNO_3$ (40 mL) and was extracted with THF (4 X 15 mL). Most of the THF was removed on a rotary evaporator, to the residue saturated aqueous $NaNO_3$ (30 mL) was added and the mixture was extracted using THF (3 X 10 mL) again. The resulting THF solution was extracted with a 16% by weight aqueous $AgNO_3$ solution (30 mL). The aqueous phase was washed with THF (3 X 10 mL), which was discarded. Solid NaCl was added to give a saturated salt solution. The resulting precipitates were filtered, washed with a small amount of water and THF. The filtrate was then extracted with THF (4 X 15 mL). The combined THF phases were dried over $MgSO_4$ and the solvent was removed by rotary evaporation. This gave 850 mg of crude product. Purification on a Redisep Gold Diol column (50 g) using 100% $Et_2O$ as eluent and a flow rate of 20 mL/min afforded (E)-2-((5,8-dihydro-4H-1,3-dioxocin-5-yl)oxy)ethanol (550 mg, 32%) with a purity of 95%.

$^{1}$H NMR (500 MHz, $CDCl_3$) δ 6.18 (ddd, J = 16.9, 10.7, 3.5 Hz, 1H), 5.82 (dd, J = 16.7, 9.3 Hz, 1H), 5.20 (d, J = 8.1 Hz, 1H), 4.52 (dd, J = 9.6, 3.6 Hz, 1H), 4.31 (td, J = 9.0, 5.3 Hz, 1H), 4.24 (m, 2H), 4.00 (t, J = 10.2 Hz, 1H), 3.80-3.75 (m, 2H), 3.75 – 3.69 (m, 1H), 3.65-3.59 (m, 1H), 3.22 (dd, J=11.6, 8.9 Hz, 1H); $^{13}$C NMR (126 MHz, $D_2O$) δ 138.52, 135.42, 97.48, 82.55, 75.95, 73.08, 70.88, 60.35; HRMS (ESI) calcd. for $C_8H_{15}O_4$ $[M+H]^+$: 175.0965, found: 175.0971.

**8,8-dibromo-3,5-dioxabicyclo[5.1.0]octane (23)[77]**

In an adaption of literature procedures[78], bromoform (28.6 g, 112 mmol, 1.50 equiv), cetrimonium bromide (2.25 g, 6.1 mmol, 0.08 equiv), $Et_3N$ (2 drops) and DCM (20 mL) were mixed and stirred for 20 min. To this solution was added 4,7-dihydro-1,3-dioxepine (7.53 g, 75.3 mmol, 1.00 equiv) and stirring was continued for an additional 10 min. The mixture was cooled in a NaCl/ice bath and 60 g of a 50% aqueous NaOH solution was added dropwise. After stirring the resulting brown suspension for 40 h at room temperature, 30 mL water, 30 mL DCM and 3 g activated charcoal were added. Following filtration of the mixture, the two phases of the filtrate were separated and then the aqueous phase was extracted using DCM (3 X 20 mL). The combined DCM phases were dried over $MgSO_4$, the solvent was removed by rotary evaporation and the crude product was purified by flash chromatography on silica gel (80 g, 60 mL/min flow rate) using 5% EtOAc in hexane as eluent. Fractions containing the product were combined and the solvent was removed giving a yellow oil which partially solidified. Trituation with 10 mL pentane at 0 °C gave pure 8,8-dibromo-3,5-dioxabicyclo [5.1.0]octane (12.6 g, 62%) as white crystals. The product can be visualized on TLC in UV if concentrated ($R_f$=0.21 using 5% EtOAc in hexane).

$^1$H NMR (250 MHz, $CDCl_3$) δ 5.05 (d, J = 7.1 Hz, 1H), 4.68-4.53 (m, 2H), 4.49 (d, J = 7.1 Hz, 1H), 3.63 (dd, J = 13.2, 6.5 Hz, 2H), 2.23 (dd, J = 8.5, 4.5 Hz, 2H); $^{13}$C NMR (63 MHz, $CDCl_3$) δ 101.37, 71.83, 35.35, 34.70.

**(1R,7S,8s)-8-bromo-3,5-dioxabicyclo[5.1.0]octane (24)[77]**

In an adaptation of the literature procedures, 8,8-dibromo-3,5-dioxabicyclo[5.1.0] octane (5.44g, 20 mmol, 1.00 equiv) was dissolved in anhydrous $Et_2O$ (80 mL) under nitrogen. The solution was cooled to -78 °C in a dry ice/acetone bath and n-BuLi (14 mL, 1.6 M in hexane, 22.4 mmol, 1.12 equiv) was added slowly via cannula alongside the inner wall of the flask. During the addition a white precipitate formed. The heterogeneous mixture was kept at -78 °C for 80 min, then 3 mL of methanol was added and stirring was continued for an additional 40 min at -78 °C. Water (0.5 mL) was then added to quench the reaction and the mixture was allowed to warm to room temperature. The mixture was dried by addition of $MgSO_4$ and then filtered. The solvents were evaporated and the crude product was dissolved in pentane and filtered again. The pentane was removed by rotary

evaporation. The resulting light yellow oil was trituated with 5 mL pentane at –10 °C giving pure (1R,7S,8s)-8-bromo-3,5-dioxabicyclo [5.1.0]octane (2.44 g, 63%) as white crystals.

$^{1}$H NMR (500 MHz, $CDCl_3$) δ 4.88 (d, J = 7.2 Hz, 1H), 4.21 (dt, J = 13.0, 2.0 Hz, 2H), 4.17 (d, J = 7.3 Hz, 1H), 4.00-3.81 (m, 2H), 3.24 (tt, J = 4.1, 0.6 Hz, 1H), 1.65-1.62 (m, 2H); $^{13}$C NMR (63 MHz, $CDCl_3$) δ 99.75, 68.44, 28.43, 18.25.

**(E)-2-(cyclooct-2-en-1-yloxy)ethanol (28)**

To (1R,7S,8r)-8-bromobicyclo[5.1.0]octane (1.01g, 5.3 mmol, 1.00 equiv) was added ethylene glycol (2 mL). To this solution was added $AgClO_4$ (2.2 g, 10.6 mmol, 2.00 equiv) in ethylene glycol (4 mL). The resulting mixture was stirred for 7 h, after filtration, the remaining solids were washed with DCM. The combined filtrates were added to 10% $AgNO_3$ solution (30 mL). This was extracted four times with DCM. These DCM extracts were discarded. To the aqueous phase NaCl was added to obtain a saturated salt solution. The resulting precipitate was filtered and washed with DCM (4 X 10 mL). The organic and aqueous phases were separated, and the aqueous phase extracted with DCM (5 X 15 mL). The combined organic phases were dried with anhydrous $MgSO_4$ and concentrated by rotary evaporation, affording 700 mg (78%) of product with a purity of 90-95%. The sample was purified by flash chromatography on **RedisepGold** silica gel (24g, 35ml/min flow rate) for analytical purposes employing a gradient of 10 to 15 % EtOAc in hexane over 11.5 minutes, giving pure (E)-2-(cyclooct-2-en-1-yloxy)ethanol (550 mg, 79% recovery).

$^{1}$H NMR (500 MHz, $CDCl_3$) δ 5.72 (ddd, J = 15.2, 11.0, 3.7 Hz, 1H), 5.48 (dd, J = 16.2, 9.4 Hz, 1H), 3.94 (td, J = 9.8, 5.5 Hz, 1H), 3.79-3.70 (m, 2H), 3.70- 3.62 (m, 1H), 3.56-3.49 (m, 1H), 2.45-2.37 (m, 1H), 2.22-2.14 (m, 2H), 2.06-1.91 (m, 2H), 1.92-1.73 (m, 2H), 1.56-1.44 (m, 1H), 1.46-1.33 (m, 1H), 0.94-0.84 (m, 1H), 0.81-0.71 (m, 1H); $^{13}$C NMR (126 MHz, $CDCl_3$) δ 134.83, 133.72, 84.47, 70.19, 61.97, 41.52, 35.65, 35.51, 28.98, 27.50; HRMS (ESI) calcd. for $C_{10}H_{19}O_2$ $[M+H]^+$: 171.1380, found: 171.1388; calcd. for $C_{10}H_{21}NO_2$ $[M+NH_4]^+$: 188.1645, found: 188.1654.

**Cyclohept-4-enone (29)[79]**

For the preparation of 1-acyl-2-vynilcyclopropanecarboxylates we followed literature procedure[64] with slight modifications: we used cis dichloro butane instead of cis dibromo butane. Reaction time was 30 h, the crude product (83%) was a 3:1 mixture of isomers, used without further purification.

For the preparation of cyclohept-4-enone we followed literature procedure (35%, 47% based on the major isomer).

$^1$H NMR (500 MHz, $CDCl_3$) δ 5.77 (ddd, J = 3.6, 2.8, 0.7 Hz, 2H), 2.70-2.55 (m, 4H), 2.40-2.25 (m, 4H); $^{13}$C NMR (126 MHz, $CDCl_3$) δ 213.53, 129.42, 42.37

**(Z)-3,4,7,8-tetrahydroazocin-2(1H)-one (32)[65]**

Literature reference was used: the first stage (the preparation of 4-cycloheptenone oxime) was complete after 2 h at room temperature, the yield was 99%. (Z)-3,4,7,8-tetrahydroazocin-2(1H)-one was purified on 40 g **RedisepGold** silica column using 20 mL/min flow for 30 minutes with a DCM (1% MeOH) to DCM (10% MeOH) gradient. 78% overall yield.

$^1$H NMR (400 MHz, $CDCl_3$) δ 6.01 (s, 1H), 5.79 (dtd, J = 12.0, 7.2, 1.6 Hz, 1H), 5.55 (dt, J = 11.5, 5.9 Hz, 1H), 3.49 (q, J = 6.7 Hz, 2H), 2.67 (t, J = 7.3 Hz, 2H), 2.50 (t, J = 7.3 Hz, 2H), 2.44 (q, J = 6.3, 5.4 Hz, 2H); $^{13}$C NMR (101 MHz, $CDCl_3$) δ 176.70, 129.30, 126.79, 40.57, 34.44, 30.23, 24.59.

**(Z)-1-(hydroxymethyl)-3,4,7,8-tetrahydroazocin-2(1H)-one (33)**

(Z)-3,4,7,8-tetrahydroazocin-2(1H)-one (3.0g (90% pure), 21.6 mmol, 1.0 equiv), formaldehyde (7.2 mL, 37% in water, 84 .0 mmol, 3.5 equiv) and KOH (66 mg, 1.2 mmol, 0.05 equiv) were mixed in ethanol (20 mL) and refluxed for 84 h. Took sample after 36 h, but the reaction was not completed yet. The solvent was removed from the reaction mixture and saturated $NaHCO_3$ was added to the residue. Extraction several times with DCM, drying over anhydrous $MgSO_4$ and removal of the solvent provided a dense oil. Trituation with $Et_2O$ gave 1.6 g of white crystals. Flash chromatography gave 1.2 g more product. Used DCM (1% MeOH) to DCM (7% MeOH) as gradient on a 40 g

**RedisepGold** silica column using 20 mL/min flow for 30 minutes. Product came around 20 minutes. 2.8 g, 83%.

$^{1}$H NMR (500 MHz, $CDCl_3$) δ 5.75 (dtt, J = 10.7, 7.4, 1.6 Hz, 1H), 5.57-5.48 (m, 1H), 4.77 (s, 2H), 3.71 (t, J = 6.6 Hz, 2H), 2.73 (dd, J = 8.2, 6.8 Hz, 2H), 2.57-2.36 (m, 4H); $^{13}$C NMR (126 MHz, $CDCl_3$) δ 175.72, 128.70, 127.10, 72.82, 46.82, 34.90, 28.82, 24.67; calcd. for $C_8H_{13}NNaO_2$ $[M+Na]^+$: 178.0838, found: 178.0843.

**(Z)-8-(2-(2-(2-methoxyethoxy)ethoxy)ethoxy)cyclooct-4-enol (36)**

(Z)-8-(2-(2-(2-methoxyethoxy)ethoxy)ethoxy)cyclooct-4-enol was prepared via a procedure analogous to literature methods[66]. Epoxide 9-oxabicyclo[6.1.0]nonane (10.8 g, 86 mmol, 1.0 equiv), tri(ethylene glycol)monomethyl ether (17.0 g, 103 mmol, 1.2 equiv) and erbium triflate (5.3 g, 8.6 mmol, 0.1 equiv) were mixed in this order and stirred overnight in a closed flask. The reaction was quenched with the addition of saturated $NaHCO_3$. The precipitate was filtered and washed several times with DCM. The aqueous filtrate was extracted with DCM, the combined DCM phases were dried over anhydrous $MgSO_4$, and the solvents were removed via rotary evaporation. Short path distillation gave 4 g of tri(ethylene glycol)monomethyl ether (at 0.1 torr, 40-60 °C bath temperature) and (Z)-8-(2-(2-(2-methoxyethoxy)ethoxy)ethoxy)cyclooct-4-enol (10.3 g, 41%), which distilled at 0.1 torr, and a bath temperature of 140-160 °C. The distilled (Z)-8-(2-(2-(2-methoxyethoxy) ethoxy) ethoxy)cyclooct-4-enol contained 5% tri(ethylene glycol) monomethyl ether and was used in subsequent reactions without further purification.

$^{1}$H NMR (500 MHz, $CDCl_3$) δ 5.68-5.40 (m, 2H), 3.78-3.72 (m, 1H), 3.72-3.63 (m, 1H), 3.63-3.56 (m, 8H), 3.56-3.46 (m, 3H), 3.35-3.29 (m, 4H), 2.52-2.22 (m, 2H), 2.21-1.93 (m, 4H), 1.73-1.44 (m, 2H); $^{13}$C NMR (126 MHz, $CDCl_3$) δ 129.58, 128.10, 83.08, 72.97, 71.75, 70.44, 70.41, 70.37 (two overlapping signals), 69.28, 58.85, 32.07, 29.59, 23.20, 22.67; calcd. for $C_{15}H_{29}O_5$ $[M+H]^+$: 289.2010, found: 289.2020.

**(E)-8-(2-(2-(2-methoxyethoxy)ethoxy)ethoxy)cyclooct-4-enol (37)**

(Z)-8-(2-(2-(2-methoxyethoxy)ethoxy)ethoxy)cyclooct-4-enol (5.2 g, 18 mmol, 1.0 equiv) and methyl benzoate (2.5 g, 18 mmol, 1.0 equiv) were dissolved in 500 mL of a 4:1 $Et_2O$/hexanes mixture. The solution was subjected to UV irradiation for 20 h in a

photochemical reactor according to literature procedures[21]. The column used for the continuous separation of the product from the reaction mixture contained 7 g silica on the bottom and 35 g $AgNO_3$ impregnated silica on the top (10% $AgNO_3$ content). After 20 h, the product-$AgNO_3$ complex was eluted from the silica column using 500 mL $Et_2O$ containing 20% DCM and 20% MeOH. The resulting organics were extracted using an aqueous 10% $AgNO_3$ solution (3 X 30 mL). The combined aqueous phases were washed with DCM (5 X 20 mL), which was discarded. To the aqueous phase brine was added, the solids were filtered, washed with DCM, and the filtrate was extracted with DCM (5 X 20 mL). The combined DCM phases were dried over anhydrous $MgSO_4$ and the solvent was removed by rotary evaporation. This gave 3.3 g (64%) of product as a 1:1 mixture of two trans isomers. Attempts to separate the two isomers on silica failed.

$^1$H NMR (500 MHz, $CDCl_3$) δ 5.69 (ddd, J = 16.0, 10.8, 3.6 Hz, 1H), 5.53 (ddd, J = 16.1, 10.7, 3.8 Hz, 1H), 5.47-5.36 (m, 2H), 4.07 (ddd, J = 8.2, 6.3, 1.7 Hz, 1H), 3.74-3.57 (m, 20H), 3.56-3.51 (m, 4H), 3.47 (dddd, J = 9.9, 5.4, 3.0, 1.5 Hz, 2H), 3.36 (two overlapping singlets, 6H), 3.20 (ddd, J = 10.7, 4.9, 1.5 Hz, 1H), 2.43-1.84 (m, 12H), 1.80-1.59 (m, 4H); $^{13}$C NMR (126 MHz, $CDCl_3$) δ 135.36, 132.89, 132.56, 132.47, 85.15, 80.28, 76.27, 71.82, 71.79, 70.97, 70.74, 70.72, 70.61, 70.58, 70.49, 70.42, 68.72, 58.88, 41.12, 38.44, 36.83, 33.00, 32.88, 32.47, 27.65, 27.50; HRMS (ESI) calcd. for $C_{15}H_{29}O_5$ $[M+H]^+$: 289.2010, found: 289.2015.

**(Z)-8-((2-(2-hydroxyethoxy)ethyl)amino)cyclooct-4-enol (38)**

To 9-oxabicyclo[6.1.0]nonane (3.0 g, 24 mmol, 1.0 equiv) was added 2-(2-aminoethoxy) ethanol (4.8 g, 48 mmol, 2.0 equiv) and the resulting mixture was heated in a microwave reactor for 1 h at 130 °C in constant temperature mode. After 1 h, the reaction was not complete, so heating was continued for 1 h at 150 °C. Trituration of the cooled reaction mixture with $Et_2O$ afforded 2.0 g of white crystals.

An additional batch of (Z)-8-((2-(2-hydroxyethoxy)ethyl)amino)cyclooct-4-enol was obtained from the reaction filtrate. First, the filtrate was concentrated in vacuuo, dissolved in excess 1N HCl, and washed with DCM (5 X 30 mL). The organic phase was discarded. The aqueous phase was basified by addition of 6N NaOH and extracted with DCM (8 X 30 mL). The combined DCM phases were dried over anhydrous $MgSO_4$, the solvent was removed by rotary evaporation and the residue was seeded with crystals from the initial

batch of product. Trituation with $Et_2O$ afforded an additional 2.6 g of white crystals. The overall yield of (Z)-8-((2-(2-hydroxyethoxy)ethyl)amino)cyclooct-4-enol was 4.6 g (85%).

$^1$H NMR (500 MHz, $CDCl_3$) δ 5.62 (dt, J = 10.8, 7.1 Hz, 1H), 5.49 (dddd, J = 10.6, 8.3, 7.0, 1.2 Hz, 1H), 3.65 (td, J = 4.5, 0.9 Hz, 2H), 3.57-3.44 (m, 4H), 3.32 (dddd, J = 8.7, 7.7, 3.5, 0.9 Hz, 1H), 2.94 (dddd, J = 12.7, 7.4, 4.3, 1.0 Hz, 1H), 2.62 (dddd, J = 12.9, 4.8, 3.7, 1.0 Hz, 1H), 2.50-2.40 (m, 1H), 2.37-2.28 (m, 1H), 2.22-2.05 (m, 3H), 2.01 (ddt, J = 14.4, 7.2, 4.9 Hz, 1H), 1.97-1.87 (m, 1H), 1.44-1.28 (m, 2H); $^{13}$C NMR (126 MHz, $CDCl_3$) δ 130.41, 128.01, 72.34, 71.76, 70.18, 61.22, 60.69, 48.03, 34.45, 32.35, 22.88, 22.72; HRMS (ESI) calcd. for $C_{12}H_{24}NO_3$ $[M+H]^+$: 230.1751, found: 230.1753.

**(Z)-3-(2-(2-hydroxyethoxy)ethyl)-3,3a,4,5,9,9a-hexahydrocycloocta[d]oxazol-2(8H)-one (39)**

(Z)-8-((2-(2-hydroxyethoxy)ethyl)amino)cyclooct-4-enol (12.9 g, 56 mmol, 1.0 equiv) and N,N′-disuccinimidyl carbonate (15.1 g, 59 mmol, 1.05 equiv) were mixed and then acetonitrile (20 mL) was added. The mixture was cooled in ice bath and $Et_3N$ (12.5 g, 124 mmol, 2.2 equiv) was added in three portions, which gave a homogenous solution. Upon allowing the solution to stir overnight, a white precipitate formed. To the reaction mixture was added $Et_2O$ (100 mL). After cooling to 5 °C, the precipitate was filtered off and discarded. The filtrate was concentrated and purified on **RedisepGold** silica gel column (80 g, 20 mL/min flow rate) by flash chromatography using a gradient from 1 to 5% MeOH in DCM over 25 minutes. Upon solvent removal, pure (Z)-3-(2-(2-hydroxyethoxy)ethyl)-3,3a,4,5,9,9a-hexahydrocycloocta[d]oxazol- 2(8H)-one (13.2 g, 92%) was obtained as a viscous oil.

$^1$H NMR (500 MHz, $CDCl_3$) δ 5.82-5.53 (m, 2H), 4.31 (dddd, J = 12.4, 8.6, 3.9, 1.4 Hz, 1H), 3.72 (ddt, J = 19.0, 8.1, 4.3 Hz, 3H), 3.67-3.49 (m, 5H), 3.24 (dddd, J = 14.6, 5.9, 4.2, 1.4 Hz, 1H), 2.44-2.05 (m, 6H), 1.72-1.51 (m, 1H), 1.40-1.31 (m, 1H); $^{13}$C NMR (126 MHz, $CDCl_3$) δ 157.91, 129.71, 129.07, 80.07, 72.32, 68.60, 61.75, 61.17, 41.48, 31.65, 29.25, 21.66, 21.01; HRMS (ESI) calcd. for $C_{13}H_{21}NNaO_4$ $[M+H]^+$: 278.1363, found: 278.1374..

**(E)-3-(2-(2-hydroxyethoxy)ethyl)-3,3a,4,5,9,9a-hexahydrocycloocta[d]oxazol-2(8H)-one (40)**

(Z)-3-(2-(2-hydroxyethoxy)ethyl)-3,3a,4,5,9,9a-hexahydrocycloocta[d]oxazol-2(8H)-one (3.8 g, 14.8 mmol, 1.0 equiv) and methyl benzoate (2.0 g, 14.8 mmol, 1.0 equiv) were dissolved in $Et_2O$ (470 mL) containing 1% MeOH. The solution was subjected to UV irradiation for 80 h in a photochemical reactor according to literature procedures[21]. The column used for the continuous separation of the product from the reaction mixture contained 7 g silica on the bottom and 35 g $AgNO_3$ impregnated silica on the top (10% $AgNO_3$ content). During the course of the reaction the quartz reaction flask was changed twice (at 30 h and 60 h) due to silver plating out in the reaction vessel.

After 80 h, the column was washed using 500 mL $Et_2O$ containing 5% MeOH. This solution was discarded. The column was then washed with MeOH (500 mL) to elute the product-$AgNO_3$ complex. The MeOH was removed by rotary evaporation at 30 °C and 30 mL of 10% aqueous $AgNO_3$ was added. This solution was washed with DCM (8 X 10 mL), which was discarded. Brine was added to the remaining aqueous solution, the solids were removed by filtration, washed with DCM and the filtrate was extracted with DCM several times. The combined DCM phases were dried over anhydrous $MgSO_4$ and the solvent was removed by rotary evaporation. This gave 3.1 g (82%) of product as a 4:1 mixture of two trans isomers.

$^1$H NMR (500 MHz, $CDCl_3$) δ 5.86 (apparent t, J = 4.3 Hz, 2H), 5.59-5.41 (m, 8H), 4.22 (apparent t, J = 9.3 Hz, 1H), 4.16-4.06 (m, 4H), 3.74-3.69 (m, 10H), 3.66-3.51 (m, 26H), 3.28- 3.19 (m, 5H), 2.59- 2.47 (m, 2H), 2.47- 2.27 (m, 18H), 2.27-2.13 (m, 12H), 2.13-2.02 (m, 2H), 1.91 (apparent qd, J = 12.0, 5.4 Hz, 4H), 1.84-1.72 (m, 1H), 1.63-1.48 (m, 5H); $^{13}$C NMR (126 MHz, $CDCl_3$) δ 157.82, 157.13, 135.96, 135.78, 134.22, 132.61, 83.63, 83.50, 72.31, 72.27, 68.46, 68.44, 64.93, 64.77, 61.65, 53.37, 41.89, 41.68, 40.27, 38.36, 37.41, 34.58, 31.93, 31.79, 25.20, 24.97; calcd. for $C_{13}H_{21}NNaO_4$ $[M+Na]^+$: 278.1363, found: 278.1375.

**(E)-2-((5,8-dihydro-4H-1,3-dioxocin-5-yl)oxy)ethyl (2,5-dioxopyrrolidin-1-yl) carbonate (41)**

(E)-2-((5,8-dihydro-4H-1,3-dioxocin-5-yl)oxy)ethanol (261 mg, 1.5 mmol, 1.0 equiv), *N,N′*-Disuccinimidyl carbonate (769 mg, 3.0 mmol, 2.0 equiv) and triethyl amine (455 mg,

630 μL, 4.5 mmol, 3.0 equiv) were mixed in MeCN (3 mL) under $N_2$ atmosphere and stirred for 5 h in the dark. Solvents were removed at 24 °C under vacuum and then purification of the crude product was performed on a Redisep Gold Diol column (50 g) using pentane (10% DCM) to 100% DCM gradient for 40 minutes at a flow rate of 30 mL/min. Removal of the solvent gave 390 mg (83%) of white foam of 95% purity.

$^1$H NMR (500 MHz, $CDCl_3$) δ 6.18 (dd, J = 16.3, 11.3 Hz, 1H), 5.90-5.81 (m, 1H), 5.18 (dd, J = 8.0, 2.8 Hz, 1H), 4.50 (dt, J = 9.3, 3.8 Hz, 2H), 4.44 (dd, J = 10.5, 5.8 Hz, 1H), 4.35- 4.25 (m, 2H), 4.21 (dd, J = 11.2, 6.9 Hz, 1H), 4.01 (td, J = 10.1, 2.6 Hz, 1H), 3.92-3.84 (m, 1H), 3.79 (dd, J = 11.2, 6.2 Hz, 1H), 3.28- 3.20 (m, 1H), 2.90- 2.79 (m, 4H); $^{13}$C NMR (101 MHz, $CDCl_3$) δ 168.50, 151.61, 138.00, 136.66, 98.37, 83.57, 77.08, 73.27, 69.80, 67.20, 25.42; HRMS (ESI) calcd. for $C_{13}H_{18}NO_8$ $[M+H]^+$: 316.1027, found: 319.1035; calcd. for $C_{13}H_{21}N_2O_8$ $[M+NH_4]^+$: 333.1292, found: 333.1300.

**(E)-2,5-dioxopyrrolidin-1-yl-(8-(2-(2-(2-methoxyethoxy)ethoxy)ethoxy)cyclooct-4-en-1-yl) carbonate (42)**

(E)-8-(2-(2-(2-methoxyethoxy)ethoxy)ethoxy)cyclooct-4-enol (1440 mg, 5.0 mmol, 1.0 equiv), *N,N'*-Disuccinimidyl carbonate (1538 mg, 6.0 mmol, 1.2 equiv) and triethyl amine (880 mg, 1200 μL, 8.75 mmol, 1.75 equiv) were mixed in MeCN (5 mL) under $N_2$ atmosphere and stirred for 2 and a half days in the dark. T the reaction mixture $Et_2O$ (20 mL) was added, the precipitate was filtered and washed with DCM (2 mL). From the filtrate the solvents were removed at 24 °C under vacuum and then purification of the crude product was performed on a silica flash column (80 g) using DCM (1% MeOH) to DCM (4% MeOH) gradient for 25 minutes at a flow rate of 60 mL/min. We collected three fractions:

300 mg of first NHS-carbonate, 500 mg of mixture of isomeric NHS-carbonates and 800 mg of starting material. The mixture could be separated on a 40 g **RedisepGold** silica column using a DCM (0.5% MeOH) to DCM (6.5% MeOH) gradient at a flow rate of 35 ml/min for 19 minutes. This gave 270 mg more of the first isomer and 200 mg of the second. 37%.

First isomer:

$^1$H NMR (400 MHz, $CDCl_3$) δ 5.62-5.55 (m, 2H), 5.14 (dd, J = 9.0, 4.2 Hz, 1H), 4.97 (td,

J = 8.9, 3.5 Hz, 1H), 3.98 (dd, J = 9.0, 5.4 Hz, 1H), 3.73 (dd, J = 10.7, 5.7 Hz, 1H), 3.72-3.58 (m, 7H), 3.57-3.51 (m, 2H), 3.48 (dt, J = 9.9, 4.8 Hz, 1H) 3.36 (s, 3H), 2.81 (s, 4H), 2.50- 2.35 (m, 1H), 2.29- 2.06 (m, 4H), 2.05-1.93 (m, 1H), 1.93-1.80 (m, 1H), 1.80-1.70 (m, 1H); $^{13}$C NMR (101 MHz, $CDCl_3$) δ 168.59, 151.01, 133.79, 133.20, 79.63, 76.01, 71.89, 70.73, 70.71, 70.65, 70.53, 68.99, 58.96, 33.12, 31.92, 28.00, 27.82, 25.42; calcd. for $C_{20}H_{35}N_2O_9$ $[M+NH_4]^+$: 447.2337, found: 447.2362.

Second isomer:

$^1$H NMR (400 MHz, $CDCl_3$) δ 5.52 (ddd, J = 10.2, 8.8, 3.4 Hz, 2H), 4.61 (ddd, J = 11.2, 4.8, 1.5 Hz, 1H), 3.82- 3.73 (m, 2H), 3.73- 3.62 (m, 8H), 3.58- 3.54 (m, 2H), 3.43 (dt, J = 8.4, 4.4 Hz, 1H), 3.38 (s, 3H), 2.81 (s, 4H), 2.52-2.41 (m, 1H), 2.41-2.16 (m, 4H), 2.11-1.99 (m, 3H); $^{13}$C NMR (101 MHz, $CDCl_3$) δ 168.80, 151.40, 133.68, 132.22, 85.83, 84.51, 77.20, 72.03, 71.94, 70.61, 70.43, 59.01, 38.82, 37.90, 32.64, 32.22, 25.47; calcd. for $C_{20}H_{35}N_2O_9$ $[M+NH_4]^+$: 447.2337, found: 447.2345.

**(E)-2,5-dioxopyrrolidin-1-yl(2-(2-(2-oxo-4,5,9,9a-tetrahydrocycloocta[d]oxazol-3(2H, 3aH, 8H)-yl)ethoxy)ethyl) carbonate (43)**

(E)-3-(2-(2-hydroxyethoxy)ethyl)-3,3a,4,5,9,9a-hexahydrocycloocta[d]oxazol-2(8H)-on (510 mg, 2.0 mmol, 1.0 equiv), *N,N'*-Disuccinimidyl carbonate (615 mg, 2.4 mmol, 1.2 equiv) and triethyl amine (354 mg, 490 µL, 3.5 mmol, 1.75 equiv) were mixed in MeCN (3 mL) under $N_2$ atmosphere and stirred for 3.5 h in the dark. Solvents were removed at 24 °C under vacuum and then purification of the crude product was performed on a silica column (24 g) using DCM (0.5% MeOH) to DCM (3% MeOH) gradient for 19 minutes at a flow rate of 25 mL/min. Removal of the solvent gave 560 mg (71%) of white foam. The first fractions contained enhanced quantity of the major isomer.

$^1$H NMR (400 MHz, $CDCl_3$) δ 5.99-5.81 (m, 1H), 5.70-5.42 (m, 6H), 4.53-4.40 (m, 6H), 4.26 (t, J = 9.6 Hz, 1H), 4.15 (dd, J = 10.7, 6.5 Hz, 3H), 3.84-3.50 (m, 20H), 3.32-3.21 (m, 3H), 2.85 (s, 14H), 2.73 (s, 1H), 2.53 (dt, J = 15.8, 8.1 Hz, 1H), 2.48-2.15 (m, 18H), 1.97 (apparent qd, J = 11.9, 5.2 Hz, 3H), 1.80 (dt, J = 21.9, 10.6 Hz, 1H), 1.72-1.48 (m, 6H); $^{13}$C NMR (101 MHz, $CDCl_3$) δ 168.45, 157.07, 151.66, 134.33, 132.81, 83.75, 70.09, 69.35, 68.12, 65.42, 41.79, 38.39, 34.73, 31.96, 31.95, 25.46; calcd. for $C_{18}H_{25}N_2O_8$

$[M+H]^+$: 397.1605, found: 397.1597.

**AZD2281-DO-TCO (45)**

4- [ [ 4-Fluoro- 3- (4- (N- (2-aminoethyl) -5-oxo-pentanamide) piperazine-1-carbonyl) phenyl] methyl]-2H-phthalazin-1-one (7.4 mg, 14.06 μmol, 1.0 equiv) was dissolved in DMF (300 μL) and triethyl amine (4.2 mg, 5.8 μL, 42.18 μmol, 3.0 equiv) was added. Then (E)-2-((5,8-dihydro-4H-1,3-dioxocin-5-yl)oxy)ethyl (2,5-dioxopyrrolidin-1-yl) carbonate (5.4 mg, 17.02 μmol, 1.2 equiv) in DCM (2 X 100 μL) was added to the mixture. The reaction was run for 30 minutes in the dark and then the crude mixture was directly loaded on a Biotage SNAP 10 g KP-C18-HS cartridge and purified applying a water (5% MeCN) to water (95% MeCN) gradient during 20 min at 15 mL/min flow rate. Lyophilization gave 5.4 mg (54%) of white powder.

$^1$H NMR (400 MHz, $CDCl_3$) δ 8.47 (d, J = 7.9 Hz, 1H), 7.87-7.69 (m, 3H), 7.39-7.29 (m, 2H), 7.07 (t, J = 8.8 Hz, 1H), 6.26 (s, 1H), 6.16 (ddd, J = 16.0, 10.5, 3.3 Hz, 1H), 5.82 (dd, J = 16.7, 9.2 Hz, 1H), 5.19 (d, J = 8.1 Hz, 1H), 4.50 (dd, J = 9.6, 3.5 Hz, 1H), 4.29 (s, 2H), 4.29-4.16 (m, 4H), 3.99 (t, J = 10.1 Hz, 1H), 3.85-3.75 (m, 3H), 3.75-3.65 (m, 3H), 3.60-3.45 (m, 3H), 3.45-3.30 (m, 6H), 3.25-3.17 (m, 1H), 2.46 (t, J = 6.9 Hz, 1H), 2.44-2.34 (m, 1H), 2.29 (t, J = 6.5 Hz, 2H), 1.97 (td, J = 14.1, 13.4, 6.5 Hz, 2H); calcd. for $C_{36}H_{44}FN_6O_9$ $[M+H]^+$: 723.3148, found: 723.3163

**AZD2281-3PEGMe-TCO (46)**

4- [ [ 4-Fluoro- 3- (4- (N- (2-aminoethyl) -5-oxo-pentanamide) piperazine-1-carbonyl) phenyl] methyl]-2H-phthalazin-1-one (7.4 mg, 14.06 μmol, 1.0 equiv) was dissolved in DMF (300 μL) and triethyl amine (4.2 mg, 5.8 μL, 42.18 μmol, 3.0 equiv) was added. Then (E)-2,5-dioxopyrrolidin-1-yl- (8- (2- (2- (2-methoxyethoxy)ethoxy)ethoxy)cyclooct-4-en-1-yl) carbonate (9.0 mg, 20.96 μmol, 1.5 equiv) in DCM (2 X 100 μL) was added to the mixture. The reaction was run for 30 minutes in the dark and then the crude mixture was directly loaded on a Biotage SNAP 10 g KP-C18-HS cartridge and purified applying a water (5% MeCN) to water (95% MeCN) gradient during 20 min at 15 mL/min flow rate. Lyophilization gave 8.3 mg (70%) of white powder.

$^1$H NMR (400 MHz, $CDCl_3$) δ 8.50-8.43 (m, 1H), 7.84-7.69 (m, 3H), 7.33 (dd, J = 8.0,

4.9 Hz, 2H), 7.06 (t, J = 8.8 Hz, 1H), 5.82-5.59 (m, 1H), 5.50 (ddd, J = 15.7, 11.3, 3.2 Hz, 1H), 5.22-5.03 (m, 1H), 4.29 (s, 2H), 3.90 (s, 1H), 3.83-3.74 (m, 3H), 3.74-3.62 (m, 10H), 3.60-3.53 (m, 5H), 3.50 (dd, J = 9.7, 4.9 Hz, 1H), 3.39 (broad s, 8H), 2.48 (t, J = 7.0 Hz, 1H), 2.41 (t, J = 6.8 Hz, 1H), 2.30 (t, J = 6.8 Hz, 2H), 2.20 – 2.09 (m, 2H), 2.06-1.90 (m, 4H), 2.90-1.70 (m, 4H), 1.66 (td, J = 14.1, 4.9 Hz, 1H); calcd. for $C_{43}H_{58}FN_6O_{10}$ $[M+H]^+$: 837.4193, found: 837.4195

**AZD2281-OX-TCO (47)**

4- [ [ 4-Fluoro- 3- (4- (N- (2-aminoethyl) -5-oxo-pentanamide) piperazine-1-carbonyl) phenyl] methyl]-2H-phthalazin-1-one (7.4 mg, 14.06 μmol, 1.0 equiv) was dissolved in DMF (300 μL) and triethyl amine (4.2 mg, 5.8 μL, 42.18 μmol, 3.0 equiv) was added. Then, (E)-2,5-dioxopyrro-lidin-1-yl(2-(2-(2-oxo-4,5,9,9a-tetrahydrocycloocta[d]oxazol-3(2H,3aH,8H)- yl)ethoxy)ethyl) carbonate (6.8 mg, 17.02 μmol, 1.2 equiv) in DCM (2 X 100 μL) was added to the mixture. The reaction was stirred for 30 minutes in the dark and then the crude mixture was directly loaded on a Biotage SNAP 10 g KP-C18-HS cartridge and purified applying a water (5% MeCN) to water (95% MeCN) gradient during 20 min at 15 mL/min flow rate. Lyophilization gave 8.3 mg (74%) of white powder.

$^1$H NMR (400 MHz, $CDCl_3$) 8.46 (dd, J = 7.3, 2.5 Hz, 1H), 7.87-7.68 (m, 3H), 7.33 (t, J = 6.1 Hz, 2H), 7.06 (t, J = 8.9 Hz, 1H), 5.64-5.44 (m, 2H), 4.29 (s, 2H), 4.27-4.23 (m, 1H), 4.16 (dd, J = 11.3, 6.4 Hz, 2H), 3.86-3.48 (m, 13H), 3.42-3.11 (m, 8H), 2.51-2.33 (m, 4H), 2.34-2.17 (m, 5H), 2.06-1.88 (m, 3H); calcd. for $C_{41}H_{51}FN_7O_9$ $[M+H]^+$: 804.3727, found: 804.3730.

## 3.3.§. Imaging experiments

### 3.3.1.§. Live cell imaging using COMBO

**Flow citometry experiments:**

Suspension culture U937 cells were cultured in RPMI (PAA, Austria) media, supplemented with 10% FCS (Hyclone) under standard conditions (5% $CO_2$, 37 °C). Cells were treated with or without 25 μM $Ac_4$ManAz metabolic glycoprotein labeling reagent (Invitrogen, UK) for 3 days. Cells were then washed twice with PBS (1,200 rpm, 3 min) and seeded onto 96-well plates at a density of $4\times10^5$/well. Cells were then stained

with COMBO-Flu (diluted in PBS with 0.5% BSA (PBS-0.5% BSA) from a DMSO stock ≥ 1:1000) at 10, 5, 2.5, 1, 0.5, 0.25 μM concentrations for 45 min at room temperature (RT). After then, cells were washed twice with PBS-0.5% BSA (2,000 rpm 2min), fixed with 4% formaldehyde for 5 min RT and washed twice with PBS-0.5% BSA twice again before being re-[redacted]0.5% BSA for FACS analysis.

**Labeling of azido-glycoproteins on HeLa Cells and Imaging by Fluorescence Microscopy**

The HeLa cells were cultured in DMEM (Sigma) media supplemented with 10% fetal calf serum (FCS, Hyclone) under standard conditions (5% $CO_2$, 37 °C). In a typical experiment $5\times10^4$ cells were seeded onto glass bottom culture dishes (P35G-0-20-C, MatTek Corp. Ashland, MA, USA) and treated with or without 50 μM $Ac_4$ManAz metabolic glycoprotein labeling reagent (Invitrogen, UK) for 2 days. Cells were then washed twice with media, stained with 12.5 μM COMBO-Flu (dissolved in DMSO and diluted from stock ≥ 1:1000) in culture media and incubated at 37 °C, 5% $CO_2$ for 1 h with images being taken at 30 min, 45 min and 60 min time-points to follow the staining progress over time. 25 μg/ml Hoechst 33342 dye (Cambridge Bioscience, UK) was also added to the media to stain the nuclei. Cells were imaged without any washing steps by a Zeiss LSM510 incubated confocal microscope (Carl Zeiss, Inc., USA) at 37 °C. Images were captured at a green channel for COMBO-Flu (excitation 488 nm, emission filtered 505-530 nm), a blue channel for Hoechst 33342 (excitation 405 nm, filtered with BP420-480) and at the differential interference correlation (DIC) channel for bright-field images.

### 3.3.2.§. Live cell imaging experiments using TCOs

Cell Lines

HT1080 cells from ATCC were grown in DMEM supplemented with 10% fetal bovine serum, 100 I.U. penicillin, 100 μg/ml streptomycin, and 2 mM L-glutamine.

PARP1-mCherry reporter construct

mCherry Protein tagged to subunit VIII of Poly ADP ribose polymerase 1 (PARP1-mRFP) was utilized to identify PARP target protein. PARP1-mCherry was constructed by PCR of human PARP1 from Open Biosystems clone 5193735 from the NIH_MGC_114 cDNA library, and cloning into pmCherry-N1 (Clontech) between XhoI and XmaI on Multiple Cloning site.

Live cell fluorescence microscopic imaging

HT1080 cells were plated at 5000 cells per well in 96-well black μ-clear bottom plates (Grenier Bio-One) and were grown for 48-72 hrs. One day before imaging, cells were transiently transfected with PARP1-mCherry DNA construct. Briefly, 6 μL of Fugene 6 (Promega) was diluted with 92.4 μL of GIBCO Opti-MEM media for 5 minutes at room temperature. After the incubation, 1.6 μL of PARP1-mCherry DNA construct (1.2 μg/μL) was added to the solution. DNA mixture was incubated at room temperature for 15 minutes. Meanwhile, media of the cells were changed with RPMI media containing 10% FBS without antibiotics. After the incubation of DNA and Fugene 6 mixture solution for 15 minutes, 5 μL of the complex was added to the corresponding wells. Cells were incubated at 37°C 5% $CO_2$ humidified incubator for overnight. Expression of fluorescent protein was briefly checked with fluorescent microscope. 2 μL of 250 μM TCO drug was added to the corresponding wells. After 30 minutes incubation, media was removed and 50 μM CFDA-Tz[80] was added to the corresponding wells. Cells were incubated for 30 minutes. After washing with growth media two times for 5 minutes each, cells were incubated for 2 h washing with the media every 30 minutes. Then they were fixed with 4% paraformaldehyde for 10 minutes. After washing with PBST three times for 5 minutes each, cells were imaged with Delta vision fluorescent microscope.

# 4.§. Appendix

## 4.1.§. Figures for kinetic measurements for the reaction of benzylamino tetrazine and different TCO's

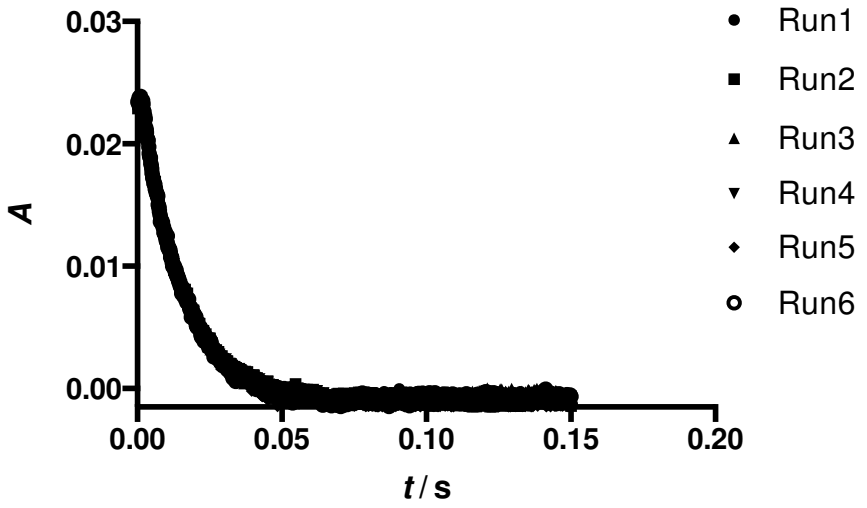


**Figure 38. Absorbance vs time, 75 μM tetrazine, 2.13 mM TCO-OH.**

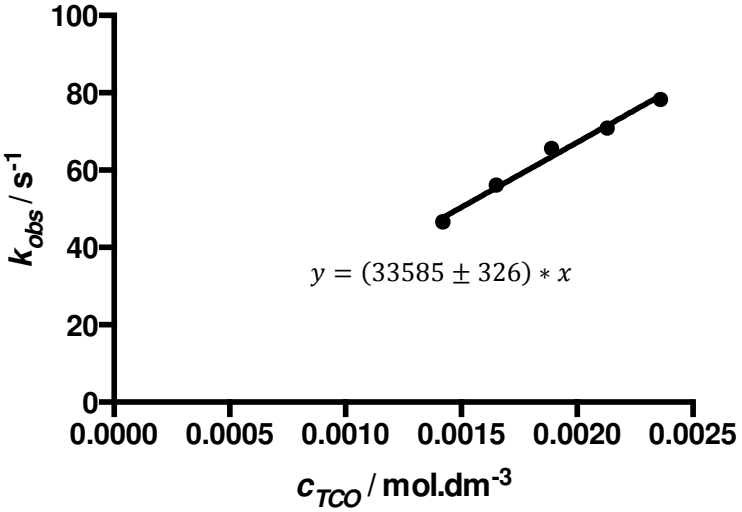


**Figure 39. Linear fit to the pseudo first order rate constants for TCO-OH.**

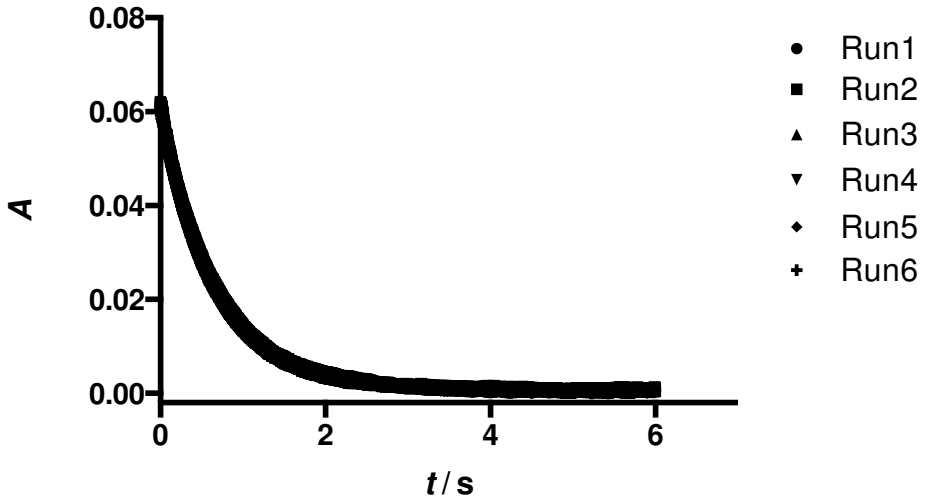


**Figure 40 Absorbance vs time, 150 μM tetrazine, 2.57 mM EG-TCO.**

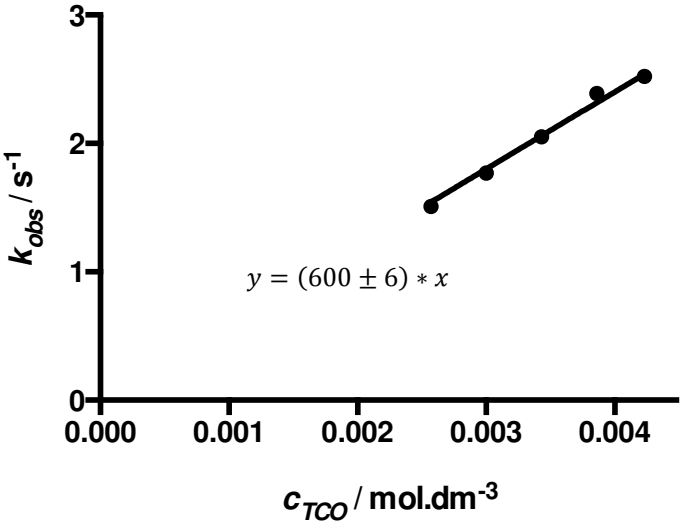


**Figure 41. Linear fit to the pseudo first order rate constants for EG-TCO.**

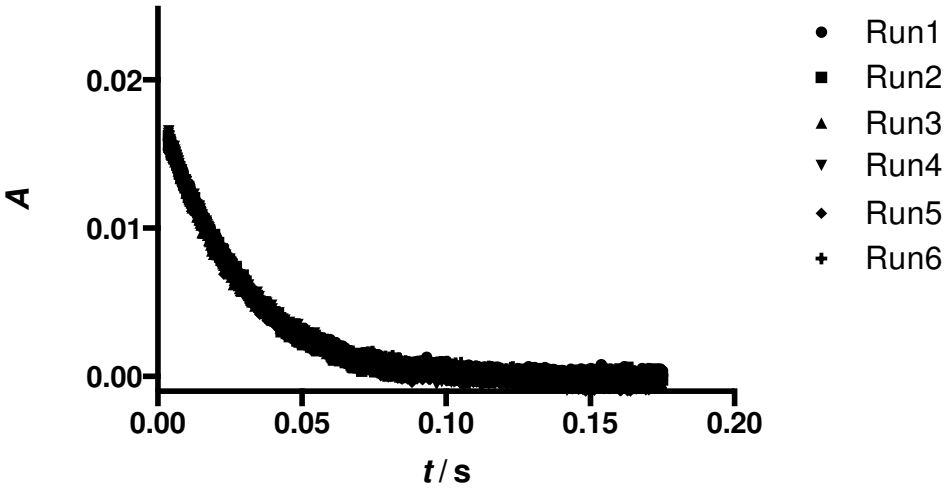


**Figure 42 Absorbance vs time, 50 μM tetrazine, 1.6 mM Oxazol-TCO.**

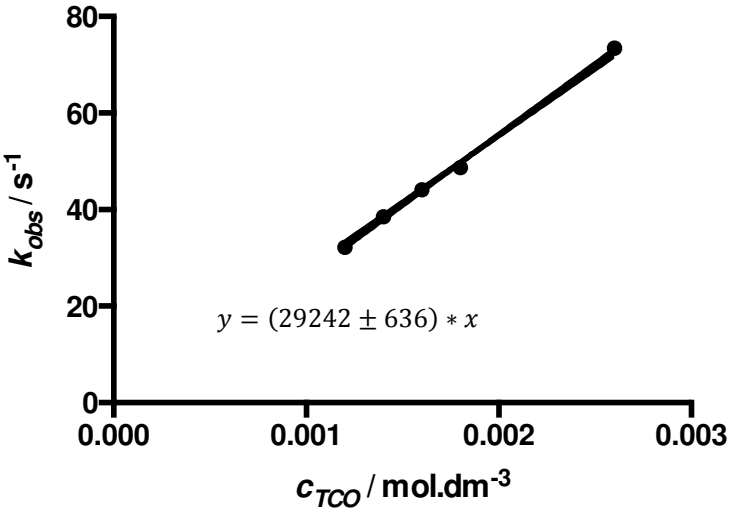


**Figure 43. Linear fit to the pseudo first order rate constants for Oxazol-TCO.**

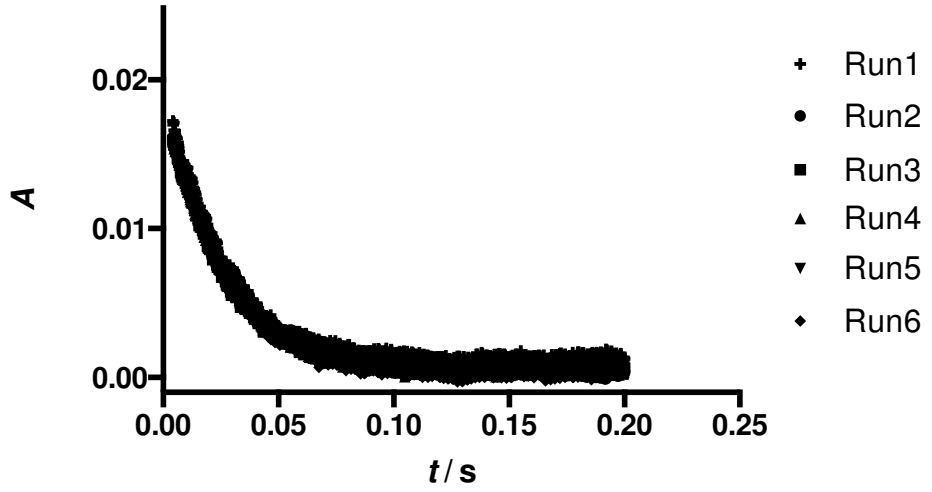


**Figure 44. Absorbance vs time, 75 μM tetrazine, 3.5 mM 3PEGMe-TCO$_A$.**

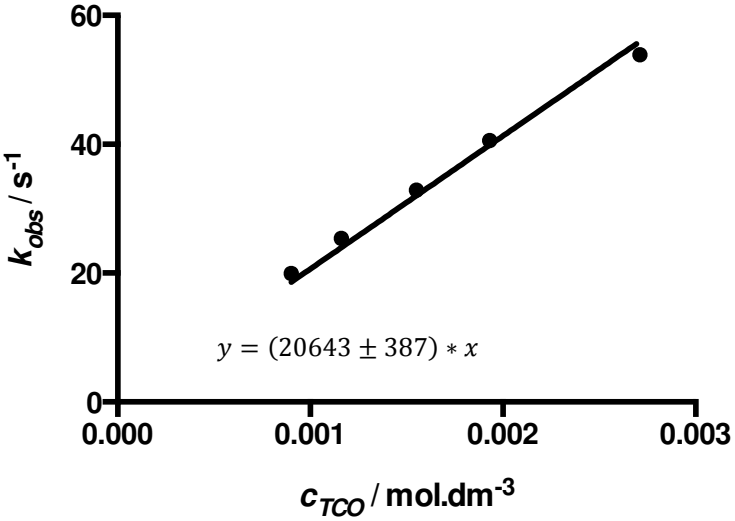


**Figure 45. Linear fit to the pseudo first order rate constants for 3PEGMe-TCO$_A$.**

## 4.2.§. Computational Data

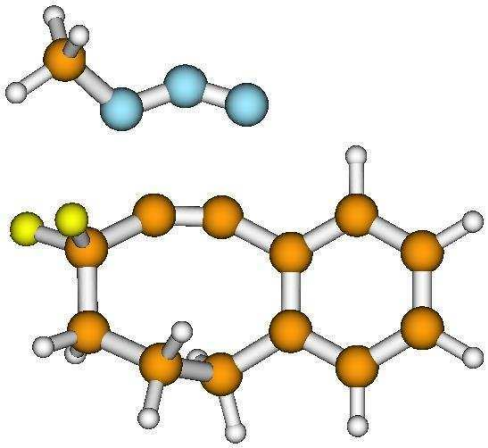

DIFBO TS1
$\Delta E^{\ddagger}$ = 11.6 kcal/mol $\Delta G^{\ddagger}$ = 24.9 kcal/mol

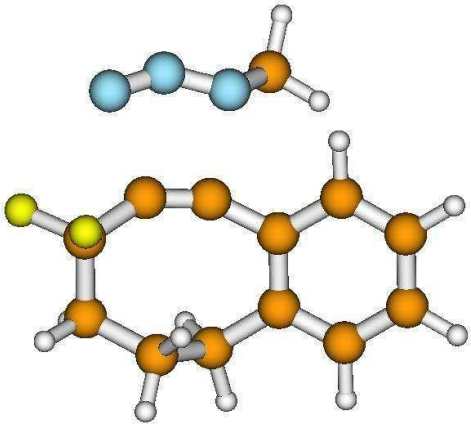

DIFBO TS2
$\Delta E^{\ddagger}$ = 13.5 kcal/mol $\Delta G^{\ddagger}$ = 26.5 kcal/mol

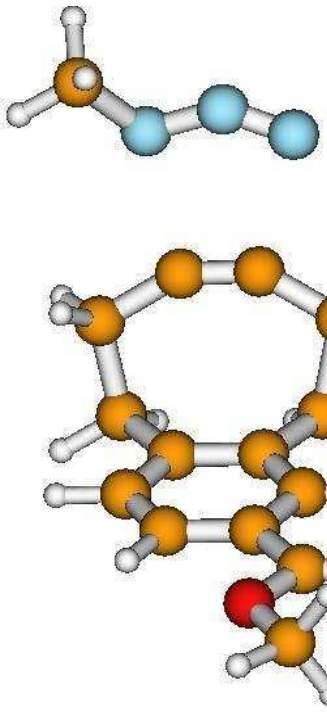

COMBO TS1
$\Delta E^{\ddagger}$ = 11.5 kcal/mol $\Delta G^{\ddagger}$ = 23.7 kcal/mol

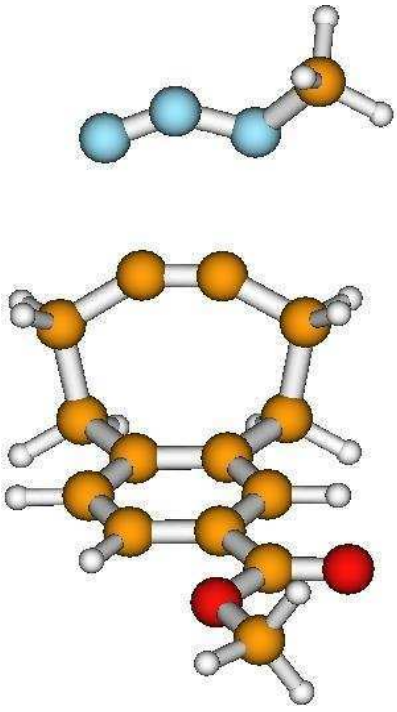

COMBO TS2
$\Delta E^{\ddagger}$ = 11.4 kcal/mol $\Delta G^{\ddagger}$ = 23.6 kcal/mol

**Figure 46. Transition-state structures and activation barriers for DIFBO and COMBO.**

**Table 9. Calculated total energies (E), enthalpies (H), Gibbs free-energies (G), and basis set superposition error (BSSE) corrections for the studied molecules. All values are given in Hartrees.**

| | *E* | *H* | *G* | BSSE |
|---|---|---|---|---|
| Methyl azide | -204.15340 | -204.09792 | -204.12988 | - |
| DIFBO | -663.09420 | -662.89503 | -662.94442 | - |
| COMBO | -692.49365 | -692.23272 | -692.28916 | - |
| DIFBO TS1 | -867.23106 | -866.97561 | -867.03668 | 0.00202 |
| DIFBO TS2 | -867.22797 | -866.97270 | -867.03394 | 0.00180 |
| COMBO TS1 | -896.63006 | -896.31312 | -896.38267 | 0.00135 |
| COMBO TS2 | -896.63035 | -896.31340 | -896.38296 | 0.00148 |

Cartesian coordinates for the studied molecules (in Å)

Methyl azide
C 0.000137 -0.000042 -0.000488
N -0.000413 -0.000667 1.473429
N 1.102616 0.000047 2.014553
N 2.055612 0.000600 2.632105
H 0.491012 -0.892461 -0.402276
H 0.489489 0.893552 -0.401519
H -1.041883 -0.000799 -0.311825

DIFBO
C 0.007146 0.001323 -0.001708
C -0.005068 0.005979 1.393999
C 1.179924 0.005121 2.129886
C 2.403318 -0.012128 1.408376
C 2.414689 -0.013536 0.009161
C 1.215625 -0.003285 -0.695403
C 3.560105 -0.096657 2.228797
C 4.242627 -0.241877 3.214977
C 4.402447 -0.726765 4.579081
C 3.055451 -0.685758 5.318680
C 1.818437 -1.071465 4.474481
C 1.163409 0.088740 3.647932
F 5.341353 -0.017050 5.296493
F 4.871975 -2.031086 4.556199
H 2.940849 0.325295 5.718581
H 3.162141 -1.361038 6.172357
H 2.065042 -1.915416 3.825195
H 1.064535 -1.445968 5.171335
H 3.363557 -0.028612 -0.513386
H 1.223994 -0.004363 -1.779014
H -0.930362 0.003298 -0.546248
H -0.954067 0.016772 1.919982
H 1.645501 1.031577 3.931581
H 0.119462 0.184935 3.955709

COMBO
C -0.028103 0.008494 0.010332
C -0.021736 0.009782 1.405916
C 1.194217 0.020012 2.075563
C 2.427018 0.018190 1.406958

| | | | |
|---|---|---|---|
| C | 2.423032 | 0.016478 | -0.013004 |
| C | 1.190405 | 0.017146 | -0.670983 |
| C | 3.672598 | 0.010886 | 2.286075 |
| C | 4.213366 | -1.419997 | 2.598694 |
| C | 4.515815 | -2.014344 | 1.297497 |
| C | 4.511604 | -2.014583 | 0.091909 |
| C | 4.202047 | -1.427869 | -1.210875 |
| C | 3.663118 | 0.004129 | -0.901762 |
| C | -1.282220 | 0.007660 | -0.791464 |
| O | -1.327229 | 0.014681 | -2.001418 |
| O | -2.390421 | -0.003489 | -0.016663 |
| C | -3.645877 | -0.008191 | -0.718059 |
| H | 5.079061 | -1.362363 | -1.862067 |
| H | 3.446178 | -2.013026 | -1.744686 |
| H | 5.093989 | -1.349981 | 3.244602 |
| H | 3.461199 | -2.002673 | 3.140573 |
| H | 4.480279 | 0.577258 | 1.816146 |
| H | 3.436725 | 0.512290 | 3.229851 |
| H | 3.419003 | 0.499333 | -1.846334 |
| H | 4.474323 | 0.574673 | -0.442642 |
| H | 1.193591 | 0.033504 | 3.160978 |
| H | -0.953917 | 0.011611 | 1.954962 |
| H | 1.161686 | 0.027131 | -1.754887 |
| H | -4.410352 | -0.018036 | 0.055923 |
| H | -3.739498 | 0.883472 | -1.339564 |
| H | -3.727017 | -0.893907 | -1.349724 |

DIFBO TS1

| | | | |
|---|---|---|---|
| C | 0.006032 | -0.017850 | -0.000884 |
| C | -0.002687 | -0.023960 | 1.393239 |
| C | 1.182988 | -0.001129 | 2.129380 |
| C | 2.412895 | 0.033876 | 1.423938 |
| C | 2.412690 | 0.051753 | 0.021875 |
| C | 1.217277 | 0.020189 | -0.687288 |
| C | 3.627396 | -0.002025 | 2.193388 |
| C | 4.261184 | -0.248491 | 3.228286 |
| C | 4.296948 | -0.898412 | 4.541536 |
| C | 2.950480 | -0.944248 | 5.263055 |
| C | 1.731927 | -1.231971 | 4.369967 |
| C | 1.147701 | 0.019695 | 3.641412 |
| F | 5.219596 | -0.310652 | 5.391121 |
| F | 4.760720 | -2.203487 | 4.373630 |
| H | 2.826565 | 0.014076 | 5.774569 |
| H | 3.055622 | -1.710853 | 6.035807 |
| H | 1.979251 | -2.014966 | 3.648112 |
| H | 0.951549 | -1.652943 | 5.008773 |
| H | 3.359420 | 0.091432 | -0.499039 |
| H | 1.232455 | 0.029587 | -1.771071 |
| H | -0.930771 | -0.038994 | -0.546487 |
| H | -0.949960 | -0.045940 | 1.922296 |
| H | 1.684494 | 0.910668 | 3.985472 |
| H | 0.108909 | 0.156344 | 3.951234 |
| N | 5.273329 | 0.842253 | 0.883495 |
| N | 6.113582 | 0.674619 | 1.663777 |
| N | 6.309137 | 0.359593 | 2.855851 |
| C | 7.554781 | -0.308454 | 3.245029 |
| H | 8.409502 | 0.357641 | 3.102124 |
| H | 7.460062 | -0.535800 | 4.303718 |
| H | 7.710020 | -1.236843 | 2.687536 |

DIFBO TS2

| | | | |
|---|---|---|---|
| C | 0.045223 | -0.008642 | -0.013998 |
| C | 0.036849 | 0.034360 | 1.379327 |
| C | 1.222334 | 0.034303 | 2.117366 |
| C | 2.450080 | 0.001293 | 1.410164 |
| C | 2.452231 | -0.043960 | 0.008833 |
| C | 1.256808 | -0.052735 | -0.700826 |
| C | 3.654240 | -0.061760 | 2.188704 |
| C | 4.309356 | -0.394583 | 3.184715 |
| C | 4.276783 | -1.176763 | 4.428842 |
| C | 2.964898 | -1.052374 | 5.203422 |
| C | 1.684222 | -1.213448 | 4.365769 |
| C | 1.191696 | 0.074906 | 3.630125 |
| N | 6.334495 | 0.401748 | 2.882171 |
| N | 6.074484 | 0.969751 | 1.907910 |
| N | 5.182469 | 1.108705 | 1.037742 |
| C | 4.994325 | 2.434022 | 0.438946 |
| F | 5.308551 | -0.850216 | 5.280482 |
| F | 4.478973 | -2.515452 | 4.109957 |
| H | 2.974580 | -0.082308 | 5.708374 |
| H | 3.010657 | -1.820151 | 5.981156 |
| H | 1.814438 | -2.032393 | 3.653071 |
| H | 0.892738 | -1.536776 | 5.046485 |
| H | 3.402403 | -0.090614 | -0.508473 |
| H | 1.270896 | -0.096794 | -1.783812 |
| H | -0.891693 | -0.011318 | -0.559549 |
| H | -0.910583 | 0.065692 | 1.907561 |
| H | 1.789301 | 0.927370 | 3.970864 |
| H | 0.164251 | 0.284194 | 3.937251 |
| H | 4.054017 | 2.394247 | -0.108751 |
| H | 4.935195 | 3.224114 | 1.193531 |
| H | 5.796890 | 2.661716 | -0.268221 |

COMBO TS1

| | | | |
|---|---|---|---|
| C | 0.006369 | -0.005044 | 0.008849 |
| C | 0.001271 | -0.005764 | 1.405980 |
| C | 1.244498 | -0.007290 | 2.083803 |
| C | 2.422647 | -0.008362 | 1.323418 |
| C | 2.412044 | 0.002541 | -0.064541 |
| C | 1.187288 | 0.004369 | -0.735812 |
| C | 1.395472 | 0.003185 | 3.596424 |
| C | 1.417467 | 1.430771 | 4.213482 |
| C | 0.151762 | 2.094506 | 3.884181 |
| C | -0.937739 | 2.108614 | 3.315441 |
| C | -1.883498 | 1.431728 | 2.414564 |
| C | -1.355101 | 0.007305 | 2.095008 |
| H | -2.000997 | 2.007958 | 1.490551 |
| H | -2.878031 | 1.364527 | 2.866387 |
| H | 2.269757 | 1.994372 | 3.817690 |
| H | 1.558676 | 1.357382 | 5.296427 |
| H | 2.330481 | -0.501204 | 3.859388 |
| H | 0.587283 | -0.559310 | 4.070034 |
| H | -1.321086 | -0.562144 | 3.027469 |
| H | -2.079582 | -0.493915 | 1.446009 |
| H | 3.376535 | -0.023674 | 1.841566 |
| H | 3.338339 | 0.000014 | -0.623477 |
| C | 1.082333 | 0.004542 | -2.220465 |
| H | -0.933387 | -0.015458 | -0.532037 |
| O | 0.041520 | -0.005831 | -2.838952 |

| | | | |
|---|---|---|---|
| O | 2.292888 | 0.019107 | -2.824237 |
| H | 3.320672 | 0.035074 | -4.564571 |
| H | 1.756216 | 0.905376 | -4.636118 |
| H | 1.777327 | -0.871792 | -4.640042 |
| C | 2.275699 | 0.022013 | -4.262026 |
| N | -1.871562 | 4.046787 | 3.899330 |
| N | -0.993064 | 4.433073 | 4.550261 |
| N | 0.098339 | 4.089547 | 5.057417 |
| C | 1.100208 | 5.114488 | 5.350474 |
| H | 0.762550 | 5.791297 | 6.141241 |
| H | 1.368793 | 5.698678 | 4.463863 |
| H | 1.985638 | 4.590154 | 5.708386 |

COMBO TS2

| | | | |
|---|---|---|---|
| C | -0.057048 | 0.000002 | -0.001199 |
| C | -0.034475 | -0.001680 | 1.400888 |
| C | 1.221287 | 0.003318 | 2.055399 |
| C | 2.379750 | 0.009666 | 1.274940 |
| C | 2.341778 | 0.021670 | -0.120650 |
| C | 1.102289 | 0.016481 | -0.764379 |
| C | 1.402925 | 0.015980 | 3.565903 |
| C | 1.429021 | 1.443473 | 4.181496 |
| C | 0.154360 | 2.100473 | 3.873399 |
| C | -0.945420 | 2.110605 | 3.324809 |
| C | -1.904927 | 1.426430 | 2.444581 |
| C | -1.375303 | 0.003490 | 2.116834 |
| H | -2.045218 | 2.000142 | 1.522124 |
| H | -2.889681 | 1.352937 | 2.916497 |
| H | 2.271139 | 2.010551 | 3.769480 |
| H | 1.589594 | 1.373255 | 5.261948 |
| H | 2.346380 | -0.481975 | 3.808942 |
| H | 0.609284 | -0.552550 | 4.057012 |
| H | -1.317261 | -0.562340 | 3.050050 |
| H | -2.110781 | -0.503752 | 1.484591 |
| H | 3.352125 | 0.001400 | 1.754927 |
| C | 3.633876 | 0.030276 | -0.858737 |
| H | 1.051031 | 0.016737 | -1.845045 |
| H | -1.018087 | -0.016058 | -0.505653 |
| O | 4.726870 | 0.035035 | -0.337140 |
| O | 3.462966 | 0.034168 | -2.200432 |
| C | 4.667225 | 0.044917 | -2.985944 |
| H | 4.337234 | 0.047369 | -4.022637 |
| H | 5.268287 | -0.840997 | -2.776090 |
| H | 5.257385 | 0.936312 | -2.768462 |
| N | -1.869986 | 4.057795 | 3.908400 |
| N | -0.977807 | 4.446314 | 4.539038 |
| N | 0.121721 | 4.104984 | 5.028828 |
| C | 1.133226 | 5.128568 | 5.292304 |
| H | 0.814333 | 5.813117 | 6.084159 |
| H | 1.385339 | 5.703907 | 4.395220 |
| H | 2.023953 | 4.603791 | 5.635953 |

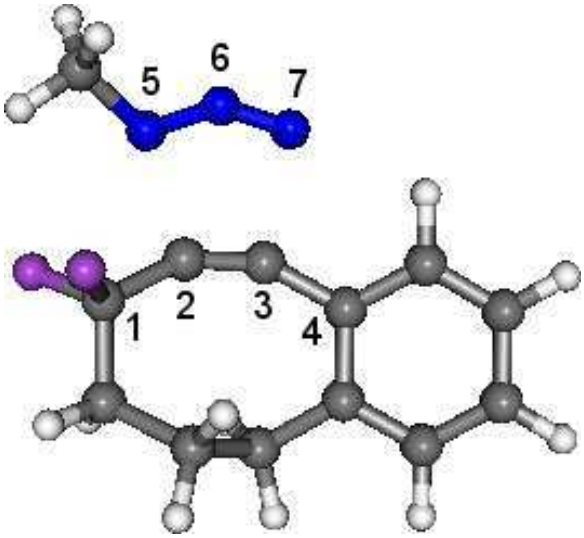



| | DIFBO | COMBO |
|---|---|---|
| $\Delta E^{\ddagger}$ [kcal/mol] | 11.6 | 11.4 |
| $\Delta G^{\ddagger}$ [kcal/mol] | 24.9 | 23.6 |
| *R*(23) [Å] | 1.238 (1.208) | 1.229 (1.206) |
| *R*(25) [Å] | 2.169 | 2.314 |
| *R*(37) [Å] | 2.267 | 2.233 |
| *α*(123) [degree] | 148.2 (159.8) | 151.1 (153.1) |
| *α*(234) [degree] | 152.2 (150.1) | 147.9 (152.8) |
| *α*(567) [degree] | 142.5 (173.2) | 142.9 (173.2) |
| HOMO [eV] | −11.0 | −9.8 |
| LUMO [eV] | 3.6 | 4.1 |

**Figure 47. Transition-state structures, barriers heights, and energies of FMOs for DIFBO and COMBO. Numbers in parentheses are the corresponding values for the equilibrium structure of the molecules. Orbital energies were obtained from Hartree-Fock/6-311G** calculations performed at the corresponding DFT geometries.**

The most important geometric parameters for the equilibrium structures of the considered molecules and for the corresponding transition states are compiled in **Figure 36.** and in

**Figure 47**. The magnitude of the distortion required to obtain the transition-state geometry can perhaps be best characterized by the $\alpha(123)$, $\alpha(234)$, and $\alpha(567)$ angles as well as the R(23) bond length. To quantify the change of the bond angles let us simply consider the sum of the three angles. If we calculate this sum for the separated molecules and for the transition states, and subtract the two values, we obtain 40.2 and 37.2 degrees for DIFBO and COMBO, respectively, which means that the overall change in the bond angles is smaller by 3 degrees for the latter compound. In addition, the elongation of the R(23) bond is also less pronounced for COMBO than that for DIFBO. Consequently, the geometry of COMBO is closer to the corresponding transition-state structure, less energy is required to distort the molecule into its transition state, and thus the activation barrier is lower.

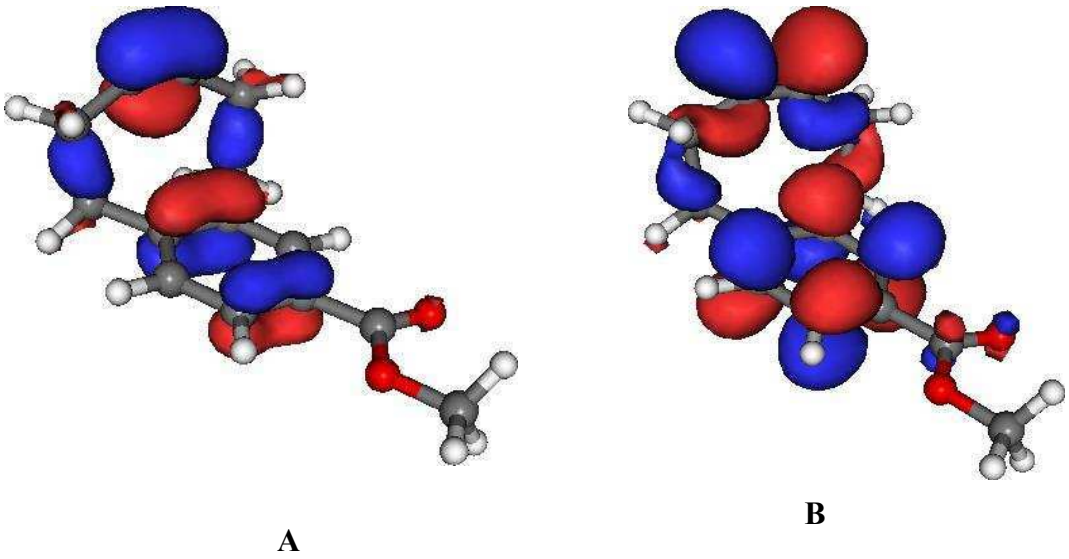

**A** **B**

**Figure 48. The FMOs of COMBO: the HOMO (a) and the LUMO+2 (b) of COMBO corresponding to the HOMO and LUMO of acetylene, respectively.**

The other important factor responsible for the lowering of the barrier height is the energy of the FMOs, which is influenced by three effects:

. The fluoro substitution $\alpha$ to the alkyne for DIFBO. As expected, the fluorination of the cyclooctine ring decreases the energies of both the HOMO and the LUMO, which was verified by calculations for DIFBO replacing the fluorine atoms by hydrogens with C–H bond lengths of 1.09 Å. We have found that both the HOMO and LUMO energies are decreased by 1.0 eV upon fluorination.

. Presence of the phenyl ring for DIFBO. We performed calculations for dimethylacetylene and 1-phenyl-1-propyne at a distorted geometry corresponding to the structure of DIFBO replacing the corresponding carbon atoms by hydrogens with C–H bond lengths of 1.09 Å. Our results show that the presence of the phenyl ring decreases the HOMO energy by 0.4 eV and increases the LUMO energy by 0.8 eV. Thus, the phenyl ring almost cancels the favorable LUMO-lowering effect of the fluorination.

. The hyperconjugation between the alkyne's $\pi$-orbitals and the $\sigma$-orbitals of the C–C bond "perpendicular" to the triple bond. To model this effect we performed calculations for acetylene at a distorted geometry corresponding to the structure of COMBO with C–H bond lengths of 1.09 Å, and we have found that the hyperconjugation significantly increases the energy of the HOMO, while the LUMO is less affected. The hyperconjugation can be illustrated by the FMOs of COMBO, which are presented in **Figure 48**. It is interesting to note that in the case of COMBO the conjugated system is extended to the whole molecule since there is also hyperconjugation between the aforementioned C–C bond and the $\pi$-orbitals of the phenyl ring.

As a result of the above effects both the HOMO and the LUMO energies are higher for COMBO than those for DIFBO (**Figure 47**), but their difference, the FMO gap is somewhat smaller for COMBO.

## 4.3.§. NMR Spectra

$^{1}H$ NMR, $CDCl_3$, 600 MHz

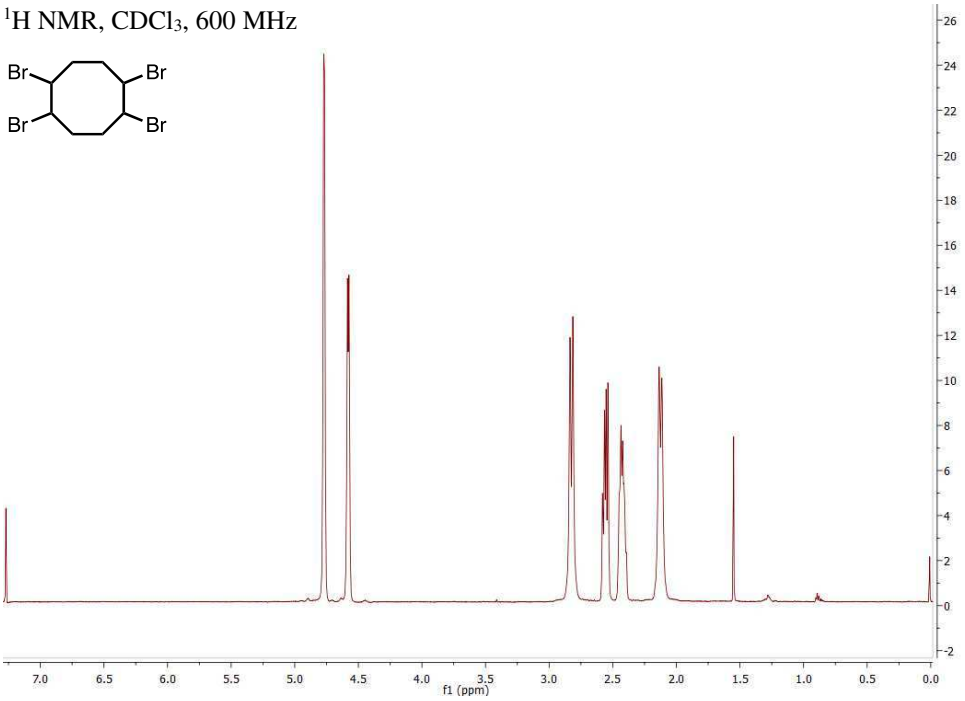


$^{13}C$ NMR, $CDCl_3$, 150 MHz

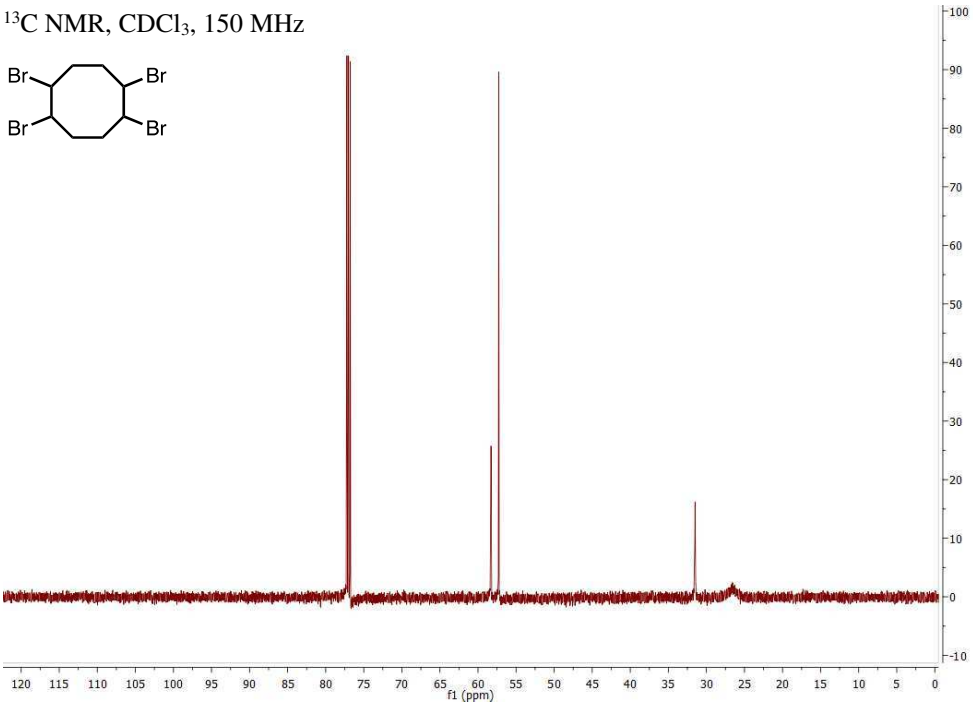

$^{1}H$ NMR, $CDCl_3$, 600 MHz

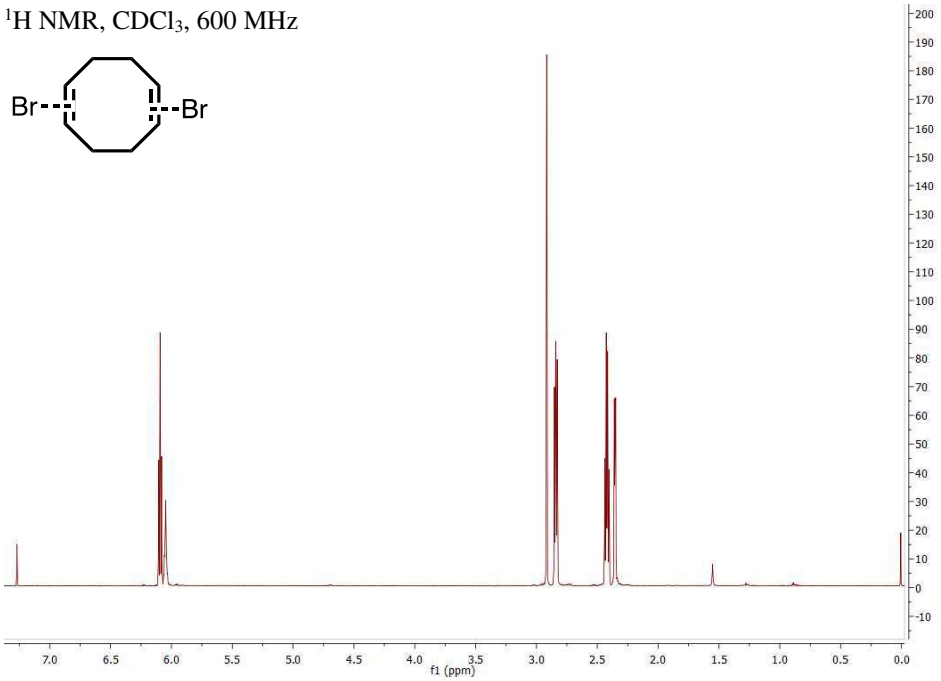


$^{13}C$ NMR, $CDCl_3$, 150 MHz

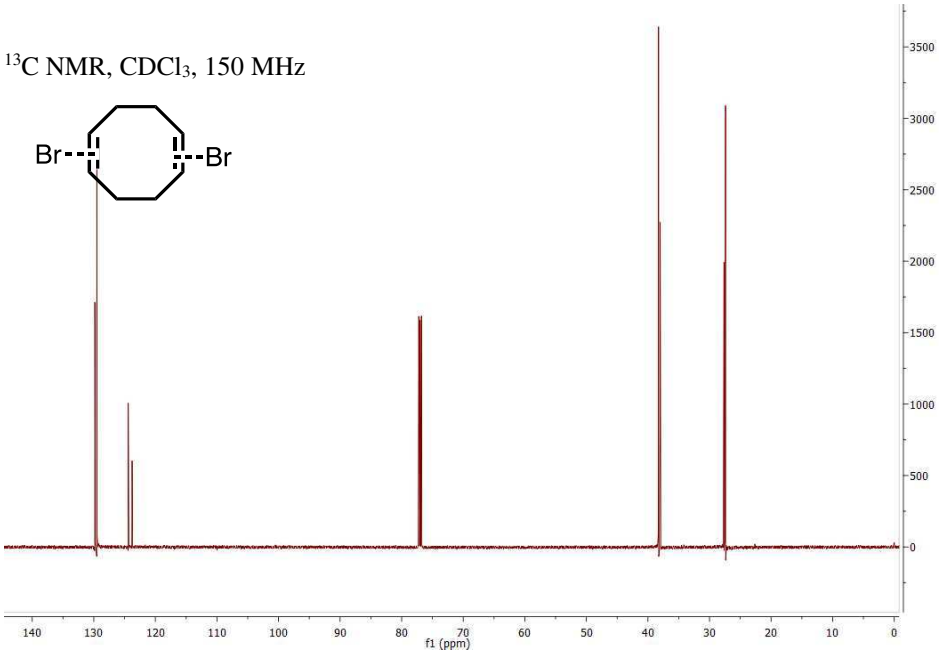

$^{1}$H NMR, $CDCl_3$, 600 MHz

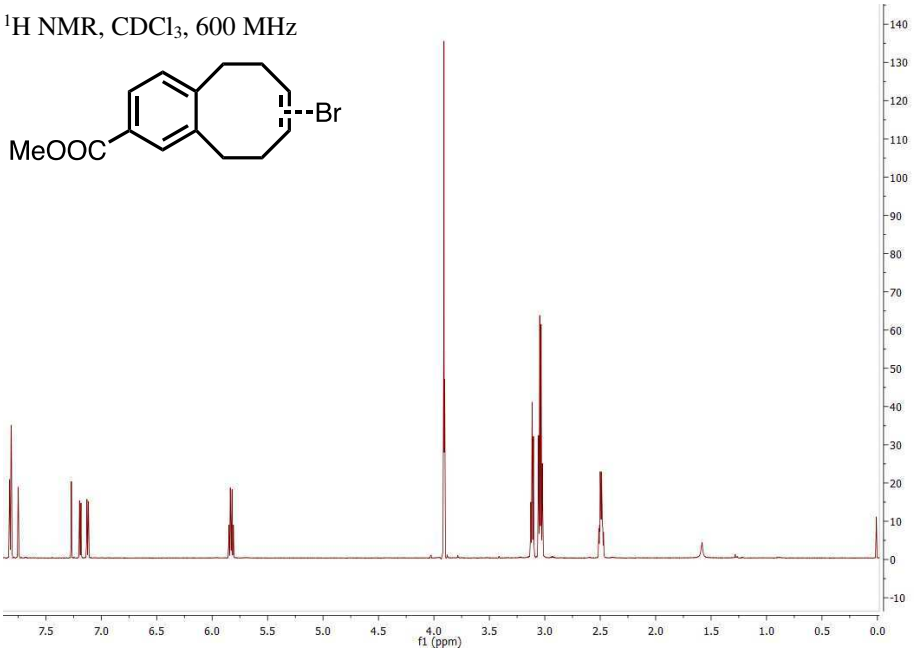


$^{13}$C NMR, $CDCl_3$, 150 MHz

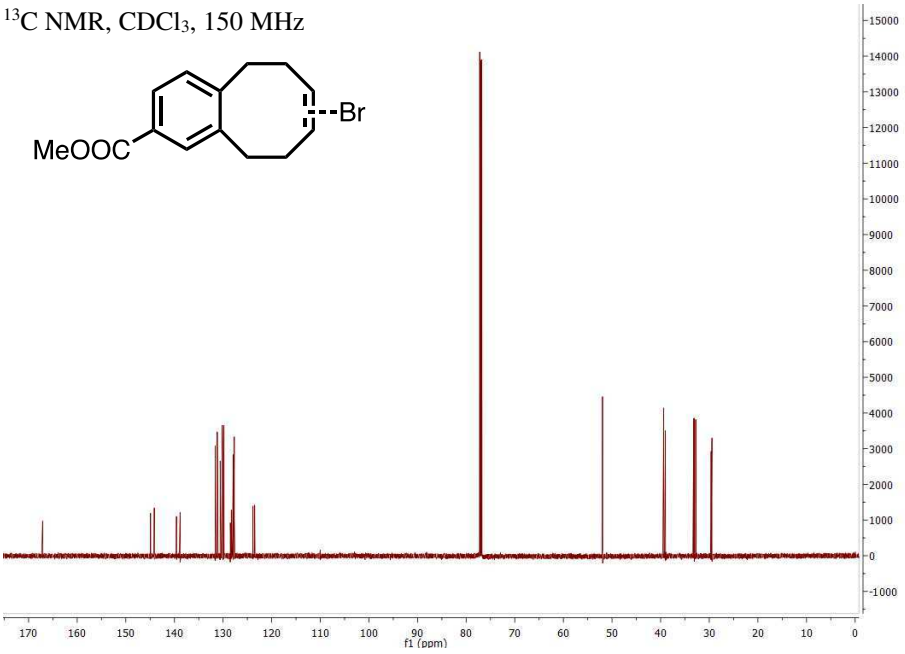

$^{1}$H NMR, $CD_3CN$, 600 MHz

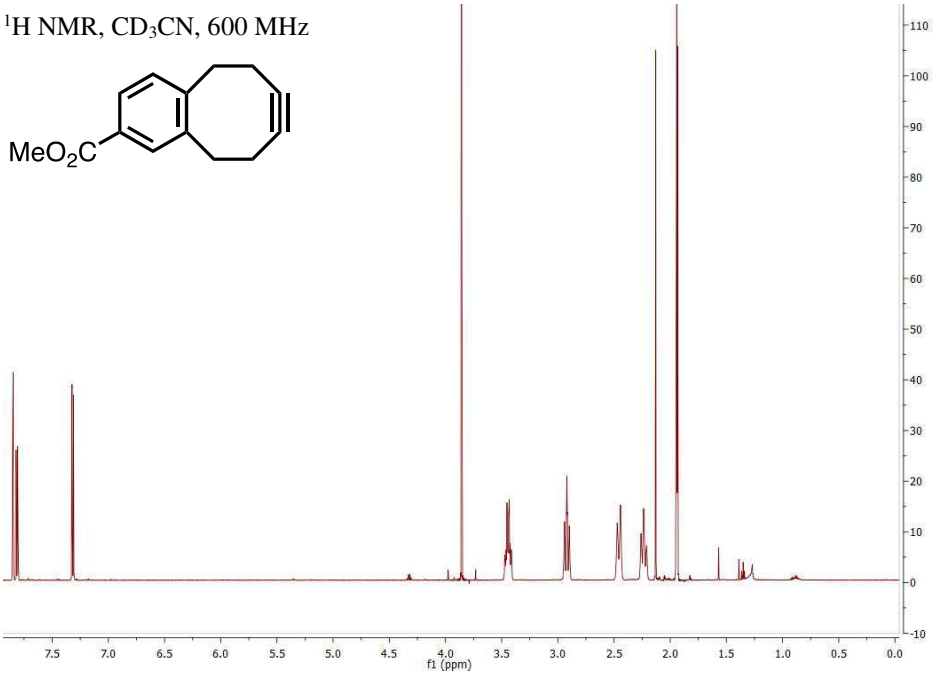


$^{13}$C NMR, $CDCl_3$, 150 MHz

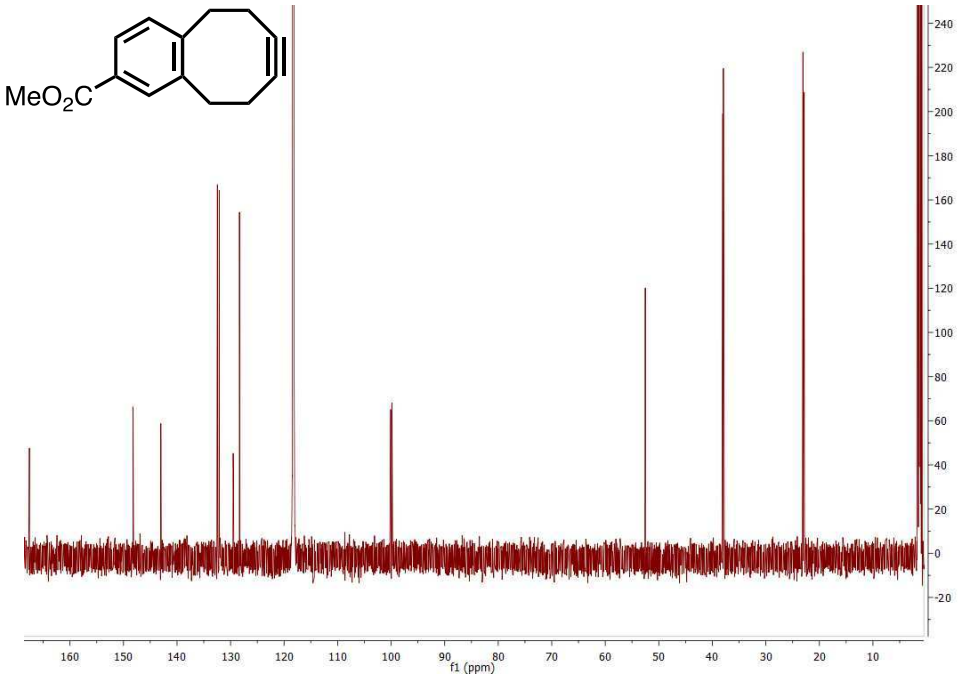

$^{1}$H NMR, $CDCl_3$, 600 MHz

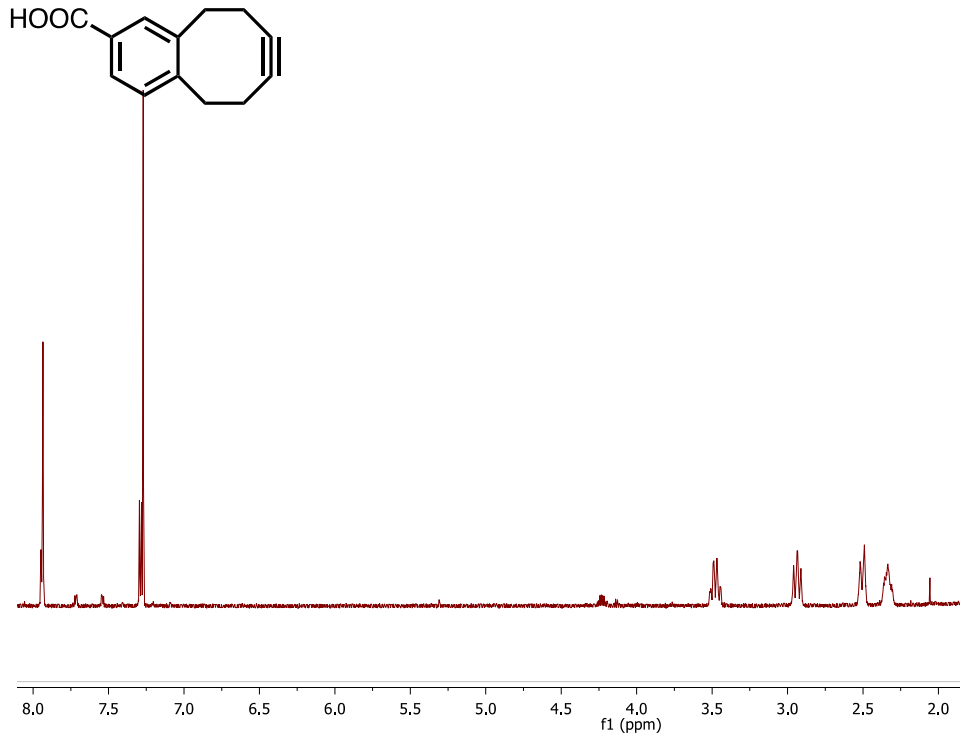


$^{13}$C NMR, $CDCl_3$, 150 MHz

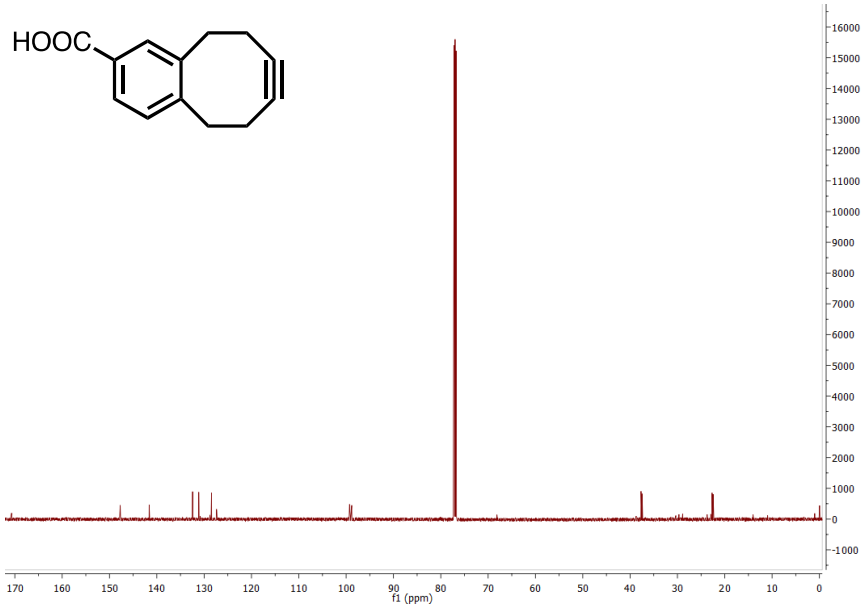

$^{1}$H NMR, $CDCl_3$, 600 MHz

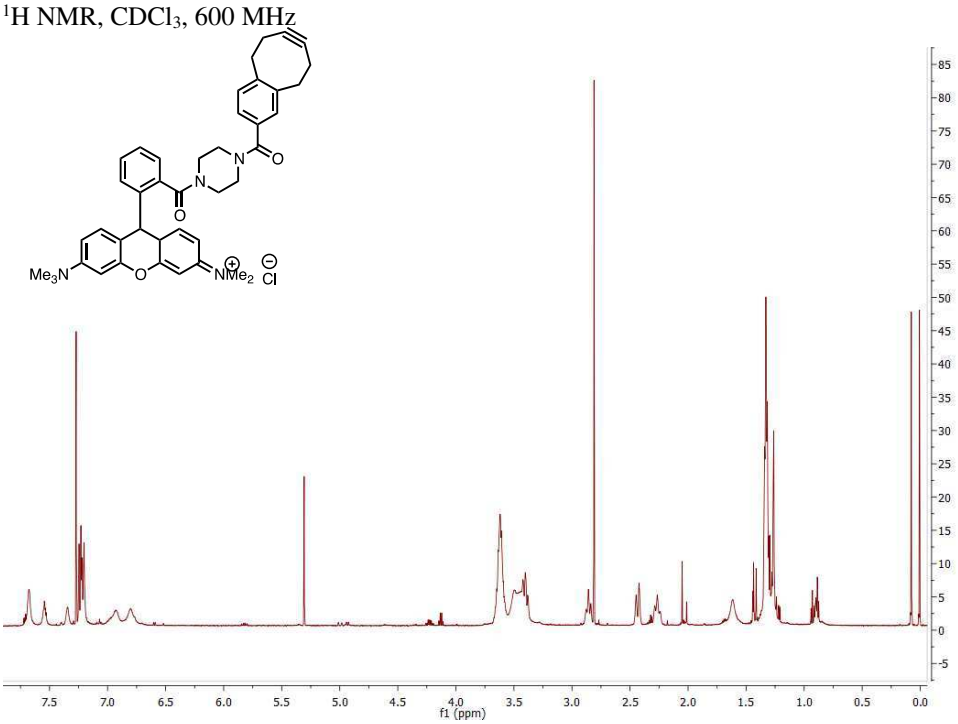


$^{13}$C NMR, $CDCl_3$, 150 MHz

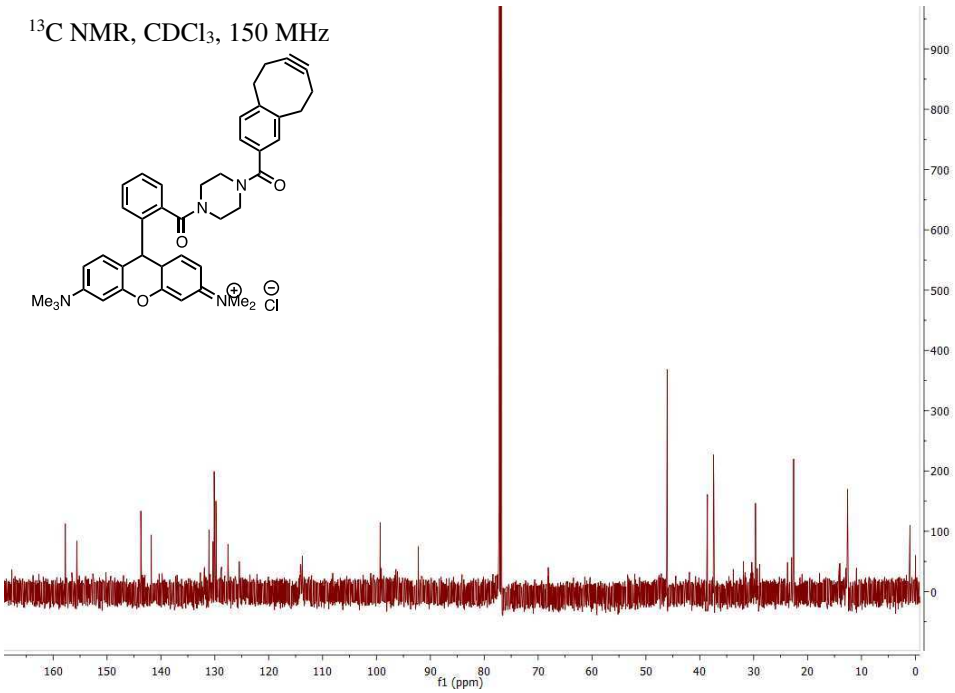

$^{1}$H NMR, $CDCl_3$, 600 MHz

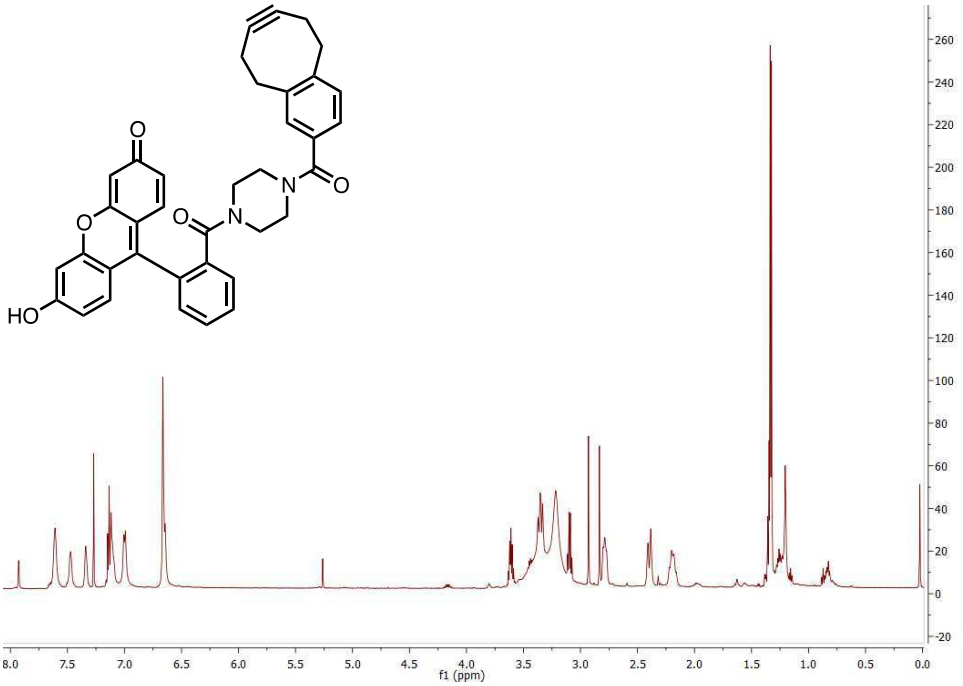


$^{13}$C NMR, $CDCl_3$, 150 MHz

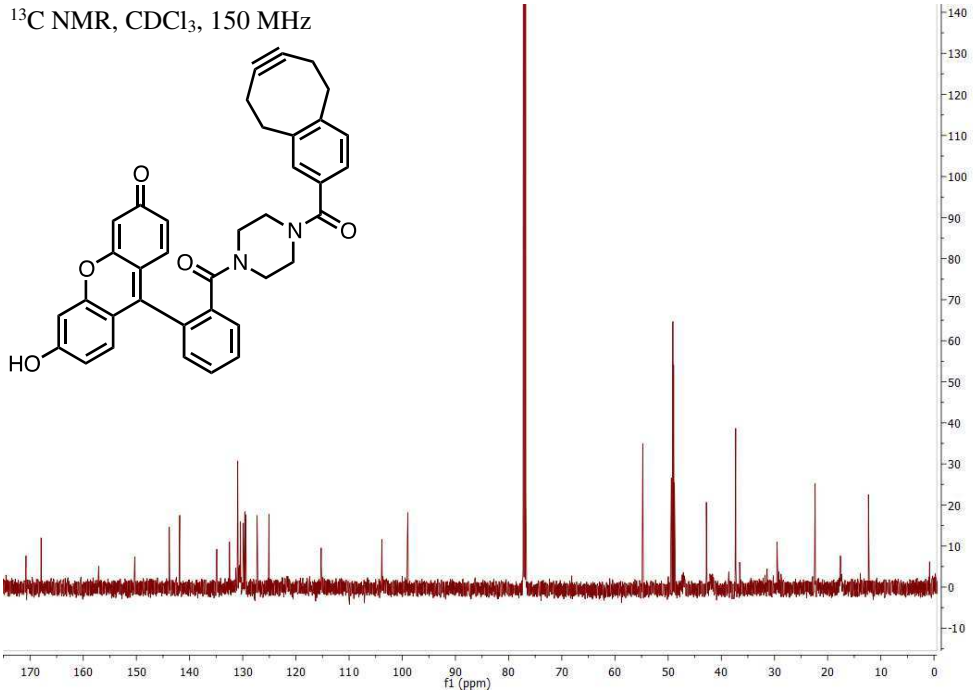

$^{1}$H NMR, $CD_3CN$, 600 MHz

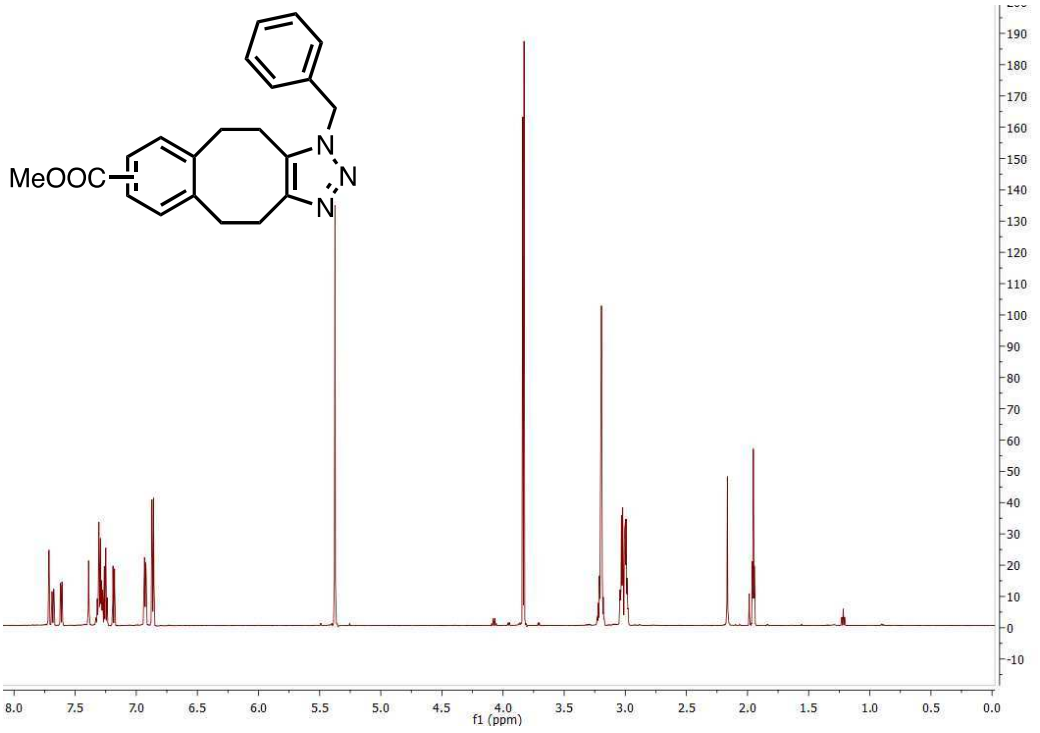


$^{3}$C NMR, $CD_3CN$, 150 MHz

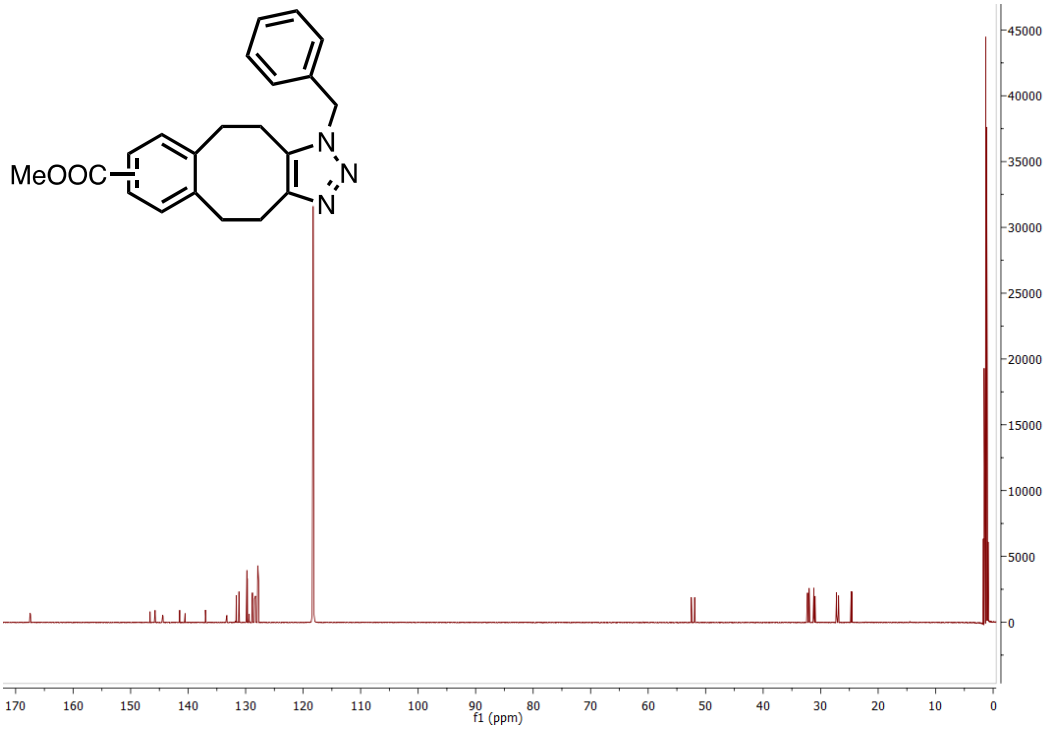

$^{1}$H NMR, $CDCl_3$, 500 MHz

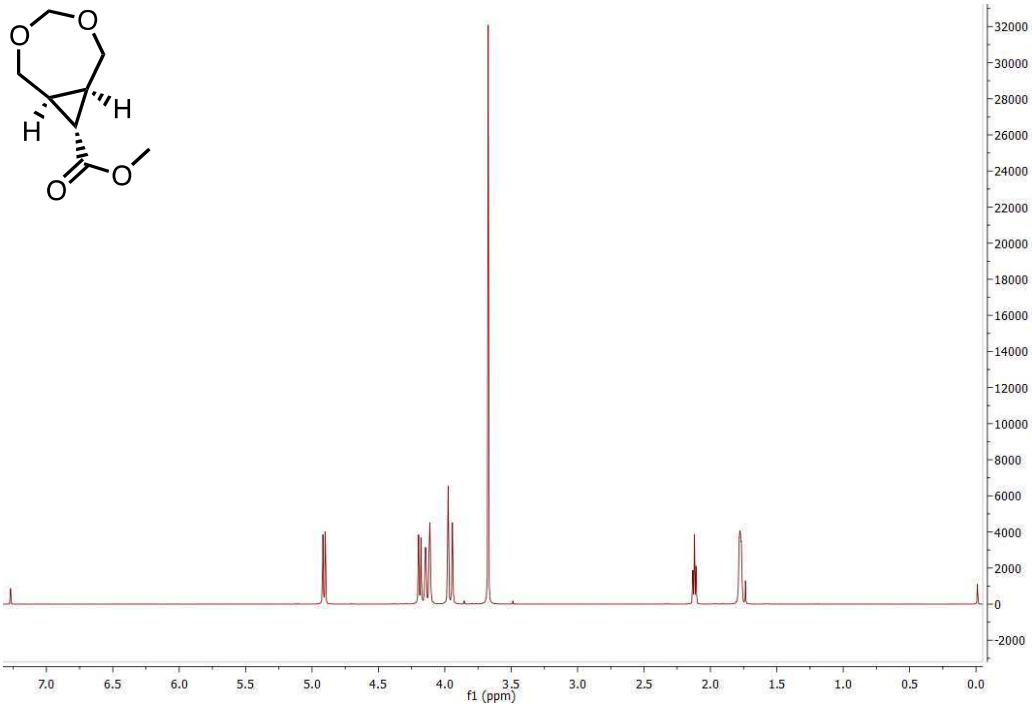


$^{13}$C NMR, $CDCl_3$ , 101 MHz

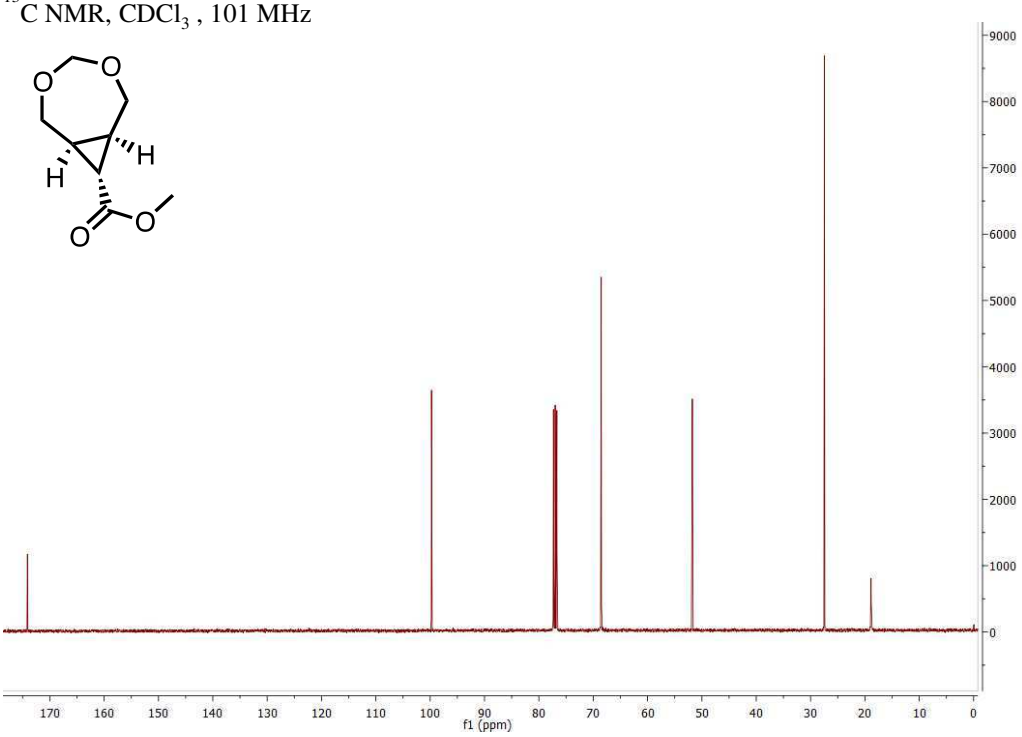

$^{1}$H NMR, $CDCl_3$, 500 MHz

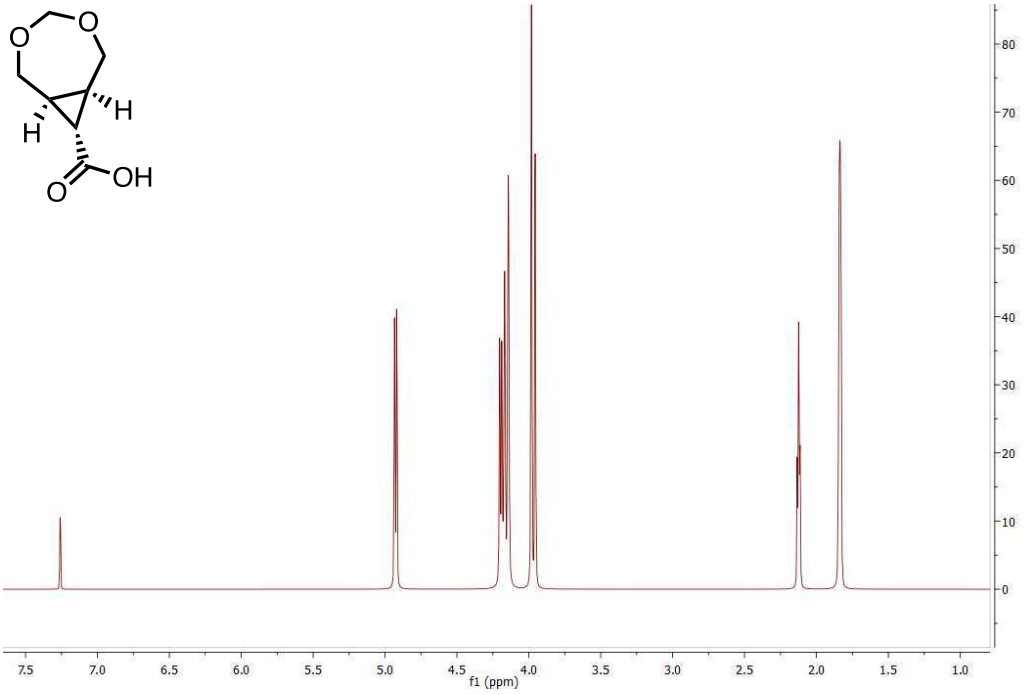


$^{13}$C NMR, $CDCl_3$, 126 MHz

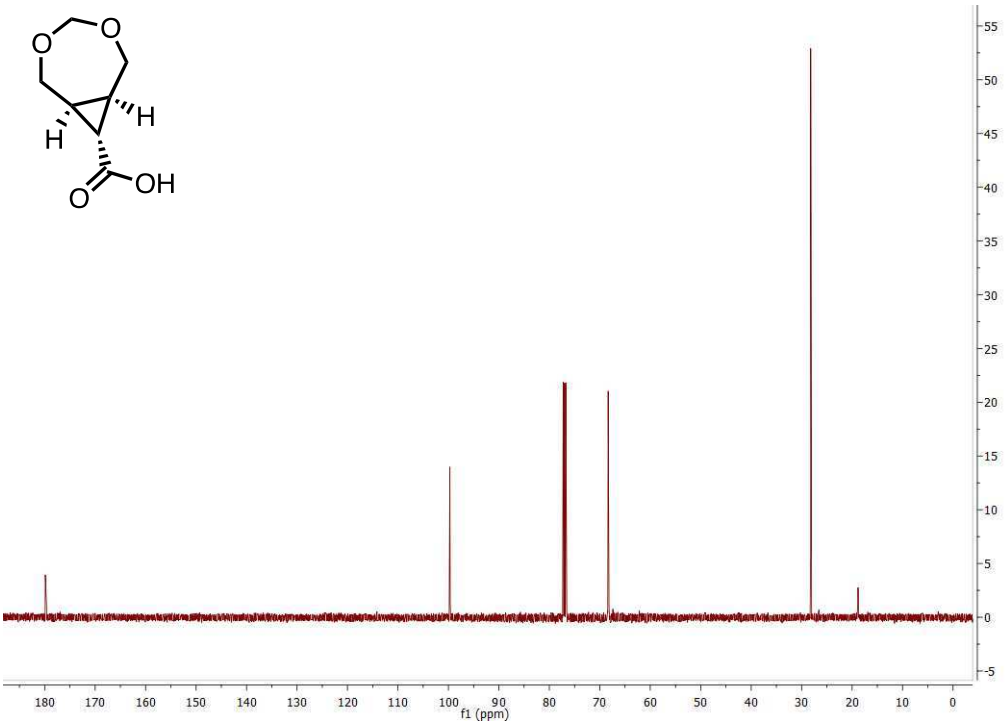

$^{1}$H NMR, DMSO-D$_6$, 500 MHz

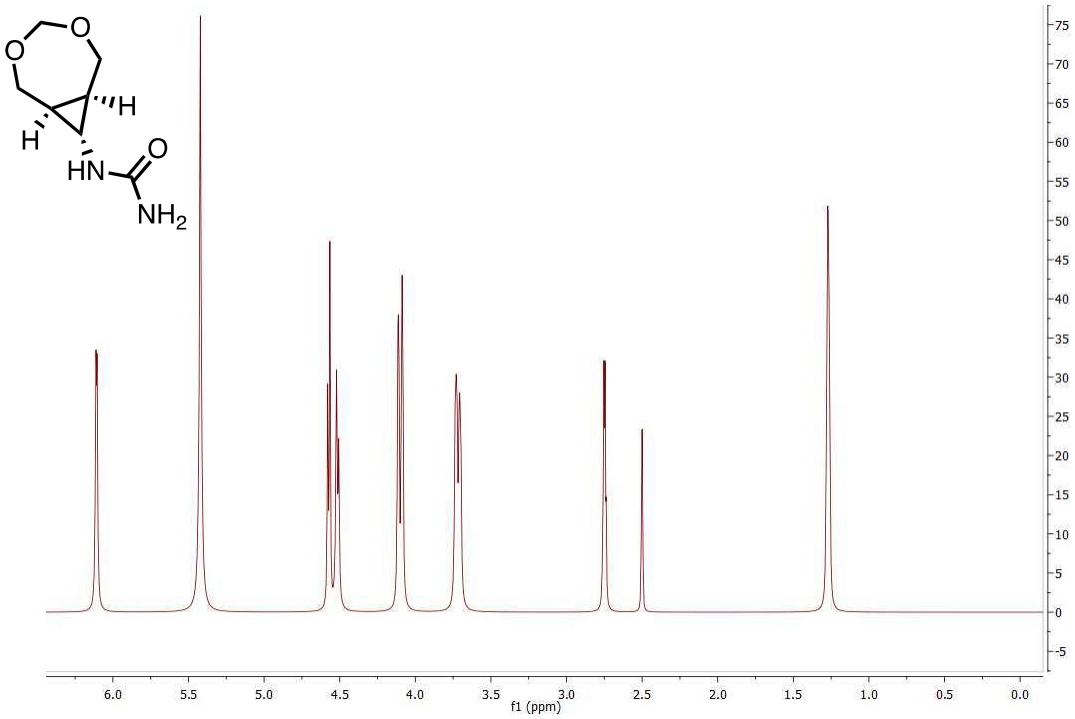


$^{13}$C NMR, DMSO-D$_6$, 126 MHz

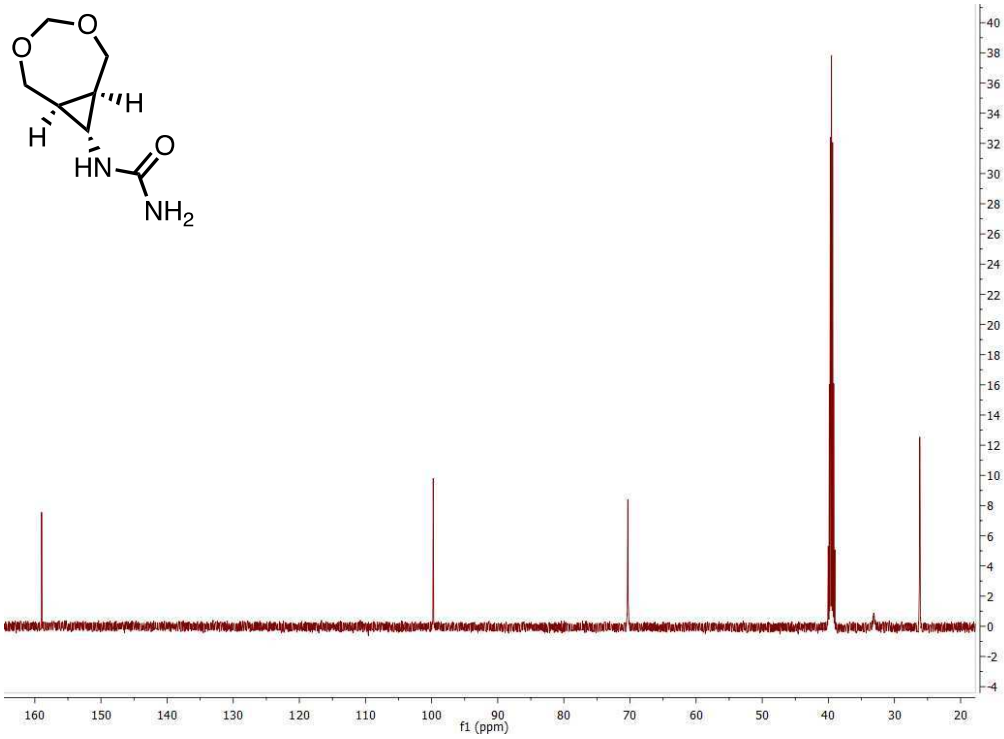

$^{1}$H NMR, DMSO-D$_6$, 250 MHz

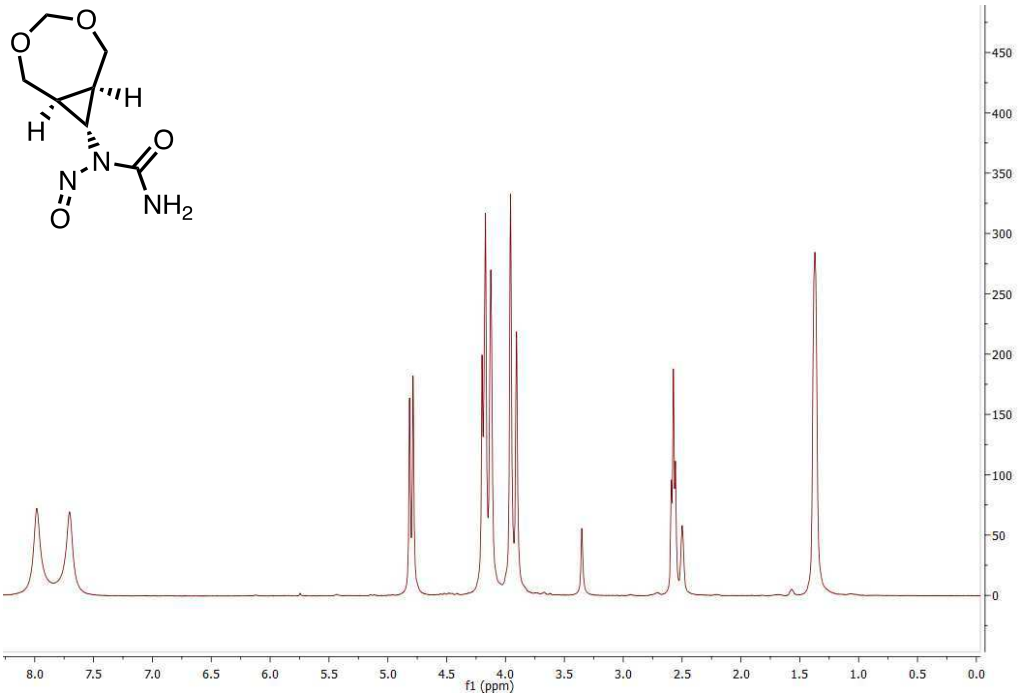


$^{13}$C NMR, DMSO-D$_6$, 63 MHz

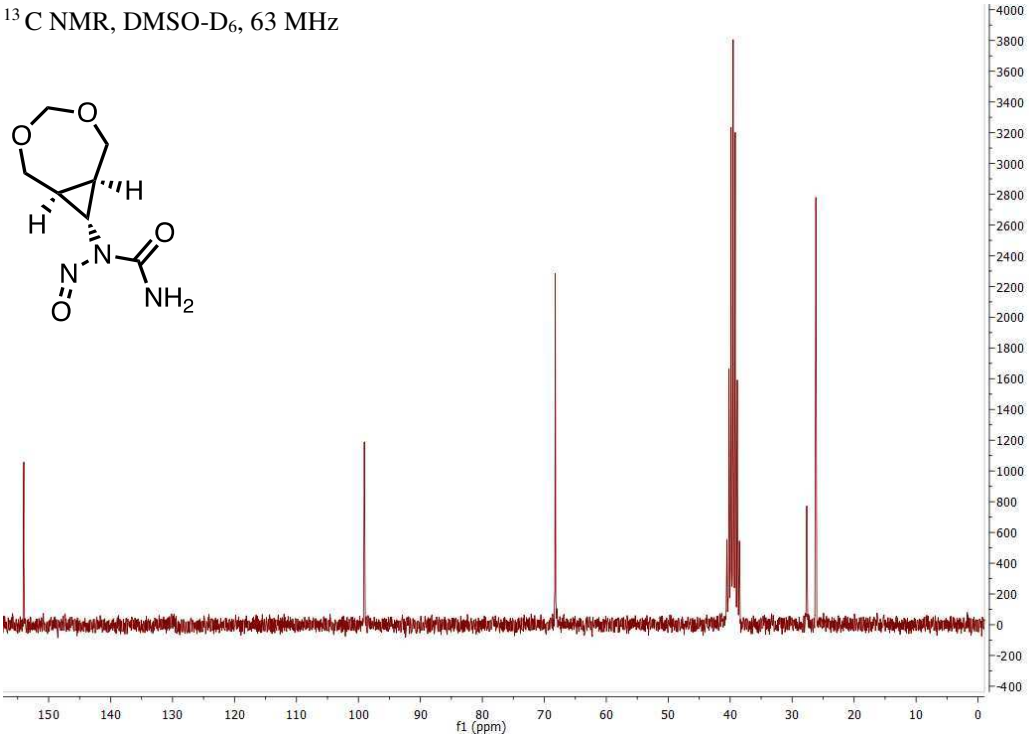

$^{1}$H NMR, $CDCl_3$, 500 MHz

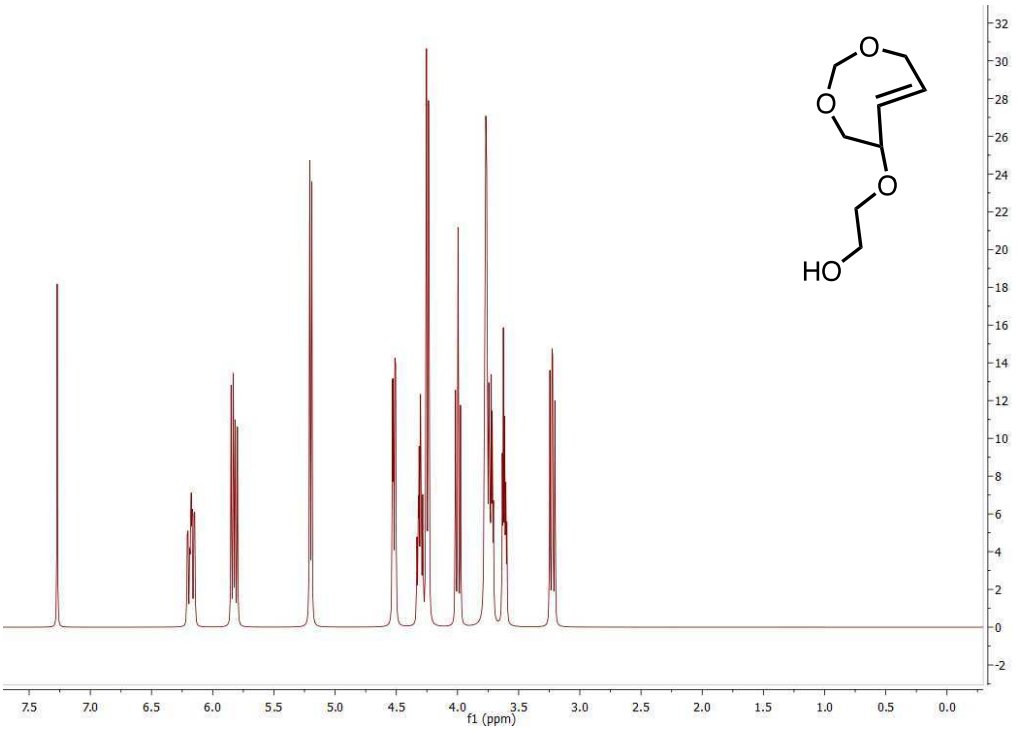


$^{13}$C NMR, $D_2O$, 126 MHz

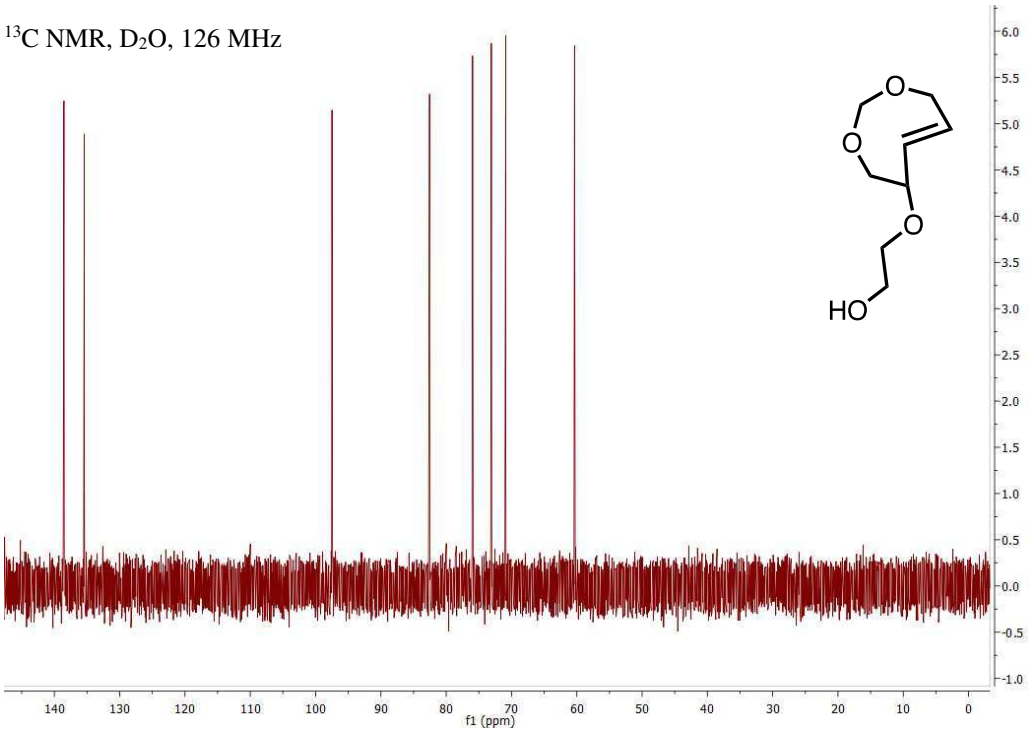

$^{1}H$ NMR, $CDCl_3$, 250 MHz

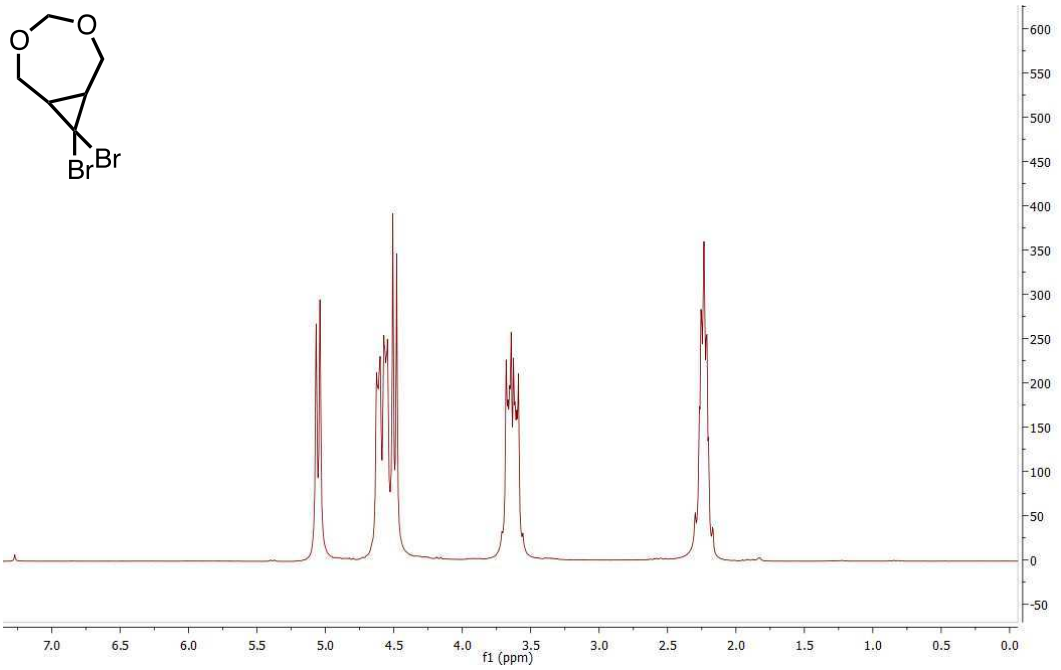


$^{13}C$ NMR, $CDCl_3$, 63 MHz

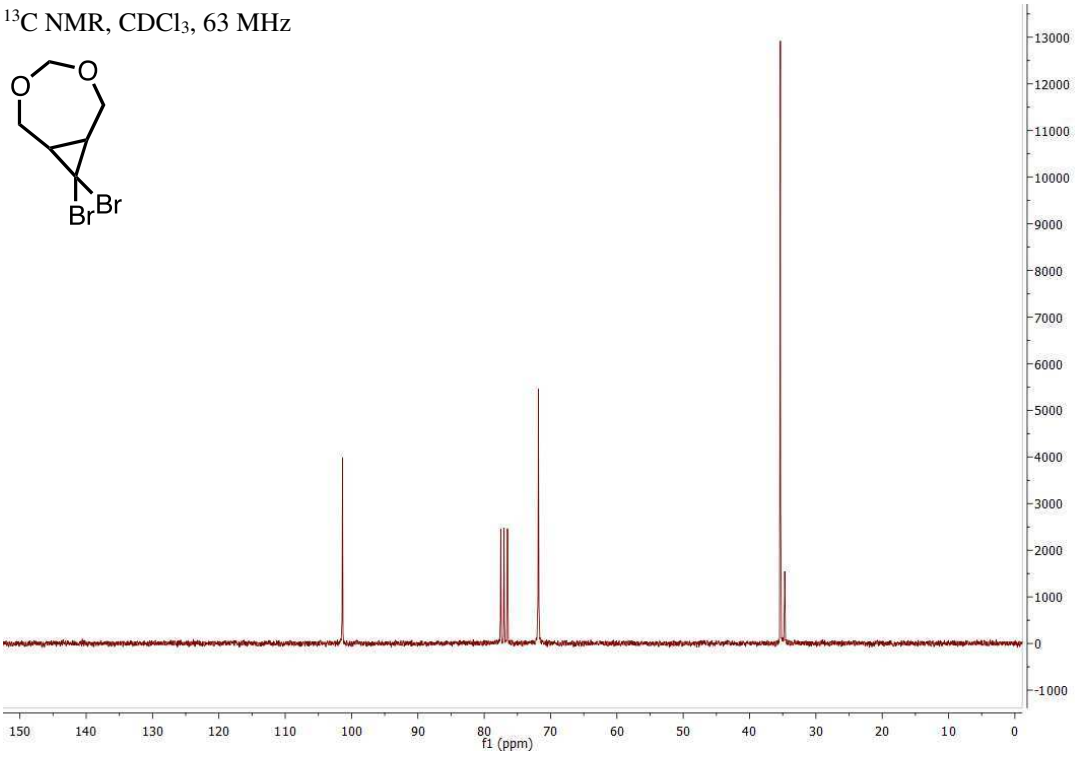

$^{1}H$, $CDCl_3$, 500 MHz

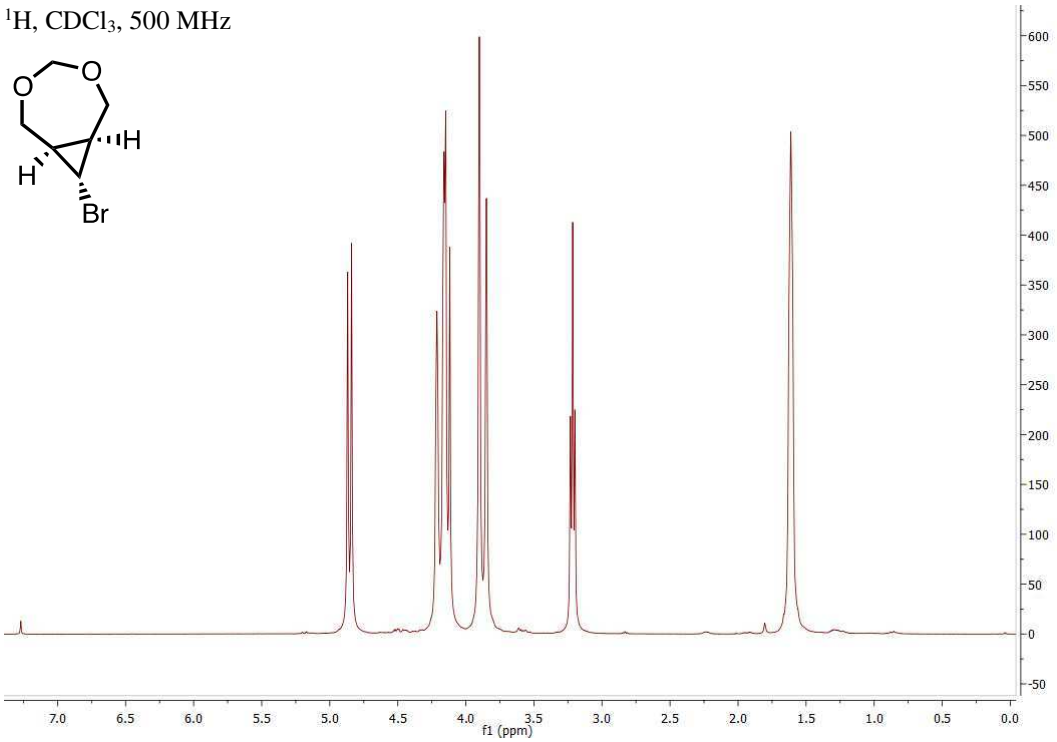


$^{13}C$ NMR, $CDCl_3$, 63 MHz

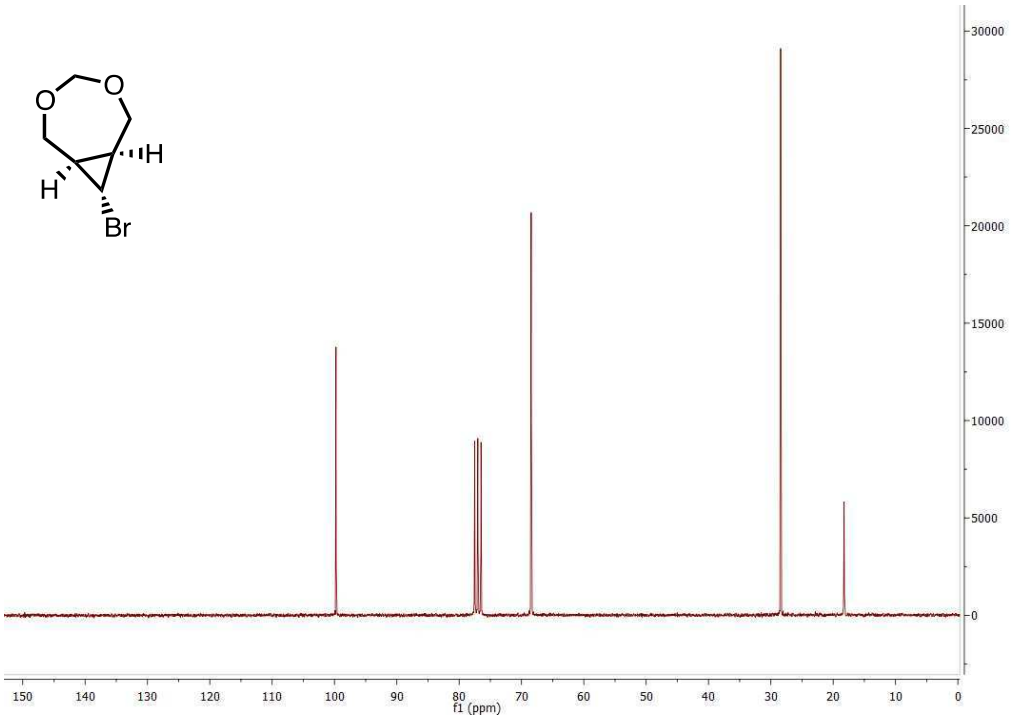

$^{1}$H NMR, $CDCl_3$, 500 MHz

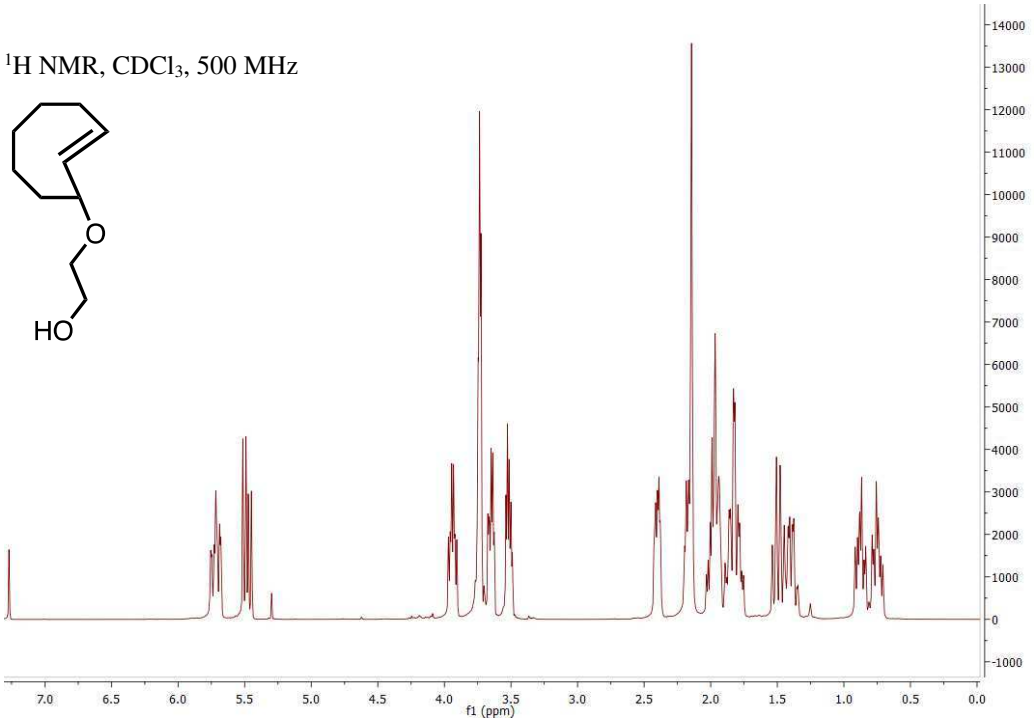


$^{13}$C NMR, $CDCl_3$, 126 MHz

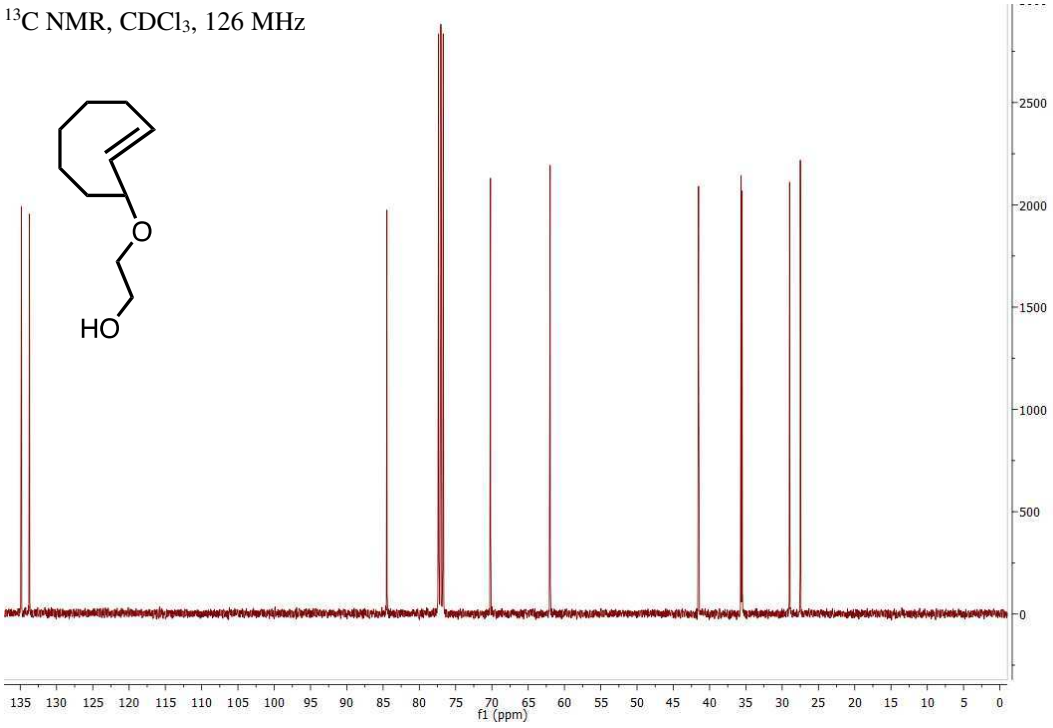

$^{1}H$ NMR, $CDCl_3$, 500 MHz

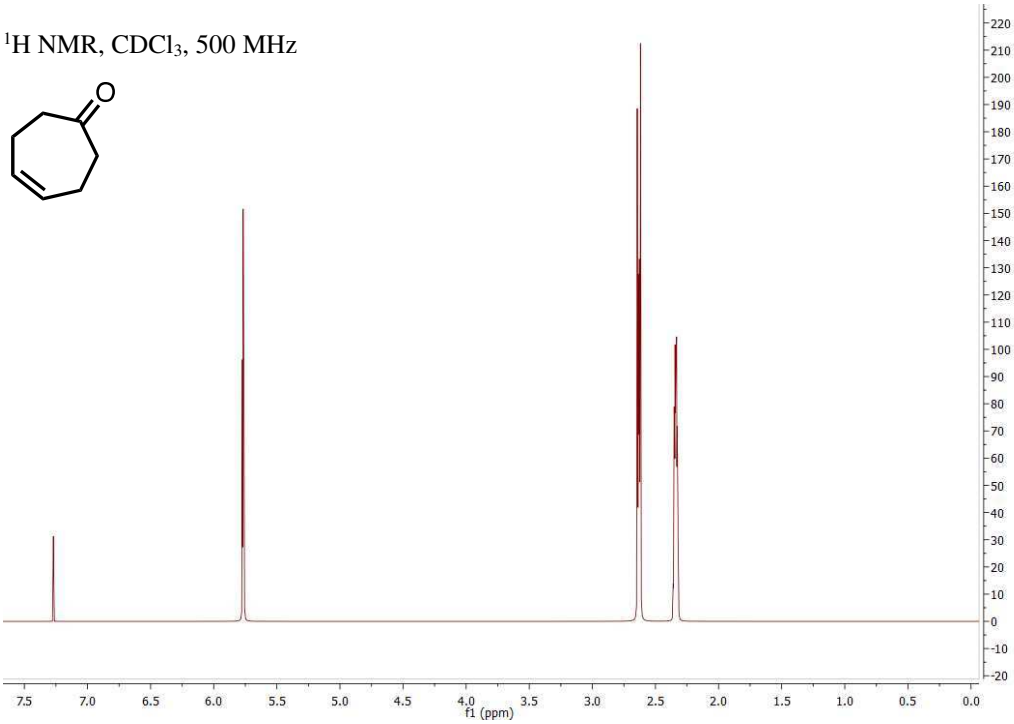


$^{13}C$ NMR, $CDCl_3$, 126 MHz

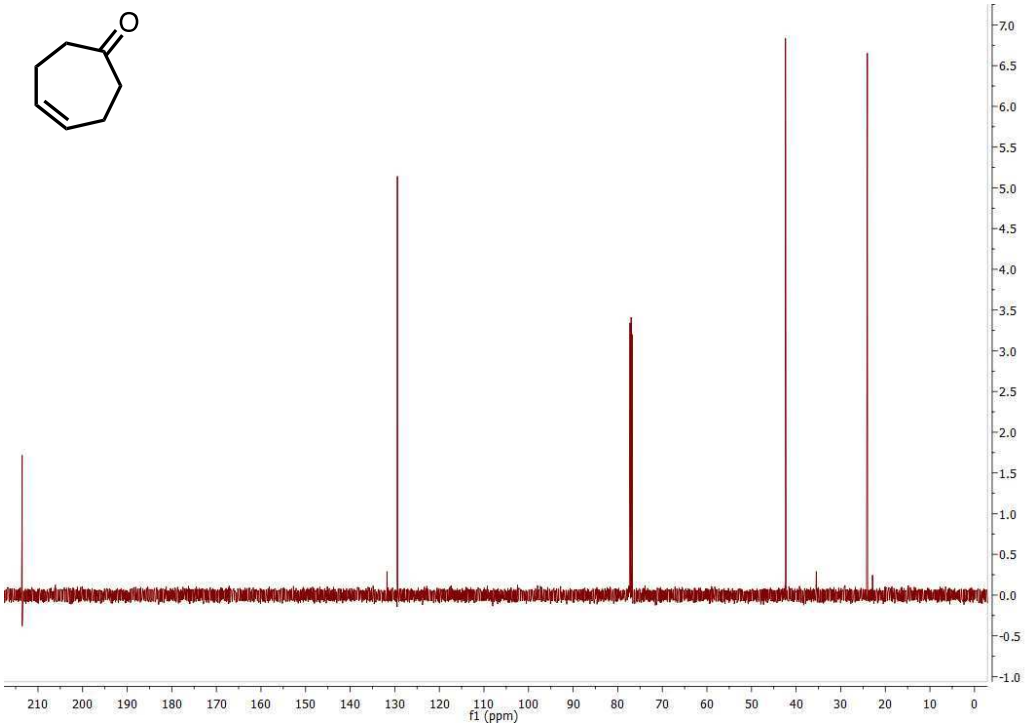

$^{1}H$ NMR, $CDCl_3$, 400 MHz

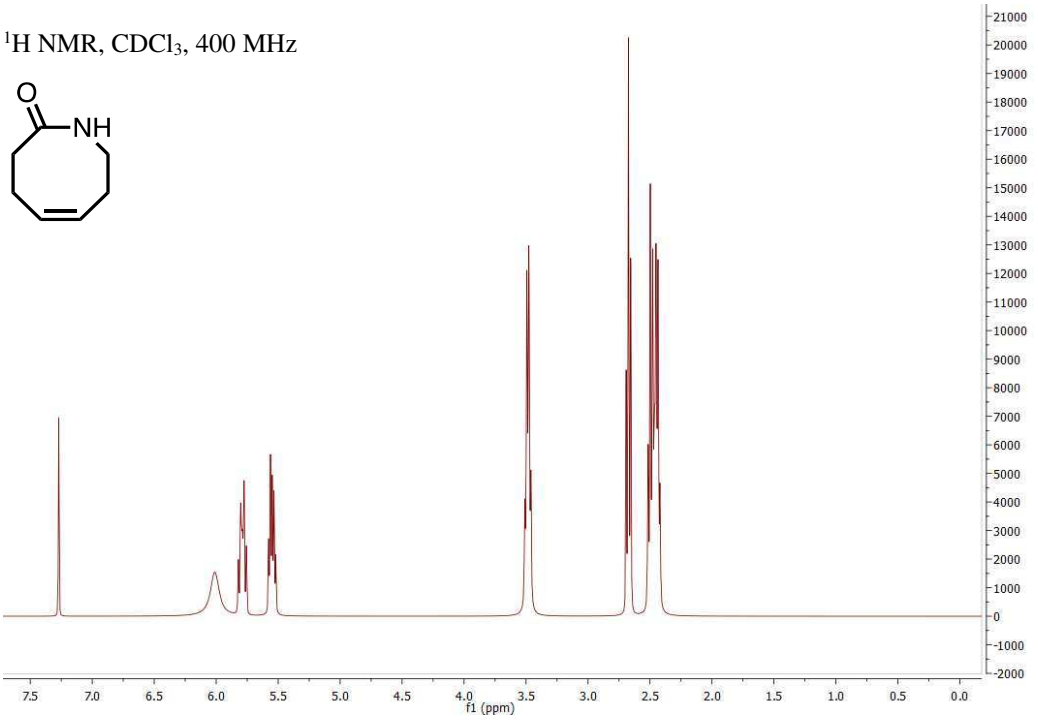


$^{13}C$ NMR, $CDCl_3$, 101 MHz

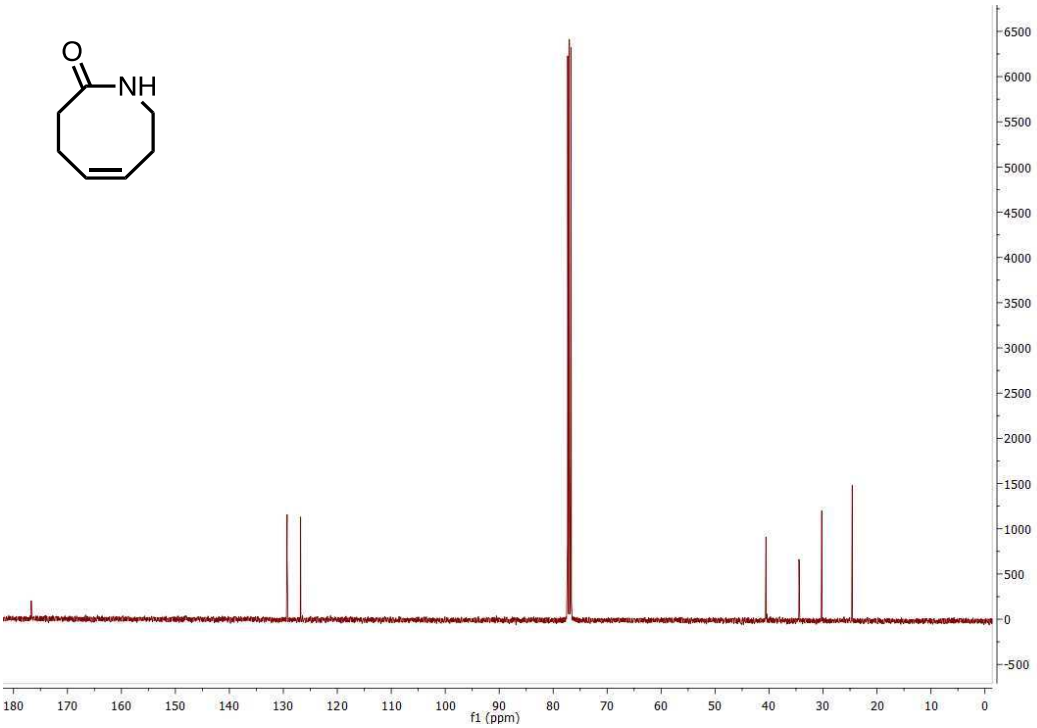

$^{1}H$ NMR, $CDCl_3$, 500 MHz

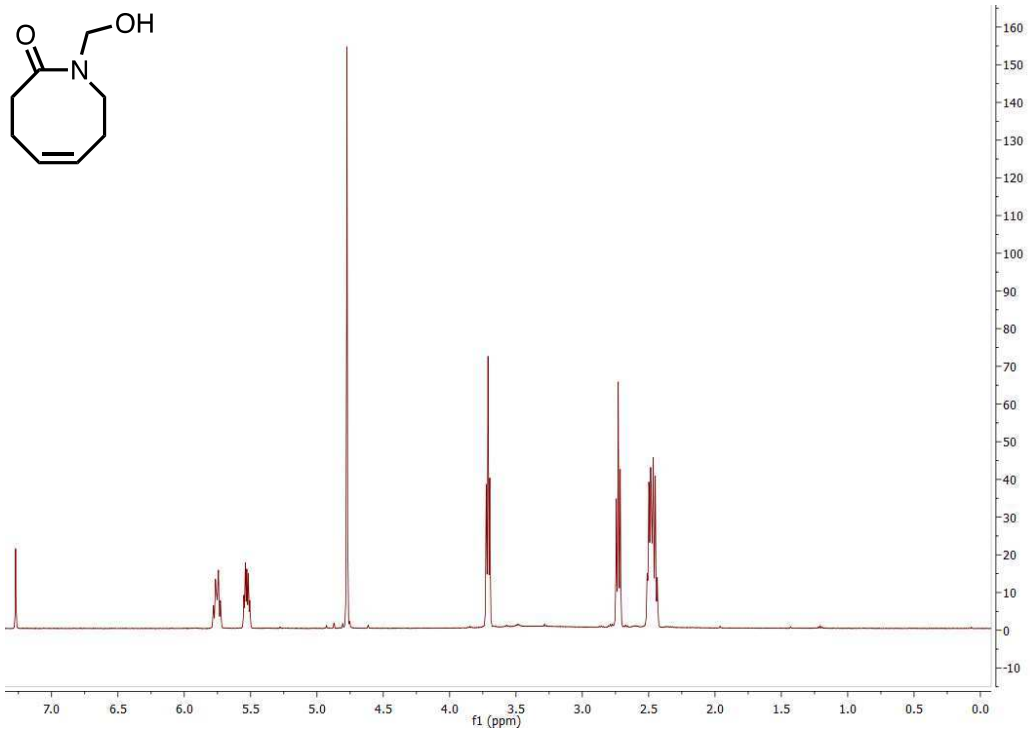


$^{13}C$ NMR, $CDCl_3$, 126 MHz

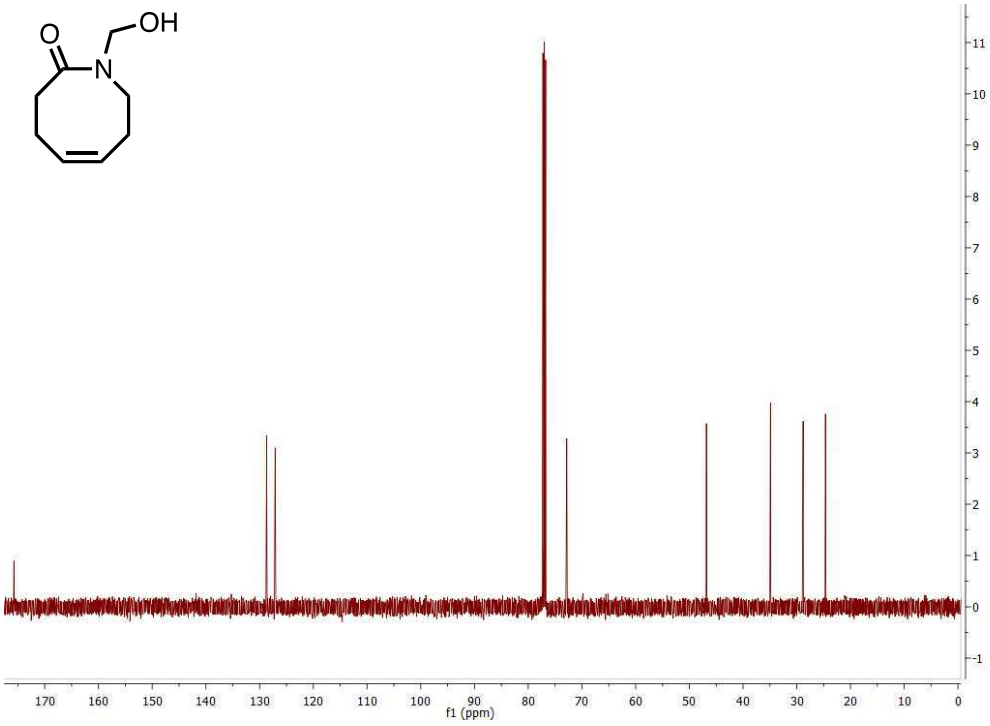

$^{1}$H NMR, $CDCl_3$, 500 MHz

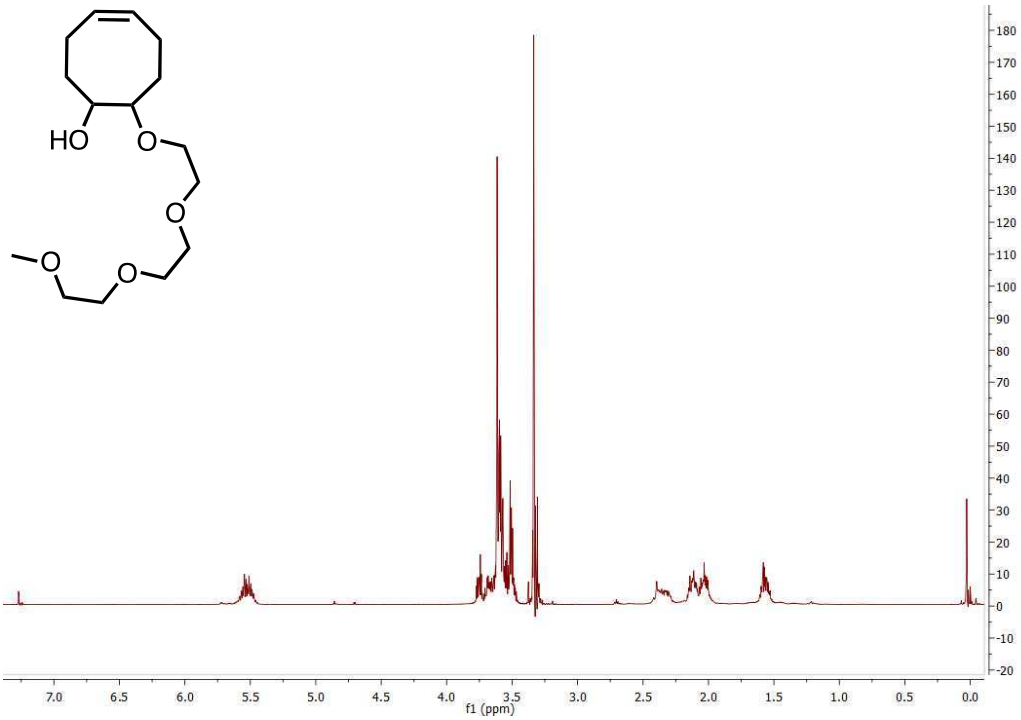


$^{13}$C NMR, $CDCl_3$, 126 MHz

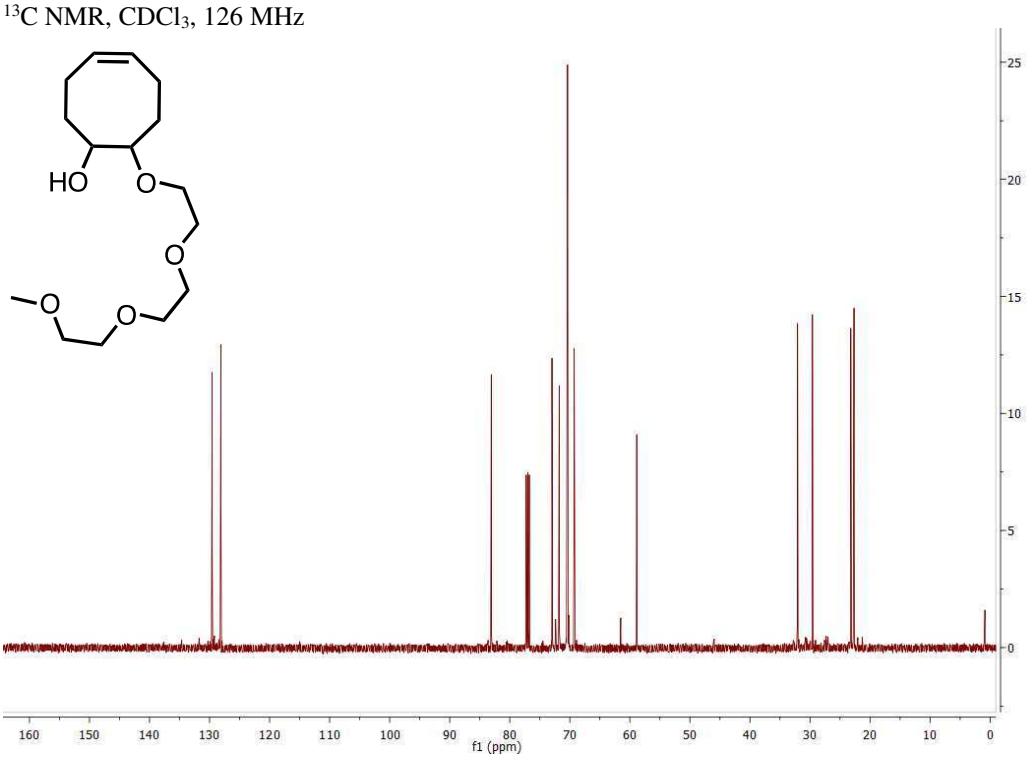

$^{1}$H NMR, $CDCl_3$, 500 MHz

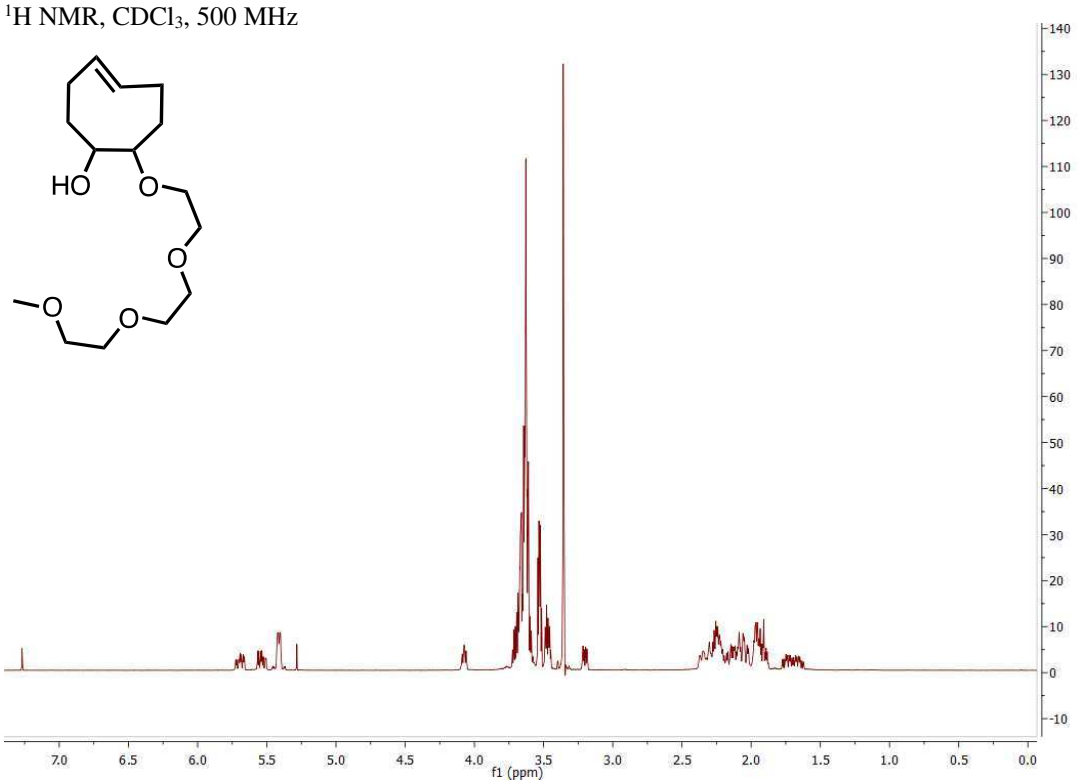


$^{13}$C NMR, $CDCl_3$, 126 MHz

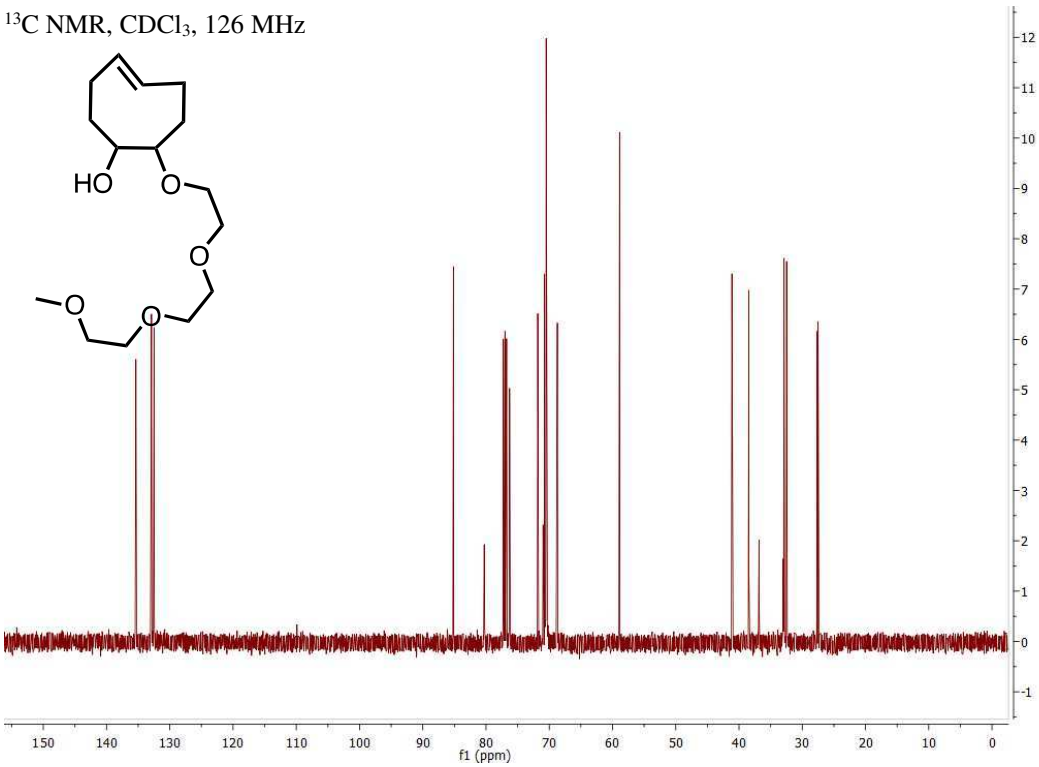

$^{1}H$ NMR, $CDCl_3$, 500 MHz

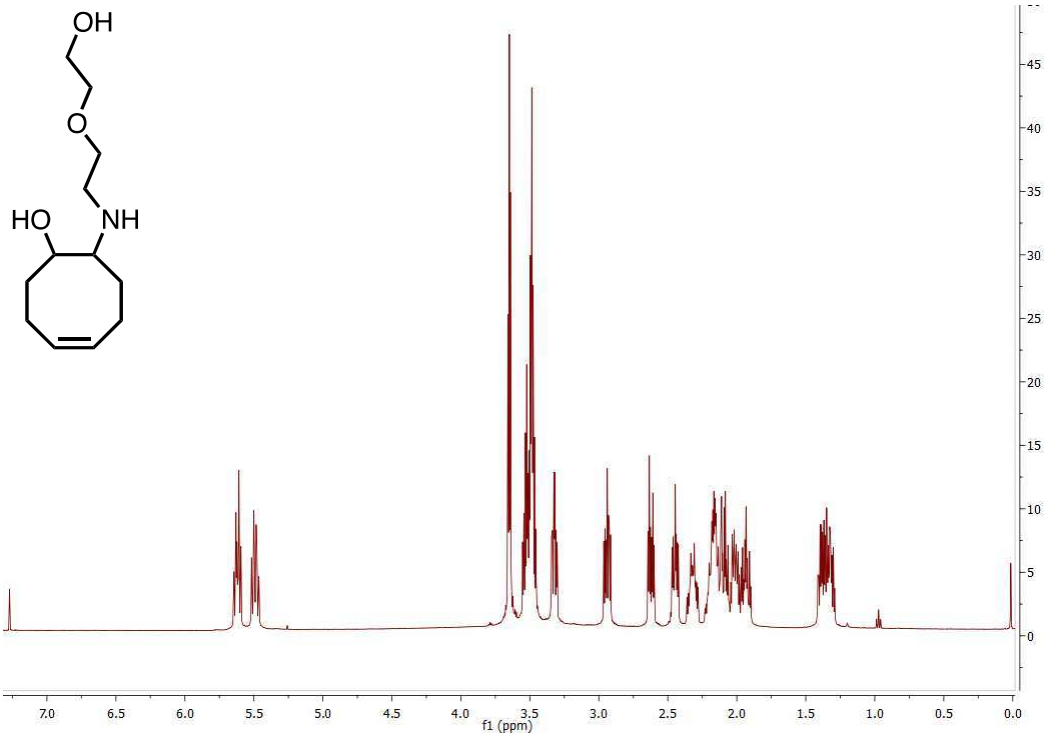


$^{13}C$ NMR, $CDCl_3$, 126 MHz

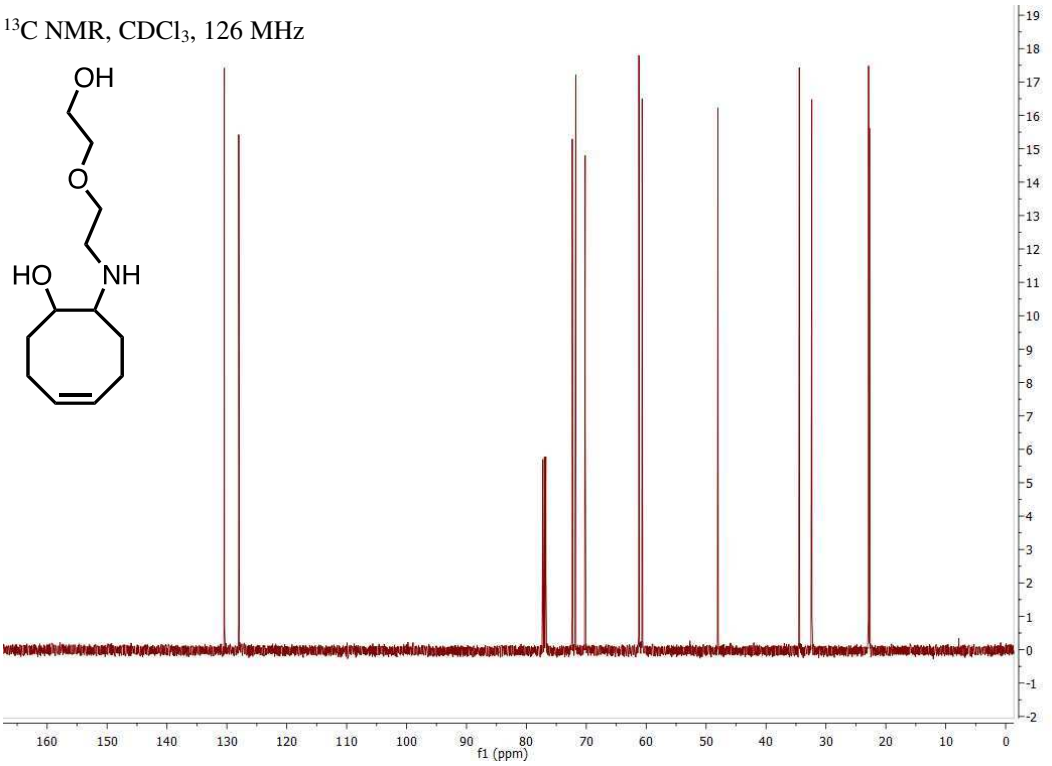

$^{1}$H NMR, $CDCl_3$, 500 MHz

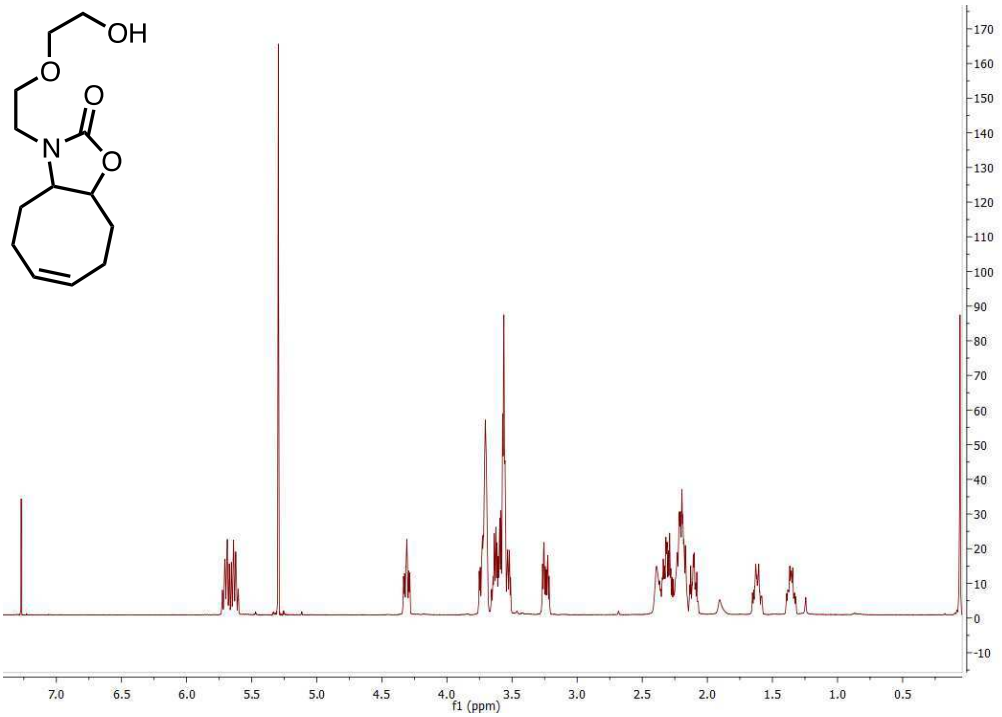


$^{13}$C NMR, $CDCl_3$, 126 MHz

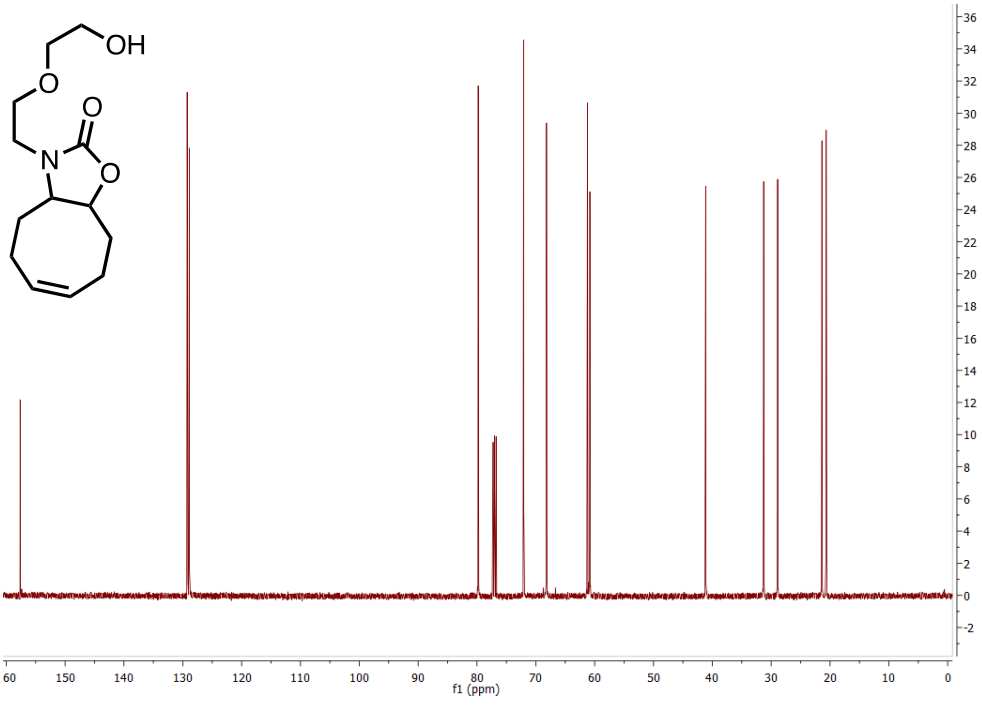

$^{1}$H NMR, $CDCl_3$, 500 MHz

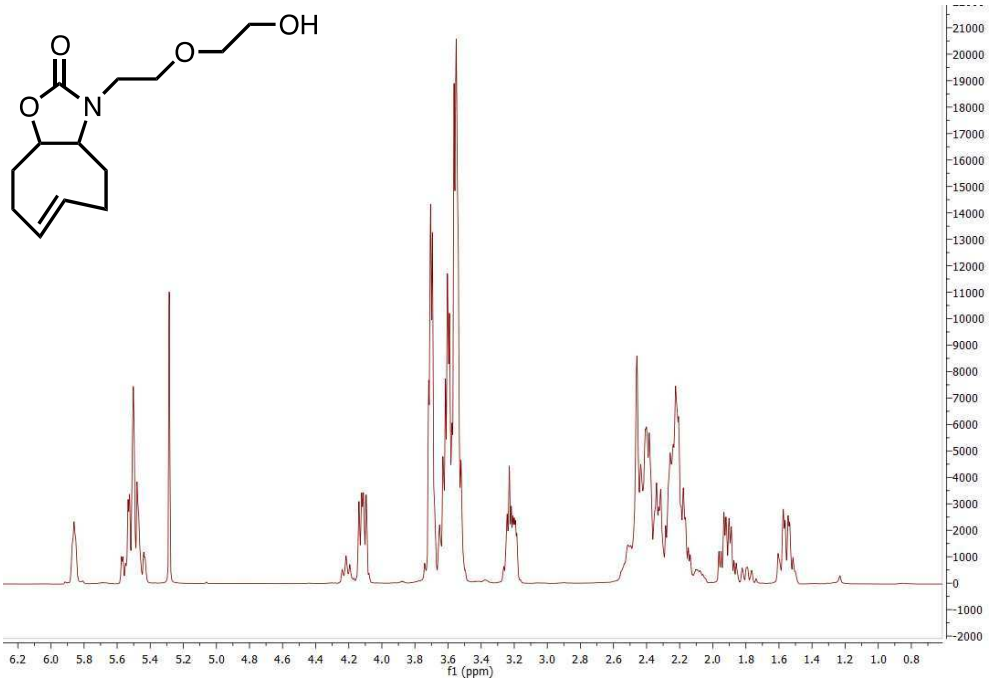


$^{13}$C NMR, $CDCl_3$, 126 MHz

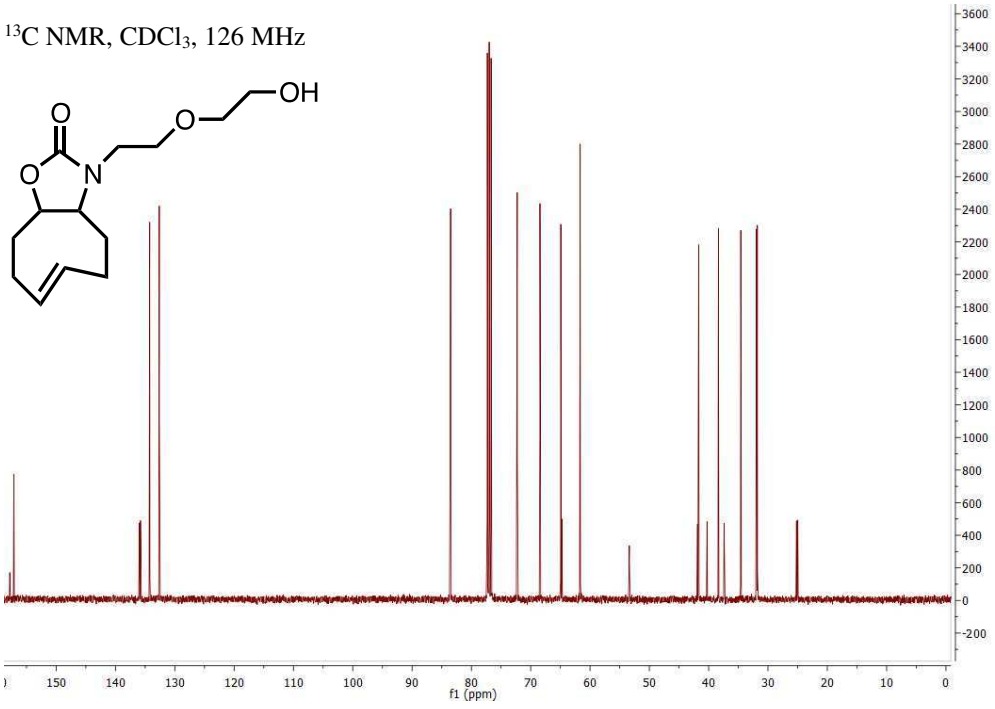

$^{1}$H NMR, $CDCl_3$, 500 MHz

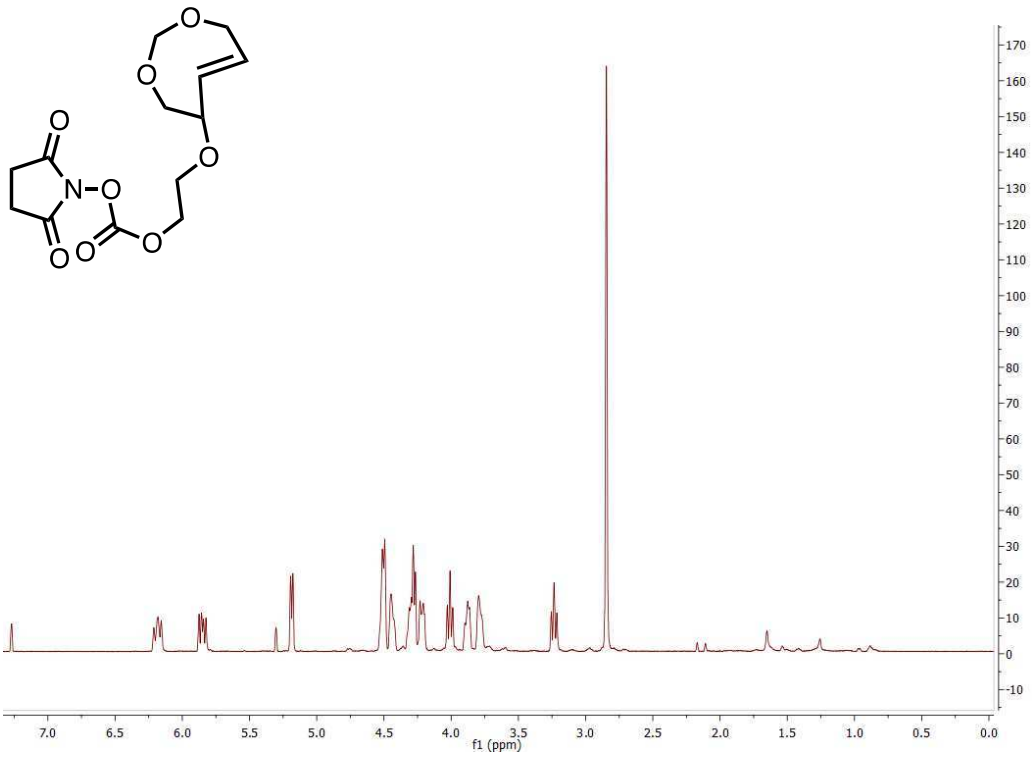


$^{13}$C NMR, $CDCl_3$, 101 MHz

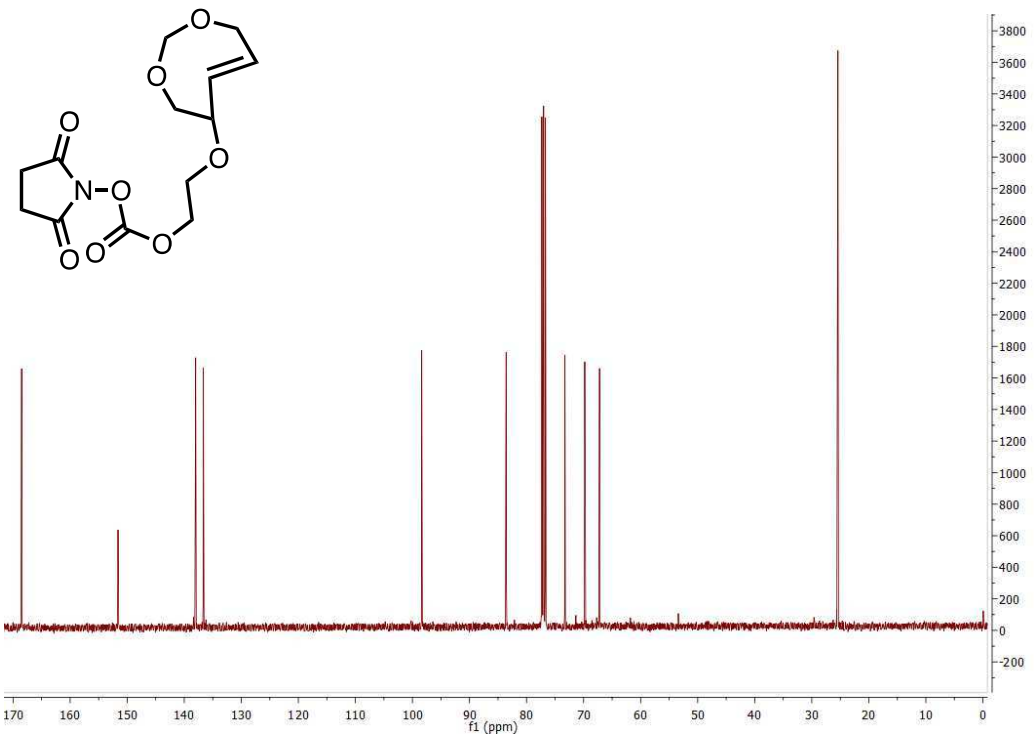

$^{1}H$ NMR, $CDCl_3$ 400 MHz

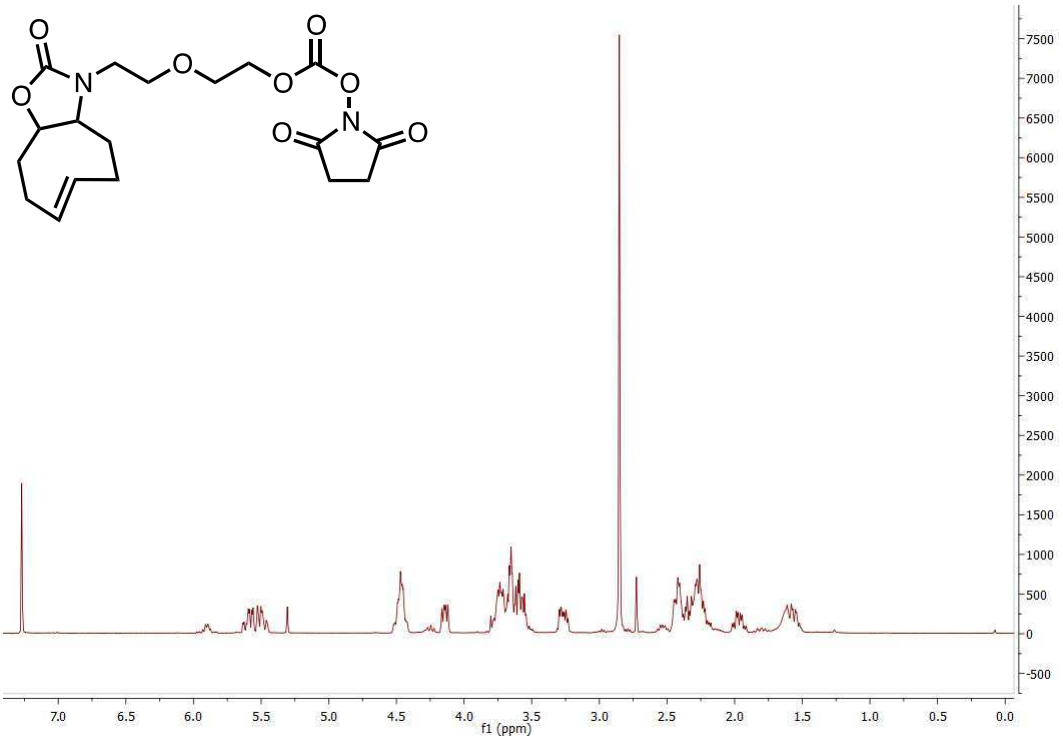


$^{13}C$ NMR, $CDCl_3$, 101 MHz

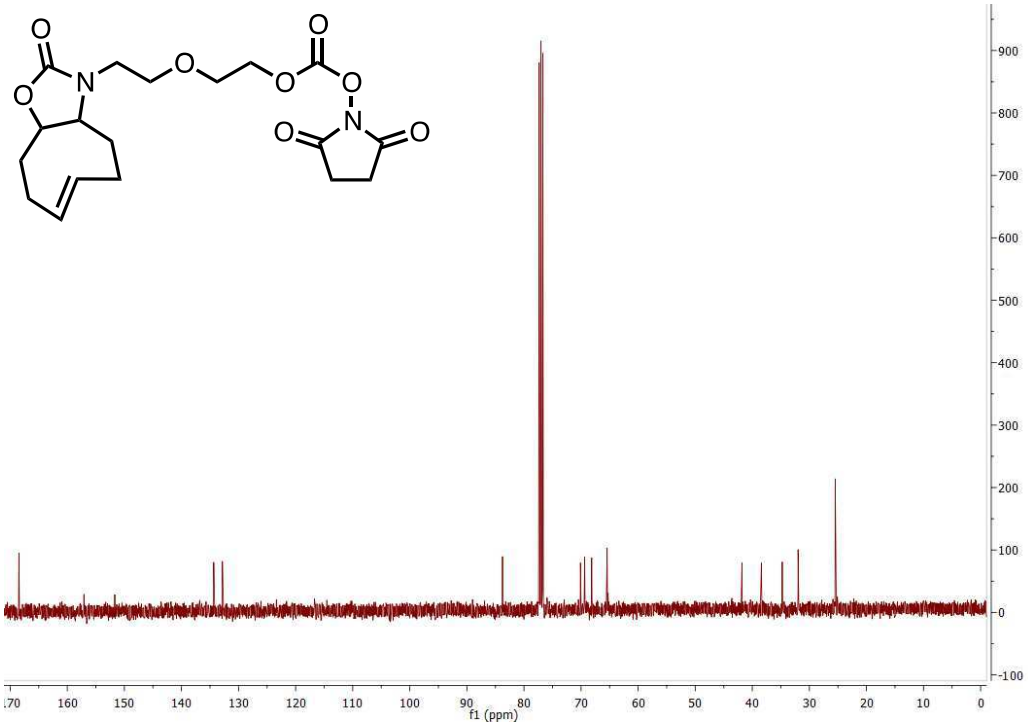

$^{1}H$ NMR, $CDCl_3$, 400 MHz

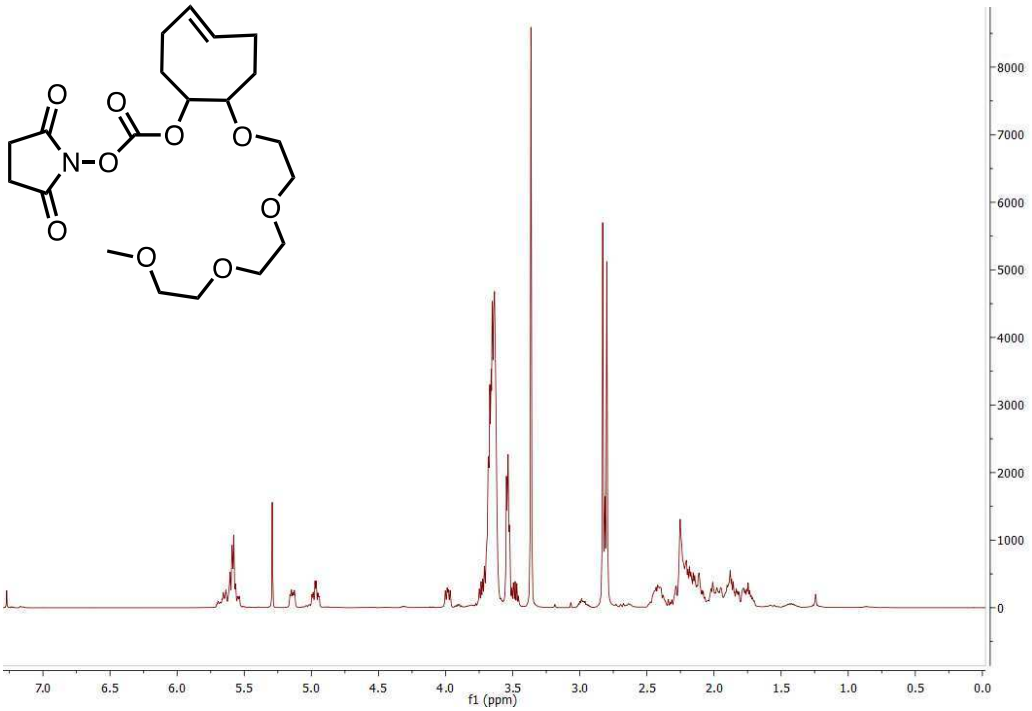


$^{13}C$ NMR, $CDCl_3$, 101 MHz

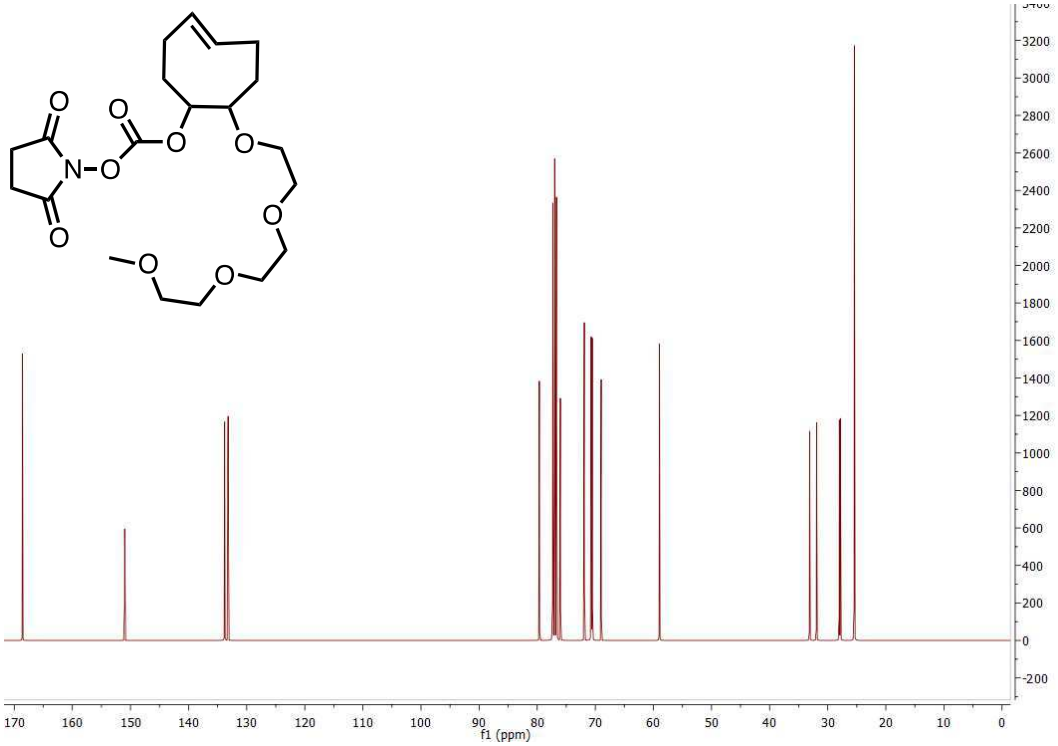

$^{1}H$ NMR, $CDCl_3$, 400 MHz

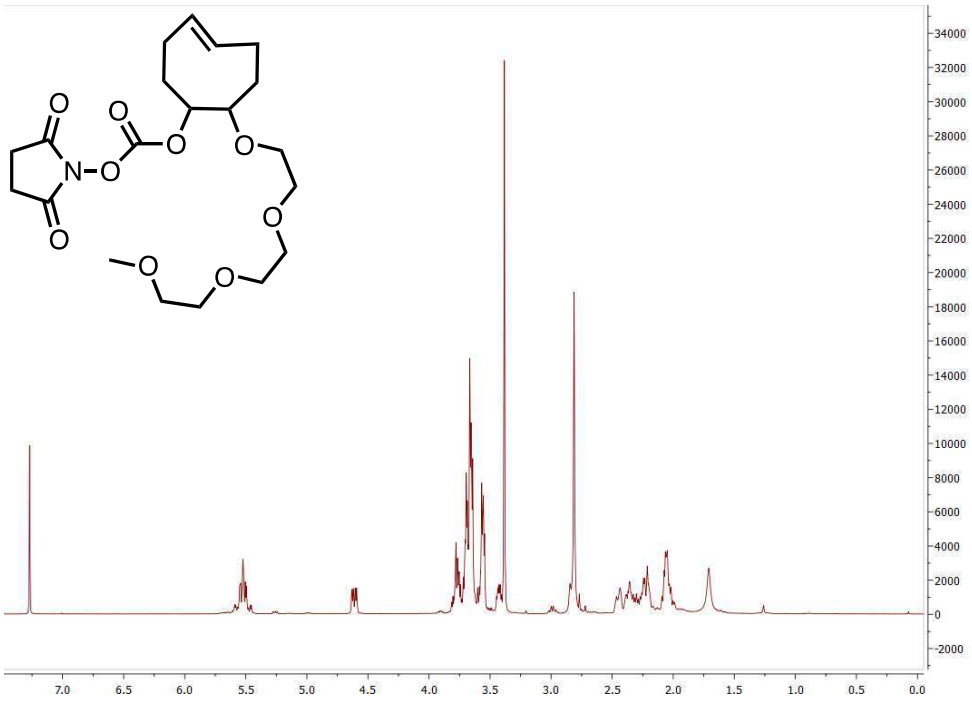


$^{13}C$ NMR, $CDCl_3$, 101 MHz

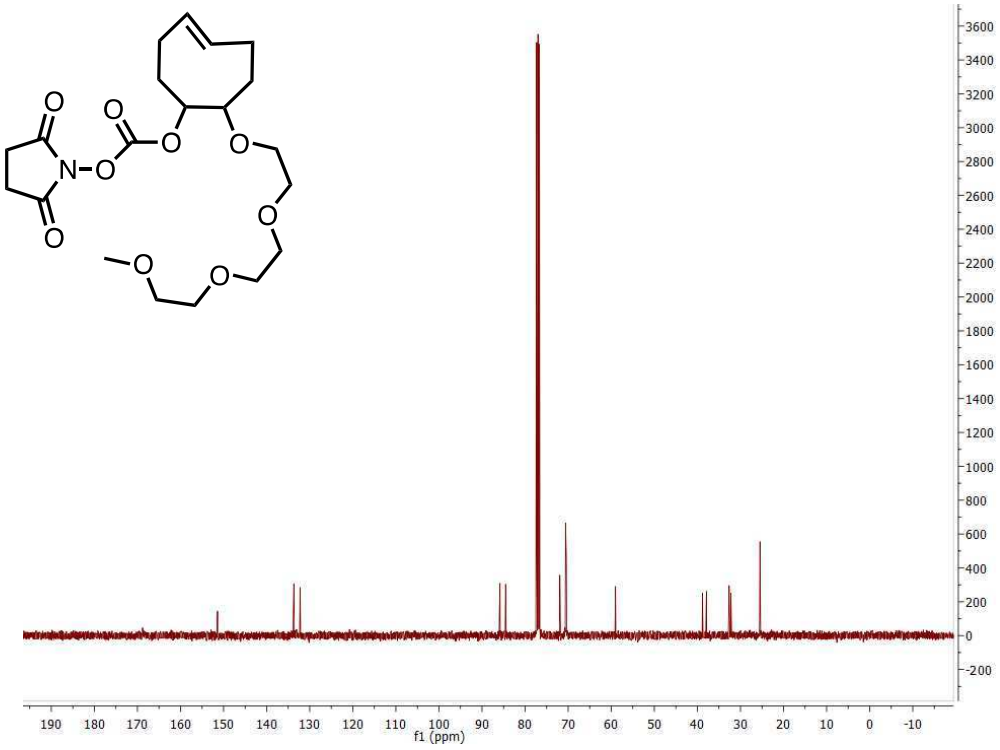

$^1$H NMR, $CDCl_3$, 400 MHz

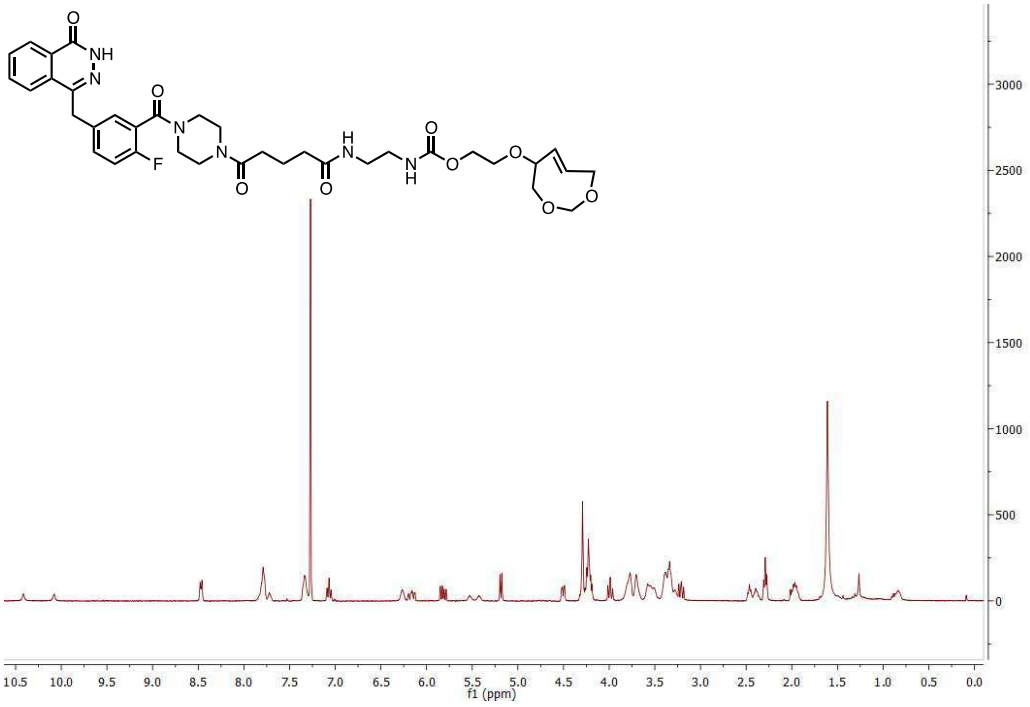


$^1$H NMR, $CDCl_3$, 400 MHz

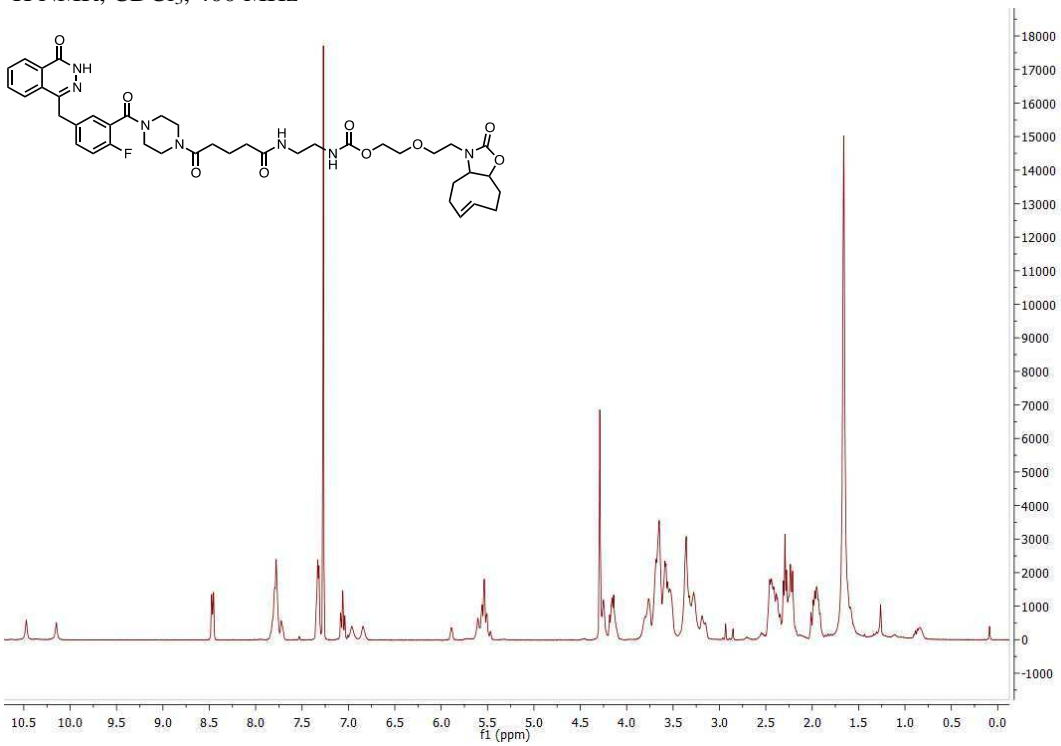

$^{1}$H NMR, $CDCl_3$, 400 MHz

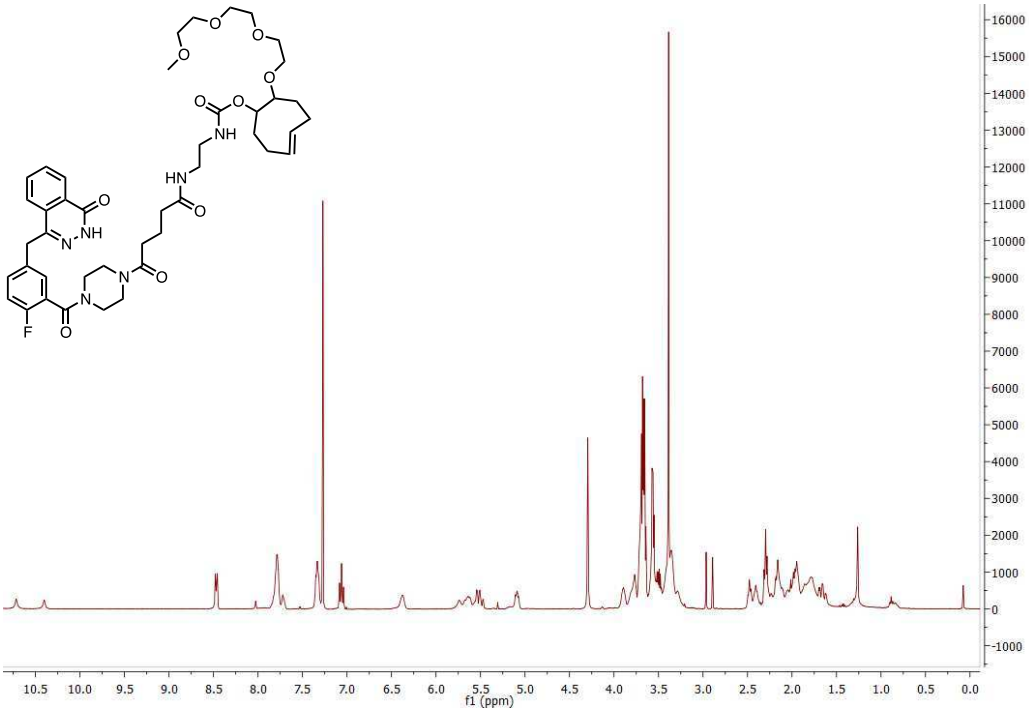

# References


[1] Agard, N. J.; Baskin, J. M.; Prescher, J. A.; Lo, A.; Bertozzi, C. R. ACS Chem. Biol. **2006**, 1, 644-648.

[2] Sletten, E. M.; Bertozzi, C. R. Acc. Chem. Res. **2011**, 44, 666-676 .

[3] Debets, M.F.; van Hest, J. C. M.; Rutjes, F. P. J. T. Org. Biomol. Chem. **2013**, 11, 6439-6455.

[4] Saxon, E.; Bertozzi, C. R. Science **2000**, 287, 2007–2010.

[5] Song, W.; Wang, Y.; Qu, J.; Lin, Q. J. Am. Chem. Soc. **2008**, 130, 9654-9655.

[6] Wang, Y.; Hu, W. J.; Song, W.; Lim, R. K. V.; Lin, Q. Org. Lett. **2008**, 10, 3725-3728.

[7] Debets, M. F.; van der Doelen, C. W. J.; Rutjes, F. P. J. T.; van Delft, F. L. ChemBioChem **2010**, 11, 1168–1184.

[8] Lin, F. L.; Hoyt, H. M.; van Halbeek, H.; Bergman, R. G.; Bertozzi, C. R. J. Am. Chem. Soc. **2005**, 127, 2686–2695.

[9] Sletten, E. M.; Bertozzi, C. R. Angew. Chem., Int. Ed. **2009**, 48, 6974–6998.

[10] Hong, V.; Presolski, S. I.; Ma, C.; Finn, M. G. Angew. Chem., Int. Ed. **2009**, 48, 9879-9883.

[11] Hong, V.; Steinmetz, N. F.; Manchester, M.; Finn, M. G. Bioconjugate Chem. **2010**, 21, 1912-1916.

[12] Del Amo, D. S.; Wang, W.; Jiang, H.; Besanceney, C.; Yan, A. C.; Levy, M.; Liu, Y.; Marlow, F. L.; Wu, P. J. Am. Chem. Soc. **2010**, 132, 16893–16899.

[13] Chang, P. V.; Chen, X.; Smyrniotis, C.; Xenakis, A.; Hu, T.; Bertozzi, C. R.; Wu, P. Angew. Chem. Int. Ed. **2009**, 121, 1-5.

[14] Herner, A.; Nikić, I.; Kállay, M.; Lemke, E. A.; Kele, P. Org. Biomol. Chem. **2013**, 11, 3297-3306.

[15] Baskin, J. M.; Prescher, J. A.; Laughlin, S. T.; Agard, N. J.; Chang, P. V.; Miller, I. A.; Lo, A.; Codelli, J. A.; Bertozzi, C. R. Proc. Natl. Acad. Sci. U.S.A. **2007**, 104, 16793-16797.

[16] Carroll, L.; Evans, H. L.; Aboagye, E. O.; Spivey, A. C. Org. Biomol. Chem. **2013**, 11, 5772-5781.

[17] Ning, X.; Guo, J.; Wolfert, M. A.; Boons, G.-J. Angew. Chem. Int. Ed. **2008**, 47, 2253-2255.

[18] Dommerholt, J.; Schmidt, S.; Temming, R.; Hendriks, L. J. A.; Rutjes, F. P. J. T.; van Hest, J. C. M.; Lefber, D. J.; Friedl, P.; van Delft F. L. Angew. Chem. Int. Ed. **2010**, 49, 9422-9425.

[19] Jewett, J. C.; Sletten, E. M.; Bertozzi, C. R. J. Am. Chem. Soc. **2010**, 132, 3688-3690.

[20] Poloukhtine, A. A.; Mbua, N. E.; Wolfert, M. A.; Boons, G-J.; Popik, V. V, J. Am. Chem. Soc. **2009**, 131, 15769-15776.

[21] Blackman, M. L.; Royzen M.; Fox, J. M. J. Am. Chem. Soc. **2008**, 130, 13518-13519.

[22] Devaraj, N. K.; Weissleder R.; Hildebrand, S. A. Bioconjugate Chem. **2008**, 19, 2297-2299.

[23] Devaraj, N. K.; Upadhyay, R.; Haun, J. B.; Hilderbrand, S. A.; Weissleder, R. Angew. Chem. Int. Ed. **2009**, 48, 7013–7016.

[24] Devaraj, N. K.; Hilderbrand, S. A.; Upadhyay, R.; Mazitschek, R.; Weissleder, R. Angew. Chem. Int. Ed. **2010**, 49, 2869-2872.

[25] Karver, M. R.; Weissleder, R.; Hilderbrand, S. A. Angew. Chem., Int. Ed. **2012**, 51, 920-922.

[26] Liang, Y.; Mackey, J. L.; Lopez, S. A.; Liu, F.; Houk, K. N. J. Am. Chem. Soc. **2012**, 134, 17904-17907.

[27] Ess, D. H.; Jones, G. O.; Houk, K. N. Org. Lett. **2008**, 10, 1633-1636.

[28] Foster, R. A. A.; Willis, M. C. Chem. Soc. Rev. **2013**, 42, 63-76.

[29] Knall, A. C.; Slugovc, C. Chem. Soc. Rev. **2013**, 42, 5131-5142.

[30] Sauer, J.; Sustmann, R. Angew. Chem. Int. Ed. Engl. **1980**, 19, 779-807.

[31] Sadashivam, D. V.; Prasad, E.; Flowers, R. A.; Birney, D. M. J. Phys. Chem. A **2006**, 110, 1288-1294.

[32] Sauer, J.; Heinrichs, G. Tetrahedron Lett. **1966**, 41, 4979-4984.

[33] Thalhammer, F.; Wallfahrer, U.; Sauer, J. Tetrahedron Lett. **1990**, 31, 6851-6854.

[34] Meier, A.; Sauer, J. Tetrahedron Lett. **1990**, 31, 6855-6856.

[35] Schuster, H.; Sichert, H.; Sauer, J. Tetrahedron Lett. **1983**, 24, 1485-1488.

[36] Sauer, J.; Heldmann, K.; Hetzenegger, J.; Krauthan, J.; Sichert, H.; Schuster, J. Eur. J. Org. Chem. **1998**, 12, 2885-2896.

[37] Wiljen, J. W.; Zavarise, S.; Engberts, J. B. F. N.; Charton, M. J. Org. Chem. **1996**, 61, 2001-2005.

[38] Sanders, B. C.; Friscourt, F.; Ledin, P. A.; Mbua, N. E.; Arumugam, S.; Guo, J.; Boltje, T. J.; Popik, V. V.; Boons, G-J. J. Am. Chem. Soc. **2011**, 133, 949-957.

[39] Sletten, E. M.; Nakamura, H.; Jewett, J. C.; Bertozzi, C. R. J. Am. Chem. Soc. **2010**, 9, 11799-11805.

[40] Chenoweth, K.; Chenoweth, D.; Goddard III, W. A. Org. Biomol. Chem. **2009**, 7, 5255-5258.

[41] (a) Krebs, A.; Odenthal, J.; Kimling, H. Tetrahedron Lett. **1975**, 16, 4663-4666.; (b) Meier, H.; Layer, M.; Zetzsche, A. Chemiker-Ztg. **1974**, 98, 460-461.

[42] Murakami, A.; Kadowaki, S.; Fujimoto, A.; Ishibashi, M.; Matsuda, T. Org. Lett. **2005,** 7, 2059-2061.

[43] Sibi, M. P.; Aasmul, M.; Hasegawa, H.; Subramanian, T. Org. Lett. **2003**, 5, 2883-2886.

[44] Detert, H.; Rose, B.; Mayer, W.; Meier, H. Chem. Ber. **1994**, 127, 1529-1532. (the procedure was modified)

[45] Meier, H.; Molz, T.; Merkle, U.; Echter, T.; Lorch, M. Liebigs. Ann. Chem. **1982**, 5, 914-923.

[46] Gaussian 03, Revision B.01, M. J. Frisch et al., Gaussian, Inc., Pittsburgh PA, 2003

[47] Ess, D. H.; Houk, K. N. J. Phys. Chem. A **2005**, 109, 9542-9553.

[48] Chang, P. V.; Prescher, J. A.; Sletten, E. M.; Baskin, J. M.; Miller, I. A.; Agard, N. J.; Loa, A.; Bertozzi, C. R. Proc. Natl. Acad. Sci. U.S.A. **2010**, 107, 1821–1826.

[49] Debets, M.; Berkel, S. van; Dommerholt, J.; Dirks, A.; Rutjes, F.; van Delft, F. Acc. Chem. Res. **2011**, 44, 805–815.

[50] Chang, P. V.; Prescher, J. A.; Hangauer, M. J.; Bertozzi, C. R. J. Am. Chem. Soc. **2007**, 129, 8400-8401.

[51] Own data

[52] Rossin, R.; Verkerk, P.; Bosch, S. van den; Vulders, R.; Verel, I.; Lub, J.; Robillard, M. Angew. Chem. Int. Ed. **2010**, 49, 3375–3378.

[53] Devaraj, N. K.; Weissleder, R. Acc. Chem. Res. **2011**, 44, 816-827.

[54] Keliher, E.; Reiner, T.; Turetsky, A.; Hilderbrand, S.; Weissleder, R. ChemMedChem **2011**, 6, 424-427.

[55] Seitchik, J. L.; Peeler, J. C.; Taylor, M. T.; Blackman, M. L.; Rhoads, T. W.; Cooley, R. B.; Refakis, C.; Fox, J. M.; Mehl, R. A. J. Am. Chem. Soc. **2012**, 134, 2898-2901.

[56] Carlson, J.; Meimetis, L.; Hilderbrand, S.; Weissleder, R. Angew. Chem. Int. Ed. **2013**, 52, 6917–6920.

[57] Wiessler, M.; Waldeck, W.; Kliem C.; Pipkorn, R.; Braun, K. Int. J. Med. Sci. **2010**, 7, 19-28.

[58] Karver, M. R.; Weissleder, R.; Hilderbrand, S. A. Bioconjugate Chem. **2011**, 22, 2263-2270.

[59] Reese, C.B.; Shaw, A. J. Am. Chem. Soc. **1970**, 92, 2566-2568.

[60] Royzen, M.; Yap, G. P. A.; Fox, J. M. J. Am. Chem. Soc. **2008**, 130, 3760-3761.

[61] Allen, F. H.; Kennard, O.; Watson, D. G.; Brammer, L.; Orpen, A. G.; Taylor, R. J. Chem. Soc., Perkin Trans. 2 **1987,** S1-S19.

[62] Jendralla, H. Chem. Ber. **1982**, 115, 201-209.

[63] Wijnen, J.W.; Zavarise, S.; Enghberts, F.N. J. Org. Chem. **1996**, 61, 2001-2005.

[64] a) Jacoby, D.; Celerier, J. P.; Haviari, G.; Petit, H.; Lhommet, G. Synthesis **1992**, 09, 884-887; b) Depres, J-P.; Greene, A. E. J. Org. Chem. **1984,** 49**,** 928-931.

[65] Wilson, S. R.; Sawicki, R. A. J. Org. Chem. **1979**, 44, 287-291.

[66] Dalpozzo, R.; Nardi, M.; Oliverio, M.; Paonessa, R.; Procopio, A. Synthesis **2009**, 20, 3433-3438.

[67] Rossin, R.; van den Bosch, S. M.; Ten Hoeve, W.; Carvelli, M.; Versteegen, R. M.; Lub, J. Bioconjugate Chem. **2013**, 24, 1210-1217.

[68] Menear, K. A.; Adcock, C.; Boulter, R.; Cockcroft, X.-I.; Copsey, L.; Cranston, A.; Dillon, K. J.; Drzewiecki, J.; Garman, S.; Gomez, S.; Javaid, H.; Kerrigan, F.; Knights, C.; Lau, A.; Loh, V. M., Jr.; Matthews, I. T. W.; Moore, S.; O'Connor, M. J.; Smith, G. C. M.; Martin, N. M. B. J. Med. Chem. **2008**, 51, 6581 – 6591.

[69] Reiner, T.; Earley, S.; Turetsky, A.; Weissleder, R. Chembiochem **2010**, 11, 2374-2377.

[70] Seyfert, D.; Lampert, R. L.; Massol, M. J. Orgmet. Chem. **1975**, 88, 255-286.

[71] Brannock, K. C.;Lappin, G. R. J. Org. Chem. **1956**, 1366-1368.

[72] Womack, E. B.; Nelson, A. B. Org. Synth. **1955**, 3, 392.

[73] Nguyen, T.; Francis M. B. Org. Lett. **2003**, 5, 3245-3248.

[74] Eglinton, G.; McCrae, W.; Raphael, R. A.; Zabkiewicz, J. A. J. Chem. Soc. C, **1969**, 474-479. (the procedure was modified)

[75] Higher reaction temperatures resulted in the decomposition of the product, while at lower temperature the tert-butyl ester of the COMBO-acid formed as well.

[76] Kirmse, W.; Olbricht, Th. Chem. Ber. **1975**, 108, 2606-2615. (procedures were modified)

[77] Taylor, K. G.; Chaney, J. J. Am .Chem. Soc. **1972**, 25, 8924-8925.

[78] Fedorenko, V. Y.; Baryshnikov, R. N.; Vafina, R. M.; Shtyrlin, Y. G.; Klimovitskii, E. N. Mendeleev Commun. **2007**, 17, 170–171.

[79] Wilson, S. R.; Wiesler, D. P. Synt. Comm. **1980**, 10, 339-343.

[80] Yang, K. S.; Budin, G.; Reiner, T.; Vinegoni, C.; Weissleder, R. Angew. Chem. Int. Ed. **2012**, 51, 6598-6603.